

Electronic Thesis and Dissertation Repository

---

11-17-2022 11:30 AM

## Regulation of Hedgehog and Wnt Signaling in Neural Differentiation of P19 Embryonal Carcinoma Cells

Danielle Margaret Spice, *The University of Western Ontario*

Supervisor: Kelly, Gregory M., *The University of Western Ontario*

A thesis submitted in partial fulfillment of the requirements for the Doctor of Philosophy degree in Biology

© Danielle Margaret Spice 2022

Follow this and additional works at: <https://ir.lib.uwo.ca/etd>



Part of the [Cell Biology Commons](#), [Developmental Biology Commons](#), and the [Developmental Neuroscience Commons](#)

---

### Recommended Citation

Spice, Danielle Margaret, "Regulation of Hedgehog and Wnt Signaling in Neural Differentiation of P19 Embryonal Carcinoma Cells" (2022). *Electronic Thesis and Dissertation Repository*. 8967.  
<https://ir.lib.uwo.ca/etd/8967>

This Dissertation/Thesis is brought to you for free and open access by Scholarship@Western. It has been accepted for inclusion in Electronic Thesis and Dissertation Repository by an authorized administrator of Scholarship@Western. For more information, please contact [wlsadmin@uwo.ca](mailto:wlsadmin@uwo.ca).

## Abstract

The Hedgehog (Hh) and Wnt protein signaling pathways are essential in the differentiation of neurons and astrocytes. As there are many known and new players involved in regulating these pathways, the role of the regulators Suppressor of Fused (SUFU) and Never in Mitosis Kinase 2 (Nek2) have either not been previously reported or have not been thoroughly explored. To address this shortfall CRISPR gene editing was used to target SUFU and Nek2 in the mouse P19 embryonal carcinoma cell model of neural differentiation. Hh and Wnt signaling were explored in normal P19 neural differentiation, which occurs in the presence of retinoic acid. Both pathways are required for the establishment of neural cell fates, however, neither is sufficient to induce both neurons and astrocyte lineages alone. SUFU was found to be required in the differentiation of astrocytes, but not neurons, and its loss resulted in the loss of the Gli3 transcription factor. The loss of Gli3 in SUFU-deficient cells resulted in constitutive expression of Hh target genes. Nek2 was required for the differentiation of both neurons and astrocytes, however, loss of function experiments did not find a clear link between Nek2, and the Hh or Wnt pathways. Instead, a mechanism was discovered where Nek2 is required to destabilize hypoxia inducible factor 1 $\alpha$ , allowing for a required metabolic shift from glycolysis to oxidative phosphorylation during the differentiation of neural cell types. Together this work shows novel mechanisms of regulating neural cell fate through the presence or absence of intracellular regulatory proteins.

## Keywords

Neuron, Astrocyte, Differentiation, Pluripotency, CRISPR, Suppressor of Fused, Never in Mitosis Kinase 2, Neural Development, Hedgehog Signaling, Wnt Signaling

## Summary for Lay Audience

During development, how specific cell types are determined requires the activation of specific information pathways. Becoming a cell that belongs to the nervous system requires, in part, activation of the Hedgehog (Hh) and Wnt signaling pathways. The cell types being explored here were neurons, cells that send and receive electrical impulses, and astrocytes, cells that support neurons. To answer questions regarding the development of these cell types a method where cells were grown in a dish that does not require live animals was used. These stem-like cells comprise the mouse P19 embryonal carcinoma model and were isolated from a mouse tumor. These cells can become any cell type in the body, and when given the vitamin A derivative, retinoic acid (RA), can become neurons and astrocytes. Through chemical studies Hh and Wnt signaling were determined to be essential during neural cell development. Two proteins involved in regulating these signaling pathways, Suppressor of Fused (SUFU) and Never in Mitosis Kinase 2 (Nek2), were investigated through loss of function experiments where a targeted gene editing approach, CRISPR, was used. Loss of SUFU showed it is vital in the development of astrocytes but not neurons; Nek2 is vital in the development of both cell types. When SUFU was lost there was over-activation of Hh signaling, resulting in the loss of Gli3, a transcription factor normally required to inhibit the Hh pathway. The connection between Nek2, Hh and Wnt signaling pathways were explored, however, there was no clear evidence showing a link. Instead, Nek2 was found to be involved in regulating how cells use sugar molecules as without it, the cells metabolize sugar via a pathway that does not require oxygen. In normal cells, however, the development of neurons and astrocytes requires a shift from an oxygen-deficient metabolic pathway, to relying exclusively on one that requires oxygen. Thus, this work sheds new light on how proteins regulate the development of specific cell types in the central nervous system and makes connections between signaling pathways, development, and metabolism.

## Co-Authorship Statement

All studies presented in this thesis were performed by Danielle M. Spice under supervision of Dr. Gregory M. Kelly. Written and experimental contributions from co-authors are listed below.

As supervisor, Dr. Gregory Kelly was involved in all stages of thesis development including project conceptualization, experimental design, data interpretation, manuscript preparation and financial assistance.

Chapter 2 titled, “Suppressor of Fused Regulation of Hedgehog Signaling is Required for Proper Astrocyte Differentiation” the presented flow cytometry work in Figure 7 was done in collaboration with Dr. Joshua Dierolf. Dr. Dierolf’s expertise was invaluable in guiding the sample preparation and in performing the flow cytometry assay and analysis. A version of this chapter has been published in *Stem Cells and Development* (Published Oct. 13, 2022, Online ahead of print: 10.1089/scd.2022.0131) and reproduced with permission.

In Chapter 3 titled, “Never in Mitosis Kinase 2 regulation of metabolism is required for neural differentiation” the presented liquid chromatography mass spectrometry in Figure 8 was done in collaboration with Dr. ’s Tyler Cooper and Gilles A. Lajoie. Dr. Cooper’s expertise was invaluable in the design of the proteomics experiment, in sample preparation, performing the assay workflow and analysis. Dr. Lajoie’s expertise in proteomics and funding acquisition for the proteomics work was also invaluable. A version of this chapter has been published in *Cellular Signaling* (Published Oct. 3, 2022, Online ahead of print: 10.1016/j.cellsig.2022.110484) and reproduced with permission.

I would like to thank Drs, Dierolf, Cooper and Lajoie for their help and expertise in collaborating on these projects.

## Acknowledgments

As Western University has been my academic home for ten years, there are many who contributed to my success over the years and in the completion of my doctoral work. Thanks are extended to my advisory committee, Dr. Thomas Drysdale, Dr. David Litchfield, and Dr. Sashko Damjanovski whose expertise and mentorship were invaluable to the development of the presented work.

I would like to thank my lab mates in the Kelly lab, both past and present for their friendship and support over the years. Tina Nicole Cuthbert and Renee Resendes I would like to thank, as although we worked together for only a short time you both showed me the importance of resiliency, hard work and seeking out what brings you joy. I would also like to give a special thank you to Dr. Mohamed Gatie, without whom my experience in graduate school would have been entirely different. Mohamed's constant support and friendship helped shape who I am as not only a scientist but a person, and I will forever be grateful for our time together. Also, special thanks go out to Alexandra Kozlov, Dr. Carlie Muir, Bradley Bork, Dr. Emily Clayton, Dr. Joshua Dierolf and Dr. Tyler Cooper for your friendship over the past years.

I would like to thank my supervisor Dr. Gregory Kelly for his guidance and mentorship over the past seven years. From learning to design better experiments, to writing my first manuscript, I learned so much from Dr. Kelly that cannot be shown in the writing and defense of a doctoral thesis. I am so glad to say I did my training in the Kelly lab, and I look forward to many years as friends and colleagues to come.

I would like to thank my parents, Ian and Kimberly Spice for your love and support throughout all my academic pursuits. Finally, I would like to thank my partner, Kyle Knight. Kyle's love and unwavering support allowed me to put as much into this degree as I could, and I will never be able to describe how much his love made all this possible.

# Table of Contents

Abstract.....	ii
Summary for Lay Audience.....	iii
Co-Authorship Statement.....	iv
Acknowledgments.....	v
Table of Contents.....	vi
List of Tables.....	x
List of Figures.....	xi
List of Abbreviations.....	xiv
Chapter 1.....	1
1 Introduction.....	1
1.1 Overview.....	1
1.2 Vertebrate neural development.....	3
1.3 Protein signaling pathways in neural differentiation.....	9
1.3.1 Hedgehog signaling in neural differentiation.....	9
1.3.2 Wnt signaling in neural differentiation.....	18
1.3.3 Other signaling pathways involved in neural differentiation.....	23
1.4 In vitro models of neural differentiation.....	31
1.4.1 Embryonal carcinoma cell models of neural differentiation.....	31
1.5 Never in mitosis kinase 2 and development.....	33
1.6 Hypothesis, Study Aims & Key Findings.....	35
1.6.1 Hypothesis.....	35
1.6.2 Study Aims & Key Findings.....	35
1.7 References.....	36
Chapter 2.....	74

2	Suppressor of Fused regulation of Hedgehog Signaling is Required for Proper Astrocyte Differentiation .....	74
2.1	Introduction.....	75
2.2	Materials and Methods.....	77
2.2.1	Cell culture & Differentiation.....	77
2.2.2	Cas9 plasmid preparation.....	77
2.2.3	Knockout lines .....	77
2.2.4	Overexpression lines.....	78
2.2.5	Real-time reverse transcriptase PCR .....	78
2.2.6	Immunoblot Analysis.....	79
2.2.7	Immunofluorescence.....	80
2.2.8	Flow Cytometry .....	80
2.3	Results.....	83
2.3.1	Retinoic acid and cell aggregation induces P19 neural differentiation.....	83
2.3.2	Hh signaling is activated early in neural differentiation.....	85
2.3.3	Early Hh signaling is required but not sufficient for neural differentiation .....	87
2.3.4	SUFU levels during neural differentiation.....	91
2.3.5	Sufu knockout activates Hedgehog signaling .....	93
2.3.6	Sufu loss activates Hh signaling through loss of Gli3 .....	98
2.3.7	Sufu knockout delays and decreases the astrocyte cell fate.....	101
2.3.8	<i>Sufu</i> or <i>Gli3</i> overexpression partially rescues astrocyte phenotype.....	107
2.4	Discussion.....	110
2.5	References.....	114
	Chapter 3.....	121
3	Never in Mitosis Kinase 2 regulation of metabolism is required for neural differentiation.....	121

3.1	Introduction.....	122
3.2	Materials and Methods.....	124
3.2.1	Cell Culture.....	124
3.2.2	Preparing CRISPR plasmids.....	124
3.2.3	Generating Nek2 deficient cell lines.....	125
3.2.4	Generating Nek2 Overexpression Cell Line.....	126
3.2.5	RT-qPCR.....	126
3.2.6	Immunoblotting.....	127
3.2.7	Immunofluorescence and Phase Contrast Imaging.....	128
3.2.8	Cell Count and Viability Assays.....	128
3.2.9	Caspase 3 Activity Assay.....	129
3.2.10	Luciferase Assay.....	129
3.2.11	LC-Mass Spectrometry.....	130
3.2.12	Statistical Analysis.....	132
3.3	Results.....	132
3.3.1	Nek2 levels are unchanged during neural differentiation.....	132
3.3.2	Nek2 regulates cell proliferation in undifferentiated cells.....	135
3.3.3	Nek2 promotes exit from pluripotency.....	143
3.3.4	Nek2 is required for neural differentiation.....	146
3.3.5	Nek2 loss and overexpression alters Hh signalling.....	150
3.3.6	Nek2 loss and overexpression alters Wnt signalling.....	153
3.3.7	Proteomic analysis identifies several differentially abundant proteins in Nek2 deficient cells.....	158
3.3.8	Loss of Nek2 promotes glycolytic metabolism.....	163
3.4	Discussion.....	164
3.5	References.....	167



Chapter 4.....	173
4 Discussion & Conclusions .....	173
4.1 Summary of Key Findings .....	173
4.2 Discussion & Significance .....	177
4.2.1 Stem cell models of neural differentiation.....	177
4.2.2 SUFU is required to regulate Hh signaling during astrocyte differentiation .....	178
4.2.3 Nek2 regulates metabolism during neural specification.....	181
4.3 Limitations & Future Directions.....	183
4.4 References.....	186
Curriculum Vitae .....	195

## List of Tables

Table 2-1: gRNA and primer sequences for CRISPR-Cas9 editing of Sufu gene.....	78
Table 2-2: RT-qPCR Primers List .....	79
Table 3-1: CRISPR-Cas9 gRNAs, primers for gRNA amplification and PCR around the cut site.....	125
Table 3-2: Primers used for RT-qPCR.....	127
Table 3-3: Q Exactive Settings for Data Acquisition .....	131

# List of Figures

Figure 1-1: Developmental Origins of Neural Cell Types.....	2
Figure 1-2: Neural tube folding .....	6
Figure 1-3: Hedgehog Signaling.....	10
Figure 1-4: Hedgehog ligand modifications .....	12
Figure 1-5: Wnt Signaling .....	22
Figure 1-6: Notch Signaling.....	24
Figure 1-7: FGF Signaling.....	27
Figure 1-8: Retinoic Acid Signaling.....	30
Figure 2-1: Flow cytometry gating strategy of P19 cells.....	82
Figure 2-2: Retinoic acid is required for P19 cell neural differentiation .....	84
Figure 2-3: Hh signaling is activated early in RA-induced differentiation .....	86
Figure 2-4: Early Hh pathway activation is required but not sufficient to induce neural lineages .....	89
Figure 2-5: DMSO alone and DMSO plus RA treatment is sufficient to induce neurons but not astrocytes .....	90
Figure 2-6: SUFU levels do not change during RA-induced neural differentiation.....	92
Figure 2-7: CRISPR-Cas9 knock out of <i>Sufu</i> activates Hh signaling in undifferentiated P19 cells .....	94
Figure 2-8: TIDE analysis of <i>Sufu</i> <sup>-/-</sup> clone (KO#2).....	95
Figure 2-9: CRISPR-Cas9 plasmid transfection and selection do not affect SUFU levels or P19 cell differentiation.....	97

Figure 2-10: <i>Sufu</i> <sup>-/-</sup> #2 maintains increased Hh signaling and causes the loss of Gli3 .....	99
Figure 2-11: <i>Sufu</i> <sup>-/-</sup> #1 maintains increased Hh signaling and causes the loss of Gli3 .....	100
Figure 2-12: <i>Sufu</i> <sup>-/-</sup> delays astrocyte formation without affecting neuron differentiation ....	102
Figure 2-13: <i>Sufu</i> <sup>-/-</sup> decreases astrocyte differentiation .....	105
Figure 2-14: pSUFU and pGli3 overexpression induces Chicken Sufu expression and rescued detection of Gli3 .....	108
Figure 2-15: <i>Sufu</i> or <i>Gli3</i> overexpression partially rescues the <i>Sufu</i> <sup>-/-</sup> phenotype.....	109
Figure 3-1: Nek2 gene expression does not change throughout RA-induced neural differentiation.....	133
Figure 3-2: Nek2 levels do not change during neural differentiation.....	134
Figure 3-3: Allele summary of NEK2 deficient cells .....	136
Figure 3-4: Altering Nek2 levels changes proliferation rate of undifferentiated cells .....	138
Figure 3-5: Nek2 deficiency inhibits proliferation without affecting apoptosis.....	140
Figure 3-6: Altering Nek2 levels alters embryoid body development and organization .....	141
Figure 3-7: Nek2 promotes exit from pluripotency .....	144
Figure 3-8: Nek2 is required for neural differentiation .....	147
Figure 3-9: NEK2 knockdown blocks differentiation of neurons and astrocytes.....	149
Figure 3-10: Hh and Wnt signaling are perturbed in Nek2 deficient and overexpressing cells .....	151
Figure 3-11: Hh signaling is affected by perturbed Nek2 levels .....	152
Figure 3-12: Wnt signaling is affected by perturbed Nek2 levels .....	154

Figure 3-13: Wnt is required for neural differentiation but is only sufficient to induce neurons ..... 156

Figure 3-14: LC-MS workflow and results of WT and KO cells ..... 159

Figure 3-15: Loss of Nek2 inhibits oxidative metabolism..... 161

Figure 4-1: Model for the role of SUFU and Nek2 in P19 neural differentiation ..... 176

## List of Abbreviations

2-DG – 2-deoxy-D-glucose

$\beta$ -TrCP –  $\beta$ -transducin repeats-containing proteins

APC – Adenomatous polyposis coli

BIO – 6-bromoindirubin-3'-oxime

BMP – Bone Morphogenic Protein

BOC – Brother of CDO

cAMP – Cyclic adenosine 3', 5'-monophosphate

CDO – Cell Adhesion Molecule-related/down regulated by oncogenes

CK1/2 – Casein kinase 1/2

CNS – Central nervous system

Cyc – Cyclopamine

Dab2 – Disabled-2

DHH – Desert Hedgehog

Disp – Dispatched

Dkk1 – Dickkopf-1

Dvl – Disheveled

ER – Endoplasmic Reticulum

ESC – Embryonic stem cell

EVC - Ellis-van Creveld protein

FGF – Fibroblast Growth Factor

FGFR – FGF receptor

FRS2 – FGFR substrate 2

Fzd – Frizzled

GAS1 – Growth Arrest Specific 1

GRB2 – Guanine nucleotide exchange factor 2

GSK3 $\beta$  – Glycogen synthase kinase 3 $\beta$

Grk2 – G-protein coupled receptor kinase 2

hESC – human embryonic stem cell

Hh - Hedgehog

Hhat – Hedgehog Acyltransferase

Hip1 – Hedgehog Interacting Protein 1

IFT – Intraflagellar Transport Proteins

IHH – Indian Hedgehog

Kif – Kinesin Family Member

LEF – Leukemia Inhibitory Factor

LRP – Low Density Lipoprotein-Related Protein

LIF – Leukemia Inhibitory Factor

MAPK – Mitogen-activated protein kinase (also known as ERK)

MAPKK – Mitogen activated protein kinase kinase (also known as MEK)

MAPKKK – Mitogen-activated protein kinase kinase kinase (also known as Raf)

mESC – Mouse embryonic stem cell

N-SHH – N-terminal cleaved Sonic Hedgehog

NEK2 – Never in Mitosis Kinase 2

NSC – Neural Stem Cell

OxPhos – Oxidative Phosphorylation

PI3K/AKT – Phosphatidylinositol-3 Kinase

PKA – cAMP dependent Protein Kinase A

Ptch – Patched

PCP – Planar Cell Polarity

Porc – Porcupine

RA – Retinoic Acid

RALDH2 – Retinaldehyde Dehydrogenase 2

RAR – Retinoic acid receptor

RARE – RA response element

RXR – Retinoid X receptor

OPC – Oligodendrocyte precursor cell

SAG – Smoothed Agonist

SAP18 – Sin3A Associated Protein 18

SHH – Sonic Hedgehog



SMO – Smoothened

SPOP – Speckle type BTB/POZ protein

SUFU – Suppressor of Fused

TCF – T cell Factor

Wls – Wntless

# Chapter 1

## 1 Introduction

In this chapter I describe what is known and what remains to be explored within the field of mouse neural differentiation. As a field, mouse neurobiology is vast and encompasses the establishment of neural structures like the spinal cord and brain during embryogenesis all the way to replenishing neural cells in the adult brain. Given this large scope, I have focused my thesis within neural cell type differentiation during embryogenesis.

### 1.1 Overview

Embryogenesis is a highly complex process that allows a single cell, known as the zygote, to become an entire animal. This tightly regulated process of cell division, self-renewal and differentiation is at the core of the fields of development and stem cell biology. In particular, the process of neural development relies heavily on the stem cell field to tease apart the intricate protein interactions and genes required for the establishment of neural cell types. The main classes of cells that exist in the central nervous system (CNS) are neurons, astrocytes, oligodendrocytes, and microglia (Figure 1-1). Neural cells, including neurons, astrocytes and oligodendrocytes derive from the ectodermal lineage from a similar pool of neuroepithelial progenitor cells (Bradl 2006). Neurons are cells that send electrical signals allowing for thoughts, memories, and movement. Astrocytes form the blood-brain barrier and are vital in providing neurons with necessary metabolites to function (Mason 2017), regulating synapse formation and neurotransmitter release from neurons and in neurotransmitter reuptake (Chung et al. 2015). Oligodendrocytes act by increasing the speed of neuron electrical impulses (Nave and Werner 2014), regulating neuron metabolism and glucose import along axons (Lee et al. 2012; Saab et al. 2016), and are required for information processing (Moore et al. 2020). Finally, are the microglia that act as the immune system in the brain and are derived from primitive macrophages of the yolk sac rather than ectodermal lineages of the embryo (Nayak et al. 2014). In mammals, the establishment of neural cell types begins during neurulation, the process by which the CNS structures take shape, establish

the boundaries of various neuron subtypes, and begins the differentiation of glial cells: astrocytes, and oligodendrocytes.

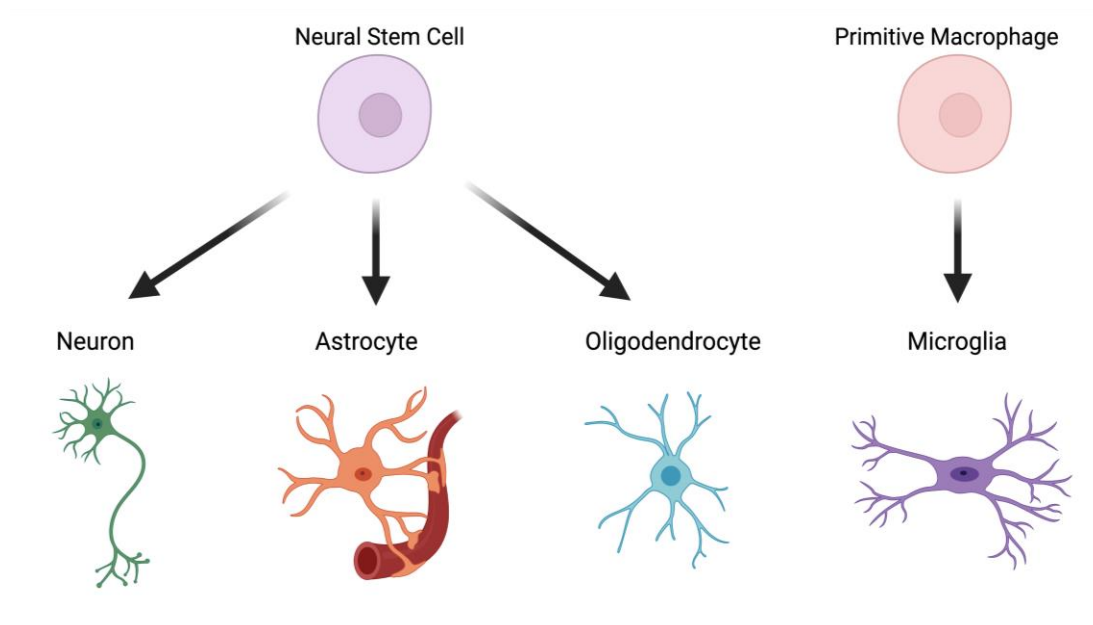


**Figure 1-1: Developmental Origins of Neural Cell Types**

Neural ectoderm cells given the proper cues will develop into neural stem cells, which then become either neurons, astrocytes, or oligodendrocytes. Microglia, although existing in the brain are not “neural” and are not derived from the same precursor population, are instead derived from primitive macrophages of the yolk sac that migrate into the CNS during embryogenesis.

Neurons, astrocytes, and oligodendrocytes originate from a single pool of cells known as neural stem cells (NSC) (Vieira et al. 2018). Stem cells, in general, are any cell that can give rise to themselves, or they can give rise to something new or different. When NSCs are provided with specific information during neurulation, and throughout nervous system development, they will become one of these specific cell types. This process, referred to as differentiation, is defined as the commitment of a cell toward a particular cell type. However, the “how” and the “when” NSCs should differentiate towards each lineage is complex and not fully understood. Given the complexity of the embryo, many researchers have relied on stem cells and their related models to explore the precise molecular mechanisms involved in regulating the differentiation of these neural cell types. Becoming a particular cell type during differentiation is dependent on the genes that the individual cells express. For instance, a neuron will express neuron-specific genes while an astrocyte will express astrocyte-specific genes.

Given neurons and astrocytes originate from a pool of progenitor cells (Vieira et al. 2018), understanding how different regulatory processes and the accompanying proteins are involved in this process is vitally important. In this thesis I will present work that seeks to address some of these unknowns in the cell fate determination of neurons and astrocytes. Towards that end, I will show how specific proteins, including the Suppressor of Fused (SUFU) and Never in Mitosis Kinase 2 (Nek2), are required in the process and will present new connections between protein signaling pathways and neural differentiation.

## 1.2 Vertebrate neural development

The development of nervous system tissue is a highly coordinated and complex process that requires input from multiple cell types and extracellular signals. In vertebrates this neurulation occurs immediately after gastrulation; the process that establishes the three germ layers: endoderm, mesoderm, and ectoderm. In vertebrates, neurulation is initiated from a flat sheet of cells dorsal to the notochord, a mesodermal structure that is essential in determining the longitudinal axis of the mammalian embryo (Placzek et al. 1990). In

most vertebrates, primary neurulation factors secreted from the notochord induce the dorsal sheet to form the floor plate and together these structures instruct the dorsal ectoderm to fold into the neural tube (Gallera 1971). Deletion and transplantation experiments in *Xenopus* and chick embryos demonstrate that the notochord is required to initiate neurulation, where the presence of two notochords causes the formation of two floor plates (van Straaten et al. 1985, 1988; Placzek et al. 1990; Yamada et al. 1991) while the absence of a notochord results in no floor plate formation and no neurulation (Smith and Schoenwolf 1989; Placzek et al. 1990). While these experiments were conducted in non-mammalian models, evidence shows that primary neurulation in mammals is equivalent in reptiles and amphibians (Gallera 1971). Despite these similarities, a more recent study in human embryos shows the location of neurulation initiation begins in the middle of the rostral-caudal axis (de Bree et al. 2018). In this study, neurulation occurred in both directions (de Bree et al. 2018) rather than starting rostrally and moving towards the caudal end of the embryo as has been reported for mouse and chicken (Gallera 1971; Nievelstein et al. 1993). Although there are minor differences between animal species, transplantation experiments in chick highlight that the process of neural ectoderm induction occurs non-cell autonomously (van Straaten et al. 1985, 1988; Placzek et al. 1990; Yamada et al. 1991). Thus, cells must be conducted towards the correct ectodermal cell lineage based on extrinsic signals from the underlying mesoderm.

Many studies have shown that after the initiation of the floor plate, the dorsal ectoderm folds to form the neural tube (Figure 1-2). To facilitate this, cells at the medial and dorsolateral hinge points must restrict their apical surface and expand their basal surface (Smith and Schoenwolf 1989). Thus, cytoskeletal rearrangements are required for neural tube folding (Burnside 1973; Rolo et al. 2018), as genetic (Chen et al. 1996; Lesko et al. 2021) and chemical inhibition (Karfunkel 1972) studies involving cytoskeleton polymerization inhibit neural tube closure. Regulation of cytoskeleton dynamics through the Wnt planar cell polarity (PCP) pathway are also vital for neural tube folding as mutations in this and other pathway components lead to neural tube folding defects (Kibar et al. 2001; Murdoch et al. 2001; Hamblet et al. 2002; Wang et al. 2006a, 2006b). Closure of the neural tube occurs when the neural folds come together and neural crest

cells “escape” from the neural tube and give rise to many structures in the face, skull, and the peripheral nervous system (Golden and Chernoff 1993). In mice and humans, unlike in birds, there are multiple sites of initiation of neural tube closure along the rostral-caudal axis (Golden and Chernoff 1993; Van Allen et al. 1993), and a failure in closure results in multiple developmental diseases including non-lethal spina bifida, and lethal anencephaly (Van Allen et al. 1993; Juriloff and Harris 2000).

Signals essential for neural tube formation include members of the Fibroblast Growth Factor (FGF), Hedgehog (Hh), Bone morphogenic protein (BMP), Notch/Delta families and retinoic acid (RA). FGF is secreted from cells of the neural tube organizer that demarcate the location of the caudal stem zone, as it moves along the rostral-caudal axis (Mathis et al. 2001; del Corral et al. 2002). As cells move through and exit the organizer, they stop expressing *Fgf8* allowing them to become notochord and floor plate (del Corral et al. 2002). Notch/Delta signaling is important in the formation of floor plate versus notochord as these cells exit the organizer, where active Notch signaling induces floor plate specification (López et al. 2003; Gray and Dale 2010; Stasiulewicz et al. 2015). The notochord secretes Sonic Hedgehog (SHH) which can also induce floor plate formation that, in turn, also secretes SHH into the developing neural fold (Yamada et al. 1991; Echelard et al. 1993; Krauss et al. 1993). Although SHH is secreted from the notochord, *Shh* expression is only required for notochord maintenance after induction, as *Shh*<sup>-/-</sup> mice can form a notochord but the structure is lost as the organizer moves caudally over time (Chiang et al. 1996). These experiments did, however, show that *Shh* is required for floor plate induction as no floor plate is observed in mice lacking *Shh* (Chiang et al. 1996) or in mice treated with antibodies blocking SHH activity (Ericson et al. 1996). SHH secretion establishes a morphogen gradient along the dorsal-ventral axis that is essential in the development of ventrally located motor and interneurons (Ericson et al. 1996, 1997). Despite *Shh* being absolutely required for motor neuron differentiation, some adjacent classes of interneurons along the dorsal-ventral axis form in the *Shh*<sup>-/-</sup> mouse (Litingtung and Chiang 2000). The role of *Shh* in the dorsal-ventral axis was primarily observed by the expression of *Shh* target genes or by immunostaining of fixed tissues (Gritli-Linde et al. 2001; Huang et al. 2007) and was not until the use of GFP-tagged SHH, was the ligand confirmed to be within the neural pore (Chamberlain et al. 2008).

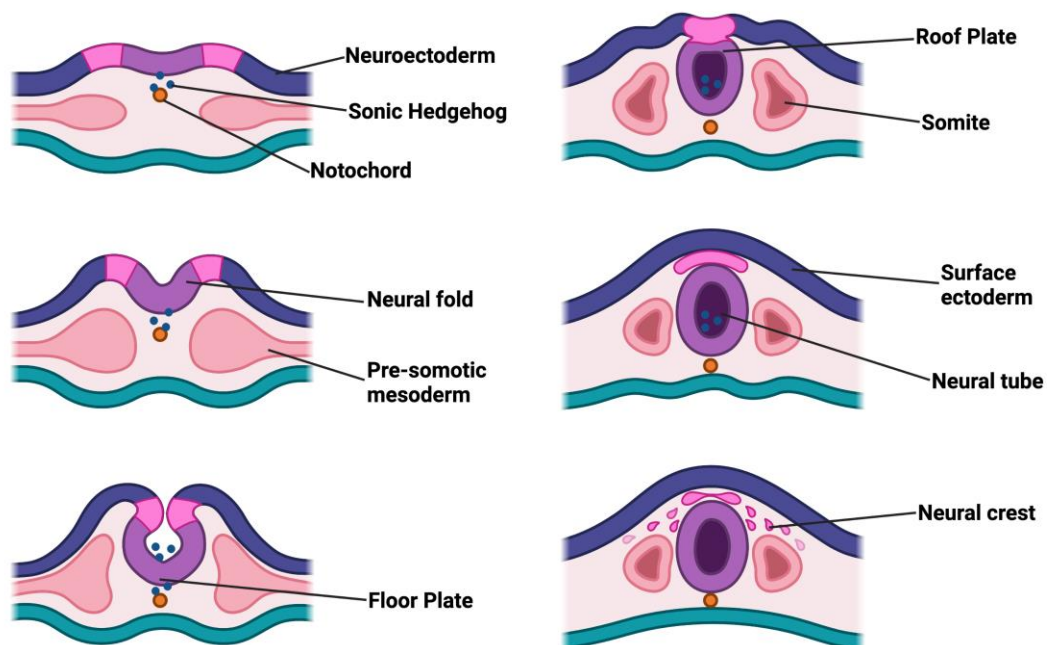


**Figure 1-2: Neural tube folding**

The notochord secretes SHH to induce the induction of the floor plate and the formation of the neural fold. Dorso-lateral hinge points cause opposing sides of the neural fold to come together to form the roof plate. BMP from the roof plate and SHH from the floor plate establish the dorsal-ventral axis creating distinct regions of motor neurons, interneurons, and sensory neurons. These regions are fine-tuned by the secretion of RA from somites. After roof plate formation the surface ectoderm detaches from the neural ectoderm as newly formed neural crest cells begin to migrate. Image created with Biorender.com.

Dorsally secreted BMP is in opposition to ventrally secreted SHH. The dorsal ectoderm secretes BMP as the neural folds come together from opposing sides to form the roof plate (Basler et al. 1993; Liem et al. 1995), where BMPs are essential in establishing dorsal sensory neurons and interneurons (Lee et al. 1998, 2000; Millonig et al. 2000). Loss of BMP family members (Lee et al. 1998, 2000), the inhibition of BMP by secreted antagonists (Chesnutt et al. 2004) and/or the loss of BMP receptors (Wine-Lee et al. 2004) results in the loss of dorsal-most sensory and interneurons. In contrast, BMP overexpression expands dorsal interneuron regions (Panchision et al. 2001; Timmer et al. 2002). BMP is also required to induce expression of canonical Wnt ligands 1 and 3 (Parr et al. 1993; Wine-Lee et al. 2004) allowing for fine-tuning of dorsal interneuron populations (Muroyama et al., 2002) and to expand the number of dorsal interneuron progenitors (Ikeya et al. 1997; Chesnutt et al. 2004). Fine-tuning of neuron populations is controlled dorsally through Wnt expression but is primarily through the secretion of RA from the paraxial, or somitic mesoderm (Maden et al. 1998; Berggren et al. 1999; del Corral et al. 2002; Molotkova et al. 2005). In support, embryos lacking RA or the RA producing enzyme RALDH2 have abnormal neural tubes, particularly lacking dorsal regions, and show decreased neuron differentiation (del Corral et al. 2003; Wilson et al. 2003, 2004; Molotkova et al. 2005). Removing RA from the developing neural tube also reduces *Bmp4*, *Bmp7*, *Wnt1* and *Wnt3a* expression, coinciding with the loss of dorsal neural cell fates and highlighting the vital role of RA in dorsal patterning (Wilson et al. 2004). Conversely, ventral neuron regions are expanded in the RA-deficient embryo, thus RA antagonizes ventral cell fates (Wilson et al. 2004). The distance of cells from the SHH or BMP source determines their responsiveness to RA, determines their gene expression profiles and interneuron cell fates. For example, ventral SHH induces the expression of the ventral interneuron transcription factor *Nkx2.2*, while RA induces the expression of *Pax6*, a transcription factor that inhibits *Nkx2.2* expression (Wilson et al. 2004; Schäfer et al. 2005). The interactions, both positively and negatively, between these signaling pathways and their downstream targets create gene regulatory networks that allows for the formation of very specific regions of neuron cell identity.

Not only is the specificity of neuron cell fate instructed by these signals along the dorsal-ventral axis, but it also exists along the rostral-caudal axis. This is particularly important



for motor neuron populations that have different developmental requirements along the trunk of the developing embryo. FGF and RA are used again along the rostral caudal axis to induce the expression of *Hox* genes (Liu et al. 2001; Bel-Vialar et al. 2002). Thus, the determination of distinct neural tube populations along multiple axes is a complex interaction of morphogen gradients that not only establishes these cell type regions, but also are involved in the differentiation of distinct cell fates.

## 1.3 Protein signaling pathways in neural differentiation

### 1.3.1 Hedgehog signaling in neural differentiation

Hedgehog (Hh) signaling (Figure 1-3), as described in Section 1.2, is important in the dorsal-ventral patterning of the vertebrate neural tube but also, in the anterior-posterior patterning of the vertebrate limb (Riddle et al. 1993; López-Martínez et al. 1995), the medial-proximal axis of the developing face (Hu and Helms 1999; Dworkin et al. 2016) and in determining neural cell identity (Ericson et al. 1996, 1997; Belgacem et al. 2016; Brady and Vaccarino 2021; Yang et al. 2021). The pathway begins following the secretion of a Hh ligand, either Indian Hedgehog (IHH), Desert Hedgehog (DHH) or SHH. IHH is involved in bone development and hematopoiesis (St-Jacques et al. 1999; Dyer et al. 2001), whereas DHH is involved in male germline development (Bitgood et al. 1996; Clark et al. 2000). SHH, as indicated above, is the ligand involved in neural development (Ericson et al. 1996, 1997; Belgacem et al. 2016; Brady and Vaccarino 2021; Yang et al. 2021) and despite it being the ligand reported *in vivo*, some *in vitro* studies have shown increased expression of all three ligands with neural induction (Wu et al. 2010; Spice et al. 2022b).

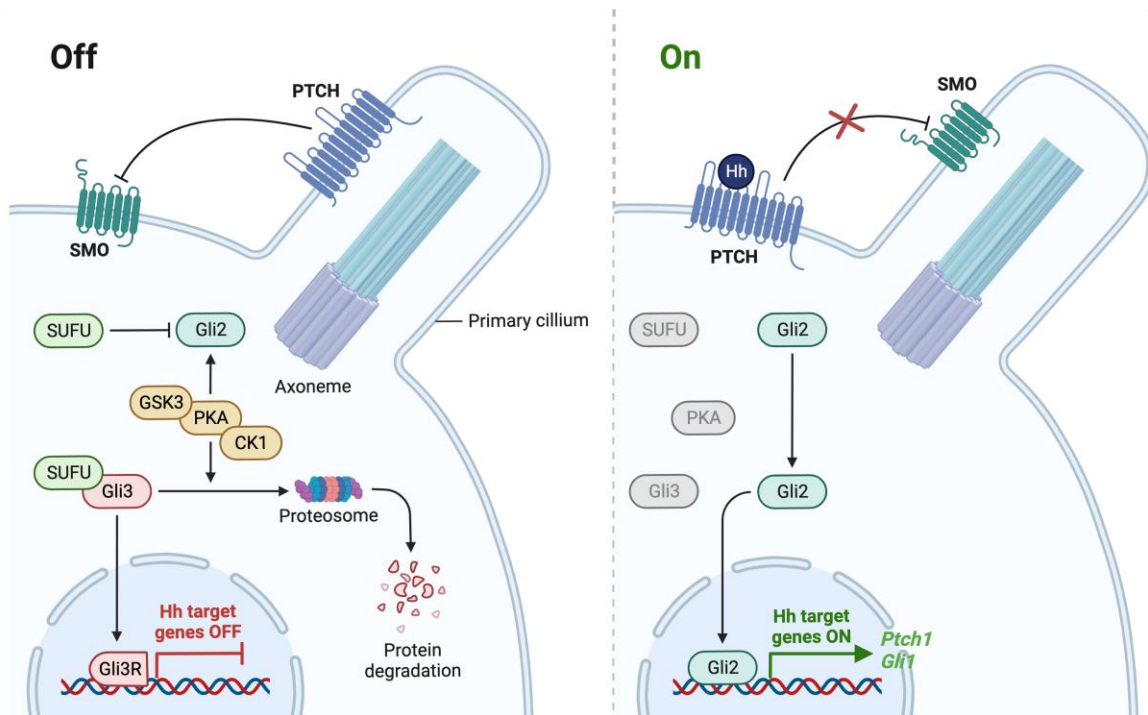


**Figure 1-3: Hedgehog Signaling**

In the absence of a Hh ligand, the Ptch receptor blocks the translocation of Smo into the primary cilium. The negative regulator of signaling, SUFU either sequesters full-length Gli2 in the cytoplasm or promotes the phosphorylation of Gli3 by PKA, GSK3 and CK1. Phosphorylated Gli3 is ubiquitinated and partially degraded by the proteasome to form a transcriptional repressor (Gli3R) to block target gene transcription. Gli3R blocks transcription as partial degradation removes the transactivation domain observed in full-length Glis leaving only its repressor domain active (Hui and Angers 2011). The presence of a Hh ligand inhibits Ptch removing it from the plasma membrane, allowing Smo into the primary cilium, which causes SUFU to dissociate from full-length Gli. Following this, Gli translocates to the nucleus and activates the transcription of target genes like *Ptch1* and *Gli1*. Image created with Biorender.com with reference to (Briscoe and Théron 2013).

Before being secreted Hh ligands must undergo post-translational modifications to be fully functional (Lee et al. 1994; Pepinsky et al. 1998; Taylor et al. 2001). Hh enters the endoplasmic reticulum (ER) and the immature ligand undergoes autoproteolytic cleavage where a cholesterol group is added and the C-terminal end of the protein is removed (Figure 1-4) (Lee et al. 1994; Ekker et al. 1995; Porter et al. 1995, 1996; Chen et al. 2011a). The C-terminal end of SHH is transported out of the ER and is degraded by the proteasome (Chen et al. 2011a), whereas the cholesterol modified N-terminus (N-SHH) is the active form of the protein. This cleavage is required as mutations in the processing region of Hh causes reduced neural induction (Lai et al. 1995) and holoprosencephaly, a failure of the forebrain to divide during brain development (Roessler et al. 1996, 2009; Traiffort et al. 2004; Maity et al. 2005). This active form is found in the neural tube and induces neuron differentiation (Fan et al. 1995; Hynes et al. 1995; Lai et al. 1995; Marti et al. 1995; Porter et al. 1995; Roelink et al. 1995). The lipidation on the C-terminal end of N-SHH, is accompanied by modification of the N-terminus with palmitic acid (Pepinsky et al. 1998). This second lipid addition is essential for function, as the non-lipidated form of the protein has an approximately 160-fold decrease in pathway activity compared to the palmitoylated version (Taylor et al. 2001; Maity et al. 2005). Palmitoylation occurs by Skinny Hedgehog or rasp in *Drosophila* (Chamoun et al. 2001; Micchelli et al. 2002), or Hedgehog acyltransferase (Hhat) in mammals (Buglino and Resh 2008, 2010). The site of modification occurs in the ER (Konitsiotis et al. 2015), and this modification is required for enhancing the activity of the ligand on receiving cells, its stabilization after secretion and its ability to form soluble multimers (Gallet et al. 2003; Chen et al. 2004; Peters et al. 2004; Callejo et al. 2006; Goetz et al. 2006; Grover et al. 2011). In mouse embryos, Hhat loss of function causes reduced SHH activity, corresponding to loss of floor plate and interneuron populations and holoprosencephaly (Dennis et al. 2012; Iulianella et al. 2018). Interestingly, the loss of floor plate and interneuron populations in Hhat loss of function embryos is rescued by mutations in the Patched (Ptch) receptor (Iulianella et al. 2018).

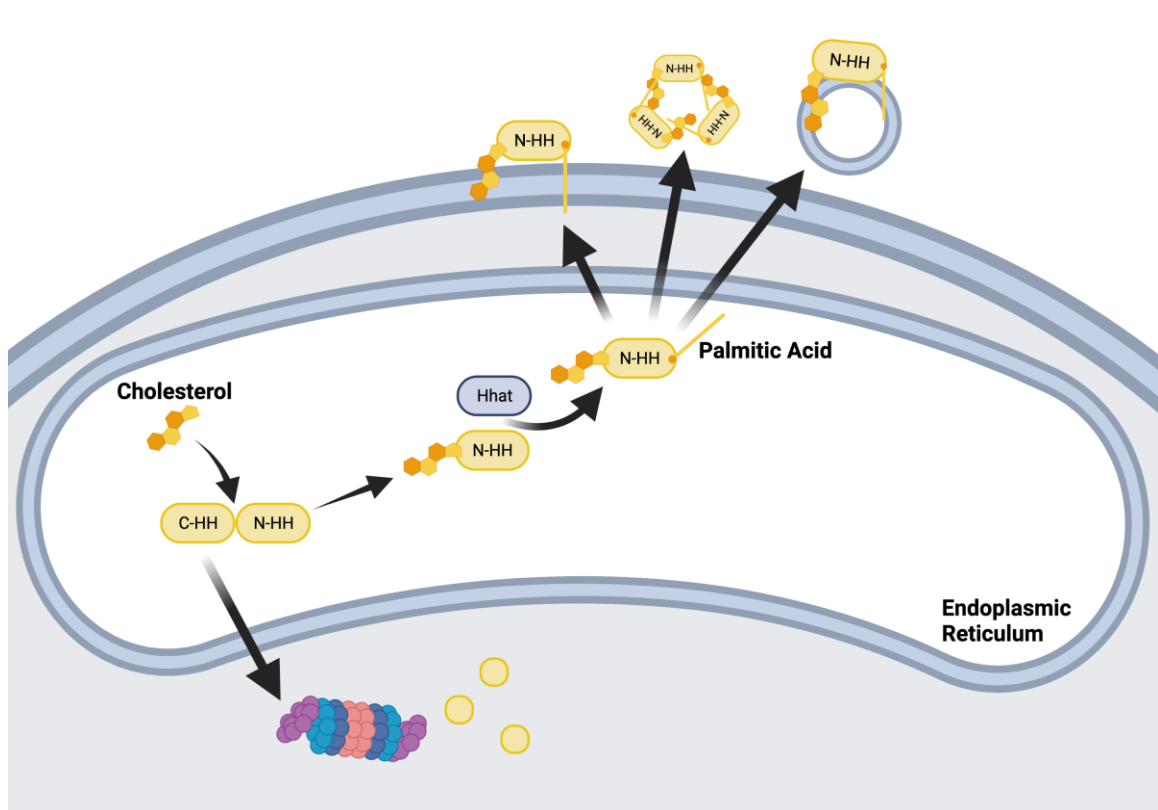


**Figure 1-4: Hedgehog ligand modifications**

In the endoplasmic reticulum, cholesterol causes the autoprolytic cleavage of the C-terminal end of the HH protein before Hedgehog acyltransferase (Hhat) adds a palmitic acid to the N-terminal end. This lipid-modified and cleave ligand is then prepared for secretion through multiple mechanisms including being incorporated into the cell surface, being packaged into multi-protein particles, and being excreted on the surface of exosomes. Image created using Biorender.com with reference to (Briscoe and Théron 2013).

Secreted SHH also requires the membrane protein Dispatched (Ma et al. 2002), which recognizes the cholesterol modification and transfers N-SHH to the secreted protein SCUBE2, shielding the cholesterol from the aqueous environment of the extracellular space (Creanga et al. 2012; Tukachinsky et al. 2012). Following secretion and diffusion, cells respond when SHH binds to its receptor Ptch (Ingham et al. 1991; Marigo et al. 1996; Stone et al. 1996), where Ptch inhibits Smo in the absence of ligand (Chen and Struhl 1996; Taipale et al. 2002), participates in limiting Hh diffusion (Chen and Struhl 1996; Briscoe et al. 2001) and together with the Hh co-receptor, Hedgehog interacting protein (Hip), bind the Hh ligand (Chuang et al. 2003). However, the Ptch-Hip1 interaction is not essential for neural development as *Hip1* loss of function mice have normal neural tubes (Chuang et al. 2003). Other receptors of SHH include CDO, BOC, GAS1, various glypicans and LRP2 (Tenzen et al. 2006; Allen et al. 2007; Yan and Lin 2009; Christ et al. 2012). Glypicans can promote or inhibit Hh activity (Yan and Lin 2009; Williams et al. 2010) whereas LRP2 promotes Hh transduction and is required to transduce Hh signaling in the developing mouse forebrain (Christ et al. 2012). CDO, BOC and GAS1, unlike Ptch, promote Hh signal transduction (Tenzen et al. 2006; Allen et al. 2007) and all three are required in the neural tube as triple knockout embryos show complete loss of ventral neurons (Allen et al. 2011). In vertebrates there are two Ptch paralogues, Ptch1 and Ptch2, both of which are Hh target genes and participate in a negative feedback loop to sequester Hh after pathway activation (Chen and Struhl 1996; Concordet et al. 1996; Goodrich et al. 1996, 1999; Hepker et al. 1997). Ptch activity is required for neural development and its loss of function leads to neural tube closure defects (Goodrich et al. 1997). Ptch overexpression also causes embryonic or early postnatal lethality with an expansion of dorsal interneuron populations and neural tube closure defects (Goodrich et al. 1999).

Suppressor of Fused (SUFU), a focus of the presented work, is a negative regulator of Hh. SUFU acts by either sequestering full length Glis in the cytoplasm, thus inhibiting their nuclear translocation, or promotes their conversion to a transcriptional repressor (Chen et al. 2009; Humke et al. 2010). When Hh is present the SUFU-Gli complex is recruited into the primary cilium where SUFU dissociates from the full-length form of the Gli activator (Haycraft et al. 2005; Humke et al. 2010; Tukachinsky et al. 2010; Chen

et al. 2011c). Kinesin-like family members are involved in this activation as the EVC/EVC2 proteins bind Smo and this complex recruits the microtubule motor protein Kif7 in the primary cilium (Yang et al. 2012). Other intraflagellar transport proteins (IFTs) (Haycraft et al. 2005) are involved as the dissociation of SUFU from Gli3 and the activation of the latter is also dependent on the IFT, Kif3a (Humke et al. 2010). Recruitment of Kif7 may be the key connection between Smo and SUFU as reducing the amount of SUFU restores the lost Hh activity and floor plate development observed in the *Kif7*<sup>-/-</sup> embryo (Law et al. 2012). The loss of function of IFT88 in the midbrain of the E9.0 mouse embryo also causes a complete loss of Hh activity and reduced dopaminergic neuron differentiation like *Gli2*<sup>-/-</sup>/*Gli3*<sup>-/-</sup> double mutants (Gazea et al. 2016).

Smo transduction of the Hh signal does not solely rely on IFT proteins, as cAMP-dependent Protein Kinase A (PKA) and casein kinase 2 (CK2) in *Drosophila* (Jia et al. 2010; Li et al. 2014), and casein kinase 1 (CK1) and GPCR kinase 2 (Grk2) in vertebrates (Chen et al. 2011b) also play a key role. For instance, Smo mutations that simulate constitutive phosphorylation of its cytoplasmic tail is sufficient to expand ventral neuron regions in the chick neural tube (Chen et al. 2011b). Grk2 is known to promote neurogenesis in the PC12 model of neuron differentiation, however, the link between Grk2 and Hh signaling was not explored in this study (Karkoulas et al. 2020). Some evidence also points to the role of CK2 and mouse neural development, where *CK2*<sup>-/-</sup> mutants have open neural tubes (Lou et al. 2008; Dominguez et al. 2011). However, these reports, like that with Grk2, have not made the connection between neural development and Hh signaling. Some of these kinases also play an essential role in regulating SUFU and Gli proteins downstream of Smo. PKA and glycogen synthase kinase 3 $\beta$  (GSK3 $\beta$ ) phosphorylate and stabilize SUFU (Chen et al. 2011c) where protein phosphatase 4 dephosphorylates SUFU in response to SHH (Liao et al. 2020). Studies have found that active Hh signaling targets SUFU for proteasomal degradation (Yue et al. 2009), however, we have found no changes in SUFU levels during neuron differentiation despite active Hh signaling (Chapter 2) (Spice et al. 2022b). Likewise, others have shown that SUFU is required for maximal Hh pathway activation in developing ventral neuron identities in the neural tube (Zhang et al. 2017). In fact, SUFU is essential during neural

tube development, as *Sufu*<sup>-/-</sup> embryos are embryonic lethal due to heart and neural tube closure defects (Cooper et al. 2005). In addition, loss of SUFU function decreases retinal neuron differentiation (Cwinn et al. 2011), reduces and delays cerebellar neuron differentiation (Kim et al. 2018) and is critical in timing the differentiation of projection neurons in the mammalian neocortex (Yabut et al. 2015). SUFU also reduces and delays astrocyte differentiation *in vitro* (Chapter 2) (Spice et al. 2022b) and is required for oligodendrocyte differentiation in the mouse forebrain (Winkler et al. 2018). These defects all support the fact that SUFU primarily acts as a negative regulator of Hh signaling as SUFU-deficient cells and embryos show constitutive expression of Hh target genes (Cooper et al. 2005; Svärd et al. 2006; Chen et al. 2009; Wu et al. 2010; Hoelzl et al. 2015, 2017; Yabut et al. 2015; Urman et al. 2016; Spice et al. 2022b). Additionally, the phosphorylation status of SUFU is critical for conferring the Hh response, as SUFU stabilization and phosphorylation can both inhibit and promote Hh target gene expression (Takenaka et al. 2007; Chen et al. 2011c). For example, ubiquitination of SUFU on Lys63 increases its association to Gli3 and promotes Gli3 conversion to a repressor (Infante et al. 2018), while other ubiquitinated sites reduce SUFU association to Gli1 and promote Hh signaling (Raducu et al. 2016). Thus, more context-specific evidence is needed to demonstrate the changes in SUFU post-translational modifications throughout neural differentiation to better understand how the presence or absence of Hh alters the activity of SUFU regulating kinases and ubiquitinating proteins.

What is clear, is that SUFU plays a key role in Gli transcription factor regulation, and that it primarily acts as a negative regulator of these factors. In vertebrates there are three Gli proteins, Gli1, Gli2 and Gli3. Gli1 acts solely as an activator as it is missing the N-terminal repressor domain while Gli2 and Gli3 can act as either activators or repressors (Dai et al. 1999; Sasaki et al. 1999). Despite the similarity between Gli2 and Gli3, they do have distinct roles within vertebrate Hh signaling. Gli2 primarily acts as the transcriptional activator, whereas Gli3 is the transcriptional repressor (Altaba 1998; Bai et al. 2002; Buttitta et al. 2003; Motoyama et al. 2003). Interestingly, in zebrafish and amphibians, who also possess three Gli proteins, Gli1 acts as the primary activator of signaling instead of Gli2 (Lee et al. 1997; Altaba 1998; Karlstrom et al. 2003; Ke et al. 2008). Nevertheless, SUFU acts to regulate Gli proteins, and it is well known that it



sequesters Gli transcription factors in the cytoplasm (Ding et al. 1999; Barnfield et al. 2005; Chen et al. 2009; Humke et al. 2010). SUFU also promotes the conversion of Gli proteins to transcriptional repressors (Chen et al. 2009; Humke et al. 2010) by protecting them from SPOP-Cul3 mediated ubiquitination and degradation (Chen et al. 2009; Wang et al. 2010) and recruiting GSK3 $\beta$ , PKA and CK1 to phosphorylate Gli proteins (Jia et al. 2005; Tempe et al. 2006; Wang and Li 2006; Pan et al. 2009). This phosphorylation recruits other ubiquitin ligases to cause partial proteasomal degradation, converting Gli to a repressor through  $\beta$ -TrCP-mediated ubiquitination (Jia et al. 2005; Wang and Li 2006; Wen et al. 2010). Gli3 is converted to the transcriptional repressor through phosphorylation (Tempe et al. 2006; Wang and Li 2006), while Gli2 phosphorylation typically results in total degradation of the protein (Bhatia et al. 2006; Pan et al. 2006). Lastly, SUFU can regulate Gli transcriptional activity by interacting with SAP18 and DNA-bound Gli3 to increase repressive activity (Cheng and Bishop 2002; Paces-Fessy et al. 2004). Gli proteins can also undergo sumoylation, another post-translational modification, that increases their activator activity *in vitro*, and in the mouse neural tube (Cox et al. 2010). Together these interactions regulate the transcriptional response of cells to Hh ligands, but how these occur following Hh activation is complex.

All three Glis have a conserved DNA-binding sequence (Kinzler and Vogelstein 1990) that exist upstream of signaling targets, including *Ptch1*, *Ptch2*, and *Hhip* (Ågren et al. 2004; Vokes et al. 2007; Lee et al. 2010) to promote a negative feedback mechanism. *Gli1* and *Boc* (Lee et al. 1997, 2010; Dai et al. 1999; Vokes et al. 2007) promote a positive feedback mechanism of these same signaling targets. Regardless of the mechanism, Gli proteins are essential in neural development as Hh signaling is lost and neural tube defects are present in *Gli2*<sup>-/-</sup>/*Gli3*<sup>-/-</sup> embryos (Buttitta et al. 2003; Motoyama et al. 2003; Gazea et al. 2016) and in embryos with only one defective Gli (Ding et al. 1998). Despite *Gli1* being a Hh target gene, it is not required for neural development as Gli1-deficient embryos have no neural defects (Park et al. 2000; Bai et al. 2002). Given the role of SHH in neural tube development and differentiation of ventral interneuron and motor neuron populations, it is not surprising that neural inducing transcription factors are also targets of Gli proteins (Motoyama et al. 2003; Lei et al. 2006; Vokes et al. 2007;

Voronova et al. 2011; Peterson et al. 2012). As shown previously, Gli activation promotes the expression of pan-neuron inducing factor *Ascl1/Mash1* (Voronova et al. 2011; Spice et al. 2022b), pan-neural factor *Sox2* (Takanaga et al. 2009; Peterson et al. 2012; Bora-Singhal et al. 2015), and ventral interneuron markers *Nkx2.2* (Lei et al. 2006; Vokes et al. 2007; Peterson et al. 2012) and *FoxA2* (Motoyama et al. 2003; Vokes et al. 2007; Peterson et al. 2012). Expression of neural-related target genes also relies on the removal of the Gli-repressor, which is sufficient for expression of the ventral interneuron marker *Nkx6.1* (Wijgerde et al. 2002; Lebel et al. 2007; Peterson et al. 2012) and motor neuron marker *Olig2* (Peterson et al. 2012). Thus, embryos lacking all three Gli proteins are capable of inducing motor neuron differentiation (Bai et al. 2004).

Hh signaling (schematic in Figure 1-3) is well known to play a vital role in neural development, and experiments involving neural differentiation and neural tube morphogenesis have been instrumental in determining the molecular mechanisms of the pathway. Loss of function experiments have highlighted the necessary roles of Hh pathway components in neural development, however, given the complexity of Hh signaling and the various times during neurogenesis that a Hh signal is required, there are still many unanswered questions. My work aimed to answer some of these questions by exploring loss of SUFU and Never in Mitosis Kinase 2 (Nek2) in neural differentiation in the P19 model, and I provide evidence that the negative regulation of Hh signaling is required for this differentiation.

### 1.3.2 Wnt signaling in neural differentiation

Wnt signaling (Figure 1-5), like Hh, is absolutely required for normal neural development as it acts to differentiate specific dorsal interneuron populations, increasing the number of dorsal neuron progenitors, and establishing the midbrain (McMahon et al. 1992; Ikeya et al. 1997; Muroyama et al. 2002; Chesnutt et al. 2004; Gibbs et al. 2017). Wnt signals are also required for *in vitro* neuron differentiation where its activation favors the specification of neurons over astrocytes (Smolich and Papkoff 1994; Tang et al. 2002; Spice et al. 2022a). Unlike Hh, that acts as a long-range morphogen of the developing central nervous system, Wnt ligands have more restricted expression along the dorsal-ventral axis and are induced through active BMP (Parr et al. 1993; Wine-Lee et al. 2004). Wnts were first discovered in 1982 (Nusse and Varmus 1982) and since then 19 mammalian Wnt ligands and at least 10 receptors have been described (Wang et al. 2012; Nusse and Clevers 2017). Given the number of ligands available to cells for signaling, it is not surprising that different Wnt-Wnt receptor combinations elicit some distinct pathway responses (Dijksterhuis et al. 2015), and ligands act alone or synergistically to activate the canonical Wnt- $\beta$ -catenin pathway (Najdi et al. 2012; Alok et al. 2017).

A parallel to Hh is the similar lipid modification observed on Wnt ligands, although with slight differences. Hh ligands are modified with cholesterol and palmitic acid (Lee et al. 1994; Ekker et al. 1995; Porter et al. 1995, 1996; Pepinsky et al. 1998; Chen et al. 2011a) while Wnt ligands are modified with palmitoleic acid, a derivative of palmitic acid (Willert et al. 2003; Zhai et al. 2004; Takada et al. 2006; Doubravska et al. 2011). The O-acyltransferase responsible for Wnt modification is Porcupine (Porc), that modifies Wnt ligands in the ER (Kadowaki et al. 1996; Zhai et al. 2004; Rios-Esteves et al. 2014). Lipid modification of Wnt is believed to restrict their diffusion from producing cells, as overexpression of Porc in the chick neural tube decreases the range of Wnt-induced proliferation of dorsal interneuron progenitors (Galli et al. 2007). Lipid modification is required for Wnt secretion (Takada et al. 2006; Doubravska et al. 2011). This hydrophobic region likely facilitates Wnt incorporation into lipoprotein particles (Panáková et al. 2005), or on the extracellular surface of secretory vesicles, exosomes, and the plasma membrane (Gross et al. 2012; Farin et al. 2016; McGough and Vincent

2016). Shuttling of Wnt into these secretory vesicles and to the plasma membrane is performed by Wntless/Evi (Wls) (Bänziger et al. 2006; Gross et al. 2012; Najdi et al. 2012). Wls is essential for pathway activity as the loss of its activity inhibits Wnt pathway activation and Wls-conditional null alleles phenocopy *Wnt-1* loss of function (Bänziger et al. 2006; Carpenter et al. 2010). More work is needed, however, to fully understand the role of Wls and Porc in neural development and differentiation as *Porc*<sup>-/-</sup> embryos are lethal at gastrulation and heterozygotes do not show neural abnormalities (Barrott et al. 2011; Biechele et al. 2011).

Lipid modification of Wnt is not only required for its secretion but it is also necessary for interacting with its primary receptor Frizzled (Fzd) (Janda et al. 2012). In the presence of Wnt, Fzd dimerizes with the Wnt co-receptor LRP5/6 (Pinson et al. 2000; Tamai et al. 2000; Janda et al. 2017) that acts to recruit the scaffolding proteins Disheveled (Dvl) and Axin to the plasma membrane (Schwarz-Romond et al. 2007; Fiedler et al. 2011; Tauriello et al. 2012). As Fzd directly interacts with Dvl (Tauriello et al. 2012) it is thought that Wnt causes Fzd-LRP5/6 dimerization that then recruits Dvl, which acts as a platform for Axin interaction with the cytoplasmic tail of LRP5/6 (Mao et al. 2001b). All these interactions, however, require the activation of kinases, GSK3 and CK1 (Tamai et al. 2004; Zeng et al. 2005), proteins also involved in transmitting the Hh signal. Given the role of Wnt in the development of dorsal neurons, it is not surprising that Fzd10 has been identified in the dorsal neural tube of *Xenopus*, and that its overexpression increases the number of sensory neurons (Garcia-Morales et al. 2009). Incidentally, *in vitro* differentiation of neurons is also enhanced by the overexpression of Fzd10 (Garcia-Morales et al. 2009). LRP6 is also essential in neural development as its loss causes midbrain defects, a reduction in dorsal interneurons in the neural tube and it inhibits the differentiation of dopaminergic neurons (Pinson et al. 2000; Castelo-Branco et al. 2010; Gray et al. 2013). In contrast, CDO, which interacts with and inhibits LRP6, loss during *in vitro* neuron differentiation increases Wnt signaling and inhibits neuron differentiation (Jeong et al. 2014). The loss of either Wnt1 or LRP6 increases neuronal differentiation of mouse embryonic stem cells (mESC) (Čajánek et al. 2009) yet others have shown increased neuron differentiation with Wnt activation (Smolich and Papkoff 1994; Tang et al. 2002; Spice et al. 2022a). However, a contradiction exists showing decreased neuron

differentiation when both Fzd and LRP6 are inhibited in human embryonic stem cell (hESC) derived neurogenesis (Bengoa-Vergniory et al. 2017). Although there are discrepancies, it is apparent that Wnt signaling and thus the presence and activity of Wnt receptors is crucial to the differentiation of neural cells.

When Wnt is present, it causes the recruitment of Dvl and Axin to interact with the intracellular domains of LRP5/6 and Fzd (Mao et al. 2001b; Schwarz-Romond et al. 2007; Fiedler et al. 2011; Tauriello et al. 2012). This recruitment of Axin to the plasma membrane causes the disassembly of the destruction complex (Roberts et al. 2011; Kim et al. 2013) and the stabilization, cytosolic accumulation, and nuclear import of  $\beta$ -catenin (Li et al. 2012). Although disassembly of the destruction complex is the commonly held belief, in some contexts Axin remains bound to  $\beta$ -catenin with Wnt activation allowing newly synthesized  $\beta$ -catenin to accumulate (Li et al. 2012). GSK3 $\beta$  activity or its ability to interact with the destruction complex is also suggested to be inhibited by phosphorylated LRP5/6 (Stamos et al. 2014). *Axin* overexpression during neural development *in vivo* causes the complete loss of midbrain structures (Yu et al. 2007) and reduced neuron differentiation in the neocortex (Hirabayashi et al. 2004). This is also supported *in vitro* as its overexpression or chemical stabilization in P19 cells or primary mouse NSC cultures inhibited the differentiation of neurons (Lyu et al. 2003; Hirabayashi et al. 2004; Spice et al. 2022a). Conversely, when GSK3 $\beta$  is chemically inhibited reports show increased Wnt signaling activity and increased neuron differentiation at the expense of astrocyte differentiation (Lange et al. 2011; Spice et al. 2022a). However, another report shows decreased neuron differentiation when GSK3 is knocked out (Kim et al. 2009). Thus, like other players, discrepancies are noted and are likely the result of how the investigations were performed. Nonetheless, the absence of a Wnt ligand promotes the degradation of  $\beta$ -catenin (Xing et al. 2003; Kohler et al. 2009; Pronobis et al. 2015), which is phosphorylated by CK1 and hyperphosphorylated by GSK3 (Liu et al. 2002). These post-translational modifications, along with GSK3 phosphorylating APC, allow the recruitment of the  $\beta$ -TrCP E3 ubiquitin ligase complex leading to the proteasomal degradation of  $\beta$ -catenin (Aberle et al. 1997; Pronobis et al. 2015).

Wnt pathway activation leads to the transcription of target genes as  $\beta$ -catenin in the nucleus interacts with T cell Factor/Leukemia Inhibitory Factor (TCF/LEF); a family of transcription factors (Behrens et al. 1996; Molenaar et al. 1996).  $\beta$ -catenin facilitates this interaction as TCF is known to bind to the inhibitory protein Groucho in the absence of Wnt (Cavallo et al. 1998; Roose et al. 1998). Targets of active Wnt signaling include cell cycle regulators *c-Myc* and *cyclin D* (He et al. 1998; Tetsu and McCormick 1999), and negative feedback genes *Dickkopf-1 (Dkk1)* (Niida et al. 2004), that acts to bind and inhibit LRP5/6 (Mao et al. 2001a), *Disabled-2 (Dab2)* (Railo et al. 2009), that acts as an Axin stabilizer (Jiang et al. 2009), and *Axin* (Lustig et al. 2002). TCF transcription factors have been explored sparingly in neural development, however, it has been reported that the overexpression of a dominant-repressor form of TCF in the chick neural tube promotes oligodendrocyte differentiation (Ye et al. 2009).

Although the canonical Wnt signaling pathway (Figure 1-5) plays a role in neural precursor cell proliferation and neural lineage differentiation, not all pathway components have been explored within the neural context. As major players in Wnt signaling also regulate Hh signaling, and that both pathways play various roles in neural development, more work is required to tease apart this crosstalk. Toward this end, I sought to explore Nek2 as a potential node of crosstalk between Wnt and Hh signaling within P19 neural differentiation. Although results presented herein do not show that Nek2 acts in this manner, they do show that Nek2 does promote Wnt signaling during neural differentiation, and its overexpression phenocopies the loss of astrocytes observed with chemical overactivation of Wnt signaling.

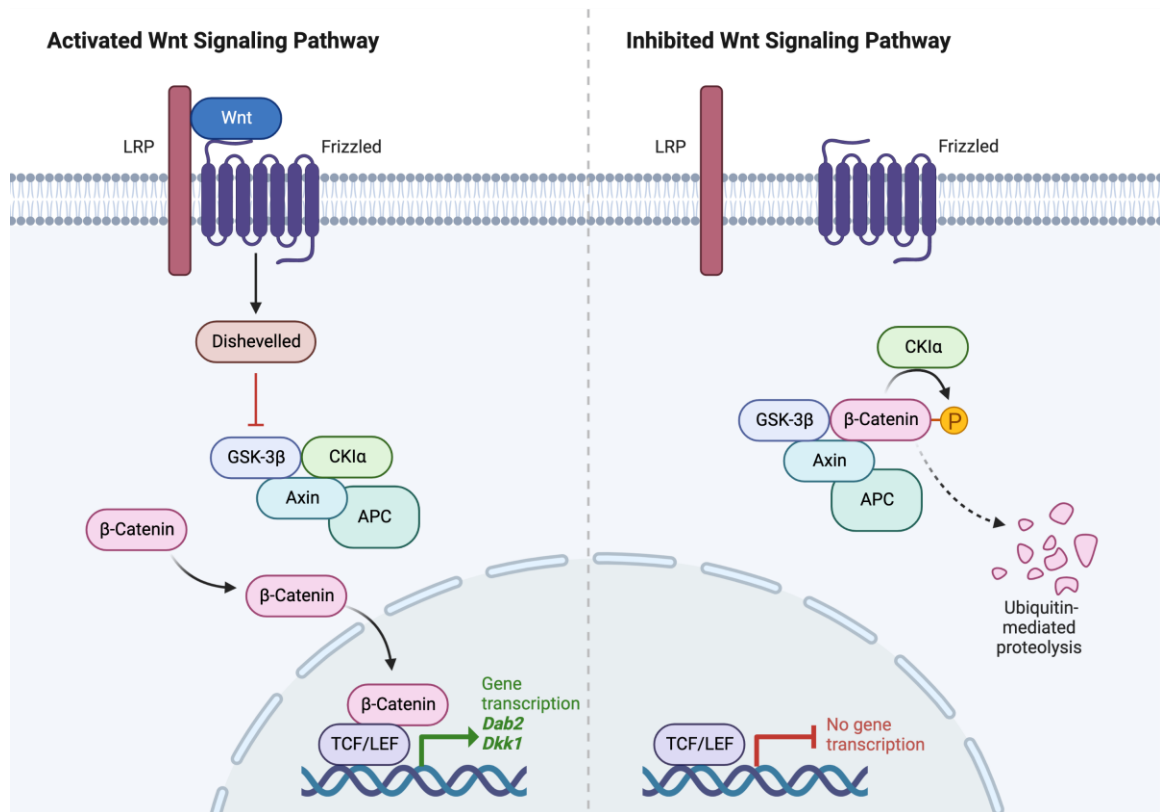


**Figure 1-5: Wnt Signaling**

In the absence of Wnt ligand the destruction complex including CK1, GSK3 $\beta$ , Axin and APC, causes the hyperphosphorylation of  $\beta$ -catenin.  $\beta$ -catenin phosphorylation causes it to be degraded by the proteasome. During canonical signaling, Wnt binds the co-receptors LRP5/6 and Frizzled, which leads to the recruitment of Dishevelled to the plasma membrane. This translocation subsequently causes the recruitment of Axin and the dissociation of the  $\beta$ -catenin destruction complex, which allows the latter to accumulate and translocate to the nucleus. Here,  $\beta$ -catenin interacts with TCF/LEF transcription factors to promote the transcription of target genes like *Dab2* and *Dkk1*. Image created with Biorender.com with reference to (Nusse and Clevers 2017).

### 1.3.3 Other signaling pathways involved in neural differentiation

Although not explored in the presented work, it is important to note other signaling pathways also have central roles in neural development, as described in Section 1.2, and pattern neural cell fate. These include the Notch/Delta signaling pathway (Figure 1-6), which works through a juxtacrine mechanism where the ligand Delta/Jagged binds the extracellular domain of the Notch receptor. This binding allows  $\gamma$ -secretase to cleave and activate the intracellular domain of Notch (NICD) (Yoon and Gaiano 2005). NICD then enters the nucleus where it activates transcription by interacting with CBF1, recombination signal binding protein  $\text{J}\kappa$  and Mastermind (Griffin et al. 2000; Yoon and Gaiano 2005). The overarching view of Notch signaling within neurogenesis is that active Notch maintains cells in a neural progenitor fate and that inhibition of Notch induces neuron differentiation. Notch does this through promoting the expression of the *Hes* transcription factors (Ryoichiro and Ohtshuka 1999) that act to inhibit the expression of neural-inducing genes like *Ascl1/Mash1* (Bertrand et al. 2002). The requirement of Notch for neural progenitor maintenance has been confirmed through many studies showing early and increased neuron differentiation in *Notch*<sup>-/-</sup> embryos (Hitoshi et al. 2002; Yoon and Gaiano 2005). This precocious neuron differentiation, however, leads to fewer differentiated neurons due to the early depletion of the neural precursor pool in these embryos (Hitoshi et al. 2002; Yoon et al. 2004). Active Notch signaling also enhances and accelerates astrocyte differentiation (Gaiano and Fishell 2002; Grandbarbe et al. 2003), and its overactivation promotes neural stem cell differentiation towards oligodendrocyte precursor cells (OPC). However, this overactivation also inhibits OPC differentiation to oligodendrocytes (Grandbarbe et al. 2003). NICD can interact with players in both the Wnt and Hh signaling pathways. Thus, the impact of Notch on neural differentiation likely goes beyond neural progenitor pool maintenance (Borggreffe et al. 2016).



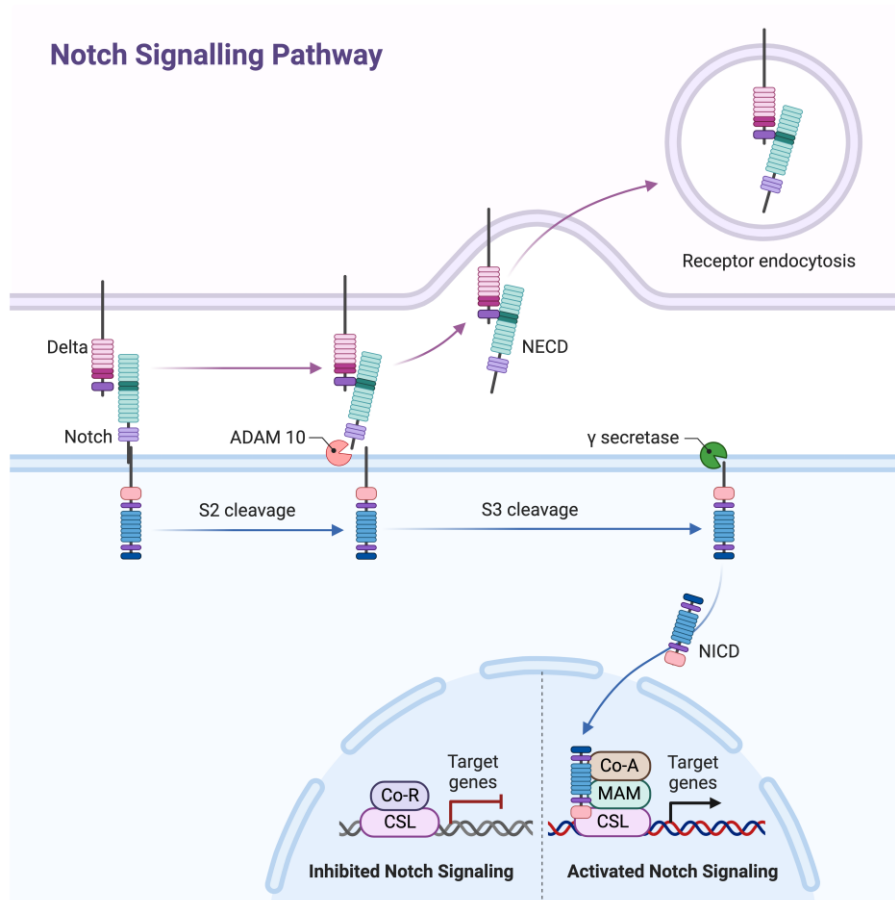


**Figure 1-6: Notch Signaling**

The Notch receptor binds the Delta ligand on an adjacent cell. Binding causes the activation of the ADAM10 and  $\gamma$ -secretase proteases to activate and release the intracellular domain of Notch (NICD), which translocates to the nucleus where it interacts with transcription factors and co-transcriptional regulators to activate transcription of target genes, like the *Hes* transcription factors. Image created with Biorender.com.

FGF signaling, described in Section 1.2, and shown in Figure 1-7, primarily functions to maintain multipotent progenitors in the caudal stem zone during neurulation (Mathis et al. 2001; del Corral et al. 2002), increase neural progenitor proliferation (McKinnon et al. 1990; Lin and Goldman 2009) and pattern the hindbrain (Sato and Nakamura 2004). FGF signaling begins with the secretion of one of 22 ligands that activate tyrosine kinase receptors (FGFR) on receiving cells (Zhang et al. 2006). As an RTK, FGFR activation results in autophosphorylation and the recruitment of guanine nucleotide exchange factor 2 (GRB2), GRB2-associated binding protein 1 (GAB), son of sevenless and FGFR substrate 2 (FRS2) (Teven et al. 2014). The recruitment of these proteins causes the activation of two downstream pathways, the mitogen-activated protein kinase (MAPK) and the phosphatidylinositol-3 kinase (PI3K)/AKT pathway (Yun et al. 2010). In the MAPK pathway, Ras activation of MAPKKK (Raf) phosphorylates and activates MAPKK (MEK), which in the cascade phosphorylates and activates MAPK (ERK) (Yun et al. 2010; Teven et al. 2014). Effectors of the MAPK pathway include c-Jun N-terminal kinase and p38 mitogen-activated kinase that through phosphorylation activate transcription factors like c-Fos and c-Jun to promote the transcription of target genes (Yun et al. 2010; Teven et al. 2014). Gene targets of MAPK signaling primarily include cell proliferation related genes, although can also include genes involved in early neural induction and neuron differentiation (Stock et al. 1992; Lamb and Harland 1995; Wilson et al. 2000; Teven et al. 2014). The PI3K/AKT pathway is also activated by FGF, where PI3K converts phosphatidylinositol-4,5-bisphosphate to phosphatidylinositol-3,4,5-triphosphate that recruits and activates AKT (Yun et al. 2010; Teven et al. 2014), which also have numerous effectors and biological responses. It remains unclear which pathway is activated by FGF, but the presence of the secreted ligands and interfering with the pathways regulated by them affect CNS development (Stock et al. 1992; Woodward et al. 1992). It is known that FGF signaling is required in cell proliferation and survival of astrocyte precursors in the neonatal rat brain (Lin and Goldman 2009) and it increases OPC proliferation while inhibiting their differentiation into oligodendrocytes (McKinnon et al. 1990). FGF is also critical in posterior neural induction as a dominant negative FGFR blocks the development of posterior neural tissue in *Xenopus* embryos (Ribisi et al. 2000), but this may be due to its effects on pattern formation rather than neural

differentiation (Holowacz and Sokol 1999). For example, *Fgf8* is sufficient to convert the diencephalon into the mesencephalon and to induce the presumptive mesencephalon to pattern the cerebellum (Sato and Nakamura 2004). That said, FGF20 participates with FGF2 to increase the differentiation of dopaminergic neurons (Takagi et al. 2005) and in P19 cells, FGF overexpression promotes neuron differentiation (Chen et al. 2006). Other *in vitro* work using human ESCs is more puzzling as it was reported that FGF must be inhibited for neural differentiation to occur (Greber et al. 2011), while blocking MAPK signaling abrogates neural differentiation (Cohen et al. 2010). Given the number of receptor-ligand combinations and the multiple cellular signaling pathways activated in response to FGF, the role of this signaling molecule during neural differentiation is not clear. Although not explored in the present work, FGF signaling is recognized as being essential in neural patterning and posterior neural cell fate.

## FGF Signaling Pathway

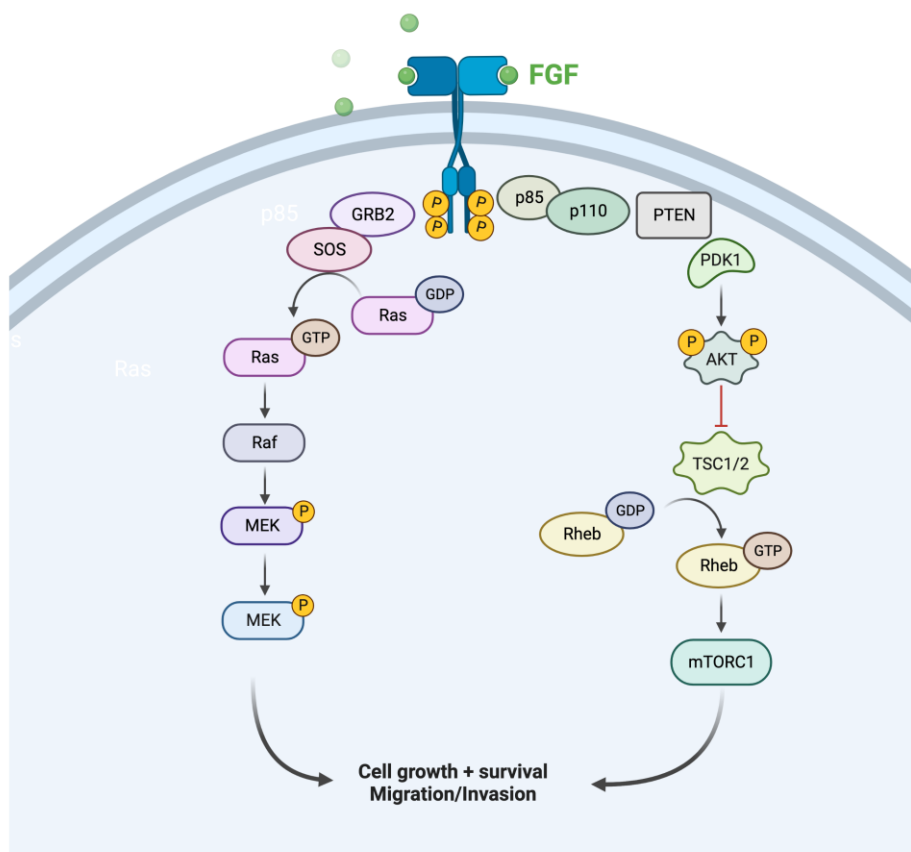


**Figure 1-7: FGF Signaling**

In the presence of fibroblast growth factor (FGF), the receptor tyrosine kinase is activated and gets autophosphorylated prior to activating the MAPK or AKT pathways. In the MAPK pathway (left), GRB2 and son of sevenless (SOS) convert inactive, GDP-bound Ras to active, GTP-bound Ras. Active Ras stimulates Raf (MAPKKK), which in the cascade phosphorylates MEK (MAPKK), required to activate MAPK (ERK), that phosphorylates pathway effectors that enter the nucleus and activate transcription of cell proliferation related genes. In the AKT pathway (right) the receptor causes the cascade to activate AKT, which inhibits the TSC proteins leading to the activation of mTORC1. This active mTORC1 complex can alter the expression of target genes that inhibit autophagy and stimulate pro-survival. Image created using Biorender.com.

Retinoic Acid (RA) signaling (Figure 1-8) is also involved in the development of neuroectodermal lineages, specifically early neural specification, and forebrain development (Maden 2007; Ghyselinck and Duester 2019). I used RA, paired with cell aggregation to induce the differentiation of the P19 cells towards neuron and astrocyte cell fates. Vitamin A, or retinol, is passively diffused into the cell where it is converted to the active RA molecule. Retinol becomes retinaldehyde through retinol dehydrogenase 10 activity (RDH) (Metzler and Sandell 2016), and retinaldehyde becomes RA through retinaldehyde dehydrogenase (RALDH) activity (Cunningham and Duester 2015). RA can diffuse into the nucleus, where it is recognized by retinoic acid (RAR) and retinoid X receptors (RXR) bound to the RA response element (RARE) sequences in the DNA (Ghyselinck and Duester 2019). Binding affects transcription and the outcomes are immense, and often unpredictable as there are up to 15,000 identified RAREs in the mammalian genome (Moutier et al. 2012). Thus during embryogenesis, the number of genes induced or repressed in response to active RA is not entirely clear, but it is well known that RA is linked to neural induction and differentiation (Jones-Villeneuve et al. 1982; McBurney et al. 1988; Wichterle et al. 2002; Skromne et al. 2007; Chatzi et al. 2011; Sturgeon et al. 2011; Shin et al. 2012; Cunningham et al. 2015). RA has been used in many *in vitro* models of neural differentiation, including but not limited to mESCs, hESCs, embryonal carcinoma cells and neuroblastoma cells (Jones-Villeneuve et al. 1982; Sidell et al. 1983; Bain et al. 1996; Schuldiner et al. 2001; Wichterle et al. 2002; Tonge and Andrews 2010). In P19 cells, an embryonal carcinoma line, RA has several roles including the induction of *FoxA1* expression during neural differentiation, which activates *Shh* expression (Tan et al. 2010) and represses the pluripotency gene *Nanog* (Chen et al. 2014). RA signaling in P19 cells has been well characterized (Edwards and McBurney 1983; Wei et al. 1989; Pratt et al. 1990; Kruyt et al. 1992; Malý and Dráber 1992; Bain and Gottlieb 1994; Taneja et al. 1996), where varying concentrations give rise to specific cell lineages and high concentrations ( $10^{-7}$  to  $10^{-5}$  M) give rise to neural phenotypes. Studies have also explored the expression patterns of RARs, RXRs and cytosolic RA binding proteins throughout neural differentiation (Wei et al. 1989; Malý and Dráber 1992; Bain and Gottlieb 1994; Taneja et al. 1996) and have established RA as the key inducer of the neural phenotype (Pratt et al. 1990; Kruyt et al. 1992). In

particular, the RAR types responsible for signaling in P19 cells are RAR $\alpha$  and RAR $\gamma$  (Taneja et al. 1996), where dominant negative RAR $\alpha$  inhibits neural differentiation (Costa and McBurney 1996), as does the inhibition of RAR/RXR dimerization (Shago et al. 1997). Cell aggregation and embryoid body formation, a key component of the *in vitro* differentiation of P19 cells (Schmidt et al. 1992), regulates the expression patterns of the RARs (Jonk et al. 1992); showing how 3D culturing and RA signaling in this model are tightly linked. Not only is the positive propagation of RA signaling involved in P19 neural differentiation, but the negative regulation via RA hydroxylase and *Cyp26* are also required (Sonneveld et al. 1999). Given the involvement of RA in neural development in P19 and other cell lines, my focus was on using it to better elucidate the Wnt and Hh signaling regulators and the crosstalk that exists between these pathways.

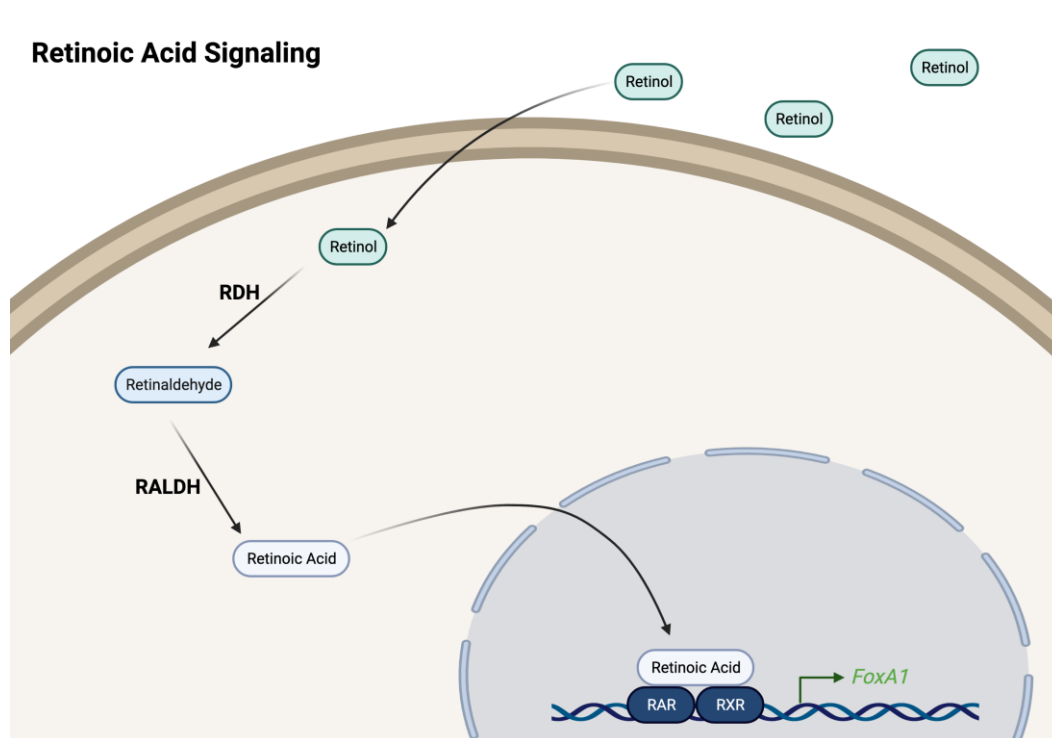


**Figure 1-8: Retinoic Acid Signaling**

Retinol in the extracellular space passively diffuses across the membrane where retinol dehydrogenase (RDH) converts retinol to retinaldehyde. Retinaldehyde is converted to retinoic acid (RA) by retinaldehyde dehydrogenase (RALDH), which diffuses into the nucleus where it binds the RAR and RXR receptors. These receptors are bound to the DNA at retinoic acid response elements (RAREs), which control the transcription of genes. Binding can regulate the expression of up to 15,000 genes, including the *FoxA1* transcription factor involved in neural differentiation. Image created using Biorender.com.

## 1.4 In vitro models of neural differentiation

Cells in culture have been used for decades to study the cellular mechanisms involved in neural induction and differentiation. *In vitro* models of differentiation provide a cost-effective approach to understanding the genes and protein signaling pathways governing the complex processes of pluripotency, proliferation, induction, and differentiation. They also corroborate what occurs *in vivo* and the utility of cultured embryonal carcinoma cells, which are stem-like cells, have set the stage for numerous stem cell studies (Kelly and Gatie 2017). For instance, the P19 embryonal carcinoma model has been used since 1982 to study neural differentiation (McBurney and Rogers 1982), but there are other models that use similar differentiation cues to generate neurons and astrocytes. The P19 model, which I used in my study will be discussed in this section.

### 1.4.1 Embryonal carcinoma cell models of neural differentiation

Embryonal carcinoma models have been used extensively in the study of differentiation. One of the first studies involved NTera2 (NT2) human embryonal carcinoma cells, which readily differentiate to neurons in the presence of RA (Andrews 1984). Other carcinoma cell lines include human SK-N-MC cells, rat PC12 cells, and mouse P19 cells, which were selected for further study. P19 cells were derived from the subcutaneous implantation of an E7.5 embryo in a mouse (McBurney and Rogers 1982), and reports have shown that given the proper cues they differentiate into cardiac and skeletal muscle or neural lineages (Jones-Villeneuve et al. 1982; Edwards and McBurney 1983; McBurney 1993). P19 cells that differentiate in the presence of RA into neural lineages require high density cell culturing and low serum conditions (Jones-Villeneuve et al. 1982; Edwards and McBurney 1983). These cells also produce astrocytes with RA treatment and cell aggregation (Jones-Villeneuve et al. 1982; Spice et al. 2022b), while protocols with monolayer cultures treated with RA in defined medium only produce neurons (Monzo et al. 2012). More importantly, the neurons produced through embryoid body (EB) formation and RA treatment are morphologically like primary neurons of the rodent brain (McBurney et al. 1988). In addition, P19-derived neurons are similarly post-mitotic (McBurney et al. 1988), form functional synapses (Morassutti et al. 1994) and produce neurotransmitters, including those made by choline acetyltransferase, tyrosine



hydroxylase, dopamine  $\beta$ -hydroxylase and glutamic acid decarboxylase (Jones-Villeneuve et al. 1983; Sharma and Notter 1988; Bain et al. 1993; Staines et al. 1994). P19 cells also produce glutamate and differentiated neurons express glutamate receptors (Ray and Gottlieb 1993) that are responsive when implanted into the adult rat brain (Magnuson et al. 1995). It is interesting to note that these implanted neurons can survive for over 30 days and points to the fundamental ability of these *in vitro* derived neurons to integrate with the CNS of the host organism (Magnuson et al. 1995).

Other signaling pathways, like those previously described, regulate neural differentiation in P19 cells. For instance, FGF signaling is involved in differentiation and is temporally regulated by RA and dependent on EB formation (Chen et al. 2006; Alam et al. 2009). MAPK and AKT are also essential in these cells as inhibition of AKT signaling (Mao and Lee 2005; Fu et al. 2020), or inhibition of c-Jun N-terminal kinase, a downstream effector of MAPK, reduces neuron differentiation (Wang et al. 2001). Notch signaling, another pathway involved in neural differentiation has not been extensively explored in P19 cells, but it is noteworthy that when these cells are cultured under hypoxic conditions, HIF1 $\alpha$  interacts with NICD (Gustafsson et al. 2005), and *Hes1* is rapidly upregulated during EB formation (Wakabayashi et al. 2000). Most relevant to my investigation are the reports showing P19 cells temporally regulating and utilizing canonical Wnt signaling to increase neuron differentiation while inhibiting astrocyte formation (Smolich and Papkoff 1994; Tang et al. 2002; Jing et al. 2009; Spice et al. 2022a). Finally, Hh signaling, also at the centre of my study, plays a key role in neural differentiation of P19 cells as reports have documented that RA induces *Shh* expression (Tan et al. 2010) and *Gli2* overexpression is sufficient to induce neurons (Voronova et al. 2011). Given the number of signaling pathways reported to be involved in P19 neural differentiation, it is likely they are playing various roles, individually and together, along the lineage commitment to differentiation timeline. Cells undergoing differentiation must be competent to respond to external signals before undergoing specification towards the neural lineage (Wilson and Edlund 2001). Specified cells can then become committed towards a neuronal or glial cell fate as distinct progenitors that can only give rise to their respective differentiated cell types (Wilson and Edlund 2001). Temporal regulation of signaling pathways is thus key

in defining these various identities throughout differentiation. It is interesting that the involvement of Wnt and Hh signaling in P19 cells both play a role in neural differentiation given the similarities and potential crosstalk that exists between the regulators of these pathways. The P19 cell model was used to explore some of these questions, specifically focusing on Sufu and Nek2. In the presented work I describe how the P19 model differentiates in the presence of RA and various chemical signaling modulators, as well as show changes in differentiation resulting from the genetic manipulations of Sufu and Nek2. Finally, I should note that many researchers have replaced embryonal carcinoma cells with embryonic stem cell lines, but I strongly believe my work highlights the power of the P19 model to elucidate fundamental molecular mechanisms related to neural differentiation.

## 1.5 Never in mitosis kinase 2 and development

The focus of this work was in exploring the role of Wnt and Hh signaling regulators in neural differentiation. Although not usually thought of when discussing these pathways, Never in mitosis kinase 2 (Nek2) has been recently identified as a regulator of both Hh and Wnt pathways (Mbom et al. 2014; Cervenka et al. 2016; Wang et al. 2016; Zhou et al. 2017). The primary role of Nek proteins is in regulating the cell cycle, where Nek2 is known to regulate centrosome disjunction before mitosis (Fry 2002; Rellos et al. 2007; Cervenka et al. 2016; Sahota et al. 2018). However, in Wnt signaling, Nek2 acts as a positive regulator through  $\beta$ -catenin and DVL (Mbom et al. 2014; Cervenka et al. 2016). In Hek293T cells Nek2 phosphorylates  $\beta$ -catenin, and blocks the interaction with  $\beta$ -TrCP to inhibit degradation (Mbom et al. 2014). This kinase also phosphorylates DVL, increasing Wnt signaling responses in this same cell type (Cervenka et al. 2016). The connection between Nek2 and Wnt signaling also occurs in colorectal cancer cells (Neal et al. 2014), lung adenocarcinoma cells (Das et al. 2013), cervical cancer cells (Xu et al. 2020), breast cancer cells (Shen et al. 2019), and hepatocellular carcinoma cells (Lin et al. 2016; Deng et al. 2019). In these cases, Nek2 overexpression caused increased  $\beta$ -catenin stabilization and target gene activity. In contrast to a role in Wnt signaling, Nek2

acts as a negative regulator of Hh signaling (Wang et al. 2016; Zhou et al. 2017). Again, in Hek293T cells, Nek2 binds, phosphorylates and stabilizes SUFU (Wang et al. 2016) and is a Hh signaling target gene that acts in a negative feedback mechanism (Zhou et al. 2017). Although cancers are associated with overactive Hh signaling, no studies currently exist linking Nek2 loss of function with Hh pathway activity in these cells. There are, however, many studies showing overactivation of Nek2 is linked to malignancy and poor patient survival (Yao et al. 2019), and to date many studies have reported this general phenomenon (Liu et al. 2014, 2017; Boulay et al. 2017; Gu et al. 2017; Can et al. 2018; Bai et al. 2021; Jian et al. 2021; Wan et al. 2021; Xing et al. 2021; Zhang et al. 2021; Xiang et al. 2022).

Despite these studies highlighting the role of Nek2 in cancer, few studies have investigated its role in embryonic development. We know Nek2 has been explored during heart development where its knockdown in *Xenopus* causes left-right asymmetry and looping defects (Joseph Endicott et al. 2015). These defects were not connected in this work to Hh or Wnt signaling, rather instead to cilia dynamics (Joseph Endicott et al. 2015). However, since Hh signaling requires cilia (Briscoe and Théron 2013), it is possible that signaling was perturbed in these embryos and it was just not explored. Nek2 overexpression studies in *Drosophila* have linked Nek2 and Wnt signaling as overexpression of Nek2 during eye development causes overactive wingless (Wnt) signaling and reduces retinal neuron differentiation (Martins et al. 2017). To my knowledge, there remains no study investigating the role of Nek2 in mammalian neurogenesis. Since *Nek2* expression has been observed in the brain of E10.5 mouse embryos (Tanaka et al. 1997) and Nek3 is required for regulating microtubule dynamics in mature neurons (Chang et al. 2009), Nek2 is very likely to have a role during neurogenesis. Toward that end, I found that Nek2 plays an essential role in neuron and astrocyte development, however, only Wnt signaling was suggested by the data to be linked to Nek2 in the P19 model. Even more surprisingly, Nek2 was found to be connected to hypoxia inducible factor 1 $\alpha$  and mitochondrial electron transport chain components to regulate metabolism during neural differentiation.

## 1.6 Hypothesis, Study Aims & Key Findings

### 1.6.1 Hypothesis

Hh and Wnt signaling are key signaling pathways that regulate neural differentiation. Although much is known about these pathways within this context, known and novel pathway regulators have not been extensively studied within neural differentiation. To address this, I used P19 embryonal carcinoma cells as a model to study the molecular mechanisms orchestrating the transitions from pluripotency to neuron and astrocyte cell fate. My objective was to explore the role of SUFU and Nek2 in neural differentiation, where I had two hypotheses: 1) I hypothesized that if Hh signaling plays a role in neural differentiation, then genetic ablation of the pathway regulator SUFU would block neural differentiation through deregulation of Hh signaling, and 2) I hypothesized that if both Hh and Wnt signaling play roles in neural differentiation, then genetic ablation of Nek2 would block differentiation through deregulation of both pathways.

### 1.6.2 Study Aims & Key Findings

#### *Chapter 2*

**Study Aim:** Determine the differentiation potential and evaluate changes to Hh signaling within SUFU-deficient cells.

**Key Finding:** SUFU deficient cells increase expression of Hh target genes through the complete loss of the Gli3 transcription factor, causing delayed and reduced astrocyte formation without altering neuron differentiation.

#### *Chapter 3*

**Study Aim:** Determine the differentiation potential and evaluate changes to Hh and Wnt signaling in cells overexpressing and lacking Nek2.

**Key Finding:** Nek2 promotes differentiation of neural precursor cells and is required for the differentiation of neurons and astrocytes through its regulation of metabolism rather than via Wnt or Hh regulation.

*Together my results support that Wnt and Hh signaling are key in P19 neural differentiation and that SUFU plays a crucial role in Hh regulation. However, the role of Nek2 in neural differentiation is not directly related to protein signaling pathway regulation and instead is linked earlier to metabolic changes in these progenitor cells.*

## 1.7 References

- Aberle, H., Bauer, A., Stappert, J., Kispert, A., and Kemler, R. 1997. B-Catenin Is a Target for the Ubiquitin-Proteasome Pathway. *EMBO Journal* **16**(13): 3797–3804. doi:10.1093/emboj/16.13.3797.
- Ågren, M., Kogerman, P., Kleman, M.I., Wessling, M., and Toftgård, R. 2004. Expression of the PTCH1 tumor suppressor gene is regulated by alternative promoters and a single functional Gli-binding site. *Gene* **330**(1–2): 101–114. doi:10.1016/j.gene.2004.01.010.
- Alam, A.H.M.K., Suzuki, H., and Tsukahara, T. 2009. Expression analysis of Fgf8a & Fgf8b in early stage of P19 cells during neural differentiation. *Cell Biol Int* **33**(9): 1032–1037. Elsevier Ltd. doi:10.1016/j.cellbi.2009.06.015.
- Allen, B.L., Song, J.Y., Izzi, L., Althaus, I.W., Kang, J.-S., Charron, F., Krauss, R.S., and McMahon, A.P. 2011. Overlapping roles and collective requirement for the co-receptors Gas1, Cdo and Boc in Shh pathway function. *Dev Cell* **20**(6): 775–787. doi:10.1016/j.devcel.2011.04.018.Overlapping.
- Allen, B.L., Tenzen, T., and McMahon, A.P. 2007. The Hedgehog-binding proteins Gas1 and Cdo cooperate to positively regulate Shh signaling during mouse development. *Genes Dev* **21**(10): 1244–1257. doi:10.1101/gad.1543607.
- Van Allen, M.I., Kalousek, D.K., Chernoff, G.F., Juriloff, D., Harris, M., McGillivray, B.C., Yong, S.L., Langlois, S., MacLeod, P.M., Chitayat, D., Friedman, J.M., Wilson, R.D., McFadden, D., Pantzar, J., Ritchie, S., and Hall, J.G. 1993. Evidence for multi-site closure of the neural tube in humans. *Am J Med Genet* **47**(5): 723–743. doi:10.1002/ajmg.1320470528.
- Alok, A., Lei, Z., Jagannathan, N.S., Kaur, S., Harmston, N., Rozen, S.G., Tucker-Kellogg, L., and Virshup, D.M. 2017. Wnt proteins synergize to activate  $\beta$ -catenin signaling. *J Cell Sci* **130**(9): 1532–1544. doi:10.1242/jcs.198093.

- Altaba, A.R.I. 1998. Combinatorial Gli gene function in floor plate and neuronal inductions by Sonic hedgehog. *Development* **125**(12): 2203–2212.
- Andrews, P.W. 1984. Retinoic acid induces neuronal differentiation of a cloned human embryonal carcinoma cell line in vitro. *Dev Biol* **103**(2): 285–293. doi:10.1016/0012-1606(84)90316-6.
- Bai, C.B., Auerbach, W., Lee, J.S., Stephen, D., and Joyner, A.L. 2002. Gli2, but not Gli1, is required for initial Shh signaling and ectopic activation of the Shh pathway. *Development* **129**: 4753–4761.
- Bai, C.B., Stephen, D., and Joyner, A.L. 2004. All mouse ventral spinal cord patterning by Hedgehog is Gli dependent and involves an activator function of Gli3. *Dev Cell* **6**(1): 103–115. doi:10.1016/S1534-5807(03)00394-0.
- Bai, R., Yuan, C., Sun, W., Zhang, J., Luo, Y., Gao, Y., Li, Y., Gong, Y., and Xie, C. 2021. Nek2 plays an active role in tumorigenesis and tumor microenvironment in non-small cell lung cancer. *Int J Biol Sci* **17**(8): 1995–2008. doi:10.7150/ijbs.59019.
- Bain, G., and Gottlieb, D.I. 1994. Expression of retinoid X receptors in P19 embryonal carcinoma cells and embryonic s. *Biochem Biophys Res Commun* **200**(3): 1252–1256.
- Bain, G., Ramkumar, T.P., Cheng, J.M., and Gottlieb, D.I. 1993. Expression of the genes coding for glutamic acid decarboxylase in pluripotent cell lines. *Molecular Brain Research* **17**(1–2): 23–30. doi:10.1016/0169-328X(93)90068-Z.
- Bain, G., Ray, W.J., Yao, M., and Gottlieb, D.I. 1996. Retinoic acid promotes neural and represses mesodermal gene expression in mouse embryonic stem cells in culture. *Biochem Biophys Res Commun* **223**(3): 691–694. doi:10.1006/bbrc.1996.0957.
- Bänziger, C., Soldini, D., Schütt, C., Zipperlen, P., Hausmann, G., and Basler, K. 2006. Wntless, a Conserved Membrane Protein Dedicated to the Secretion of Wnt Proteins from Signaling Cells. *Cell* **125**(3): 509–522. doi:10.1016/j.cell.2006.02.049.
- Barnfield, P.C., Zhang, X., Thanabalasingham, V., Yoshida, M., and Hui, C.C. 2005. Negative regulation of Gli1 and Gli2 activator function by Suppressor of fused through multiple mechanisms. *Differentiation* **73**(8): 397–405. International Society of Differentiation. doi:10.1111/j.1432-0436.2005.00042.x.
- Barrott, J.J., Cash, G.M., Smith, A.P., Barrow, J.R., and Murtaugh, L.C. 2011. Deletion of mouse Porcn blocks Wnt ligand secretion and reveals an ectodermal etiology of human focal dermal hypoplasia/Goltz syndrome. *Proc Natl Acad Sci U S A* **108**(31): 12752–12757. doi:10.1073/pnas.1006437108.

- Basler, K., Edlund, T., Jessell, T.M., and Yamada, T. 1993. Control of cell pattern in the neural tube: Regulation of cell differentiation by dorsalin-1, a novel TGF $\beta$  family member. *Cell* **73**(4): 687–702. doi:10.1016/0092-8674(93)90249-P.
- Behrens, J., Von Kries, J.P., Kühl, M., Bruhn, L., Wedlich, D., Grosschedl, R., and Birchmeier, W. 1996. Functional interaction of  $\beta$ -catenin with the transcription factor LEF-1. *Nature* **382**: 638–642. doi:10.1038/382638a0.
- Belgacem, Y.H., Hamilton, A.M., Shim, S., Spencer, K.A., and Borodinsky, L.N. 2016. The many hats of Sonic hedgehog signaling in nervous system development and disease. *J Dev Biol* **4**(4). doi:10.3390/jdb4040035.
- Bel-Vialar, S., Itasaki, N., and Krumlauf, R. 2002. Initiating Hox gene expression: in the early chick neural tube differential sensitivity to FGF and RA signaling subdivides the HoxB genes into two distinct groups. *Development* **129**: 5103–5115. doi:10.3999/jscpt.23.43.
- Bengoa-Vergniory, N., Gorroño-Etxebarria, I., López-Sánchez, I., Marra, M., Di Chiaro, P., and Kypta, R. 2017. Identification of Noncanonical Wnt Receptors Required for Wnt-3a-Induced Early Differentiation of Human Neural Stem Cells. *Mol Neurobiol* **54**(8): 6213–6224. *Molecular Neurobiology*. doi:10.1007/s12035-016-0151-5.
- Berggren, K., McCaffery, P., Dräger, U., and Forehand, C.J. 1999. Differential distribution of retinoic acid synthesis in the chicken embryo as determined by immunolocalization of the retinoic acid synthetic enzyme, RALDH-2. *Dev Biol* **210**(2): 288–304. doi:10.1006/dbio.1999.9286.
- Bertrand, N., Castro, D.S., and Guillemot, F. 2002. Proneural genes and the specification of neural cell types. *Nat Rev Neurosci* **3**(7): 517–530. doi:10.1038/nrn874.
- Bhatia, N., Thiyagarajan, S., Elcheva, I., Saleem, M., Dlugosz, A., Mukhtar, H., and Spiegelman, V.S. 2006. Gli2 is targeted for ubiquitination and degradation by  $\beta$ -TrCP ubiquitin ligase. *Journal of Biological Chemistry* **281**(28): 19320–19326. © 2006 ASBMB. Currently published by Elsevier Inc; originally published by American Society for Biochemistry and Molecular Biology. doi:10.1074/jbc.M513203200.
- Biechele, S., Cox, B.J., and Rossant, J. 2011. Porcupine homolog is required for canonical Wnt signaling and gastrulation in mouse embryos. *Dev Biol* **355**(2): 275–285. Elsevier Inc. doi:10.1016/j.ydbio.2011.04.029.
- Bitgood, M.J., Shen, L., and McMahon, A.P. 1996. Sertoli cell signaling by Desert hedgehog regulates the male germline. *Current Biology* **6**(3): 298–304. doi:10.1016/S0960-9822(02)00480-3.

- Bora-Singhal, N., Perumal, D., Nguyen, J., and Chellappan, S. 2015. Gli1-Mediated Regulation of Sox2 Facilitates Self-Renewal of Stem-Like Cells and Confers Resistance to EGFR Inhibitors in Non-Small Cell Lung Cancer. *Neoplasia* **17**(7): 538–551. The Authors. doi:10.1016/j.neo.2015.07.001.
- Borggreffe, T., Lauth, M., Zwijsen, A., Huylebroeck, D., Oswald, F., and Giaimo, B.D. 2016. The Notch intracellular domain integrates signals from Wnt, Hedgehog, TGF $\beta$ /BMP and hypoxia pathways. *Biochim Biophys Acta Mol Cell Res* **1863**(2): 303–313. The Authors. doi:10.1016/j.bbamcr.2015.11.020.
- Boulay, G., Awad, M.E., Riggi, N., Archer, T.C., Iyer, S., Boonseng, W.E., Rossetti, N.E., Naigles, B., Rengarajan, S., Volorio, A., Kim, J.C., Mesirov, J.P., Tamayo, P., Pomeroy, S.L., Aryee, M.J., and Rivera, M.N. 2017. OTX2 activity at distal regulatory elements shapes the chromatin landscape of group 3 medulloblastoma. *Cancer Discov* **7**(3): 288–301. doi:10.1158/2159-8290.CD-16-0844.
- Bradl, M. 2006. Progenitors and Precursors of Neurons and Glial Cells. *In The Cell Cycle in the Central Nervous System. Edited by D. Janigro.* Humana Press, Totowa, NJ. pp. 23–29. doi:10.1007/978-1-59745-021-8\_3.
- Brady, M. V., and Vaccarino, F.M. 2021. Role of shh in patterning human pluripotent cells towards ventral forebrain fates. *Cells* **10**(4). doi:10.3390/cells10040914.
- de Bree, K., de Bakker, B.S., and Oostra, R.-J. 2018. The development of the human notochord. *PLoS One* **13**(10): e0205752. doi:10.1126/science.aag0053.Funding.
- Briscoe, J., Chen, Y., Jessell, T.M., and Struhl, G. 2001. A hedgehog-insensitive form of Patched provides evidence for direct long-range morphogen activity of Sonic hedgehog in the neural tube. *Mol Cell* **7**(6): 1279–1291. doi:10.1016/S1097-2765(01)00271-4.
- Briscoe, J., and Théron, P.P. 2013. The mechanisms of Hedgehog signalling and its roles in development and disease. *Nat Rev Mol Cell Biol* **14**(7): 418–431. doi:10.1038/nrm3598.
- Buglino, J.A., and Resh, M.D. 2008. Hhat is a palmitoyltransferase with specificity for N-palmitoylation of Sonic Hedgehog. *Journal of Biological Chemistry* **283**(32): 22076–22088. © 2008 ASBMB. Currently published by Elsevier Inc; originally published by American Society for Biochemistry and Molecular Biology. doi:10.1074/jbc.M803901200.
- Buglino, J.A., and Resh, M.D. 2010. Identification of conserved regions and residues within hedgehog acyltransferase critical for palmitoylation of Sonic hedgehog. *PLoS One* **5**(6): 17–20. doi:10.1371/journal.pone.0011195.



- Burnside, B. 1973. Microtubules and Microfilaments in Amphibian Neurulation. *American Zoology* **13**: 989–1006.
- Buttitta, L., Mo, R., Hui, C.C., and Fan, C.M. 2003. Interplays of Gli2 and Gli3 and their requirement in mediating Shh-dependent sclerotome induction. *Development* **130**(25): 6233–6243. doi:10.1242/dev.00851.
- Čajánek, L., Ribeiro, D., Liste, I., Parish, C.L., Bryja, V., and Arenas, E. 2009. Wnt/ $\beta$ -catenin signaling blockade promotes neuronal induction and dopaminergic differentiation in embryonic stem cells. *Stem Cells* **27**(12): 2917–2927. doi:10.1002/stem.210.
- Callejo, A., Torroja, C., Quijada, L., and Guerrero, I. 2006. Hedgehog lipid modifications are required for Hedgehog stabilization in the extracellular matrix. *Development* **133**(3): 471–483. doi:10.1242/dev.02217.
- Can, L., Nadiminti, K., Zhu, Y., Jethava, Y., Frech, I., Tricot, G.J., and Zhan, F. 2018. The Nek2 Genetic Knockout Mouse Model Provides Novel Treatment Strategies in Myeloma and Lymphoma. *Blood* **132**(Supplement 1): 5612–5612. American Society of Hematology. doi:10.1182/blood-2018-99-115099.
- Carpenter, A.C., Rao, S., Wells, J.M., Campbell, K., and Lang, R.A. 2010. Generation of mice with a conditional null allele for Wntless. *Genesis* **48**(9): 554–558. doi:10.1002/dvg.20651.
- Castelo-Branco, G., Andersson, E.R., Minina, E., Sousa, K.M., Ribeiro, D., Kokubu, C., Imai, K., Prakash, N., Wurst, W., and Arenas, E. 2010. Delayed dopaminergic neuron differentiation in Lrp6 mutant mice. *Developmental Dynamics* **239**(1): 211–221. doi:10.1002/dvdy.22094.
- Cavallo, R.A., Cox, R.T., Moline, M.M., Roose, J., Polevoy, G.A., Clevers, H., Peifer, M., and Bejsovec, A. 1998. *Drosophila* Tcf and Groucho interact to repress Wingless signalling activity. *Nature* **395**: 604–608. doi:10.1038/255242a0.
- Cervenka, I., Valnohova, J., Bernatik, O., Harnos, J., Radsetoulal, M., Sedova, K., Hanakova, K., Potesil, D., Sedlackova, M., Salasova, A., Steinhart, Z., Angers, S., Schulte, G., Hampl, A., Zdrahal, Z., and Bryja, V. 2016. Dishevelled is a NEK2 kinase substrate controlling dynamics of centrosomal linker proteins. *Proc Natl Acad Sci U S A* **113**(33): 9304–9309. doi:10.1073/pnas.1608783113.
- Chamberlain, C.E., Jeong, J., Guo, C., Allen, B.L., and McMahon, A.P. 2008. Notochord-derived Shh concentrates in close association with the apically positioned basal body in neural target cells and forms a dynamic gradient during neural patterning. *Development* **135**(6): 1097–1106. doi:10.1242/dev.013086.

- Chamoun, Z., Mann, R.K., Nellen, D., Von Kessler, D.P., Bellotto, M., Beachy, P.A., and Basler, K. 2001. Skinny Hedgehog, an acyltransferase required for palmitoylation and activity of the Hedgehog signal. *Science* (1979) **293**(5537): 2080–2084. doi:10.1126/science.1064437.
- Chang, J., Baloh, R.H., and Milbrandt, J. 2009. The NIMA-family kinase Nek3 regulates microtubule acetylation in neurons. *J Cell Sci* **122**(13): 2274–2282. doi:10.1242/jcs.048975.
- Chatzi, C., Brade, T., and Duyster, G. 2011. Retinoic acid functions as a key gabaergic differentiation signal in the basal ganglia. *PLoS Biol* **9**(4). doi:10.1371/journal.pbio.1000609.
- Chen, J., Chang, S., Duncan, S.A., Okano, H.J., Fishell, G., and Aderem, A. 1996. Disruption of the MacMARCKS gene prevents cranial neural tube closure and results in anencephaly. *Proc Natl Acad Sci U S A* **93**(13): 6275–6279. doi:10.1073/pnas.93.13.6275.
- Chen, M.H., Li, Y.J., Kawakami, T., Xu, S.M., and Chuang, P.T. 2004. Palmitoylation is required for the production of a soluble multimeric Hedgehog protein complex and long-range signaling in vertebrates. *Genes Dev* **18**(6): 641–659. doi:10.1101/gad.1185804.
- Chen, M.H., Wilson, C.W., Li, Y.J., Law, K.K. Lo, Lu, C.S., Gacayan, R., Zhang, X., Hui, C.C., and Chuang, P.T. 2009. Cilium-independent regulation of Gli protein function by Sufu in Hedgehog signaling is evolutionarily conserved. *Genes Dev* **23**(16): 1910–1928. doi:10.1101/gad.1794109.
- Chen, T., He, S., Zhang, Z., Gao, W., Yu, L., and Tan, Y. 2014. Foxal contributes to the repression of Nanog expression by recruiting Grg3 during the differentiation of pluripotent P19 embryonal carcinoma cells. *Exp Cell Res* **326**(2): 326–335. doi:10.1016/j.yexcr.2014.04.020.
- Chen, W., Caihong, X., Wei, B., Li, L., Lin, W., Chen, Y.-G., Ang, S.-L., and Jing, N. 2006. Cell aggregation-induced FGF8 elevation is essential for P19 cell neural differentiation. *Mol Biol Cell* **17**(July): 3075–3084. doi:10.1091/mbc.e05-11-1087.
- Chen, X., Tukachinsky, H., Huang, C.H., Jao, C., Chu, Y.R., Tang, H.Y., Mueller, B., Schulman, S., Rapoport, T.A., and Salic, A. 2011a. Processing and turnover of the Hedgehog protein in the endoplasmic reticulum. *Journal of Cell Biology* **192**(5): 825–838. doi:10.1083/jcb.201008090.
- Chen, Y., Sasai, N., Ma, G., Yue, T., Jia, J., Briscoe, J., and Jiang, J. 2011b. Sonic Hedgehog dependent Phosphorylation by CK1 $\alpha$  and GRK2 is required for Ciliary Accumulation and Activation of Smoothed. *PLoS Biol* **9**(6). doi:10.1371/journal.pbio.1001083.

- Chen, Y., and Struhl, G. 1996. Dual roles for patched in sequestering and transducing Hedgehog. *Cell* **87**(3): 553–563. doi:10.1016/S0092-8674(00)81374-4.
- Chen, Y., Yue, S., Xie, L., Pu, X.H., Jin, T., and Cheng, S.Y. 2011c. Dual phosphorylation of suppressor of fused (Sufu) by PKA and GSK3 $\beta$  regulates its stability and localization in the primary cilium. *Journal of Biological Chemistry* **286**(15): 13502–13511. doi:10.1074/jbc.M110.217604.
- Cheng, S.Y., and Bishop, J.M. 2002. Suppressor of Fused represses Gli-mediated transcription by recruiting the SAP18-mSin3 corepressor complex. *Proc Natl Acad Sci U S A* **99**(8): 5442–7. doi:10.1073/pnas.082096999.
- Chesnutt, C., Burrus, L.W., Brown, A.M.C., and Niswander, L. 2004. Coordinate regulation of neural tube patterning and proliferation by TGF $\beta$  and WNT activity. *Dev Biol* **274**(2): 334–347. doi:10.1016/j.ydbio.2004.07.019.
- Chiang, C., Litington, Y., Lee, E., Young, K.E., Corden, J.L., Westphal, H., and Beachy, P.A. 1996. Cyclopia and defective axial patterning in mice lacking Sonic hedgehog gene function. *Nature* **383**: 407–413.
- Christ, A., Christa, A., Kur, E., Lioubinski, O., Bachmann, S., Willnow, T.E., and Hammes, A. 2012. LRP2 Is an Auxiliary SHH Receptor Required to Condition the Forebrain Ventral Midline for Inductive Signals. *Dev Cell* **22**(2): 268–278. Elsevier Inc. doi:10.1016/j.devcel.2011.11.023.
- Chuang, P.T., Kawcak, T., and McMahon, A.P. 2003. Feedback control of mammalian Hedgehog signaling by the Hedgehog-binding protein, Hip1, modulates Fgf signaling during branching morphogenesis of the lung. *Genes Dev* **17**(3): 342–347. doi:10.1101/gad.1026303.
- Chung, W.S., Allen, N.J., and Eroglu, C. 2015. Astrocytes control synapse formation, function, and elimination. *Cold Spring Harb Perspect Biol* **7**(9). Cold Spring Harbor Laboratory Press. doi:10.1101/cshperspect.a020370.
- Clark, A.M., Garland, K.K., and Russell, L.D. 2000. Desert hedgehog (Dhh) gene is required in the mouse testis for formation of adult-type Leydig cells and normal development of peritubular cells and seminiferous tubules. *Biol Reprod* **63**(6): 1825–1838. doi:10.1095/biolreprod63.6.1825.
- Cohen, M.A., Itsykson, P., and Reubinoff, B.E. 2010. The role of FGF-signaling in early neural specification of human embryonic stem cells. *Dev Biol* **340**(2): 450–458. doi:10.1016/j.ydbio.2010.01.030.The.

- Concordet, J.P., Lewis, K.E., Moore, J.W., Goodrich, L. V., Johnson, R.L., Scott, M.P., and Ingham, P.W. 1996. Spatial regulation of a zebrafish patched homologue reflects the roles of sonic hedgehog and protein kinase A in neural tube and somite patterning. *Development* **122**(9): 2835–2846. doi:10.1242/dev.122.9.2835.
- Cooper, A.F., Yu, K.P., Brueckner, M., Brailey, L.L., Johnson, L., McGrath, J.M., and Bale, A.E. 2005. Cardiac and CNS defects in a mouse with targeted disruption of suppressor of fused. *Development* **132**(19): 4407–4417. doi:10.1242/dev.02021.
- del Corral, R.D., Breitkreuz, D.N., and Storey, K.G. 2002. Onset of neuronal differentiation is regulated by paraxial mesoderm and requires attenuation of FGF signalling. *Development* **169**1: 1681–1691.
- del Corral, R.D., Olivera-Martinez, I., Goriely, A., Gale, E., Maden, M., and Storey, K. 2003. Opposing FGF and retinoid pathways control ventral neural pattern, neuronal differentiation and segmentation during body axis extension. *Cell Press* **40**: 65–79.
- Costa, S.L., and McBurney, M.W. 1996. Dominant negative mutant of retinoic acid receptor $\alpha$  inhibits retinoic acid-induced P19 cell differentiation by binding to DNA. *Exp Cell Res* **225**: 35–43. doi:10.1006/excr.1996.0154.
- Cox, B., Briscoe, J., and Ulloa, F. 2010. SUMOylation by *pias1* regulates the activity of the hedgehog dependent gli transcription factors. *PLoS One* **5**(8). doi:10.1371/journal.pone.0011996.
- Creanga, A., Glenn, T.D., Mann, R.K., Saunders, A.M., Talbot, W.S., and Beachy, P.A. 2012. *Scube/You* activity mediates release of dually lipid-modified Hedgehog signal in soluble form. *Genes Dev* **26**(12): 1312–1325. doi:10.1101/gad.191866.112.
- Cunningham, T.J., Brade, T., Sandell, L.L., Lewandoski, M., Trainor, P.A., Colas, A., Mercola, M., and Duester, G. 2015. Retinoic acid activity in undifferentiated neural progenitors is sufficient to fulfill its role in restricting *Fgf8* expression for somitogenesis. *PLoS One* **10**(9): 1–15. doi:10.1371/journal.pone.0137894.
- Cunningham, T.J., and Duester, G. 2015. Mechanisms of retinoic acid signalling and its roles in organ and limb development. *Nat Rev Mol Cell Biol* **16**(2): 110–123. Nature Publishing Group. doi:10.1038/nrm3932.
- Cwinn, M.A., Mazerolle, C., McNeill, B., Ringuette, R., Thurig, S., Hui, C.C., and Wallace, V.A. 2011. Suppressor of fused is required to maintain the multipotency of neural progenitor cells in the retina. *Journal of Neuroscience* **31**(13): 5169–5180. doi:10.1523/JNEUROSCI.5495-10.2011.
- Dai, P., Akimaru, H., Tanaka, Y., Maekawa, T., Nakafuku, M., and Ishii, S. 1999. Sonic hedgehog-induced activation of the *Gli1* promoter is mediated by *GLI3*. *Journal of Biological Chemistry* **274**(12): 8143–8152. © 1999 ASBMB. Currently published

by Elsevier Inc; originally published by American Society for Biochemistry and Molecular Biology. doi:10.1074/jbc.274.12.8143.

- Das, T.K., Dana, D., Paroly, S.S., Perumal, S.K., Singh, S., Jhun, H., Pendse, J., Cagan, R.L., Talele, T.T., and Kumar, S. 2013. Centrosomal kinase Nek2 cooperates with oncogenic pathways to promote metastasis. *Oncogenesis* **2**(9): e69-14. Nature Publishing Group. doi:10.1038/oncis.2013.34.
- Deng, L., Sun, J., Chen, X., Liu, L., and Wu, D. 2019. Nek2 augments sorafenib resistance by regulating the ubiquitination and localization of  $\beta$ -catenin in hepatocellular carcinoma. *J Exp Clin Cancer Res* **38**(1): 316. *Journal of Experimental & Clinical Cancer Research*. doi:10.1186/s13046-019-1311-z.
- Dennis, J.F., Kurosaka, H., Iulianella, A., Pace, J., Thomas, N., Beckham, S., Williams, T., and Trainor, P.A. 2012. Mutations in Hedgehog Acyltransferase (Hhat) Perturb Hedgehog Signaling, Resulting in Severe Acrania-Holoprosencephaly-Agnathia Craniofacial Defects. *PLoS Genet* **8**(10). doi:10.1371/journal.pgen.1002927.
- Dijksterhuis, J.P., Baljinnyam, B., Stanger, K., Sercan, H.O., Ji, Y., Andres, O., Rubin, J.S., Hannoush, R.N., and Schulte, G. 2015. Systematic mapping of WNT-FZD protein interactions reveals functional selectivity by distinct WNT-FZD pairs. *Journal of Biological Chemistry* **290**(11): 6789–6798. © 2015 ASBMB. Currently published by Elsevier Inc; originally published by American Society for Biochemistry and Molecular Biology. doi:10.1074/jbc.M114.612648.
- Ding, Q., Fukami, S.I., Meng, X., Nishizaki, Y., Zhang, X., Sasaki, H., Dlugosz, A., Nakafuku, M., and Hui, C.C. 1999. Mouse suppressor of fused is a negative regulator of Sonic hedgehog signaling and alters the subcellular distribution of Gli1. *Current Biology* **9**(19): 1119–1122. doi:10.1016/S0960-9822(99)80482-5.
- Ding, Q., Motoyama, J., Gasca, S., Mo, R., Sasaki, H., Rossant, J., and Hui, C. 1998. Diminished Sonic hedgehog signaling and lack of floor plate differentiation in Gli2 mutant mice. *Development* **125**: 2533–2543. doi:10.1242/dev.125.14.2533.
- Dominguez, I., Degano, I.R., Chea, K., Cha, J., Toselli, P., and Seldin, D.C. 2011. CK2 $\alpha$  is essential for embryonic morphogenesis. *Mol Cell Biochem* **356**(1–2): 209–216. doi:10.1007/s11010-011-0961-8.
- Doubravaska, L., Krausova, M., Gradl, D., Vojtechova, M., Tumova, L., Lukas, J., Valenta, T., Pospichalova, V., Fafulek, B., Plachy, J., Sebesta, O., and Korinek, V. 2011. Fatty acid modification of Wnt1 and Wnt3a at serine is prerequisite for lipidation at cysteine and is essential for Wnt signalling. *Cell Signal* **23**(5): 837–848. doi:10.1016/j.cellsig.2011.01.007.

- Dworkin, S., Boglev, Y., Owens, H., and Goldie, S.J. 2016. The role of Sonic hedgehog in craniofacial patterning, morphogenesis and cranial neural crest survival. *J Dev Biol* **4**(3). doi:10.3390/jdb4030024.
- Dyer, M. a, Farrington, S.M., Mohn, D., Munday, J.R., and Baron, M.H. 2001. Indian hedgehog activates hematopoiesis and vasculogenesis and can respecify prospective neurectodermal cell fate in the mouse embryo. *Development* **128**(10): 1717–1730.
- Echelard, Y., Epstein, D.J., St-Jacques, B., Shen, L., Mohler, J., McMahon, J.A., and McMahon, A.P. 1993. Sonic hedgehog, a member of a family of putative signaling molecules, is implicated in the regulation of CNS polarity. *Cell* **75**(7): 1417–1430. doi:10.1016/0092-8674(93)90627-3.
- Edwards, M.K.S., and McBurney, M.W. 1983. The concentration of retinoic acid determines the differentiated cell types formed by a teratocarcinoma cell line. *Dev Biol* **98**: 187–191. doi:10.1016/0012-1606(83)90348-2.
- Ekker, S.C., Ungar, A.R., Greenstein, P., von Kessler, D.P., Porter, J.A., Moon, R.T., and Beachy, P.A. 1995. Patterning activities of vertebrate hedgehog proteins in the developing eye and brain. *Current Biology* **5**(8): 944–955. doi:10.1016/S0960-9822(95)00185-0.
- Ericson, J., Morton, S., Kawakami, A., Roelink, H., and Jessell, T.M. 1996. Two critical periods of Sonic Hedgehog signaling required for the specification of motor neuron identity. *Cell* **87**(4): 661–673. doi:10.1016/S0092-8674(00)81386-0.
- Ericson, J., Rashbass, P., Schedl, A., Brenner-Morton, S., Kawakami, A., Van Heyningen, V., Jessell, T.M., and Briscoe, J. 1997. Pax6 controls progenitor cell identity and neuronal fate in response to graded Shh signaling. *Cell* **90**(1): 169–180. doi:10.1016/S0092-8674(00)80323-2.
- Fan, C.M., Porter, J.A., Chiang, C., Chang, D.T., Beachy, P.A., and Tessier-Lavigne, M. 1995. Long-range sclerotome induction by sonic hedgehog: Direct role of the amino-terminal cleavage product and modulation by the cyclic AMP signaling pathway. *Cell* **81**(3): 457–465. doi:10.1016/0092-8674(95)90398-4.
- Farin, H.F., Jordens, I., Mosa, M.H., Basak, O., Korving, J., Tauriello, D.V.F., De Punder, K., Angers, S., Peters, P.J., Maurice, M.M., and Clevers, H. 2016. Visualization of a short-range Wnt gradient in the intestinal stem-cell niche. *Nature* **530**(7590): 340–343. Nature Publishing Group. doi:10.1038/nature16937.
- Fiedler, M., Mendoza-Topaz, C., Rutherford, T.J., Mieszczanek, J., and Bienz, M. 2011. Dishevelled interacts with the DIX domain polymerization interface of Axin to interfere with its function in down-regulating  $\beta$ -catenin. *Proc Natl Acad Sci U S A* **108**(5): 1937–1942. doi:10.1073/pnas.1017063108.

- Fry, A.M. 2002. The Nek2 protein kinase: A novel regulator of centrosome structure. *Oncogene* **21**(40 REV. ISS. 4): 6184–6194. doi:10.1038/sj.onc.1205711.
- Fu, F., Li, L.S., Li, R., Deng, Q., Yu, Q.X., Yang, X., Pan, M., Han, J., Zhen, L., Zhang, L.N., Lei, T.Y., Li, D.Z., and Liao, C. 2020. All-trans-retinoid acid induces the differentiation of P19 cells into neurons involved in the PI3K/Akt/GSK3 $\beta$  signaling pathway. *J Cell Biochem* **121**(11): 4386–4396. doi:10.1002/jcb.29659.
- Gaiano, N., and Fishell, G. 2002. The role of Notch in promoting glial and neural stem cell fates. *Annu Rev Neurosci* **25**: 471–490. doi:10.1146/annurev.neuro.25.030702.130823.
- Gallera, J. 1971. Primary induction in birds. *Adv Morphog* **9**: 149–180. United States. doi:10.1016/b978-0-12-028609-6.50008-x.
- Gallet, A., Rodriguez, R., Ruel, L., and Therond, P.P. 2003. Cholesterol modification of Hedgehog is required for trafficking and movement, revealing an asymmetric cellular response to Hedgehog. *Dev Cell* **4**(2): 191–204. doi:10.1016/S1534-5807(03)00031-5.
- Galli, L.M., Barnes, T.L., Secrest, S.S., Kadowaki, T., and Burrus, L.W. 2007. Porcupine-mediated lipid-modification regulates the activity and distribution of Wnt proteins in the chick neural tube. *Development* **134**(18): 3339–3348. doi:10.1242/dev.02881.
- Garcia-Morales, C., Liu, C.H., Abu-Elmagd, M., Hajihosseini, M.K., and Wheeler, G.N. 2009. Frizzled-10 promotes sensory neuron development in *Xenopus* embryos. *Dev Biol* **335**(1): 143–155. Elsevier Inc. doi:10.1016/j.ydbio.2009.08.021.
- Gazea, M., Tasouri, E., Tolve, M., Bosch, V., Kabanova, A., Gojak, C., Kurtulmus, B., Novikov, O., Spatz, J., Pereira, G., Hübner, W., Brodski, C., Tucker, K.L., and Blaess, S. 2016. Primary cilia are critical for Sonic hedgehog-mediated dopaminergic neurogenesis in the embryonic midbrain. *Dev Biol* **409**(1): 55–71. Elsevier. doi:10.1016/j.ydbio.2015.10.033.
- Ghyselinck, N.B., and Duester, G. 2019. Retinoic acid signaling pathways. *Development* **146**: dev167502. doi:10.1242/dev.167502.
- Gibbs, H.C., Chang-Gonzalez, A., Hwang, W., Yeh, A.T., and Lekven, A.C. 2017. Midbrain-Hindbrain Boundary Morphogenesis: At the Intersection of Wnt and Fgf Signaling. *Front Neuroanat* **11**: 1–17. doi:10.3389/fnana.2017.00064.
- Goetz, J.A., Singh, S., Suber, L.M., Kull, F.J., and Robbins, D.J. 2006. A highly conserved amino-terminal region of Sonic Hedgehog is required for the formation of its freely diffusible multimeric form. *Journal of Biological Chemistry* **281**(7): 4087–4093. © 2006 ASBMB. Currently published by Elsevier Inc; originally published

- by American Society for Biochemistry and Molecular Biology.  
doi:10.1074/jbc.M511427200.
- Golden, J.A., and Chernoff, G.F. 1993. Intermittent pattern of neural tube closure in two strains of mice. *Teratology* **47**(1): 73–80. doi:10.1002/tera.1420470112.
- Goodrich, L. V., Johnson, R.L., Milenkovic, L., McMahon, J.A., and Scott, M.P. 1996. Conservation of the hedgehog/patched signaling pathway from flies to mice: Induction of a mouse patched gene by Hedgehog. *Genes Dev* **10**(3): 301–312. doi:10.1101/gad.10.3.301.
- Goodrich, L. V., Jung, D., Higgins, K.M., and Scott, M.P. 1999. Overexpression of *ptc1* inhibits induction of Shh target genes and prevents normal patterning in the neural tube. *Dev Biol* **211**(2): 323–334. doi:10.1006/dbio.1999.9311.
- Goodrich, L. V., Milenković, L., Higgins, K.M., and Scott, M.P. 1997. Altered neural cell fates and medulloblastoma in mouse patched mutants. *Science* (1979) **277**(5329): 1109–1113. doi:10.1126/science.277.5329.1109.
- Grandbarbe, L., Bouissac, J., Rand, M., Hrabé de Angelis, M., Artavanis-Tsakonas, S., and Mohier, E. 2003. Delta-Notch signaling controls the generation of neurons/glia from neural stem cells in a stepwise process. *Development* **130**(7): 1391–1402. doi:10.1242/dev.00374.
- Gray, J.D., Kholmanskikh, S., Castaldo, B.S., Hansler, A., Chung, H., Klotz, B., Singh, S., Brown, A.M.C., and Ross, M.E. 2013. LRP6 exerts non-canonical effects on Wnt signaling during neural tube closure. *Hum Mol Genet* **22**(21): 4267–4281. doi:10.1093/hmg/ddt277.
- Gray, S.D., and Dale, J.K. 2010. Notch signalling regulates the contribution of progenitor cells from the chick Hensen's node to the floor plate and notochord. *Development* **137**(4): 561–568. doi:10.1242/dev.041608.
- Greber, B., Coulon, P., Zhang, M., Moritz, S., Frank, S., Müller-Molina, A.J., Araúzo-Bravo, M.J., Han, D.W., Pape, H.C., and Schöler, H.R. 2011. FGF signalling inhibits neural induction in human embryonic stem cells. *EMBO Journal* **30**(24): 4874–4884. doi:10.1038/emboj.2011.407.
- Griffin, J.D., Artavanis-Tsakonas, S., Lake, R., Blacklow, S.C., Aster, J.C., and Wu, L. 2000. MAML1, a human homologue of *Drosophila* mastermind, is a transcriptional co-activator for NOTCH receptors. *Nat Genet* **26**(4): 484–489.
- Gritli-Linde, A., Lewis, P., McMahon, A.P., and Linde, A. 2001. The whereabouts of a morphogen: Direct evidence for short- and graded long-range activity of Hedgehog signaling peptides. *Dev Biol* **236**(2): 364–386. doi:10.1006/dbio.2001.0336.



- Gross, J.C., Chaudhary, V., Bartscherer, K., and Boutros, M. 2012. Active Wnt proteins are secreted on exosomes. *Nat Cell Biol* **14**(10): 1036–1045. Nature Publishing Group. doi:10.1038/ncb2574.
- Grover, V.K., Valadez, J.G., Bowman, A.B., and Cooper, M.K. 2011. Lipid modifications of Sonic hedgehog ligand dictate cellular reception and signal response. *PLoS One* **6**(7): 1–12. doi:10.1371/journal.pone.0021353.
- Gu, Z., Xia, J., Xu, H., Frech, I., Tricot, G., and Zhan, F. 2017. NEK2 promotes aerobic glycolysis in multiple myeloma through regulating splicing of pyruvate kinase. *J Hematol Oncol* **10**: 1–11. *Journal of Hematology & Oncology*. doi:10.1186/s13045-017-0392-4.
- Gustafsson, M. V., Zheng, X., Pereira, T., Gradin, K., Jin, S., Lundkvist, J., Ruas, J.L., Poellinger, L., Lendahl, U., and Bondesson, M. 2005. Hypoxia requires Notch signaling to maintain the undifferentiated cell state. *Dev Cell* **9**(5): 617–628. doi:10.1016/j.devcel.2005.09.010.
- Hamblet, N.S., Lijam, N., Ruiz-Lozano, P., Wang, J., Yang, Y., Luo, Z., Mei, L., Chien, K.R., Sussman, D.J., and Wynshaw-Boris, A. 2002. Dishevelled 2 is essential for cardiac outflow tract development, somite segmentation and neural tube closure. *Development* **129**(24): 5827–5838. doi:10.1242/dev.00164.
- Haycraft, C.J., Banizs, B., Aydin-Son, Y., Zhang, Q., Michaud, E.J., and Yoder, B.K. 2005. Gli2 and Gli3 localize to cilia and require the intraflagellar transport protein Polaris for processing and function. *PLoS Genet* **1**(4): e53. doi:10.1371/journal.pgen.0010053.
- He, T.C., Sparks, A.B., Rago, C., Hermeking, H., Zawel, L., Da Costa, L.T., Morin, P.J., Vogelstein, B., and Kinzler, K.W. 1998. Identification of c-MYC as a target of the APC pathway. *Science (1979)* **281**(5382): 1509–1512. doi:10.1126/science.281.5382.1509.
- Hepker, J., Wang, Q.T., Motzny, C.K., Holmgren, R., and Orenic, T.V. 1997. *Drosophila cubitus interruptus* forms a negative feedback loop with and regulates expression of Hedgehog target genes. *Development* **124**(2): 549–558. doi:10.1242/dev.124.2.549.
- Hirabayashi, Y., Itoh, Y., Tabata, H., Nakajima, K., Akiyama, T., Masuyama, N., and Gotoh, Y. 2004. The Wnt/ $\beta$ -catenin pathway directs neuronal differentiation of cortical neural precursor cells. *Development* **131**(12): 2791–2801. doi:10.1242/dev.01165.
- Hitoshi, S., Alexson, T., Tropepe, V., Donoviel, D., Elia, A.J., Nye, J.S., Conlon, R.A., Mak, T.W., Bernstein, A., and Van Der Kooy, D. 2002. Notch pathway molecules are essential for the maintenance, but not the generation, of mammalian neural stem cells. *Genes Dev* **16**(7): 846–858. doi:10.1101/gad.975202.

- Hoelzl, M.A., Heby-Henricson, K., Bilousova, G., Rozell, B., Kuiper, R. V., Kasper, M., Toftgård, R., and Teglund, S. 2015. Suppressor of Fused Plays an Important Role in Regulating Mesodermal Differentiation of Murine Embryonic Stem Cells In Vivo. *Stem Cells Dev* **24**(21): 2547–2560. doi:10.1089/scd.2015.0050.
- Hoelzl, M.A., Heby-Henricson, K., Gerling, M., Dias, J.M., Kuiper, R. v., Trünkle, C., Bergström, Å., Ericson, J., Toftgård, R., and Teglund, S. 2017. Differential requirement of SUFU in tissue development discovered in a hypomorphic mouse model. *Dev Biol* **429**(1): 132–146. Elsevier Inc. doi:10.1016/j.ydbio.2017.06.037.
- Holowacz, T., and Sokol, S. 1999. FGF is required for posterior neural patterning but not for neural induction. *Dev Biol* **205**(2): 296–308. doi:10.1006/dbio.1998.9108.
- Hu, D., and Helms, J.A. 1999. The role of Sonic hedgehog in normal and abnormal craniofacial morphogenesis. *Development* **126**(21): 4873–4884. doi:10.1242/dev.126.21.4873.
- Huang, X., Litingtung, Y., and Chiang, C. 2007. Region-specific requirement for cholesterol modification of sonic hedgehog in patterning the telencephalon and spinal cord. *Development* **134**(11): 2095–2105. doi:10.1242/dev.000729.
- Hui, C., and Angers, S. 2011. Gli proteins in development and disease. *Annu Rev Cell Dev Biol* **27**(1): 513–537. doi:10.1146/annurev-cellbio-092910-154048.
- Humke, E.W., Dorn, K. V., Milenkovic, L., Scott, M.P., and Rohatgi, R. 2010. The output of Hedgehog signaling is controlled by the dynamic association between Suppressor of Fused and the Gli proteins. *Genes Dev* **24**(7): 670–682. doi:10.1101/gad.1902910.
- Hynes, M., Porter, J.A., Chiang, C., Chang, D., Tessier-Lavigne, M., Beachy, P.A., and Rosenthal, A. 1995. Induction of midbrain dopaminergic neurons by Sonic hedgehog. *Neuron* **15**(1): 35–44. doi:10.1016/0896-6273(95)90062-4.
- Ikeya, M., Lee, S.M.K., Johnson, J.E., McMahon, A.P., and Takada, S. 1997. Wnt signalling required for expansion of neural crest and cns progenitors. *Nature* **389**(6654): 966–970. doi:10.1038/40146.
- Infante, P., Faedda, R., Bernardi, F., Bufalieri, F., Severini, L.L., Alfonsi, R., Mazzà, D., Siler, M., Coni, S., Po, A., Petroni, M., Ferretti, E., Mori, M., De Smaele, E., Canettieri, G., Capalbo, C., Maroder, M., Screpanti, I., Kool, M., Pfister, S.M., Guardavaccaro, D., Gulino, A., and Di Marcotullio, L. 2018. Itch/ $\beta$ -Arrestin2-dependent non-proteolytic ubiquitylation of SuFu controls Hedgehog signalling and medulloblastoma tumorigenesis. *Nat Commun* **9**: 976. doi:10.1038/s41467-018-03339-0.

- Ingham, P.W., Taylor, A.M., and Nakano, Y. 1991. Role of the *Drosophila* patched gene in positional signalling. *Nature* **353**(6340): 184–187. doi:10.1038/353184a0.
- Iulianella, A., Sakai, D., Kurosaka, H., and Trainor, P.A. 2018. Ventral neural patterning in the absence of Shh activity gradient from the floor plate. *Developmental Dynamics* **247**(1): 170–184. doi:10.1002/dvdy.24590.Ventral.
- Janda, C.Y., Dang, L.T., You, C., Chang, J., Lau, W. De, Zhong, Z.A., Yan, K.S., Marecic, O., Siepe, Di., Li, X., Moody, J.D., Williams, B.O., Clevers, H., Piehler, J., Baker, D., Kuo, C.J., and Garcia, K.C. 2017. Surrogate Wnt agonists that phenocopy canonical Wnt and  $\beta$ -catenin signalling. *Nature* **545**(7653): 234–237. Nature Publishing Group. doi:10.1038/nature22306.
- Janda, C.Y., Waghray, D., Levin, A.M., Thomas, C., and Garcia, K.C. 2012. Structural basis of Wnt recognition by frizzled. *Science* (1979) **336**(6090): 59–64. doi:10.1126/science.1222879.
- Jeong, M.H., Ho, S.M., Vuong, T.A., Jo, S.B., Liu, G., Aaronson, S.A., Leem, Y.E., and Kang, J.S. 2014. Cdo suppresses canonical Wnt signalling via interaction with Lrp6 thereby promoting neuronal differentiation. *Nat Commun* **5**. Nature Publishing Group. doi:10.1038/ncomms6455.
- Jia, H., Liu, Y., Xia, R., Tong, C., Yue, T., Jiang, J., and Jia, J. 2010. Casein kinase 2 promotes Hedgehog signaling by regulating both smoothed and Cubitus interruptus. *Journal of Biological Chemistry* **285**(48): 37218–37226. doi:10.1074/jbc.M110.174565.
- Jia, J., Zhang, L., Zhang, Q., Tong, C., Wang, B., Hou, F., Amanai, K., and Jiang, J. 2005. Phosphorylation by double-time/CKI $\epsilon$  and CKI $\alpha$  targets Cubitus Interruptus for Slimb/ $\beta$ -TRCP-mediated proteolytic processing. *Dev Cell* **9**(6): 819–830. doi:10.1016/j.devcel.2005.10.006.
- Jian, F., Sun, Y., Sun, Q., Zhang, B., and Bian, L. 2021. NEK2 regulates cellular proliferation and cabergoline sensitivity in pituitary adenomas. *J Cancer* **12**(7): 2083–2091. doi:10.7150/jca.52937.
- Jiang, Y., Luo, W., and Howe, P.H. 2009. Dab2 stabilizes Axin and attenuates Wnt/ $\beta$ -catenin signaling by preventing protein phosphatase (PP1)-Axin interactions. *Oncogene* **28**(33): 2999–3007. doi:10.1038/onc.2009.157.Dab2.
- Jing, X.T., Wu, H.T., Wu, Y., Ma, X., Liu, S.H., Wu, Y.R., Ding, X.F., Peng, X.Z., Qiang, B.Q., Yuan, J.G., Fan, W.H., and Fan, M. 2009. DIXDC1 promotes retinoic acid-induced neuronal differentiation and inhibits gliogenesis in P19 cells. *Cell Mol Neurobiol* **29**(1): 55–67. doi:10.1007/s10571-008-9295-9.

- Jones-Villeneuve, E.M., McBurney, M.W., Rogers, K.A., and Kalnins, V.I. 1982. Retinoic acid induces embryonal carcinoma cells to differentiate into neurons and glial cells. *J Cell Biol* **94**(2): 253–262. doi:10.1083/jcb.94.2.253.
- Jones-Villeneuve, E.M., Rudnicki, M.A., Harris, J.F., and McBurney, M.W. 1983. Retinoic acid-induced neural differentiation of embryonal carcinoma cells. *Mol Cell Biol* **3**(12): 2271–2279. doi:10.1128/mcb.3.12.2271.
- Jonk, L.J.C., de Jonge, M.E.J., Kruyt, F.A.E., Mummery, C.L., van der Saag, P.T., and Kruijer, W. 1992. Aggregation and cell cycle dependent retinoic acid receptor mRNA expression in P19 embryonal carcinoma cells. *Mech Dev* **36**(3): 165–172. doi:10.1016/0925-4773(92)90067-T.
- Joseph Endicott, S., Basu, B., Khokha, M., and Brueckner, M. 2015. The nima-like kinase nek2 is a key switch balancing cilia biogenesis and resorption in the development of left-right asymmetry. *Development (Cambridge)* **142**(23): 4068–4079. doi:10.1242/dev.126953.
- Juriloff, D.M., and Harris, M.J. 2000. Mouse models for neural tube closure defects. *Hum Mol Genet* **9**(6): 993–1000. doi:10.1093/hmg/9.6.993.
- Kadowaki, T., Wilder, E., Klingensmith, J., Zachary, K., and Perrimon, N. 1996. The segment polarity gene porcupine encodes a putative multitransmembrane protein involved in Wingless processing. *Genes Dev* **10**(24): 3116–3128. doi:10.1101/gad.10.24.3116.
- Karfunkel, P. 1972. The activity of microtubules and microfilaments in neurulation in the chick. *Journal of Experimental Zoology* **181**(3): 289–301. doi:10.1002/jez.1401810302.
- Karkoulias, G., McCrink, K.A., Maning, J., Pollard, C.M., Desimine, V.L., Patsouras, N., Psallidopoulos, M., Taraviras, S., Lymperopoulos, A., and Flordellis, C. 2020. Sustained GRK2-dependent CREB activation is essential for  $\alpha$ 2-adrenergic receptor-induced PC12 neuronal differentiation. *Cell Signal* **66**(August 2019): 109446. Elsevier. doi:10.1016/j.cellsig.2019.109446.
- Karlstrom, R.O., Tyurina, O. V., Kawakami, A., Nishioka, N., Talbot, W.S., Sasaki, H., and Schier, A.F. 2003. Genetic analysis of zebrafish gli1 and gli2 reveals divergent requirements for gli genes in vertebrate development. *Development* **130**(8): 1549–1564. doi:10.1242/dev.00364.
- Ke, Z., Kondrichin, I., Gong, Z., and Korzh, V. 2008. Combined activity of the two Gli2 genes of zebrafish play a major role in Hedgehog signaling during zebrafish neurodevelopment. *Molecular and Cellular Neuroscience* **37**(2): 388–401. doi:10.1016/j.mcn.2007.10.013.

- Kelly, G.M., and Gatie, M.I. 2017. Mechanisms Regulating Stemness and Differentiation in Embryonal Carcinoma Cells. *Stem Cells Int* **2017**. doi:10.1155/2017/3684178.
- Kibar, Z., Vogan, K.J., Groulx, N., Justice, M.J., Underhill, D.A., and Gros, P. 2001. Ltap, a mammalian homolog of *Drosophila* Strabismus/Van Gogh, is altered in the mouse neural tube mutant Loop-tail. *Nat Genet* **28**(3): 251–255. doi:10.1038/90081.
- Kim, J.J., Jiwani, T., Erwood, S., Loree, J., and Rosenblum, N.D. 2018. Suppressor of fused controls cerebellar neuronal differentiation in a manner modulated by GLI3 repressor and Fgf15. *Developmental Dynamics* **247**(1): 156–169. doi:10.1002/dvdy.24526.
- Kim, S.E., Huang, H., Zhao, M., Zhang, X., Zhang, A., Semonov, M. V., MacDonald, B.T., Zhang, X., Abreu, J.G., Peng, L., and He, X. 2013. Wnt stabilization of  $\beta$ -catenin reveals principles for morphogen receptor-scaffold assemblies. *Science* (1979) **340**(6134): 867–870. doi:10.1126/science.1232389.
- Kim, W.Y., Wang, X., Wu, Y., Doble, B.W., Patel, S., Woodgett, J.R., and Snider, W.D. 2009. GSK-3 is a master regulator of neural progenitor homeostasis. *Nat Neurosci* **12**(11): 1390–1397. doi:10.1038/nn.2408.
- Kinzler, K.W., and Vogelstein, B. 1990. The GLI gene encodes a nuclear protein which binds specific sequences in the human genome. *Mol Cell Biol* **10**(2): 634–642. doi:10.1128/mcb.10.2.634-642.1990.
- Kohler, E.M., Chandra, S.H.V., Behrens, J., and Schneikert, J. 2009.  $\beta$ -Catenin degradation mediated by the CID domain of APC provides a model for the selection of APC mutations in colorectal, desmoid and duodenal tumours. *Hum Mol Genet* **18**(2): 213–226. doi:10.1093/hmg/ddn338.
- Konitsiotis, A.D., Jovanović, B., Ciepla, P., Spitaler, M., Lanyon-Hogg, T., Tate, E.W., and Magee, A.I. 2015. Topological analysis of hedgehog acyltransferase, a multipalmitoylated transmembrane protein. *Journal of Biological Chemistry* **290**(6): 3293–3307. doi:10.1074/jbc.M114.614578.
- Krauss, S., Concordet, J.P., and Ingham, P.W. 1993. A functionally conserved homolog of the *Drosophila* segment polarity gene *hh* is expressed in tissues with polarizing activity in zebrafish embryos. *Cell* **75**(7): 1431–1444. doi:10.1016/0092-8674(93)90628-4.
- Kruyt, F.A.E., van der Veer, L.J., Mader, S., van den Brink, C.E., Feijen, A., Jonk, L.J.C., Kruijer, W., and van der Saag, P.T. 1992. Retinoic acid resistance of the variant embryonal carcinoma cell line RAC65 is caused by expression of a truncated RAR $\alpha$ . *Differentiation* **49**: 27–37. International Society of Differentiation. doi:10.1111/j.1432-0436.1992.tb00766.x.

- Lai, C.J., Ekker, S.C., Beachy, P.A., and Moon, R.T. 1995. Patterning of the neural ectoderm of *Xenopus laevis* by the amino-terminal product of hedgehog autoproteolytic cleavage. *Development* **121**(8): 2349–2360. doi:10.1242/dev.121.8.2349.
- Lamb, T.M., and Harland, R.M. 1995. Fibroblast growth factor is a direct neural inducer, which combined with noggin generates anterior-posterior neural pattern. *Development* **121**(11): 3627–3636. doi:10.1242/dev.121.11.3627.
- Lange, C., Mix, E., Frahm, J., Glass, Ä., Müller, J., Schmitt, O., Schmöle, A.C., Klemm, K., Ortinau, S., Hübner, R., Frech, M.J., Wree, A., and Rolfs, A. 2011. Small molecule GSK-3 inhibitors increase neurogenesis of human neural progenitor cells. *Neurosci Lett* **488**(1): 36–40. Elsevier Ireland Ltd. doi:10.1016/j.neulet.2010.10.076.
- Law, K.K. Lo, Makino, S., Mo, R., Zhang, X., Puviindran, V., and Hui, C. chung. 2012. Antagonistic and Cooperative Actions of Kif7 and Sufu Define Graded Intracellular Gli Activities in Hedgehog Signaling. *PLoS One* **7**(11): 3–10. doi:10.1371/journal.pone.0050193.
- Lebel, M., Mo, R., Shimamura, K., and Hui, C. chung. 2007. Gli2 and Gli3 play distinct roles in the dorsoventral patterning of the mouse hindbrain. *Dev Biol* **302**(1): 345–355. doi:10.1016/j.ydbio.2006.08.005.
- Lee, E.Y., Ji, H., Ouyang, Z., Zhou, B., Ma, W., Vokes, S.A., McMahon, A.P., Wong, W.H., and Scott, M.P. 2010. Hedgehog pathway-regulated gene networks in cerebellum development and tumorigenesis. *Proc Natl Acad Sci U S A* **107**(21): 9736–9741. doi:10.1073/pnas.1004602107.
- Lee, J., Platt, K.A., Censullo, P., and Ruiz I Altaba, A. 1997. Gli1 is a target of Sonic hedgehog that induces ventral neural tube development. *Development* **124**(13): 2537–2552. doi:10.1242/dev.124.13.2537.
- Lee, J.J., Ekker, S.C., Von Kessler, D.P., Porter, J.A., Sun, B.I., and Beachy, P.A. 1994. Autoproteolysis in hedgehog protein biogenesis. *Science* (1979) **266**(5190): 1528–1537. doi:10.1126/science.7985023.
- Lee, K.J., Dietrich, P., and Jessell, T.M. 2000. Genetic ablation reveals that the roof plate is essential for dorsal interneuron specification. *Nature* **403**(6771): 734–740. doi:10.1038/35001507.
- Lee, K.J., Mendelsohn, M., and Jessell, T.M. 1998. Neuronal patterning by BMPs: A requirement for GDF7 in the generation of a discrete class of commissural interneurons in the mouse spinal cord. *Genes Dev* **12**(21): 3394–3407. doi:10.1101/gad.12.21.3394.

- Lee, Y., Morrison, B.M., Li, Y., Lengacher, S., Farah, M.H., Hoffman, P.N., Liu, Y., Tsingalia, A., Jin, L., Zhang, P.W., Pellerin, L., Magistretti, P.J., and Rothstein, J.D. 2012. Oligodendroglia metabolically support axons and contribute to neurodegeneration. *Nature* **487**(7408): 443–448. doi:10.1038/nature11314.
- Lei, Q., Jeong, Y., Misra, K., Li, S., Zelman, A.K., Epstein, D.J., and Matisse, M.P. 2006. Wnt Signaling Inhibitors Regulate the Transcriptional Response to Morphogenetic Shh-Gli Signaling in the Neural Tube. *Dev Cell* **11**(3): 325–337. doi:10.1016/j.devcel.2006.06.013.
- Lesko, A.C., Keller, R., Chen, P., and Sutherland, A. 2021. Scribble mutation disrupts convergent extension and apical constriction during mammalian neural tube closure. *Dev Biol* **478**(January): 59–75. Elsevier Ltd. doi:10.1016/j.ydbio.2021.05.013.
- Li, S., Ma, G., Wang, B., and Jiang, J. 2014. Hedgehog induces formation of PKA-smoothed complexes to promote smoothed phosphorylation and pathway activation. *Sci Signal* **7**(332): 1–15. doi:10.1126/scisignal.2005414.
- Li, V.S.W., Ng, S.S., Boersema, P.J., Low, T.Y., Karthaus, W.R., Gerlach, J.P., Mohammed, S., Heck, A.J.R., Maurice, M.M., Mahmoudi, T., and Clevers, H. 2012. Wnt Signaling through Inhibition of  $\beta$ -Catenin Degradation in an Intact Axin1 Complex. *Cell* **149**(6): 1245–1256. Elsevier Inc. doi:10.1016/j.cell.2012.05.002.
- Liao, H., Cai, J., Liu, C., Shen, L., Pu, X., Yao, Y., Han, B., Yu, T., Cheng, S.Y., and Yue, S. 2020. Protein phosphatase 4 promotes Hedgehog signaling through dephosphorylation of Suppressor of fused. *Cell Death Dis* **11**(8). Springer US. doi:10.1038/s41419-020-02843-w.
- Liem, K.F., Tremml, G., Roelink, H., and Jessell, T.M. 1995. Dorsal differentiation of neural plate cells induced by BMP-mediated signals from epidermal ectoderm. *Cell* **82**(6): 969–979. doi:10.1016/0092-8674(95)90276-7.
- Lin, G., and Goldman, J.E. 2009. An FGF-responsive astrocyte precursor isolated from the neonatal forebrain. *Glia* **57**(6): 592–603. doi:10.1002/glia.20788.
- Lin, S., Zhou, S., Jiang, S., Liu, X., Wang, Y., Zheng, X., Zhou, H., Li, X., and Cai, X. 2016. NEK2 regulates stem-like properties and predicts poor prognosis in hepatocellular carcinoma. *Oncol Rep* **36**(2): 853–862. doi:10.3892/or.2016.4896.
- Litingtung, Y., and Chiang, C. 2000. Specification of ventral neuron types is mediated by an antagonistic interaction between Shh and Gli3. *Nat Neurosci* **3**(10): 979–985. doi:10.1038/79916.
- Liu, C., Li, Y., Semenov, M., Han, C., Baeg, G., Tan, Y., Zhang, Z., Lin, X., He, X., and Signaling, C. 2002. Control of B-Catenin Phosphorylation / Degradation by a Dual-Kinase Mechanism. *Cell* **108**: 837–847.

- Liu, H., Liu, B., Hou, X., Pang, B., Guo, P., Jiang, W., Ding, Q., Zhang, R., Xin, T., Guo, H., Xu, S., and Pang, Q. 2017. Overexpression of NIMA-related kinase 2 is associated with poor prognoses in malignant glioma. *J Neurooncol* **132**(3): 409–417. Springer US. doi:10.1007/s11060-017-2401-4.
- Liu, J.P., Laufer, E., and Jessell, T.M. 2001. Assigning the positional identity of spinal motor neurons: Rostrocaudal patterning of Hox-c expression by FGFs, Gdf11, and retinoids. *Neuron* **32**(6): 997–1012. doi:10.1016/S0896-6273(01)00544-X.
- Liu, X., Gao, Y., Lu, Y., Zhang, J., Li, L., and Yin, F. 2014. Upregulation of NEK2 is associated with drug resistance in ovarian cancer. *Oncol Rep* **31**(2): 745–754. doi:10.3892/or.2013.2910.
- López, S.L., Paganelli, A.R., Rosato Siri, M. V., Ocaña, O.H., Franco, P.G., and Carrasco, A.E. 2003. Notch activates sonic hedgehog and both are involved in the specification of dorsal midline cell-fates in *Xenopus*. *Development* **130**(10): 2225–2238. doi:10.1242/dev.00443.
- López-Martínez, A., Chang, D.T., Chiang, C., Porter, J.A., Ros, M.A., Simandl, B.K., Beachy, P.A., and Fallon, J.F. 1995. Limb-patterning activity and restricted posterior localization of the amino-terminal product of Sonic hedgehog cleavage. *Current Biology* **5**(7): 791–796. doi:10.1016/S0960-9822(95)00156-4.
- Lou, D.Y., Dominguez, I., Toselli, P., Landesman-Bollag, E., O'Brien, C., and Seldin, D.C. 2008. The Alpha Catalytic Subunit of Protein Kinase CK2 Is Required for Mouse Embryonic Development. *Mol Cell Biol* **28**(1): 131–139. doi:10.1128/mcb.01119-07.
- Lustig, B., Jerchow, B., Sachs, M., Weiler, S., Pietsch, T., Rarsten, U., Van De Wetering, M., Clevers, H., Schlag, P.M., Birchmeier, W., and Behrens, J. 2002. Negative feedback loop of Wnt signaling through upregulation of conductin/axin2 in colorectal and liver tumors. *Mol Cell Biol* **22**(4): 1184–1193. doi:10.1128/mcb.22.4.1184-1193.2002.
- Lyu, J., Costantini, F., Jho, E. hoon, and Joo, C. ki. 2003. Ectopic expression of axin blocks neuronal differentiation of embryonic carcinoma P19 cells. *Journal of Biological Chemistry* **278**(15): 13487–13495. doi:10.1074/jbc.M300591200.
- Ma, Y., Erkner, A., Gong, R., Yao, S., Taipale, J., Basler, K., and Beachy, P.A. 2002. Hedgehog-mediated patterning of the mammalian embryo requires transporter-like function of dispatched. *Cell* **111**(1): 63–75. doi:10.1016/S0092-8674(02)00977-7.
- Maden, M. 2007. Retinoic acid in the development, regeneration and maintenance of the nervous system. *Nat Rev Neurosci* **8**(10): 755–765. doi:10.1038/nrn2212.



- Maden, M., Sonneveld, E., Van der Saag, P.T., and Gale, E. 1998. The distribution of endogenous retinoic acid in the chick embryo: Implications for developmental mechanisms. *Development* **125**(21): 4133–4144. doi:10.1242/dev.125.21.4133.
- Magnuson, D.S.K., Morassutti, D.J., McBurney, M.W., and Marshall, K.C. 1995. Neurons derived from P19 embryonal carcinoma cells develop responses to excitatory and inhibitory neurotransmitters. *Developmental Brain Research* **90**(1–2): 141–150. doi:10.1016/0165-3806(96)83494-8.
- Maity, T., Fuse, N., and Beachy, P.A. 2005. Molecular mechanisms of Sonic hedgehog mutant effects in holoprosencephaly. *Proc Natl Acad Sci U S A* **102**(47): 17026–17031. doi:10.1073/pnas.0507848102.
- Malý, P., and Dráber, P. 1992. Retinoic acid-induced changes in differentiation-defective embryonal carcinoma RAC65 cells. *FEBS Lett* **311**(2): 102–106. doi:10.1016/0014-5793(92)81377-X.
- Mao, B., Wu, W., Li, Y., Stannek, P., Glinka, A., and Niehrs, C. 2001a. LDL-receptor-related protein 6 is a receptor for Dickkopf proteins. *Nature* **411**: 321–325.
- Mao, J., Wang, J., Liu, B., Pan, W., Farr, G.H., Flynn, C., Yuan, H., Takada, S., Kimelman, D., Li, L., and Wu, D. 2001b. Low-density lipoprotein receptor-related protein-5 binds to Axin and regulates the canonical Wnt signaling pathway. *Mol Cell* **7**(4): 801–809. doi:10.1016/S1097-2765(01)00224-6.
- Mao, Y., and Lee, A.W.M. 2005. A novel role for Gab2 in bFGF-mediated cell survival during retinoic acid-induced neuronal differentiation. *Journal of Cell Biology* **170**(2): 305–316. doi:10.1083/jcb.200505061.
- Marigo, V., Davey, R.A., Zuo, Y., Cunningham, J.M., and Tabin, C.J. 1996. Biochemical evidence that Patched is the Hedgehog receptor. *Nature* **384**: 176–179.
- Marti, E., Bumcrot, D.A., Takada, R., and McMahon, A.P. 1995. Requirement of 19K form of Sonic hedgehog for induction of distinct ventral cell types in CNS explants. *Nature* **375**: 322–325.
- Martins, T., Meghini, F., Florio, F., and Kimata, Y. 2017. The APC/C Coordinates Retinal Differentiation with G1 Arrest through the Nek2-Dependent Modulation of Wntless Signaling. *Dev Cell* **40**(1): 67–80. Elsevier Inc. doi:10.1016/j.devcel.2016.12.005.
- Mason, S. 2017, February 2. Lactate shuttles in neuroenergetics-homeostasis, allostasis and beyond. *Frontiers Research Foundation*. doi:10.3389/fnins.2017.00043.

- Mathis, L., Kulesa, P.M., and Fraser, S.E. 2001. FGF receptor signalling is required to maintain neural progenitors during Hensen's node progression. *Nat Cell Biol* **3**(6): 559–566. doi:10.1038/35078535.
- Mbom, B.C., Siemers, K.A., Ostrowski, M.A., Nelson, W.J., and Barth, A.I.M. 2014. Nek2 phosphorylates and stabilizes B-catenin at mitotic centrosomes downstream of Plk1. *Mol Biol Cell* **25**(7): 977–991. doi:10.1091/mbc.E13-06-0349.
- McBurney, M. 1993. P19 embryonal carcinoma cells. *International Journal of Developmental Biology* **140**: 135–140.
- McBurney, M.W., Reuhl, K.R., Ally, a I., Nasipuri, S., Bell, J.C., and Craig, J. 1988. Differentiation and maturation of embryonal carcinoma-derived neurons in cell culture. *The Journal of Neuroscience* **8**(3): 1063–73. doi:10.1523/JNEUROSCI.08-03-01063.1988.
- McBurney, M.W., and Rogers, B.J. 1982. Isolation of male embryonal carcinoma cells and their chromosome replication patterns. *Dev Biol* **89**(2): 503–508. doi:10.1016/0012-1606(82)90338-4.
- McGough, I.J., and Vincent, J.P. 2016. Exosomes in developmental signalling. *Development* **143**(14): 2482–2493. doi:10.1242/dev.126516.
- McKinnon, R.D., Matsui, T., Dubois-Dalcq, M., and Aaronson, S.A. 1990. FGF modulates the PDGF-driven pathway of oligodendrocyte development. *Neuron* **5**(5): 603–614. doi:10.1016/0896-6273(90)90215-2.
- McMahon, A.P., Joyner, A.L., Bradley, A., and McMahon, J.A. 1992. The midbrain-hindbrain phenotype of Wnt-1- Wnt-1- mice results from stepwise deletion of engrailed-expressing cells by 9.5 days postcoitum. *Cell* **69**(4): 581–595. doi:10.1016/0092-8674(92)90222-X.
- Metzler, M.A., and Sandell, L.L. 2016. Enzymatic metabolism of vitamin A in developing vertebrate embryos. *Nutrients* **8**(12): 1–21. doi:10.3390/nu8120812.
- Micchelli, C.A., The, I., Selva, E., Mogila, V., and Perrimon, N. 2002. rasp, a putative transmembrane acyltransferase, is required for Hedgehog. *Development* **129**(4): 843–851.
- Millonig, J.H., Millen, K.J., and Hatten, M.E. 2000. The mouse Dreher gene *Lmx1a* controls formation of the roof plate in the vertebrate CNS. *Nature* **403**(6771): 764–769. doi:10.1038/35001573.
- Molenaar, M., Van De Wetering, M., Oosterwegel, M., Peterson-Maduro, J., Godsave, S., Korinek, V., Roose, J., Destree, O., and Clevers, H. 1996. XTcf-3 transcription

- factor mediates  $\beta$ -catenin-induced axis formation in xenopus embryos. *Cell* **86**(3): 391–399. doi:10.1016/S0092-8674(00)80112-9.
- Molotkova, N., Molotkov, A., Sirbu, I.O., and Duester, G. 2005. Requirement of mesodermal retinoic acid generated by Raldh2 for posterior neural transformation. *Mech Dev* **122**(2): 145–155. doi:10.1016/j.mod.2004.10.008.
- Monzo, H.J., Park, T.I.H., Montgomery, J.M., Faull, R.L.M., Dragunow, M., and Curtis, M.A. 2012. A method for generating high-yield enriched neuronal cultures from P19 embryonal carcinoma cells. *J Neurosci Methods* **204**(1): 87–103. Elsevier B.V. doi:10.1016/j.jneumeth.2011.11.008.
- Moore, S., Meschkat, M., Ruhwedel, T., Trevisiol, A., Tzvetanova, I.D., Bettefeld, A., Kusch, K., Kole, M.H.P., Strenzke, N., Möbius, W., de Hoz, L., and Nave, K.A. 2020. A role of oligodendrocytes in information processing. *Nat Commun* **11**(1). Nature Research. doi:10.1038/s41467-020-19152-7.
- Morassutti, D.J., Staines, W.A., Magnuson, D.S.K., Marshall, K.C., and McBurney, M.W. 1994. Murine embryonal carcinoma-derived neurons survive and mature following transplantation into adult rat striatum. *Neuroscience* **58**(4): 753–763. doi:10.1016/0306-4522(94)90452-9.
- Motoyama, J., Milenkovic, L., Iwama, M., Shikata, Y., Scott, M.P., and Hui, C.C. 2003. Differential requirement for Gli2 and Gli3 in ventral neural cell fate specification. *Dev Biol* **259**(1): 150–161. doi:10.1016/S0012-1606(03)00159-3.
- Moutier, E., Ye, T., Choukrallah, M.A., Urban, S., Osz, J., Chatagnon, A., Delacroix, L., Langer, D., Rochel, N., Moras, D., Benoit, G., and Davidson, I. 2012. Retinoic acid receptors recognize the mouse genome through binding elements with diverse spacing and topology. *Journal of Biological Chemistry* **287**(31): 26328–26341. © 2012 ASBMB. Currently published by Elsevier Inc; originally published by American Society for Biochemistry and Molecular Biology. doi:10.1074/jbc.M112.361790.
- Murdoch, J.N., Doudney, K., Paternotte, C., Copp, A.J., and Stanier, P. 2001. Severe neural tube defects in the loop-tail mouse result from mutation of Lpp1, a novel gene involved in floor plate specification. *Hum Mol Genet* **10**(22): 2593–2601. doi:10.1093/hmg/10.22.2593.
- Muroyama, Y., Fujihara, M., Ikeya, M., Kondoh, H., and Takada, S. 2002. Wnt signaling plays an essential role in neuronal specification of the dorsal spinal cord. *Genes Dev* **16**(5): 548–553. doi:10.1101/gad.937102.
- Najdi, R., Proffitt, K., Sprowl, S., Kaur, S., Yu, J., Covey, T.M., Virshup, D.M., and Waterman, M.L. 2012. A uniform human Wnt expression library reveals a shared

- secretory pathway and unique signaling activities. *Differentiation* **84**(2): 203–213. Elsevier. doi:10.1016/j.diff.2012.06.004.
- Nave, K.A., and Werner, H.B. 2014. Myelination of the nervous system: Mechanisms and functions. *In Annual Review of Cell and Developmental Biology*. Annual Reviews Inc. pp. 503–533. doi:10.1146/annurev-cellbio-100913-013101.
- Nayak, D., Roth, T.L., and McGavern, D.B. 2014. Microglia development and function. *Annu Rev Immunol* **32**: 367–402. doi:10.1146/annurev-immunol-032713-120240.Microglia.
- Neal, C.P., Fry, A.M., Moreman, C., McGregor, A., Garcea, G., Berry, D.P., and Manson, M.M. 2014. Overexpression of the Nek2 kinase in colorectal cancer correlates with beta-catenin relocalization and shortened cancer-specific survival. *J Surg Oncol* **110**(7): 828–838. doi:10.1002/jso.23717.
- Nievelstein, R.A., Hartwig, N.G., Vermeij-Keers, C., and Valk, J. 1993. Embryonic development of the mammalian caudal neural tube. *Teratology* **48**(1): 21–31. United States. doi:10.1002/tera.1420480106.
- Niida, A., Hiroko, T., Kasai, M., Furukawa, Y., Nakamura, Y., Suzuki, Y., Sugano, S., and Akiyama, T. 2004. DKK1, a negative regulator of Wnt signaling, is a target of the  $\beta$ -catenin/TCF pathway. *Oncogene* **23**(52): 8520–8526. doi:10.1038/sj.onc.1207892.
- Nusse, R., and Clevers, H. 2017. Wnt/ $\beta$ -Catenin Signaling, Disease, and Emerging Therapeutic Modalities. *Cell* **169**(6): 985–999. Elsevier Inc. doi:10.1016/j.cell.2017.05.016.
- Nusse, R., and Varmus, H.E. 1982. Many tumors induced by the mouse mammary tumor virus contain a provirus integrated in the same region of the host genome. *Cell* **31**: 99–109. doi:https://doi.org/10.1016/0092-8674(82)90409-3.
- Paces-Fessy, M., Boucher, D., Petit, E., Paute-Briand, S., and Blanchet-Tournier, M.-F. 2004. The negative regulator of Gli, Suppressor of fused (Sufu), interacts with SAP18, Galectin3 and other nuclear proteins. *Biochemical Journal* **378**(2): 353–362. doi:10.1042/bj20030786.
- Pan, Y., Bai, C.B., Joyner, A.L., and Wang, B. 2006. Sonic hedgehog Signaling Regulates Gli2 Transcriptional Activity by Suppressing Its Processing and Degradation. *Mol Cell Biol* **26**(9): 3365–3377. doi:10.1128/mcb.26.9.3365-3377.2006.
- Pan, Y., Wang, C., and Wang, B. 2009. Phosphorylation of Gli2 by protein kinase A is required for Gli2 processing and degradation and the Sonic Hedgehog-regulated

- mouse development. *Dev Biol* **326**(1): 177–189. Elsevier Inc. doi:10.1016/j.ydbio.2008.11.009.
- Panáková, D., Sprong, H., Marois, E., Thiele, C., and Eaton, S. 2005. Lipoprotein particles are required for Hedgehog and Wingless signalling. *Nature* **435**(7038): 58–65. doi:10.1038/nature03504.
- Panchision, D.M., Pickel, J.M., Studer, L., Lee, S.H., Turner, P.A., Hazel, T.G., and McKay, R.D.G. 2001. Sequential actions of BMP receptors control neural precursor cell production and fate. *Genes Dev* **15**(16): 2094–2110. doi:10.1101/gad.894701.
- Park, H.L., Bai, C., Platt, K.A., Matise, M.P., Beeghly, A., Hui, C.-C., Nakashima, M., and Joyner, A.L. 2000. Mouse *Gli1* mutants are viable but have defects in SHH signaling in combination with a *Gli2* mutation. *Development* **127**: 1593–1605.
- Parr, B.A., Shea, M.J., Vassileva, G., and McMahon, A.P. 1993. Mouse Wnt genes exhibit discrete domains of expression in the early embryonic CNS and limb buds. *Development* **119**(1): 247–261. doi:10.1242/dev.119.1.247.
- Pepinsky, R.B., Zeng, C., Went, D., Rayhorn, P., Baker, D.P., Williams, K.P., Bixler, S.A., Ambrose, C.M., Garber, E.A., Miatkowski, K., Taylor, F.R., Wang, E.A., and Galdes, A. 1998. Identification of a palmitic acid-modified form of human Sonic hedgehog. *Journal of Biological Chemistry* **273**(22): 14037–14045. © 1998 ASBMB. Currently published by Elsevier Inc; originally published by American Society for Biochemistry and Molecular Biology. doi:10.1074/jbc.273.22.14037.
- Peters, C., Wolf, A., Wagner, M., Kuhlmann, J., and Waldmann, H. 2004. The cholesterol membrane anchor of the Hedgehog protein confers stable membrane association to lipid-modified proteins. *Proc Natl Acad Sci U S A* **101**(23): 8531–8536. doi:10.1073/pnas.0308449101.
- Peterson, K.A., Nishi, Y., Ma, W., Vedenko, A., Shokri, L., Zhang, X., McFarlane, M., Baizabal, J.M., Junker, J.P., van Oudenaarden, A., Mikkelsen, T., Bernstein, B.E., Bailey, T.L., Bulyk, M.L., Wong, W.H., and McMahon, A.P. 2012. Neural-specific *Sox2* input and differential *Gli*-binding affinity provide context and positional information in *Shh*-directed neural patterning. *Genes Dev* **26**(24): 2802–2816. doi:10.1101/gad.207142.112.
- Pinson, K.I., Brennan, J., Monkley, S., Avery, B.J., and Skarnes, W.C. 2000. An LDL-receptor-related protein mediates Wnt signalling in mice. *Nature* **407**: 535–538. doi:10.1038/35035124.
- Placzek, M., Tessier-Lavigne, M., Yamada, T., Jessell, T., and Dodd, J. 1990. Mesodermal control of neural cell identity: Floor plate induction by the notochord. *Science* (1979) **250**(4983): 985–988. doi:10.1126/science.2237443.

- Porter, J.A., von Kessler, D.P., Ekker, S.C., Young, K.E., Lee, J.J., Moses, K., and Beachy, P.A. 1995. The product of hedgehog autoproteolytic cleavage active in local and long-range signaling. *Nature* **374**: 363–374. doi:10.1038/374363a0.
- Porter, J.A., Young, K.E., and Beachy, P.A. 1996. Cholesterol Modification of Hedgehog Signaling Proteins in Animal Development. *Science* (1979) **274**(5285): 255–259.
- Pratt, M.A.C., Kralova, J., and Mcburney, M.W. 1990. Gene in a Retinoic Acid-Nonresponsive Embryonal Carcinoma Cell. *Mol Cell Biol* **10**(12): 6445–6453. doi:10.1128/mcb.10.12.6445.
- Pronobis, M.I., Rusan, N.M., and Peifer, M. 2015. A novel GSK3-regulated APC:Axin interaction regulates Wnt signaling by driving a catalytic cycle of efficient  $\beta$ catenin destruction. *Elife* **4**: e08022. doi:10.7554/eLife.08022.
- Raducu, M., Fung, E., Serres, S., Infante, P., Barberis, A., Fischer, R., Bristow, C., Thézénas, M., Finta, C., Christianson, J.C., Buffa, F.M., Kessler, B.M., Sibson, N.R., Di Marcotullio, L., Toftgård, R., and D'Angiolella, V. 2016. SCF (Fbx117) ubiquitylation of Sufu regulates Hedgehog signaling and medulloblastoma development. *EMBO J* **35**(13): 1400–1416. doi:10.15252/embj.201593374.
- Railo, A., Pajunen, A., Itäranta, P., Naillat, F., Vuoristo, J., Kilpeläinen, P., and Vainio, S. 2009. Genomic response to Wnt signalling is highly context-dependent - Evidence from DNA microarray and chromatin immunoprecipitation screens of Wnt/TCF targets. *Exp Cell Res* **315**(16): 2690–2704. Elsevier Inc. doi:10.1016/j.yexcr.2009.06.021.
- Ray, W.J., and Gottlieb, D.I. 1993. Expression of ionotropic glutamate receptor genes by P19 embryonal carcinoma cells. *Biochem Biophys Res Commun* **197**(3): 1475–1482. doi:10.1006/bbrc.1993.2643.
- Rellos, P., Ivins, F.J., Baxter, J.E., Pike, A., Nott, T.J., Parkinson, D.M., Das, S., Howell, S., Fedorov, O., Qi, Y.S., Fry, A.M., Knapp, S., and Smerdon, S.J. 2007. Structure and regulation of the human Nek2 centrosomal kinase. *Journal of Biological Chemistry* **282**(9): 6833–6842. © 2007 ASBMB. Currently published by Elsevier Inc; originally published by American Society for Biochemistry and Molecular Biology. doi:10.1074/jbc.M609721200.
- Ribisi, S., Mariani, F. V., Amar, E., Lamb, T.M., Frank, D., and Harland, R.M. 2000. Ras-mediated FGF signaling is required for the formation of posterior but not anterior neural tissue in *Xenopus laevis*. *Dev Biol* **227**(1): 183–196. doi:10.1006/dbio.2000.9889.
- Riddle, R.D., Johnson, R.L., Laufer, E., and Tabin, C. 1993. Sonic hedgehog mediates the polarizing activity of the ZPA. *Cell* **75**(7): 1401–1416. doi:10.1016/0092-8674(93)90626-2.

- Rios-Esteves, J., Haugen, B., and Resh, M.D. 2014. Identification of key residues and regions important for porcupine-mediated Wnt acylation. *Journal of Biological Chemistry* **289**(24): 17009–17019. © 2014 ASBMB. Currently published by Elsevier Inc; originally published by American Society for Biochemistry and Molecular Biology. doi:10.1074/jbc.M114.561209.
- Roberts, D.M., Pronobis, M.I., Poulton, J.S., Waldmann, J.D., Stephenson, E.M., Hanna, S., and Peifer, M. 2011. Deconstructing the  $\beta$ catenin destruction complex: Mechanistic roles for the tumor suppressor APC in regulating Wnt signaling. *Mol Biol Cell* **22**(11): 1845–1863. doi:10.1091/mbc.E10-11-0871.
- Roelink, H., Porter, J.A., Chiang, C., Tanabe, Y., Chang, D.T., Beachy, P.A., and Jessell, T.M. 1995. Floor plate and motor neuron induction by different concentrations of the amino-terminal cleavage product of sonic hedgehog autoproteolysis. *Cell* **81**(3): 445–455. doi:10.1016/0092-8674(95)90397-6.
- Roessler, E., Belloni, E., Gaudenz, K., Jay, P., Berta, P., Scherer, S.W., Tsui, L.-C., and Muenke, M. 1996. Mutations in the human Sonic Hedgehog gene cause holoprosencephaly. *Nat Genet* **14**: 357–360.
- Roessler, E., El-jaick, K.B., Dubourg, C., Vélez, J.I., Solomon, B.D., Pineda-Alvarez, D.E., Lachawan, F., Zhou, N., Ouspenskaia, M., Paulussen, A., Smeets, H.J., Hehr, U., Bendavid, C., Bale, S., Odent, S., David, V., and Muenke, M. 2009. The mutational spectrum of holoprosencephaly-associated changes within the Shh gene in humans predicts loss-of-function through either key structural alterations of the ligand or its altered synthesis. *Hum Mutat* **30**(10): E921–E935. doi:10.1002/humu.21090.The.
- Rolo, A., Escuin, S., Greene, N.D.E., and Copp, A.J. 2018. Rho GTPases in mammalian spinal neural tube closure. *Small GTPases* **9**(4): 283–289. Taylor & Francis. doi:10.1080/21541248.2016.1235388.
- Roose, J., Molenaar, M., Peterson, J., Hurenkamp, J., Brantjes, H., Moerer, P., Van De Wetering, M., Destrée, O., and Clevers, H. 1998. The *Xenopus* Wnt effector XTcf-3 interacts with Groucho-related transcriptional repressors. *Nature* **395**(6702): 608–612. doi:10.1038/26989.
- Ryoichiro, K., and Ohtshuka, T. 1999. The Notch-Hes pathway in mammalian neural development. *Cell Res* **9**: 179–188.
- Saab, A.S., Tzvetavona, I.D., Trevisiol, A., Baltan, S., Dibaj, P., Kusch, K., Möbius, W., Goetze, B., Jahn, H.M., Huang, W., Steffens, H., Schomburg, E.D., Pérez-Samartín, A., Pérez-Cerdá, F., Bakhtiari, D., Matute, C., Löwel, S., Griesinger, C., Hirrlinger, J., Kirchhoff, F., and Nave, K.A. 2016. Oligodendroglial NMDA Receptors

- Regulate Glucose Import and Axonal Energy Metabolism. *Neuron* **91**(1): 119–132. Cell Press. doi:10.1016/j.neuron.2016.05.016.
- Sahota, N., Sabir, S., O'Regan, L., Blot, J., Zalli, D., Baxter, J., Barone, G., and Fry, A. 2018. NEKs, NIMA-Related Kinases. *In* *Encyclopedia of Signaling Molecules*. Edited by S. Choi. Springer International Publishing, Cham. pp. 3407–3419. doi:10.1007/978-3-319-67199-4\_17.
- Sasaki, H., Nishizaki, Y., Hui, C.C., Nakafuku, M., and Kondoh, H. 1999. Regulation of Gli2 and Gli3 activities by an amino-terminal repression domain: Implication of Gli2 and Gli3 as primary mediators of Shh signaling. *Development* **126**(17): 3915–3924. doi:10.1242/dev.126.17.3915.
- Sato, T., and Nakamura, H. 2004. The Fgf8 signal causes cerebellar differentiation by activating the Ras-ERK signaling pathway. *Development* **131**(17): 4275–4285. doi:10.1242/dev.01281.
- Schäfer, M., Kinzel, D., Neuner, C., Schartl, M., Volf, J.N., and Winkler, C. 2005. Hedgehog and retinoid signalling confines nkx2.2b expression to the lateral floor plate of the zebrafish trunk. *Mech Dev* **122**(1): 43–56. doi:10.1016/j.mod.2004.09.002.
- Schmidt, J.W., Brugge, J.S., and Nelson, W.J. 1992. pp60src tyrosine kinase modulates P19 embryonal carcinoma cell fate by inhibiting neuronal but not epithelial differentiation. *Journal of Cell Biology* **116**(4): 1019–1033. doi:10.1083/jcb.116.4.1019.
- Schuldiner, M., Eiges, R., Eden, A., Yanuka, O., Itskovitz-Eldor, J., Goldstein, R.S., and Benvenisty, N. 2001. Induced neuronal differentiation of human embryonic stem cells. *Brain Res* **913**(2): 201–205. doi:10.1016/S0006-8993(01)02776-7.
- Schwarz-Romond, T., Fiedler, M., Shibata, N., Butler, P.J.G., Kikuchi, A., Higuchi, Y., and Bienz, M. 2007. The DIX domain of Dishevelled confers Wnt signaling by dynamic polymerization. *Nat Struct Mol Biol* **14**(6): 484–492. doi:10.1038/nsmb1247.
- Shago, M., Flock, G., Leung Hagesteijn, C.Y., Woodside, M., Grinstein, S., Giguère, V., and Dedhar, S. 1997. Modulation of the retinoic acid and retinoid X receptor signaling pathways in P19 embryonal carcinoma cells by calreticulin. *Exp Cell Res* **230**: 50–60. doi:10.1006/excr.1996.3408.
- Sharma, S., and Notter, M.F.D. 1988. Characterization of neurotransmitter phenotype during neuronal differentiation of embryonal carcinoma cells. *Dev Biol* **125**: 246–254. doi:10.1016/0012-1606(88)90208-4.



- Shen, H., Yan, W., Yuan, J., Wang, Z., and Wang, C. 2019. Nek2B activates the wnt pathway and promotes triple-negative breast cancer chemotherapy-resistance by stabilizing  $\beta$ -catenin. *Journal of Experimental and Clinical Cancer Research* **38**(1): 1–17. *Journal of Experimental & Clinical Cancer Research*. doi:10.1186/s13046-019-1231-y.
- Shin, E., Palmer, M.J., Li, M., and Fricker, R.A. 2012. GABAergic Neurons from Mouse Embryonic Stem Cells Possess Functional Properties of Striatal Neurons In Vitro, and Develop into Striatal Neurons In Vivo in a Mouse Model of Huntington's Disease. *Stem Cell Rev Rep* **8**(2): 513–531. doi:10.1007/s12015-011-9290-2.
- Sidell, N., Altman, A., Haussler, M.R., and Seeger, R.C. 1983. Effects of Retinoic Acid (RA) on the Growth and Phenotypic Expression of Several Human Neuroblastoma Cell Lines. *Exp Cell Res* **148**: 21–30.
- Skromne, I., Thorsen, D., Hale, M., Prince, V.E., and Ho, R.K. 2007. Repression of the hindbrain developmental program by Cdx factors is required for the specification of the vertebrate spinal cord. *Development* **134**(11): 2147–2158. doi:10.1242/dev.002980.
- Smith, J.L., and Schoenwolf, G.C. 1989. Notochordal induction of cell wedging in the chick neural plate and its role in neural tube formation. *J Exp Zool* **250**(1): 49–62. United States. doi:10.1002/jez.1402500107.
- Smolich, B.D., and Papkoff, J. 1994. Regulated Expression of Wnt Family Members during Neuroectodermal Differentiation of P19 Embryonal Carcinoma Cell: Overexpression of Wnt-1 Perturbs Normal Differentiation-Specific Properties. *Dev Biol* **166**: 300–310.
- Sonneveld, E., Van Den Brink, C.E., Tertoolen, L.G.J., Van Der Burg, B., and Van Der Saag, P.T. 1999. Retinoic acid hydroxylase (CYP26) is a key enzyme in neuronal differentiation of embryonal carcinoma cells. *Dev Biol* **213**(2): 390–404. doi:10.1006/dbio.1999.9381.
- Spice, D.M., Cooper, T.T., Lajoie, G.A., and Kelly, G.M. 2022a. Never in Mitosis Kinase 2 regulation of metabolism is required for neural differentiation. *Cell Signal* **100**: 110484. doi: 10.1016/j.cellsig.2022.110484.
- Spice, D.M., Dierolf, J., and Kelly, G.M. 2022b. Suppressor of Fused regulation of Hedgehog Signaling is Required for Proper Astrocyte Differentiation. *Stem Cells Dev*: 1–20. doi:10.1089/scd.2022.0131.
- Staines, W.A., Morassutti, D.J., Reuhl, K.R., ally, A.I., and McBurney, M.W. 1994. Neurons derived from P19 embryonal carcinoma cells have varied morphologies and neurotransmitters. *Neuroscience* **58**(4): 735–751. doi:10.1016/0306-4522(94)90451-0.

- Stamos, J.L., Chu, M.L.H., Enos, M.D., Shah, N., and Weis, W.I. 2014. Structural basis of GSK-3 inhibition by N-terminal phosphorylation and by the Wnt receptor LRP6. *Elife* **2014**(3): 1–22. doi:10.7554/eLife.01998.
- Stasiulewicz, M., Gray, S.D., Mastromina, I., Silva, J.C., Björklund, M., Seymour, P.A., Booth, D., Thompson, C., Green, R.J., Hall, E.A., Serup, P., and Kim Dale, J. 2015. A conserved role for Notch signaling in priming the cellular response to Shh through ciliary localisation of the key Shh transducer Smo. *Development* **142**(13): 2291–2303. doi:10.1242/dev.125237.
- St-Jacques, B., Hammerschmidt, M., and McMahon, A.P. 1999. Indian hedgehog signaling regulates proliferation and differentiation of chondrocytes and is essential for bone formation. *Genes Dev* **13**(16): 2072–2086. doi:10.1101/gad.13.16.2072.
- Stock, A., Kuzis, K., Woodward, W.R., Nishi, R., and Eckenstein, F.P. 1992. Localization of acidic fibroblast growth factor in specific subcortical neuronal populations. *Journal of Neuroscience* **12**(12): 4688–4700. doi:10.1523/jneurosci.12-12-04688.1992.
- Stone, D.M., Hynes, M., Armanini, M., Swanson, T.A., Gu, Q., Johnson, R.L., Scott, M.P., Pennica, D., Goddard, A., Phillips, H., Noll, M., Hooper, J.E., De Sauvage, F., and Rosenthal, A. 1996. The tumour-suppressor gene patched encodes a candidate receptor for Sonic hedgehog. *Nature* **384**(6605): 129–134. doi:10.1038/384129a0.
- van Straaten, H.W., Hekking, J.W., Thors, F., Wiertz-Hoessels, E.L., and Drukker, J. 1985. Induction of an additional floor plate in the neural tube. *Acta Morphol Neerl Scand* **23**(2): 91–97. Netherlands.
- van Straaten, H.W., Hekking, J.W., Wiertz-Hoessels, E.J., Thors, F., and Drukker, J. 1988. Effect of the notochord on the differentiation of a floor plate area in the neural tube of the chick embryo. *Anat Embryol (Berl)* **177**(4): 317–324. Germany. doi:10.1007/BF00315839.
- Sturgeon, K., Kaneko, T., Biemann, M., Gauthier, A., Chawengsaksophak, K., and Cordes, S.P. 2011. Cdx1 refines positional identity of the vertebrate hindbrain by directly repressing Mafk expression. *Development* **138**(1): 65–74. doi:10.1242/dev.058727.
- Svärd, J., Henricson, K.H., Persson-Lek, M., Rozell, B., Lauth, M., Bergström, Å., Ericson, J., Toftgård, R., and Teglund, S. 2006. Genetic elimination of suppressor of fused reveals an essential repressor function in the mammalian hedgehog signaling pathway. *Dev Cell* **10**(2): 187–197. doi:10.1016/j.devcel.2005.12.013.

- Takada, R., Satomi, Y., Kurata, T., Ueno, N., Norioka, S., Kondoh, H., Takao, T., and Takada, S. 2006. Monounsaturated Fatty Acid Modification of Wnt Protein: Its Role in Wnt Secretion. *Dev Cell* **11**(6): 791–801. doi:10.1016/j.devcel.2006.10.003.
- Takagi, Y., Takahashi, J., Saiki, H., Morizane, A., Hayashi, T., Kishi, Y., Fukuda, H., Okamoto, Y., Koyanagi, M., Ideguchi, M., Hayashi, H., Imazato, T., Kawasaki, H., Suemori, H., Omachi, S., Iida, H., Itoh, N., Nakatsuji, N., Sasai, Y., and Hashimoto, N. 2005. Dopaminergic neurons generated from monkey embryonic stem cells function in a Parkinson primate model. *Journal of Clinical Investigation* **115**(1): 102–109. doi:10.1172/JCI21137.
- Takanaga, H., Tsuchida-Straeten, N., Nishide, K., Watanabe, A., Aburatani, H., and Kondo, T. 2009. Gli2 Is a Novel Regulator of Sox2 Expression in Telencephalic Neuroepithelial Cells. *Stem Cells* **27**(1): 165–174. doi:10.1634/stemcells.2008-0580.
- Takenaka, K., Kise, Y., and Miki, H. 2007. GSK3 $\beta$  positively regulates Hedgehog signaling through Sufu in mammalian cells. *Biochem Biophys Res Commun* **353**(2): 501–508. doi:10.1016/j.bbrc.2006.12.058.
- Tamai, K., Semenov, M., Kato, Y., Spokony, R., Liu, C., Katsuyama, Y., Hess, F., Saint-Jeannet, J.-P., and He, X. 2000. LDL-receptor-related proteins in Wnt signal transduction. *Nature* **407**: 530--535.
- Tamai, K., Zeng, X., Liu, C., Zhang, X., Harada, Y., Chang, Z., and He, X. 2004. A Mechanism for Wnt Coreceptor Activation. *Mol Cell* **13**(1): 149–156. doi:10.1016/S1097-2765(03)00484-2.
- Tan, Y., Xie, Z., Ding, M., Wang, Z., Yu, Q., Meng, L., Zhu, H., Huang, X., Yu, L., Meng, X., and Chen, Y. 2010. Increased levels of FoxA1 transcription factor in pluripotent P19 embryonal carcinoma cells stimulate neural differentiation. *Stem Cells Dev* **19**(9): 1365–1374. doi:10.1089/scd.2009.0386.
- Tanaka, K., Parvinen, M., and Nigg, E.A. 1997. The in vivo expression pattern of mouse Nek2, a NIMA-related kinase, indicates a role in both mitosis and meiosis. *Exp Cell Res* **237**(2): 264–274. doi:10.1006/excr.1997.3788.
- Taneja, R., Roy, B., Plassat, J.L., Zusi, C.F., Ostrowski, J., Reczek, P.R., and Chambon, P. 1996. Cell-type and promoter-context dependent retinoic acid receptor (RAR) redundancies for RAR $\beta$ 2 and Hoxa-1 activation in F9 and P19 cells can be artifactually generated by gene knockouts. *Proc Natl Acad Sci U S A* **93**(12): 6197–6202. doi:10.1073/pnas.93.12.6197.
- Tang, K., Yang, J., Gao, X., Wang, C., Liu, L., Kitani, H., Atsumi, T., and Jing, N. 2002. Wnt-1 promotes neuronal differentiation and inhibits gliogenesis in P19 cells. *Biochem Biophys Res Commun* **293**(1): 167–173. doi:10.1016/S0006-291X(02)00215-2.

- Tauriello, D.V.F., Jordens, I., Kirchner, K., Slootstra, J.W., Kruitwagen, T., Bouwman, B.A.M., Noutsou, M., Rüdiger, S.G.D., Schwamborn, K., Schambony, A., and Maurice, M.M. 2012. Wnt/ $\beta$ -catenin signaling requires interaction of the Dishevelled DEP domain and C terminus with a discontinuous motif in Frizzled. *Proc Natl Acad Sci U S A* **109**(14). doi:10.1073/pnas.1114802109.
- Taylor, F.R., Wen, D., Garber, E.A., Carmillo, A.N., Baker, D.P., Arduini, R.M., Williams, K.P., Weinreb, P.H., Rayhorn, P., Hronowski, X., Whitty, A., Day, E.S., Boriack-Sjodin, A., Shapiro, R.I., Galdes, A., and Pepinsky, R.B. 2001. Enhanced potency of human Sonic hedgehog by hydrophobic modification. *Biochemistry* **40**(14): 4359–4371. doi:10.1021/bi002487u.
- Tempe, D., Casas, M., Karaz, S., Blanchet-Tournier, M.-F., and Concordet, J.-P. 2006. Multisite protein kinase A and glycogen synthase kinase 3 phosphorylation leads to Gli3 ubiquitination by SCF TrCP. *Mol Cell Biol* **26**(11): 4316–4326. doi:10.1128/MCB.02183-05.
- Tenzen, T., Allen, B.L., Cole, F., Kang, J.S., Krauss, R.S., and McMahon, A.P. 2006. The Cell Surface Membrane Proteins Cdo and Boc Are Components and Targets of the Hedgehog Signaling Pathway and Feedback Network in Mice. *Dev Cell* **10**(5): 647–656. doi:10.1016/j.devcel.2006.04.004.
- Tetsu, O., and McCormick, F. 1999. Beta-Catenin regulates expression of cyclinD1 in colon carcinomacells Osamu. *Nature* **398**(April): 422.
- Teven, C.M., Farina, E.M., Rivas, J., and Reid, R.R. 2014. Fibroblast growth factor (FGF) signaling in development and skeletal diseases. *Genes Dis* **1**(2): 199–213. Elsevier Ltd. doi:10.1016/j.gendis.2014.09.005.
- Timmer, J.R., Wang, C., and Niswander, L. 2002. BMP signaling patterns the dorsal and intermediate neural tube via regulation of homeobox and helix-loop-helix transcription factors. *Development* **129**(10): 2459–2472. doi:10.1242/dev.129.10.2459.
- Tonge, P.D., and Andrews, P.W. 2010. Retinoic acid directs neuronal differentiation of human pluripotent stem cell lines in a non-cell-autonomous manner. *Differentiation* **80**(1): 20–30. Elsevier. doi:10.1016/j.diff.2010.04.001.
- Traiffort, E., Dubourg, C., Faure, H., Rognan, D., Odent, S., Durou, M.R., David, V., and Ruat, M. 2004. Functional characterization of Sonic hedgehog mutations associated with holoprosencephaly. *Journal of Biological Chemistry* **279**(41): 42889–42897. doi:10.1074/jbc.M405161200.

- Tukachinsky, H., Kuzmickas, R.P., Jao, C.Y., Liu, J., and Salic, A. 2012. Dispatched and Scube Mediate the Efficient Secretion of the Cholesterol-Modified Hedgehog Ligand. *Cell Rep* **2**(2): 308–320. doi:10.1016/j.celrep.2012.07.010.
- Tukachinsky, H., Lopez, L. V., and Salic, A. 2010. A mechanism for vertebrate Hedgehog signaling: Recruitment to cilia and dissociation of SuFu-Gli protein complexes. *Journal of Cell Biology* **191**(2): 415–428. doi:10.1083/jcb.201004108.
- Urman, N.M., Mirza, A., Atwood, S.X., Whitson, R.J., Sarin, K.Y., Tang, J.Y., and Oro, A.E. 2016. Tumor-derived suppressor of fused mutations reveal hedgehog pathway interactions. *PLoS One* **11**(12): e0168031. doi:10.1371/journal.pone.0168031.
- Vieira, M.S., Santos, A.K., Vasconcellos, R., Goulart, V.A.M., Parreira, R.C., Kihara, A.H., Ulrich, H., and Resende, R.R. 2018. Neural stem cell differentiation into mature neurons: Mechanisms of regulation and biotechnological applications. *Biotechnol Adv* **36**(7): 1946–1970. Elsevier. doi:10.1016/j.biotechadv.2018.08.002.
- Vokes, S.A., Ji, H., McCuine, S., Tenzen, T., Giles, S., Zhong, S., Longabaugh, W.J.R., Davidson, E.H., Wong, W.H., and McMahan, A.P. 2007. Genomic characterization of Gli-activator targets in sonic hedgehog-mediated neural patterning. *Development* **134**(10): 1977–1989. doi:10.1242/dev.001966.
- Voronova, A., Fischer, A., Ryan, T., al Madhoun, A., and Skerjanc, I.S. 2011. *Ascl1/Mash1* is a novel target of *Gli2* during *Gli2*-induced neurogenesis in P19 EC cells. *PLoS One* **6**(4): e19174. doi:10.1371/journal.pone.0019174.
- Wakabayashi, N., Kageyama, R., Habu, T., Doi, T., Morita, T., Nozaki, M., Yamamoto, M., and Nishimune, Y. 2000. A novel cis-acting element regulates HES-1 gene expression in P19 embryonal carcinoma cells treated with retinoic acid. *J Biochem* **128**(6): 1087–1095. doi:10.1093/oxfordjournals.jbchem.a022837.
- Wan, H., Xu, L., Zhang, H., Wu, F., Zeng, W., and Li, T. 2021. High expression of NEK2 promotes gastric cancer progression via activating AKT signaling. *J Physiol Biochem* **77**(1): 25–34. *Journal of Physiology and Biochemistry*. doi:10.1007/s13105-020-00776-8.
- Wang, B., and Li, Y. 2006. Evidence for the direct involvement of  $\beta$ TrCP in Gli3 protein processing. *Proc Natl Acad Sci U S A* **103**(1): 33–38. doi:10.1073/pnas.0509927103.
- Wang, C., Pan, Y., and Wang, B. 2010. Suppressor of fused and Spop regulate the stability, processing and function of Gli2 and Gli3 full-length activators but not their repressors. *Development* **137**(12): 2001–2009. doi:10.1242/dev.052126.
- Wang, H., Ikeda, S., Kanno, S. ichiro, Guang, L.M., Ohnishi, M., Sasaki, M., Kobayashi, T., and Tamura, S. 2001. Activation of c-Jun amino-terminal kinase is required for

- retinoic acid-induced neural differentiation of P19 embryonal carcinoma cells. *FEBS Lett* **503**: 91–96. doi:10.1016/S0014-5793(01)02699-0.
- Wang, J., Hamblet, N.S., Mark, S., Dickinson, M.E., Brinkman, B., Segil, N., Fraser, S.E., Chen, P., Wallingford, J.B., and Wynshaw-Boris, A. 2006a. Dishevelled genes mediate a conserved mammalian PCP pathway to regulate convergent extension during neurulation. *Development* **133**(9): 1767–1778. doi:10.1242/dev.02347.
- Wang, J., Sinha, T., and Wynshaw-Boris, A. 2012. Wnt signaling in mammalian development: Lessons from mouse genetics. *Cold Spring Harb Perspect Biol* **4**(5): 6. doi:10.1101/cshperspect.a007963.
- Wang, Y., Guo, N., and Nathans, J. 2006b. The role of Frizzled3 and Frizzled6 in neural tube closure and in the planar polarity of inner-ear sensory hair cells. *Journal of Neuroscience* **26**(8): 2147–2156. doi:10.1523/JNEUROSCI.4698-05.2005.
- Wang, Y., Li, Y., Hu, G., Huang, X., Rao, H., Xiong, X., Luo, Z., Lu, Q., and Luo, S. 2016. Nek2A phosphorylates and stabilizes SuFu: A new strategy of Gli2/Hedgehog signaling regulatory mechanism. *Cell Signal* **28**(9): 1304–1313. Elsevier Inc. doi:10.1016/j.cellsig.2016.06.010.
- Wei, L.N., Blaner, W.S., Goodman, D.S., and Nguyen-Huu, M.C. 1989. Regulation of the cellular retinoidbinding proteins and their messenger ribonucleic acids during P19 embryonal carcinoma cell differentiation induced by retinoic acid. *Molecular Endocrinology* **3**(3): 454–463. doi:10.1210/mend-3-3-454.
- Wen, X., Lai, C.K., Evangelista, M., Hongo, J.-A., de Sauvage, F.J., and Scales, S.J. 2010. Kinetics of Hedgehog-Dependent Full-Length Gli3 Accumulation in Primary Cilia and Subsequent Degradation. *Mol Cell Biol* **30**(8): 1910–1922. doi:10.1128/MCB.01089-09.
- Wichterle, H., Lieberam, I., Porter, J.A., and Jessell, T.M. 2002. Directed differentiation of embryonic stem cells into motor neurons. *Cell* **110**(3): 385–397. doi:10.1016/S0092-8674(02)00835-8.
- Wijgerde, M., McMahon, J.A., Rule, M., and McMahon, A.P. 2002. A direct requirement for hedgehog signaling for normal specification of all ventral progenitor domains in the presumptive mammalian spinal cord. *Genes Dev* **16**(22): 2849–2864. doi:10.1101/gad.1025702.
- Willert, K., Brown, J.D., Danenberg, E., Duncan, A.W., Weissman, I.L., Reya, T., Yates III, J.R., and Nusse, R. 2003. Wnt proteins are lipid-modified and can act as stem cell growth factors. *Nature* **423**: 448–452.
- Williams, E.H., Pappano, W.N., Saunders, A.M., Kim, M.S., Leahy, D.J., and Beachy, P.A. 2010. Dally-like core protein and its mammalian homologues mediate

- stimulatory and inhibitory effects on Hedgehog signal response. *Proc Natl Acad Sci U S A* **107**(13): 5869–5874. doi:10.1073/pnas.1001777107.
- Wilson, L., Gale, E., Chambers, D., and Maden, M. 2004. Retinoic acid and the control of dorsoventral patterning in the avian spinal cord. *Dev Biol* **269**(2): 433–446. doi:10.1016/j.ydbio.2004.01.034.
- Wilson, L., Gale, E., and Maden, M. 2003. The role of retinoic acid in the morphogenesis of the neural tube. *J Anat* **203**(4): 357–368. doi:10.1046/j.1469-7580.2003.00230.x.
- Wilson, S.I., and Edlund, T. 2001. Neural induction: Toward a unifying mechanism. *Nat Neurosci* **4**(11s): 1161–1168. doi:10.1038/nn747.
- Wilson, S.I., Graziano, E., Harland, R., Jessell, T.M., and Edlund, T. 2000. An early requirement for FGF signalling in the acquisition of neural cell fate in the chick embryo. *Current Biology* **10**(8): 421–429. doi:10.1016/S0960-9822(00)00431-0.
- Wine-Lee, L., Ahn, K.J., Richardson, R.D., Mishina, Y., Lyons, K.M., and Crenshaw, E.B. 2004. Signaling through BMP type 1 receptors is required for development of interneuron cell types in the dorsal spinal cord. *Development* **131**(21): 5393–5403. doi:10.1242/dev.01379.
- Winkler, C.C., Yabut, O.R., Fregoso, S.P., Gomez, H.G., Dwyer, B.E., Pleasure, S.J., and Franco, S.J. 2018. The dorsal wave of neocortical oligodendrogenesis begins embryonically and requires multiple sources of sonic hedgehog. *Journal of Neuroscience* **38**(23): 5237–5250. doi:10.1523/JNEUROSCI.3392-17.2018.
- Woodward, W.R., Nishi, R., Meshul, C.K., Williams, T.E., Coulombe, M., and Eckenstein, F.P. 1992. Nuclear and cytoplasmic localization of basic fibroblast growth factor in astrocytes and CA2 hippocampal neurons. *Journal of Neuroscience* **12**(1): 142–152. doi:10.1523/jneurosci.12-01-00142.1992.
- Wu, S.M., Choo, A.B.H., Yap, M.G.S., and Chan, K.K.K. 2010. Role of Sonic hedgehog signaling and the expression of its components in human embryonic stem cells. *Stem Cell Res* **4**(1): 38–49. Elsevier B.V. doi:10.1016/j.scr.2009.09.002.
- Xiang, J., Alafate, W., Wu, W., Wang, Y., Li, X., Xie, W., Bai, X., Li, R., Wang, M., and Wang, J. 2022. NEK2 enhances malignancies of glioblastoma via NIK/NF- $\kappa$ B pathway. *Cell Death Dis* **13**(1): 1–13. Springer US. doi:10.1038/s41419-022-04512-6.
- Xing, Y., Clements, W.K., Kimelman, D., and Xu, W. 2003. Crystal structure of a  $\beta$ -catenin/Axin complex suggests a mechanism for the  $\beta$ -catenin destruction complex. *Genes Dev* **17**(22): 2753–2764. doi:10.1101/gad.1142603.

- Xing, Z., Zhang, M., Wang, X., Liu, J., Liu, G., Feng, K., and Wang, X. 2021. Silencing of Nek2 suppresses the proliferation, migration and invasion and induces apoptosis of breast cancer cells by regulating ERK/MAPK signaling. *J Mol Histol* **52**(4): 809–821. Springer Netherlands. doi:10.1007/s10735-021-09979-9.
- Xu, T., Zeng, Y., Shi, L., Yang, Q., Chen, Y., Wu, G., Li, G., and Xu, S. 2020. Targeting NEK2 impairs oncogenesis and radioresistance via inhibiting the Wnt1/ $\beta$ -catenin signaling pathway in cervical cancer. *Journal of Experimental and Clinical Cancer Research* **39**(1): 1–13. *Journal of Experimental & Clinical Cancer Research*. doi:10.1186/s13046-020-01659-y.
- Yabut, O.R., Fernandez, G., Yoon, K., Pleasure, S.J., Yabut, O.R., Fernandez, G., Huynh, T., Yoon, K., and Pleasure, S.J. 2015. Suppressor of Fused Is critical for maintenance of neuronal progenitor identity during corticogenesis. *Cell Rep* **12**(12): 2021–2034. The Authors. doi:10.1016/j.celrep.2015.08.031.
- Yamada, T., Placzek, M., Tanaka, H., Dodd, J., and Jessell, T.M. 1991. Control of cell pattern in the developing nervous system: Polarizing activity of the floor plate and notochord. *Cell* **64**(3): 635–647. doi:10.1016/0092-8674(91)90247-V.
- Yan, D., and Lin, X. 2009. Shaping morphogen gradients by proteoglycans. *Cold Spring Harb Perspect Biol* **1**(3). doi:10.1101/cshperspect.a002493.
- Yang, C., Chen, W., Chen, Y., and Jiang, J. 2012. Smoothed transduces Hedgehog signal by forming a complex with Evc/Evc2. *Cell Res* **22**(11): 1593–1604. Nature Publishing Group. doi:10.1038/cr.2012.134.
- Yang, C., Qi, Y., and Sun, Z. 2021. The Role of Sonic Hedgehog Pathway in the Development of the Central Nervous System and Aging-Related Neurodegenerative Diseases. *Front Mol Biosci* **8**(July): 1–7. doi:10.3389/fmolb.2021.711710.
- Yao, Y., Su, J., Zhao, L., Luo, N., Long, L., and Zhu, X. 2019. NIMA-related kinase 2 overexpression is associated with poor survival in cancer patients: A systematic review and meta-analysis. *Cancer Manag Res* **11**: 455–465. doi:10.2147/CMAR.S188347.
- Ye, F., Chen, Y., Hoang, T., Montgomery, R.L., Zhao, X.H., Bu, H., Hu, T., Taketo, M.M., Van Es, J.H., Clevers, H., Hsieh, J., Bassel-Duby, R., Olson, E.N., and Lu, Q.R. 2009. HDAC1 and HDAC2 regulate oligodendrocyte differentiation by disrupting the B-catenin-TCF interaction. *Nat Neurosci* **12**(7): 829–838. Nature Publishing Group. doi:10.1038/nn.2333.
- Yoon, K., and Gaiano, N. 2005. Notch signaling in the mammalian central nervous system: Insights from mouse mutants. *Nat Neurosci* **8**(6): 709–715. doi:10.1038/nn1475.



- Yoon, K., Nery, S., Rutlin, M.L., Radtke, F., Fishell, G., and Gaiano, N. 2004. Fibroblast growth factor receptor signaling promotes radial glial identity and interacts with Notch1 signaling in telencephalic progenitors. *Journal of Neuroscience* **24**(43): 9497–9506. doi:10.1523/JNEUROSCI.0993-04.2004.
- Yu, H.M.I., Liu, B., Costantini, F., and Hsu, W. 2007. Impaired neural development caused by inducible expression of Axin in transgenic mice. *Mech Dev* **124**(2): 146–156. doi:10.1016/j.mod.2006.10.002.
- Yue, S., Chen, Y., and Cheng, S.Y. 2009. Hedgehog signaling promotes the degradation of tumor suppressor Sufu through the ubiquitin-proteasome pathway. *Oncogene* **28**(4): 492–499. doi:10.1038/onc.2008.403.
- Yun, Y.R., Won, J.E., Jeon, E., Lee, S., Kang, W., Jo, H., Jang, J.H., Shin, U.S., and Kim, H.W. 2010. Fibroblast growth factors: Biology, function, and application for tissue regeneration. *J Tissue Eng*: 218142. doi:10.4061/2010/218142.
- Zeng, X., Tamai, K., Doble, B., Li, S., Huang, H., Habas, R., Okamura, H., Woodgett, J., and He, X. 2005. A dual-kinase mechanism for Wnt co-receptor phosphorylation and activation. *Nature* **438**(7069): 873–877. doi:10.1038/nature04185.
- Zhai, L., Chaturvedi, D., and Cumberledge, S. 2004. Drosophila Wnt-1 undergoes a hydrophobic modification and is targeted to lipid rafts, a process that requires porcupine. *Journal of Biological Chemistry* **279**(32): 33220–33227. © 2004 ASBMB. Currently published by Elsevier Inc; originally published by American Society for Biochemistry and Molecular Biology. doi:10.1074/jbc.M403407200.
- Zhang, X., Huang, X., Xu, J., Li, E., Lao, M., Tang, T., Zhang, G., Guo, C., Zhang, X., Chen, W., Yadav, D.K., Bai, X., and Liang, T. 2021. NEK2 inhibition triggers anti-pancreatic cancer immunity by targeting PD-L1. *Nat Commun* **12**(1). Springer US. doi:10.1038/s41467-021-24769-3.
- Zhang, X., Ibrahimi, O.A., Olsen, S.K., Umemori, H., Mohammadi, M., and Ornitz, D.M. 2006. Receptor specificity of the fibroblast growth factor family: The complete mammalian FGF family. *Journal of Biological Chemistry* **281**(23): 15694–15700. © 2006 ASBMB. Currently published by Elsevier Inc; originally published by American Society for Biochemistry and Molecular Biology. doi:10.1074/jbc.M601252200.
- Zhang, Z., Shen, L., Law, K., Zhang, Z., Liu, X., Hua, H., Li, S., Huang, H., Yue, S., Hui, C., and Cheng, S.Y. 2017. Suppressor of Fused Chaperones Gli Proteins To Generate Transcriptional Responses to Sonic Hedgehog Signaling. *Mol Cell Biol* **37**(3): 1–18. doi:10.1128/mcb.00421-16.

Zhou, F., Huang, D., Li, Y., Hu, G., Rao, H., Lu, Q., Luo, S., and Wang, Y. 2017.  
Nek2A/SuFu feedback loop regulates Gli-mediated Hedgehog signaling pathway.  
Int J Oncol **50**(2): 373–380. doi:10.3892/ijo.2016.3819.

## Chapter 2

### 2 Suppressor of Fused regulation of Hedgehog Signaling is Required for Proper Astrocyte Differentiation

Hedgehog signaling is essential for vertebrate development, however, less is known about the negative regulators that influence this pathway. Using the mouse P19 embryonal carcinoma cell model, Suppressor of Fused (SUFU), a negative regulator of the Hedgehog pathway, was investigated during retinoic acid-induced neural differentiation. We found Hedgehog signaling increased activity in the early phase of differentiation but was reduced during terminal differentiation of neurons and astrocytes. This early increase in pathway activity was required for neural differentiation, however, it alone was not sufficient to induce neural lineages. SUFU, which regulates signaling at the level of Gli, remained relatively unchanged during differentiation, but its loss through CRISPR-Cas9 gene editing resulted in ectopic expression of Hedgehog target genes. Interestingly, these SUFU-deficient cells were unable to differentiate towards neural lineages without retinoic acid, and when directed towards these lineages they showed delayed and decreased astrocyte differentiation; neuron differentiation was unaffected. Ectopic activation of Hh target genes in SUFU-deficient cells remained throughout retinoic acid-induced differentiation and this was accompanied by the loss of Gli3, despite the presence of the *Gli3* message. Thus, the study indicates the proper timing and proportion of astrocyte differentiation requires SUFU, likely acting through Gli3, to reduce Hh signaling during late-stage differentiation.

## 2.1 Introduction

Hedgehog (Hh) signaling plays pivotal roles in neural development, where Sonic Hedgehog (SHH) is essential in patterning the differentiation of motor neurons and interneurons in the neural tube (Wilson and Maden 2005) and inducing differentiation of cerebellar neurons and glial cells (Dahmane and Ruiz 1999). When Hh ligand is absent, the transmembrane receptor Patched (PTCH) inhibits the transmembrane protein Smoothed (SMO) from translocating to the plasma membrane of the primary cilium (Briscoe and Thérond 2013). Inhibition allows the Suppressor of Fused (SUFU) to sequester full-length Gli transcription factors (Han et al. 2015) or promotes Gli phosphorylation (Tempe et al. 2006) and partial proteosomal degradation into a truncated repressor (Humke et al. 2010; Hui and Angers 2011). In the presence of Hh, however, PTCH is inhibited, which allows the SUFU-Gli complex to be recruited into the primary cilium (Haycraft et al. 2005). SUFU dissociates from Gli allowing the translocation of Gli to the nucleus where it acts as a transcriptional activator (Humke et al. 2010). In vertebrates there are three Gli proteins, with Gli1 serving solely as an activator as *Gli1* is a Hh target gene, present only after activation of the pathway (Hui and Angers 2011). Gli2 and Gli3 are either transcriptional activators or repressors, with Gli3 acting primarily as a repressor (Hui and Angers 2011). Thus, while Hh target gene transcription is tightly regulated through Gli, other proteins regulate Glis. One of these is SUFU, a regulator of Gli processing that is key to Hh pathway activation. Through the reduced processing and stability of the Gli3 repressor (Makino et al. 2015), *Sufu* loss of function alleles cause constitutive expression of Hh target genes in the absence of a Hh ligand (Cooper et al. 2005; Svärd et al. 2006; Cwinn et al. 2011). Loss of *Sufu* in humans causes medulloblastoma tumor growth (Taylor et al. 2002; Smith et al. 2018) and Nevoid Basal Cell Carcinoma Syndrome (Urman et al. 2016; Smith et al. 2018), while mouse embryos containing a targeted deletion of *Sufu* are embryonic lethal at E9.5 due to neural tube closure defects (Cooper et al. 2005). Furthermore, the loss of *Sufu* function in the mouse retina restricts retinal neuron differentiation (Cwinn et al. 2011) and in the cerebellum results in developmental delays in neuron differentiation (Kim et al. 2018) and cerebellum mispatterning (Kim et al. 2011).

In the present study an *in vitro* system utilizing the mouse P19 embryonal carcinoma cell line was employed to study when the Hedgehog pathway is activated, its requirement during differentiation and the effects of *Sufu* loss of function on neural cell fate. The cell line is readily differentiated into neural lineages in the presence of retinoic acid (RA) (McBurney et al. 1982). RA causes P19 cells to develop functional neurons and supporting astrocytes (McBurney et al. 1988), and although this is well-known, few studies have investigated the role of Hh signaling in this system (Voronova et al. 2011; Lin et al. 2012). Of these, one study showed the overexpression of a constitutively active *Gli2* promotes neuronal differentiation (Voronova et al. 2011), but another revealed the knockdown of *Gli2* causes the same phenotype (Lin et al. 2012). Thus, these and many unanswered questions remain, and though Hh signaling is precisely controlled *in vivo*, how SUFU is involved in determining neuron and astrocyte cell fate decisions is not known. To address this shortfall, this study aims to better understand the essential role of SUFU in neuroectodermal differentiation. Using the P19 cell model and timeline investigations, we show when Hh signaling is required during RA-induced neural differentiation, and through genetic ablation of *Sufu*, demonstrate that there is an essential role for SUFU in astrocyte determination.

## 2.2 Materials and Methods

### 2.2.1 Cell culture & Differentiation

P19 embryonal carcinoma cells (a gift from Dr. Lisa Hoffman, Lawson Health Research Institute, London, ON) and Sufu knockout (*Sufu*<sup>-/-</sup>, described below) P19 cells were cultured on adherent tissue culture plates in DMEM containing 5% fetal bovine serum and 1% pen/strep at 37°C and 5% CO<sub>2</sub>. Cells were passaged every 4 days or at 70% confluency, whichever occurred first. To induce neural differentiation, approximately 1.05x10<sup>6</sup> cells were cultured on bacterial grade Petri dishes for 4 days in 0.5 μM RA to form embryoid bodies (EB) (McBurney et al. 1988). Next, EBs were resuspended and plated on adherent tissue culture dishes in the presence of 0.5 μM RA, for a total of 10, 14 or 17 days. Untreated controls were grown as described, but without RA. For Smoothed Agonist (SAG; EMD Millipore) and Cyclopamine (Cyc; EMD Millipore) studies, cells were cultured as above but in the presence of 0.5 μM RA plus 10 nM SAG or 10 μM Cyc, or 10 nM SAG alone during EB formation; then replated as described above in the presence of 0.5 μM RA or were left untreated for the SAG-only treatment.

### 2.2.2 Cas9 plasmid preparation

The pSpCas9(BB)-2A-Puro (PX459) V2.0 (Addgene plasmid: 62988) was used, where sgRNAs for Sufu (Supplementary Table 1) were cloned into the PX459 vector (Ran et al. 2013). Briefly, sgRNAs were amplified and phosphorylated, the vector digested using the BbsI restriction enzyme, and vector and sgRNA were incubated at room temperature for 1.5 h for ligation. Ligated plasmids were transformed into competent bacteria, colonies were selected, and isolated plasmids were sequenced at the London Regional Genomics Centre (Robarts Research Institute, London, ON) using the U6 primer (Supplementary Table 1).

### 2.2.3 Knockout lines

PX459-sgRNA plasmid (2 μg) was transfected using 10 μL of Lipofectamine 2000 (Invitrogen). After 4 h, media was changed, and cells were grown to 70% confluency for clonal selection. Selection media containing 1 μg/mL puromycin was replaced every 24 h

for 4 days, and then cells were grown in complete media without puromycin until ready to be passaged. Knockout genotypes were determined by collecting genomic DNA (Qiagen DNeasy® Blood & Tissue kit, 69504), and performing standard PCR (DreamTaq Master Mix (2X), Thermo Scientific) with *Sufu*-specific primers (Table 2-1). Amplicons were sequenced at the London Regional Genomics Centre and compared to wildtype sequences using pair-wise sequence alignment (Geneious 2021™). KO line #2 sequencing was examined using TIDE analysis (<http://shinyapps.datacurators.nl/tide/>) (Brinkman et al. 2014) to further investigate the nature of the allele. TIDE analysis was unable to interrogate KO line #1 as the length of deletion was outside of the tool parameters.

**Table 2-1: gRNA and primer sequences for CRISPR-Cas9 editing of *Sufu* gene**

CRISPR-Cas9		
<i>Sufu</i> gRNA	GGCTGATAACTGACATGCGG	
	<b>Forward Primer (5' → 3')</b>	<b>Reverse Primer (5' → 3')</b>
<i>Sufu</i> gRNA	CACCGGGCTGATAACTGACATGCGG	AAACCCGCATGTCAGTTATCAGCCC
<i>Sufu</i> PCR	CTCCATCCCACCTGTAGAGTTC	AGCAAGGTTTTCTCACTCAAG
<i>U6</i>	GGGCAGGAAGAGGGCCTAT	

## 2.2.4 Overexpression lines

*Sufu* KO #2 was transfected with 2 µg of either 1436 pcDNA3 Flag HA (Addgene plasmid: 10792), a pcDNA Flag HA vector with the *Sufu* open reading frame cloned from pcDNA Su(fu) (CT #116) (Addgene plasmid: 13857) (Pearse et al. 1999) using BamHI (New England Biolabs) and XhoI (New England Biolabs) restriction enzymes, or *hGli3* flag3x (Addgene plasmid: 84921) using Lipofecatime 2000 (Invitrogen). Cells were incubated for 4 hours in the presence of plasmid, media was then changed, and cells were grown to 70% confluency. Transfected cells were treated with 500 µg/mL neomycin (G418) selection media every 48 hours for 2 weeks.

## 2.2.5 Real-time reverse transcriptase PCR

To determine relative mRNA expression levels total RNA was collected from RA-treated cells at various time points using QiaShredder (Qiagen) and RNeasy (Qiagen) kits. cDNA

was made using a High-Capacity cDNA Reverse Transcription Kit (Thermo Fisher Scientific) and amplification was performed using gene-specific primers (Table 2-2). RT-qPCR was done using 500 nM of each reverse and forward primers, 10  $\mu$ L of SensiFAST SYBR No-ROX Mix (Bioline), and 1  $\mu$ L of cDNA template. Samples were analyzed using a CFX Connect Real-Time PCR Detection System (Bio-Rad) using the comparative cycle threshold method ( $2^{-\Delta\Delta C_t}$ ). Relative expression was normalized to *L14* and untreated or wildtype untreated controls to determine fold change expression.

**Table 2-2: RT-qPCR Primers List**

Gene	qRT-PCR	
	Forward Primer (5' → 3')	Reverse Primer (5' → 3')
<i>L14</i>	GGGTGGCCTACATTTCTTCG	GAGTACAGGGTCCATCCACTAAA
<i>Shh</i>	AAAGCTGACCCCTTAGCCTA	TTCGGAGTTTCTTGTGATCTTCC
<i>Ihh</i>	GACTCATTGCCTCCAGAAGT	CCAGGTAGTAGGGTCACATTGC
<i>Dhh</i>	ACCCCGACATAATCTTCAAGGAT	GTAATCCGGGCCACATGTTT
<i>Smo</i>	CCTGACTTTCTGCGTTGC	GGTCTGACACTGAATCCG
<i>Ptch1</i>	AAAGAAGTGCAGCAAGTTTTTG	CTTCTCCTATCTTCTGACGGGT
<i>Ptch2</i>	CTCCGCACCTCATATCCTAGC	TCCCAGGAAGAGCACTTTGC
<i>Sufu</i>	CGGACCCCTTGACTATGTTA	CTTCAGACGAAACGTCAACTCA
<i>Gli1</i>	GGAAGTCCTATTCACGCCTGA	CAACCTTCTTGCTCACACATGTAAG
<i>Gli2</i>	TACCTCAACCTGTGGATGC	CTACCAGCGAGTTGGGAGAG
<i>Gli3</i>	CTGTCCGCTTAGGATCTGTTG	GCTCTTCAGCAAGTGGTTC
<i>Ascl1</i>	ACTTGAAGTCTATGGCGGGTT	CCAGTTGGTAAAGTCCAGCAG
<i>NeuroD1</i>	GCATGCACGGGCTGAACGC	GGGATGCACCGGGAAGGAAG
<i>NeuroG1</i>	CCAGCGACACTGAGTCCTG	CGGGCCATAGGTGAAGTCTT
<i>GFAP</i>	CCAAGCCAAACACGAAGCTAA	CATTTGCCGCTCTAGGGACTC
<i>S100b</i>	TGGTTGCCCTCATTGATGTCT	CTCGTTGTGATAAGCTCCTCAG
<i>Aldh1l1</i>	CATCCAGACCTCCGATACTTC	ACAATACCACAGACCCCAAC
<i>Chicken Sufu</i>	ACGGGCAAGGAATCTTGGAG	ACTCTCTCTTGCAGATGCGG

## 2.2.6 Immunoblot Analysis

Cells were lysed in 2% SDS buffer containing 62.5 mM Tris-HCL pH 6.8, 10% glycerol, 5% mercapto-2-ethanol and 1X Halt Protease Inhibitor Cocktail (Thermo Scientific; 1:200). Proteins were separated using SDS-PAGE, then transferred to PVDF membranes (Bio-Rad, 1620177). Membranes were probed with primary antibodies to  $\beta$ -III-tubulin (1:1000; Cell Signaling Technology), GLI3 (1:1000; R&D Systems), SUFU (1:1000;



abcam), GFAP (1:1000; Invitrogen) and  $\beta$ -actin (1:10,000; Santa Cruz Biotechnology) and then with the appropriate HRP-conjugated secondary antibodies (1:10,000, Sigma). Signals were detected using the Immobilon® Classico Western HRP Substrate (Millipore) and imaged using a Chemi Doc Touch System (Bio-Rad).

### 2.2.7 Immunofluorescence

Cells were differentiated, as stated previously, on coverslips coated with poly-L-lysine hydrobromide (Sigma), fixed with 4% paraformaldehyde for 10 min and permeabilized in 0.2% Triton-X-100 for 10 min at room temperature. Coverslips were incubated for 30 min in 1% Bovine Serum Albumin, 22.52 mg/mL glycine and 0.1% Tween-20, then overnight in a humidity chamber with  $\beta$ -III-tubulin (TUJ1, 1:400; Cell Signaling Technology) and GFAP (1:500; Invitrogen). Incubation in secondary antibodies (1:400), Alexa Fluor™ 660 goat anti-mouse IgG (Invitrogen) and Goat anti-Rabbit IgG Alexa Fluor Plus 488 (Invitrogen) was done in the dark for 1 h at room temperature. Coverslips were mounted onto microscope slides using Slowfade™ Gold antifade reagent with DAPI (Invitrogen) and cells were examined using a Zeiss AxioImager Z1 Compound Fluorescence Microscope at the Integrated Microscopy Facility, Biotron (Western University, London, ON). Images were analyzed using ImageJ.

### 2.2.8 Flow Cytometry

Cells, differentiated as stated previously, were washed with ice cold PBS without magnesium or chloride (PBS(-/-)) (Thermo Fisher) and dissociated with 0.25% Trypsin. Trypsin was deactivated with DMEM/F12 (Thermo Fisher) containing 10% ES-grade FBS (Thermo Fisher), and cells were centrifuged at 300 g for 5 minutes and reconstituted in PBS(-/-). Cells were counted using a trypan blue assay, separated to approximately  $1.0 \times 10^6$  cells per tube, and washed in Flow Cytometry Staining Buffer (10% FBS in PBS(-/-)). Cells were fixed using 4% formaldehyde in PBS(-/-) for 10 min at room temperature, washed with ice cold PBS(-/-) and permeabilized with 0.2% Triton-X-100 in PBS(-/-) for 10 min. Cells were incubated with or without 1  $\mu$ L of GFAP Monoclonal Antibody (GA5), Alexa Fluor 488, eBioscience™ (Invitrogen) per million cells for 1 h at room temperature, and then washed with PBS (-/-), strained using a 40  $\mu$ m strainer

(Falcon™) and analyzed using a BD FACSCanto II flow cytometer at the London Regional Flow Cytometry Facility (Robarts Research Institute). Data were analyzed using FlowJo (BD). Flow cytometry gating strategy is reported in Figure 2-1.

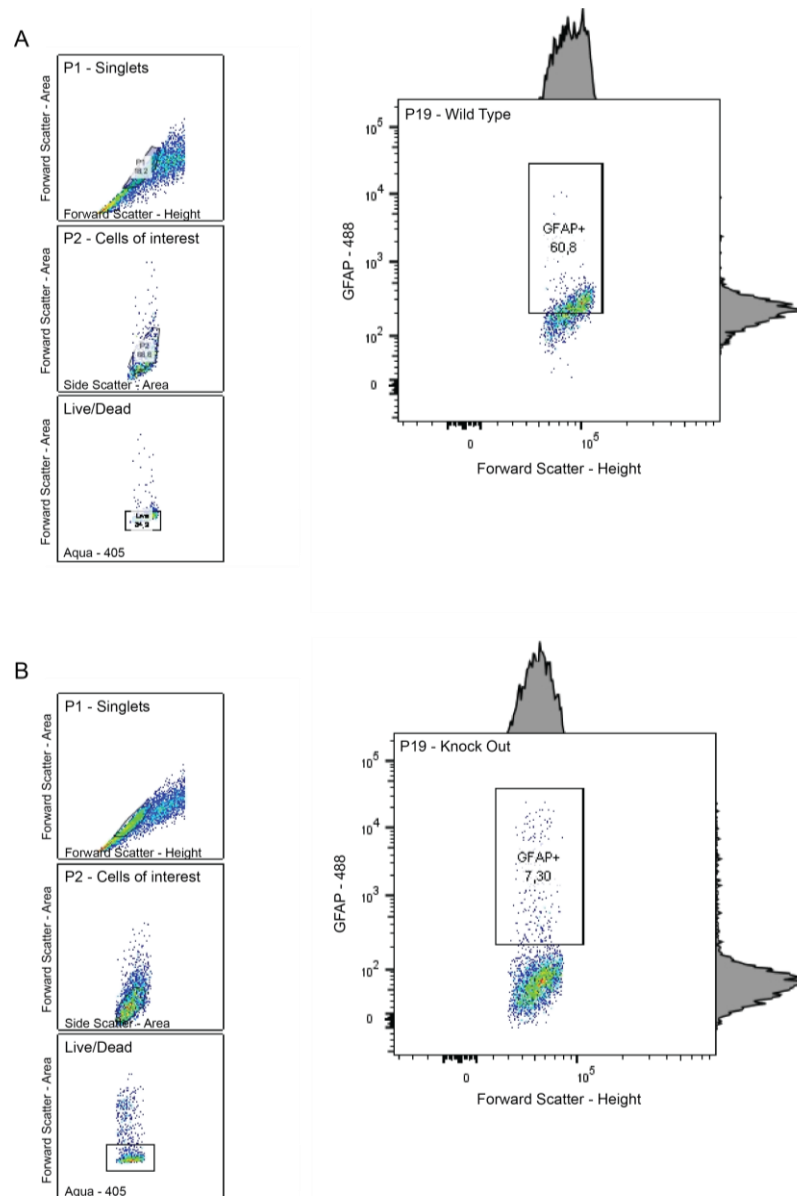


**Figure 2-1: Flow cytometry gating strategy of P19 cells**

Flow cytometric gating scheme of P19 wild type (**A**) and knock out (**B**) cells. Wild type P19 cell doublets were removed by gating for a second population (P1) examining forward scatter – height versus forward scatter – area. Cells of interest were selected by gating for side scatter – area versus forward scatter – area in a secondary population (P2). Live cells were distinguished from dead cells by gating through a comparison of a live/dead Zombie Aqua™ stain (405) versus forward scatter – area. The final gating threshold isolates cells positive for GFAP staining (488).

## 2.3 Results

### 2.3.1 Retinoic acid and cell aggregation induces P19 neural differentiation

To induce neural differentiation cells were treated for 4 days in 0.5  $\mu$ M RA to form EB, which were then plated for a total of 10 days to form neurons or 17 days to form astrocytes (Figure 2-2A). Differentiation was confirmed with RT-qPCR of *NeuroD1*, *NeuroG1* and *Ascl1* increasing and subsequently decreasing expression (Figure 2-2B). As expected (Jones-Villeneuve et al. 1982), the neuronal marker,  $\beta$ -III-tubulin was detected following RA treatment at 10 days (Figure 2-2C) and coinciding with prominent signals for Glial Fibrillary Acid Protein (GFAP), an astrocyte marker, that increased by day 17 (Figure 2-2C). Neither marker was prominent in cells undergoing spontaneous differentiation in the absence of RA (Figure 2-2C), and together confirmed that neurons and astrocytes differentiated by RA.

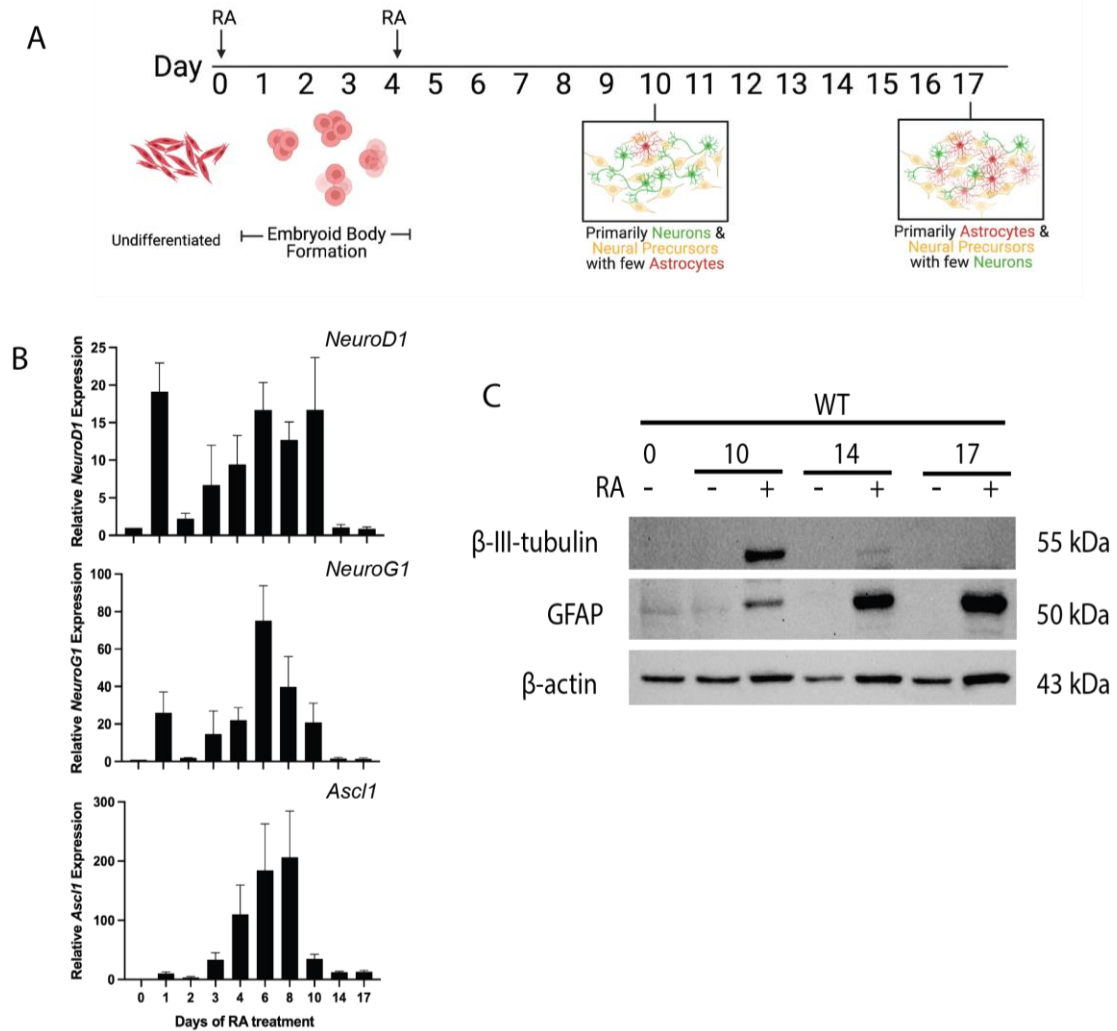


**Figure 2-2: Retinoic acid is required for P19 cell neural differentiation**

(A) Schematic of *in vitro* differentiation of P19 cells toward neural lineages. (B) RT-qPCR of *NeuroG1*, *NeuroD1*, and *Ascl1* expression on days 0-17 of RA-induced differentiation. (C) Immunoblot of β-III-tubulin and GFAP on days 0-17 of RA-induced differentiation. N=3. Bars represent mean values ± s.e.m. Panel A was created using BioRender.com.

### 2.3.2 Hh signaling is activated early in neural differentiation

Since reports note that Shh signaling is vital in vertebrate neural differentiation (Dahmane and Ruiz 1999; Wilson and Maden 2005; Briscoe and Thérond 2013), RT-qPCR was used to explore Hh component expression throughout RA treatment of P19 cells. Hh ligands *Dhh*, *Ihh*, and *Shh* were significantly upregulated after 1 day of RA treatment ( $P < 0.001$ ,  $0.01$  and  $0.05$ , respectively), as was *Gli1* ( $P < 0.001$ ), a Hh target gene, before returning to basal levels (Figure 2-3A). Expression of *Ptch1*, *Ptch2*, *Smo*, *Gli2*, *Gli3* and *Sufu* (Figure 2-3A) were also confirmed. Since *Gli3* can serve as an activator or repressor (Hui and Angers 2011), *Gli3* levels were explored throughout RA induced differentiation. Full-length *Gli3* (*Gli3FL*) was significantly increased 1 day after RA treatment (Figure 2-3B and C), whereas *Gli3* repressor (*Gli3R*) was increased at days 2, 4 and 6 of RA treatment. As the activation of Hh signaling is dependent on the ratio between *Gli3FL* and *Gli3R*, this ratio was examined, and results showed an increase in the *Gli3FL* to *Gli3R* ratio 1 day after RA treatment (Figure 2-3C). Given these data, it would appear that Hh pathway activity is increased early in neural differentiation of P19 cells, where it subsequently returns to basal levels coinciding with neuron and astrocyte differentiation.

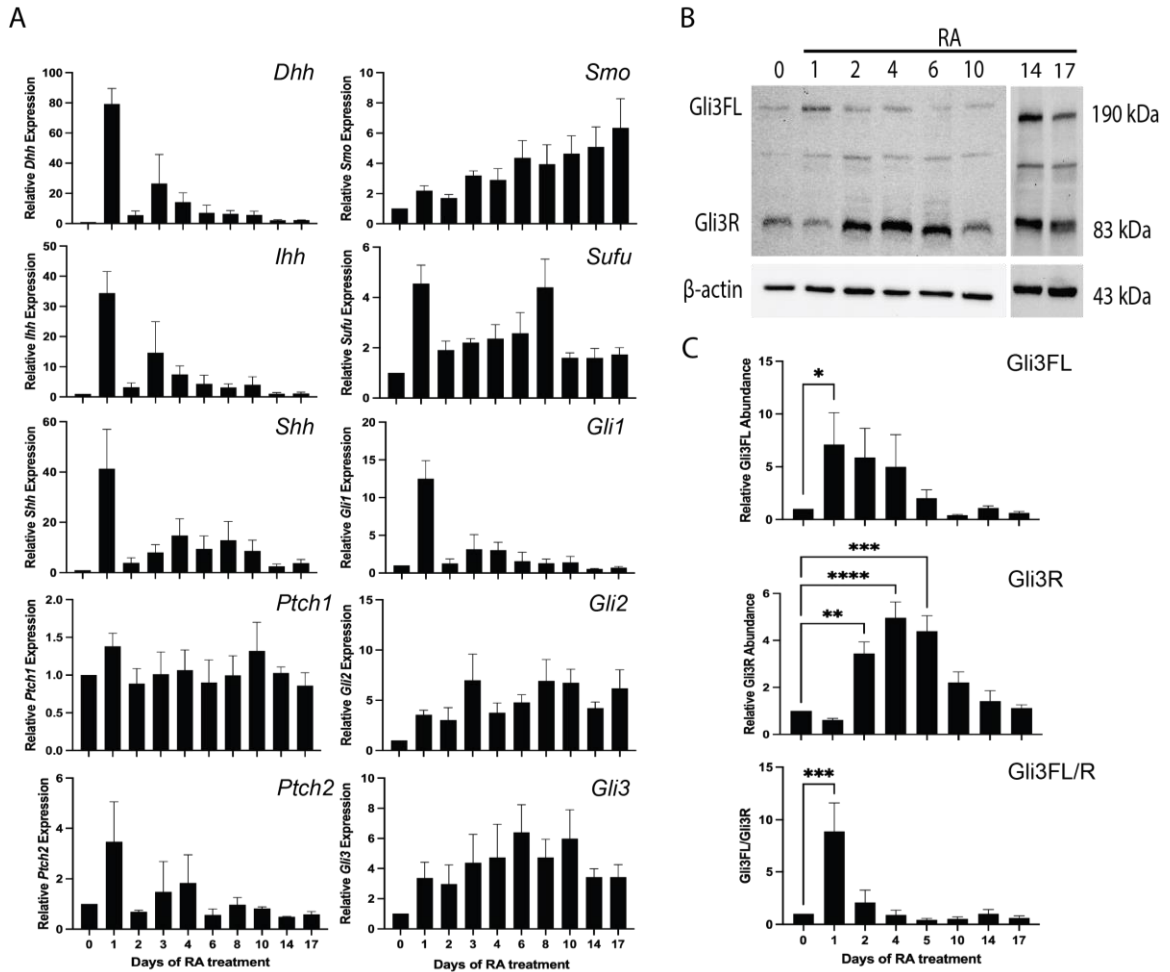


**Figure 2-3: Hh signaling is activated early in RA-induced differentiation**

(A) RT-qPCR showing expression of Hh ligands *Dhh*, *Ihh*, *Shh*, receptors *Ptch1* and *Ptch2*, intermediate pathway components *Smo* and *Sufu*, Hh target gene and transcription factors *Gli1*, *Gli2* and *Gli3* on days 0-17 of RA-induced differentiation. (B) Immunoblot of Gli3 full length (Gli3FL) and Gli3 repressor (Gli3R) on days 0-17 of RA treatment. (C) Densitometric analysis of Gli3FL, Gli3R and the Gli3FL to Gli3R ratio of immunoblot in B. N=3. Bars represent mean values  $\pm$  s.e.m. P-values were determined by One-way ANOVA with Tukey's post-hoc analysis, \* $P < 0.05$ , \*\* $P < 0.01$ , \*\*\* $P < 0.001$ , \*\*\*\* $P < 0.0001$ .

### 2.3.3 Early Hh signaling is required but not sufficient for neural differentiation

To first address if activation of Hh signaling would affect differentiation, cells were treated with 0.5  $\mu$ M RA (RA), 0.5  $\mu$ M RA plus 10 nM SAG on day zero (RA + SAG d0), 10 nM SAG alone on day zero (SAG d0) or 10 nM SAG on day 0 with subsequent 0.5  $\mu$ M RA treatment on day 4 (SAG d0 + RA d4). Immunoblots showed  $\beta$ -III-tubulin in RA, RA + SAG d0 and SAG d0 + RA d4 treatments but not in SAG d0 treatment alone on day 10 (Figure 2-4A). Densitometric analysis revealed an increase in  $\beta$ -III-tubulin intensity in the RA + SAG d0 treatment compared to RA alone, but no difference between RA alone and the SAG d0 + RA d4 treatment (Figure 2-4B). Experiments allowing cell aggregation for 4 days in the absence of RA, then subsequent 0.5  $\mu$ M RA treatment at day 4 (DMSO d0 + RA d4), also showed the  $\beta$ -III-tubulin signal at day 10, as did cells in the presence of DMSO only (DMSO d0 + DMSO d4); however, both treatments were significantly less than the RA treatment alone (Figure 2-5A and B). Therefore, SAG over-activation of Hh signaling, in the presence of RA, appeared to enhance the neuron cell fate while SAG alone was not sufficient to induce neurons.

Immunoblot analysis of GFAP showed detection on day 17 in the RA and RA + SAG d0 treatments, but no signals were seen in the SAG d0 alone treatment (Figure 2-4A). Furthermore, densitometric analysis showed increased GFAP intensity in the RA + SAG d0 treatment compared to RA treatment alone (Figure 2-4C). A GFAP band was also seen in the SAG d0 + RA d4 treatment (Figure 2-4A), but densitometric analysis revealed that this signal was not significantly different from the SAG d0 alone treatment (Figure 2-4C). DMSO d0 + RA d4 cells also showed this low level of GFAP at day 17 (Figure 2-5A), indicating that RA treatment at this later time was sufficient to induce astrocytes; however, not to the extent observed with the initial RA treatment. As the changes to neural cell fates in the presence of SAG were subtle, we confirmed SAG activation of Hh was occurring in these cells through a luciferase assay (Figure 2-5D). Thus, it appears from immunoblot data that supplementing the initial RA treatment with SAG increases astrocyte differentiation, but activation of Hh signaling alone using SAG was not sufficient to induce the astrocyte fate.



Since early Hh pathway activation enhances neural cell fates, would its attenuation affect neural differentiation? Cells were treated with either 0.5  $\mu$ M RA (RA) or 0.5  $\mu$ M RA plus 10  $\mu$ M Cyc on day 0 (RA + Cyc d0); both with subsequent RA treatments on day 4. Immunoblot analysis of  $\beta$ -III-tubulin on day 10 showed signals in both RA and RA + Cyc treatments (Figure 2-4D), but densitometry revealed the intensity was significantly reduced with Cyc treatment (Figure 2-4E). Cyc also had dramatic effects on GFAP levels, eliminating the response induced by RA (Figure 2-4D and F). Experiments with cells treated with RA plus the Cyc vehicle (RA + DMSO d0) showed no significant change in either marker (Figure 2-5C). These results suggest that inhibition of the Hh pathway attenuates neuron and astrocyte cell fates, and thus is required for proper differentiation of these cell types.

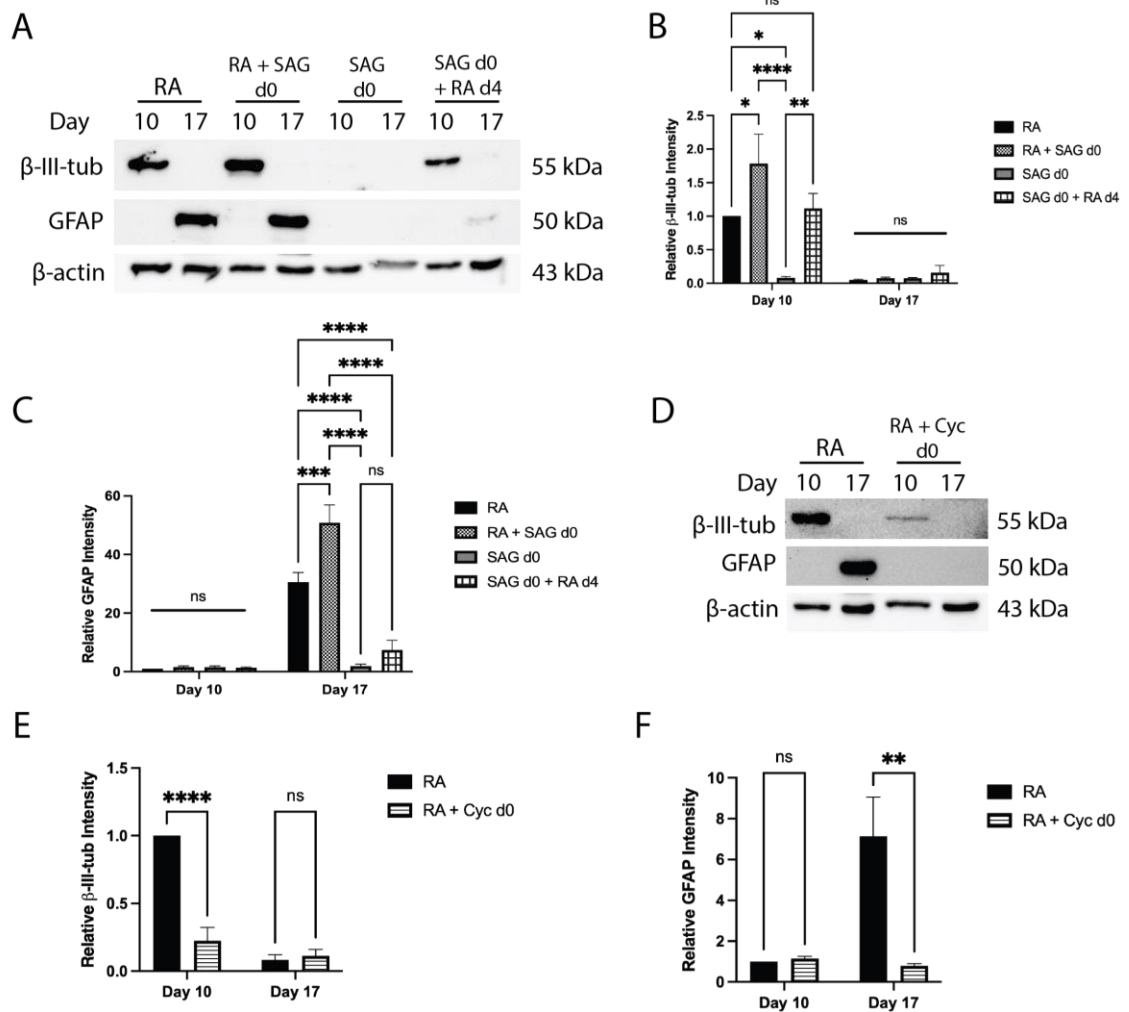


**Figure 2-4: Early Hh pathway activation is required but not sufficient to induce neural lineages**

(A) Immunoblot of  $\beta$ -III-tubulin and GFAP on days 10 and 17 of cells treated with RA alone, RA plus SAG on day 0 (RA + SAG d0), SAG alone on day 0 (SAG d0) or SAG on day 0 plus RA on day 4 (SAG d0 + RA d4) treatment. (B) Densitometry of  $\beta$ -III-tubulin and (C) of GFAP from immunoblot in A. (D) Immunoblot of  $\beta$ -III-tubulin and GFAP on days 10 and 17 of cells treated with RA or RA plus Cyclopamine (Cyc) (RA + Cyc d0) on day 0. (E) Densitometry of  $\beta$ -III-tubulin and (F) GFAP from immunoblot in D. N=3. Bars represent mean values  $\pm$  s.e.m. P-values were determined by Two-way ANOVA with Sidak's post-hoc analysis, \* $P < 0.05$ , \*\* $P < 0.01$ , \*\*\* $P < 0.001$ , \*\*\*\* $P < 0.0001$ .

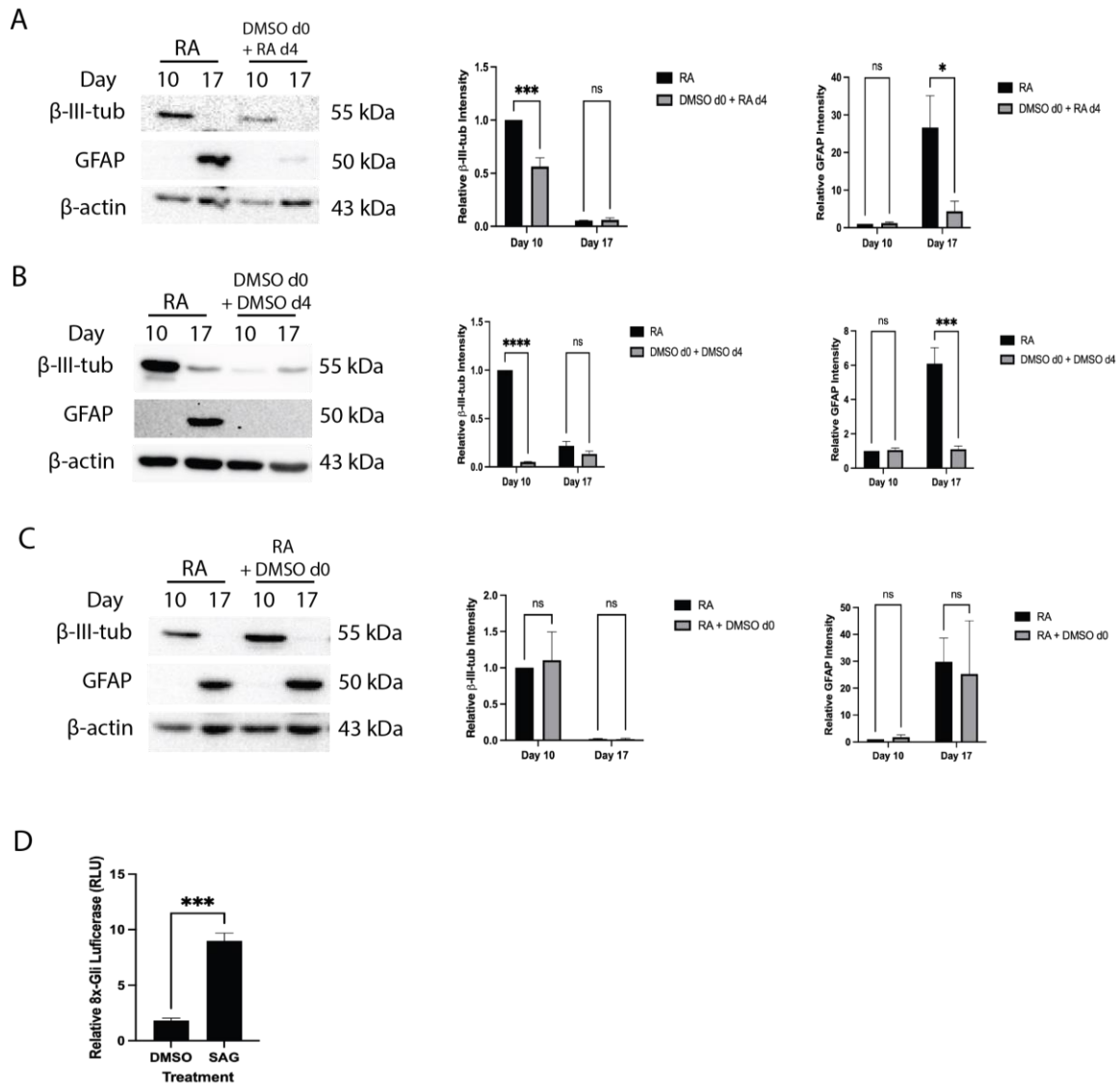


**Figure 2-5: DMSO alone and DMSO plus RA treatment is sufficient to induce neurons but not astrocytes**

Immunoblots and densitometry analyses of  $\beta$ -III-tubulin and GFAP in cells treated with RA or (A) DMSO on day 0 and 0.5  $\mu$ M RA on day 4 (DMSO d0 + RA d4), (B) DMSO treatments on days 0 and 4 (DMSO d0 + DMSO d4) and (C) RA plus DMSO on day 0 (RA + DMSO d0). (D) Luciferase assay of Gli responsive reporter in DMSO and SAG treated undifferentiated cells. N=3. Bars represent mean values  $\pm$  s.e.m. P-values were determined by Two-way ANOVA with Sidak's post-hoc analysis. \* $P < 0.05$ , \*\*\* $P < 0.001$ , \*\*\*\* $P < 0.0001$ .

#### 2.3.4 SUFU levels during neural differentiation

SUFU negatively regulates Gli activity and as reported by Humke et al. (Humke et al. 2010), promotes Gli3 conversion to a repressor. To determine its role in Hh signaling seen in P19 cells, *Sufu* gene expression was examined and found to be moderately increased on day 1, 8 and 10 of RA treatment (Figure 2-3A); however, at the protein level no changes were seen across any timepoints of RA treatment (Figure 2-6). Since *Sufu* expression and protein levels remain largely unchanged it is tempting to speculate that the early activation of the Hh pathway is controlled by the cellular localization or post-translational modification status of SUFU.

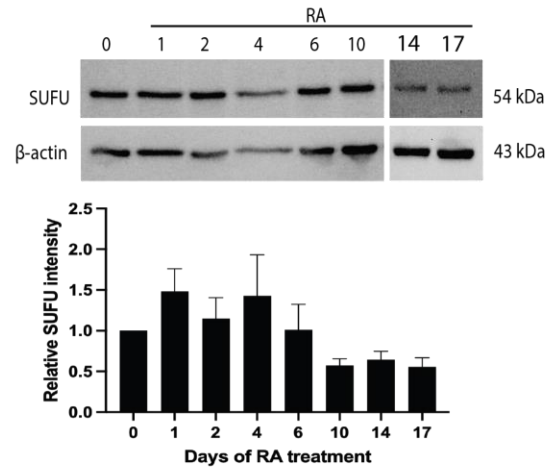


**Figure 2-6: SUFU levels do not change during RA-induced neural differentiation**

Immunoblot of SUFU at select times during RA treatment and corresponding densitometry. N=3. Bars represent mean values  $\pm$  s.e.m. P-values were determined by One-way ANOVA with Tukey's post-hoc analysis.

### 2.3.5 *Sufu* knockout activates Hedgehog signaling

Since SUFU acts as an essential regulator of Gli3 (Humke et al. 2010) and Gli2 (Humke et al. 2010; Han et al. 2015), its loss was expected to induce Hh signaling. To test this, CRISPR-Cas9 was used to target exon 6 of the *Sufu* gene (Figure 2-7A), resulting in clones with an 81 bp deletion (KO #1) that spans the intron-exon boundary between intron 5 and exon 6 and another with a 1 bp insertion (KO #2). Sequence alignment, TIDE analysis (Brinkman et al. 2014) and in silico translation of clones revealed a premature stop codon shortly after the mutation (Figure 2-8). Immunoblot analyses using a SUFU antibody targeted to the C-terminus of SUFU, a region reported to be required for GLI binding (Dunaeva et al. 2003; Han et al. 2015), was detected in untreated WT cells, but was not in either mutant clone (Figure 2-7B). SUFU levels were also unchanged in Cas9 vector transfected cells without SUFU-specific gRNA (labeled PX459), in addition to vector transfected cells showing no change in differentiation marker abundance compared to WT cells (Figure 2-9). To determine other effects, *Sufu*<sup>-/-</sup> alleles caused a decrease in cell numbers compared to WT cells cultured to 96 h (Figure 2-7C); however, MTT analysis at the same time points showed no change in MTT absorbance (Figure 2-7D). As predicted, KOs showed increased expression of Hh targets *Gli1*, *Ptch1*, and *Ascl1* in undifferentiated cultures (Figure 2-7E). Thus, the data shows the loss of SUFU does not greatly affect the proliferation of undifferentiated cells, contrary to that reported in mouse neural stem cells of the dentate gyrus (Noguchi et al. 2019), and instead it induced Hh target gene expression in P19 cells.

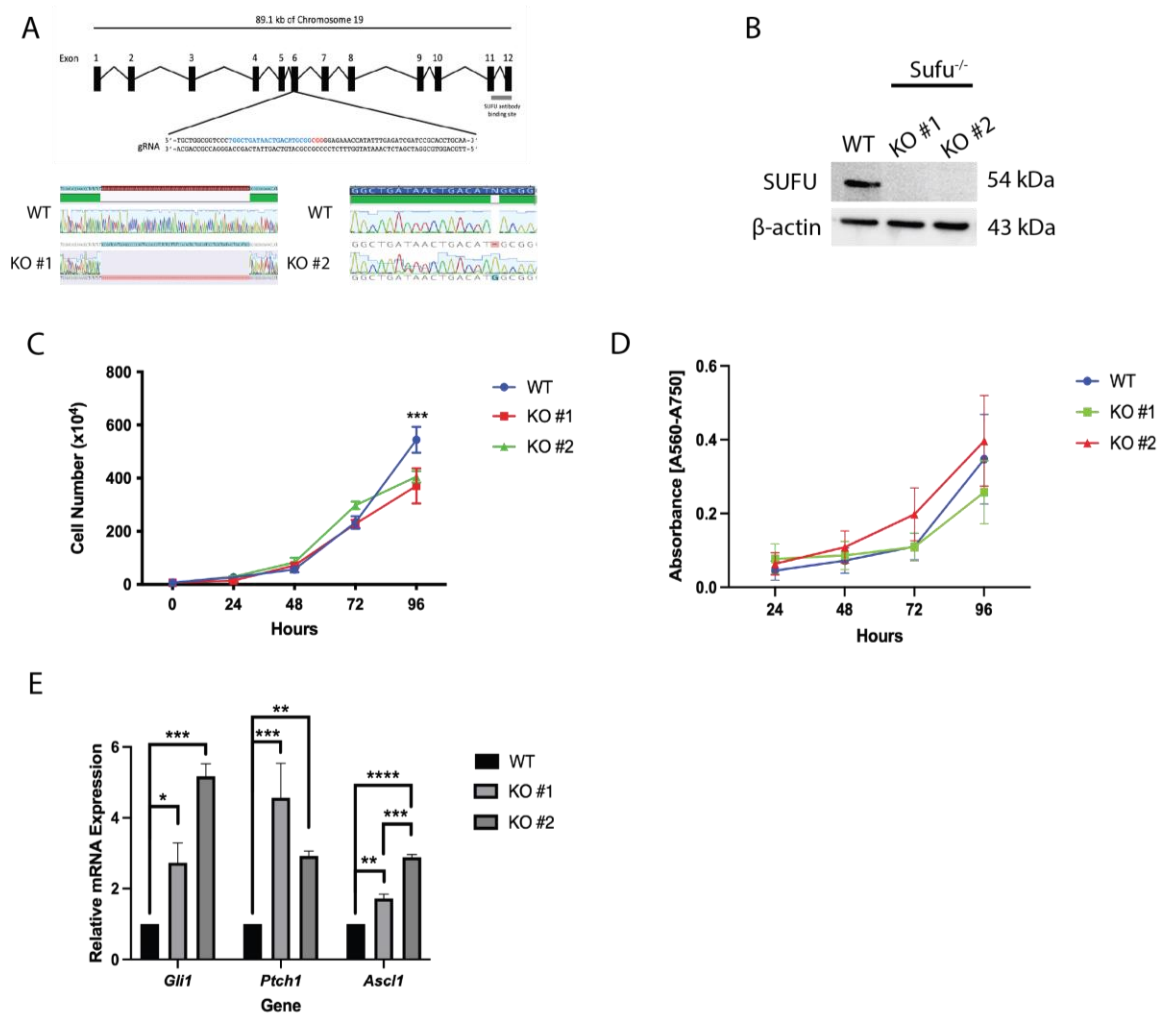


**Figure 2-7: CRISPR-Cas9 knock out of *Sufu* activates Hh signaling in undifferentiated P19 cells**

(A) Schematic showing gRNA targeting exon 6 of the *Sufu* gene yielding two KO clones. (B) Immunoblot of SUFU levels in wildtype (WT) and *Sufu*<sup>-/-</sup> clones. (C) Cell count curves of WT and *Sufu*<sup>-/-</sup> clones between 0-96 hours and (D) MTT assay of the difference in absorbance of MTT reagent in WT and KO cells at 560nm and 750nm. (E) Expression of *Gli1*, *Ptch1* and *Ascl1* in WT and *Sufu*<sup>-/-</sup> clones in undifferentiated cultures. N=3. Bars represent mean values  $\pm$  s.e.m. P-values for C and D were determined by Two-way ANOVA with Sidak's post-hoc analysis and for E were determined by One-way ANOVA with Tukey's post-hoc analysis. \* $P < 0.05$ , \*\* $P < 0.01$ , \*\*\* $P < 0.001$ , \*\*\*\* $P < 0.0001$ .

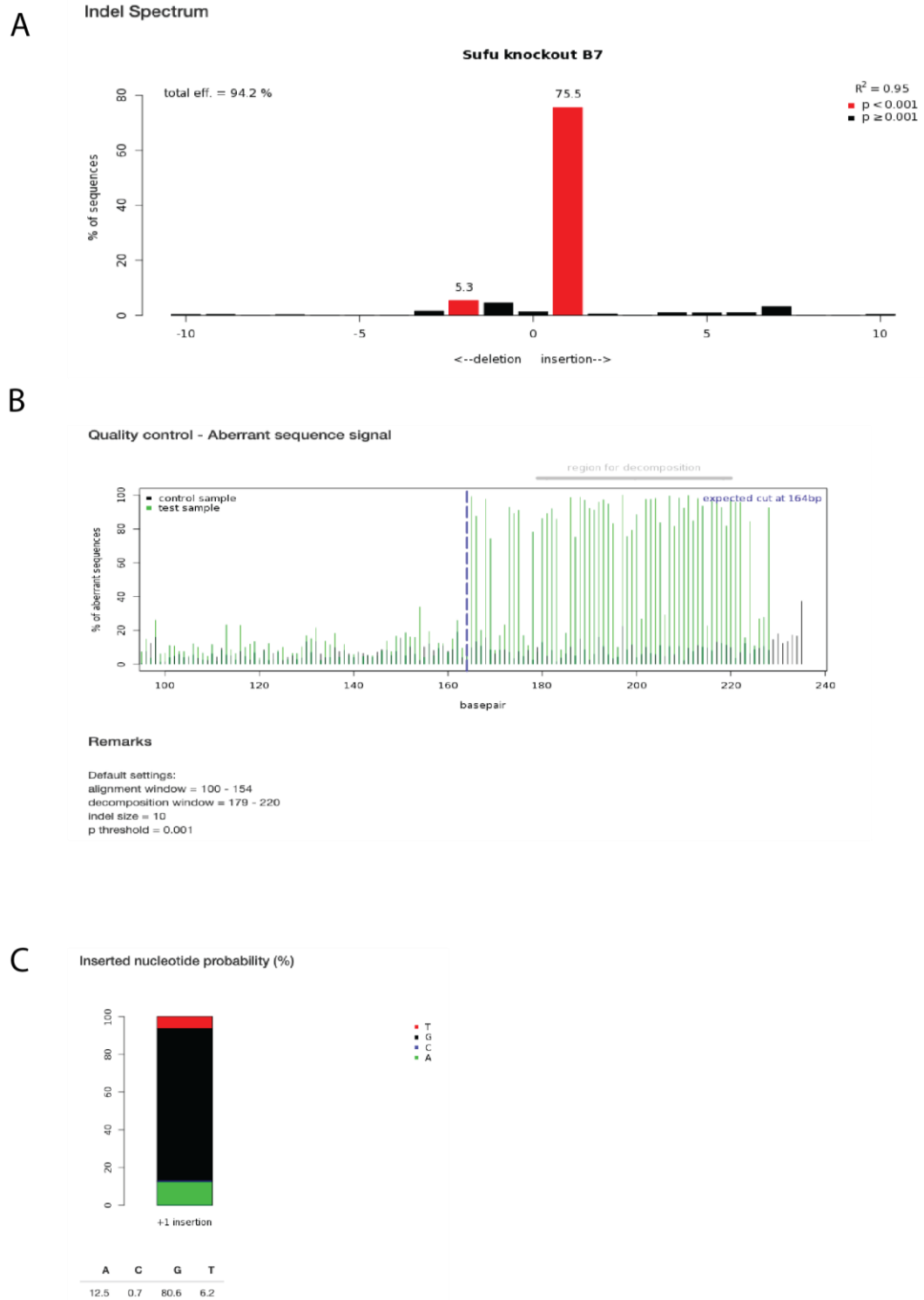


**Figure 2-8: TIDE analysis of *Sufu*<sup>-/-</sup> clone (KO#2)**



**(A)** Indel spectrum analysis showing predicted mutant allele after sequence alignment. Bars represent percent of sequences identified during analysis, with red bars being statistically significant. **(B)** Aberrant sequence analysis after sequence alignment. Black lines represent wildtype sequence and green lines represent alignment of mutant sequence. Dashed line represents the predicted cut site. Taller green compared to black lines indicate a likely mutation. **(C)** Inserted nucleotide probability score after Indel spectrum analysis.

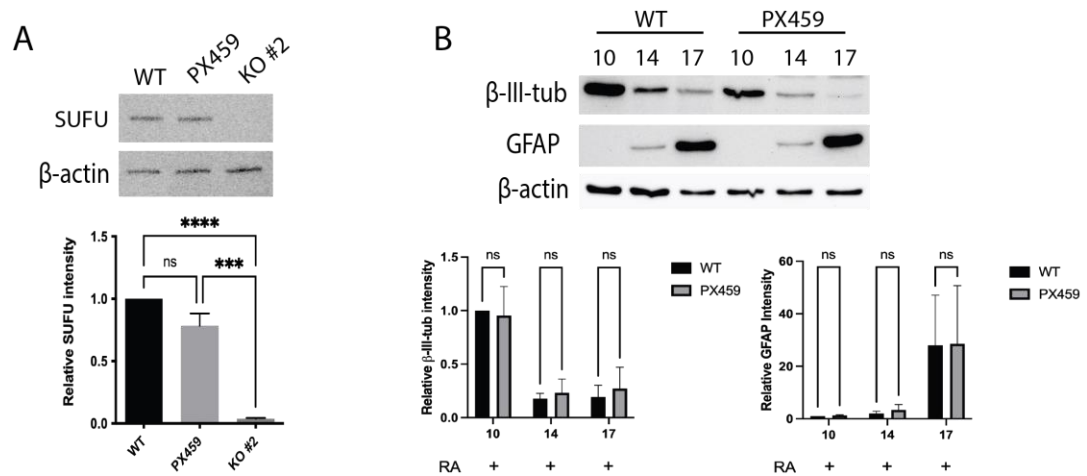


**Figure 2-9: CRISPR-Cas9 plasmid transfection and selection do not affect SUFU levels or P19 cell differentiation**

Immunoblots and corresponding densitometry of (A) SUFU and (B) differentiation markers  $\beta$ -III-tubulin and GFAP. N=3. Bars represent mean values  $\pm$  s.e.m. P-values of SUFU levels were determined by One-way ANOVA with Tukey's post-hoc analysis. Differentiation marker P-values were determined by Two-way ANOVA with Sidak's post-hoc analysis. \*\*\* $P < 0.001$ , \*\*\*\* $P < 0.0001$ .

### 2.3.6 Sufu loss activates Hh signaling through loss of Gli3

RT-qPCR was used to determine if the observed activation of Hh signaling in the KO lines was maintained throughout RA-induced differentiation. *Sufu*<sup>-/-</sup> cells treated with RA maintained higher *Gli1* (Figure 2-10A and Figure 2-11A) and *Ptch1* (Figure 2-10B and Figure 2-11B) expression compared to that in WT cells. Since previous work also showed the connection between SUFU and Gli3 processing (Humke et al. 2010), and we were particularly interested in *Gli3* expression and protein levels. Results show no significant differences in *Gli3* expression between *Sufu*<sup>-/-</sup> and WT cells in KO#2 (Figure 2-10C), however, significantly decreased *Gli3* levels were observed at days 10, 14 and 17 in KO #1 (Figure 2-11C). At the protein level, neither the Gli3 repressor nor full-length Gli3 were detected in KO #2 (Figure 2-10D), and this was consistent with KO #1 having decreased or absent Gli3 levels (Figure 2-11D). Thus, the loss of SUFU, specifically the region of the polypeptide required for Gli3 processing, likely contributes to post-translational perturbations to Gli3, causing its loss and the observed higher expression of Hh target genes.

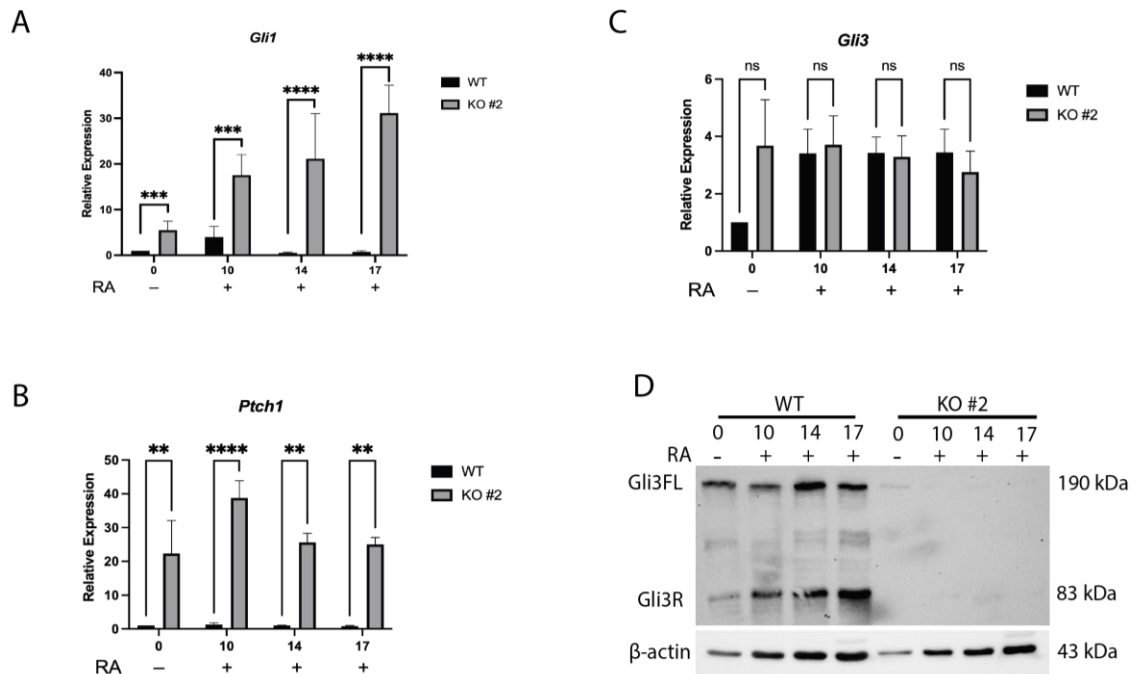


**Figure 2-10: *Sufu*<sup>-/-</sup> #2 maintains increased Hh signaling and causes the loss of Gli3**

Expression of (A) *Gli1* and (B) *Ptch1* and (C) *Gli3* in wildtype (WT) and *Sufu*<sup>-/-</sup> KO #2 cells on days 0-17. (D) Immunoblot of Gli3 full length (Gli3FL) and Gli3 repressor (Gli3R) in WT and *Sufu*<sup>-/-</sup> KO #2 cells on days 0-17. N=3. Bars represent mean values  $\pm$  s.e.m. P-values were determined by Two-way ANOVA with Sidak's post-hoc analysis. \* $P < 0.05$ , \*\* $P < 0.01$ , \*\*\* $P < 0.001$ , \*\*\*\* $P < 0.0001$ .

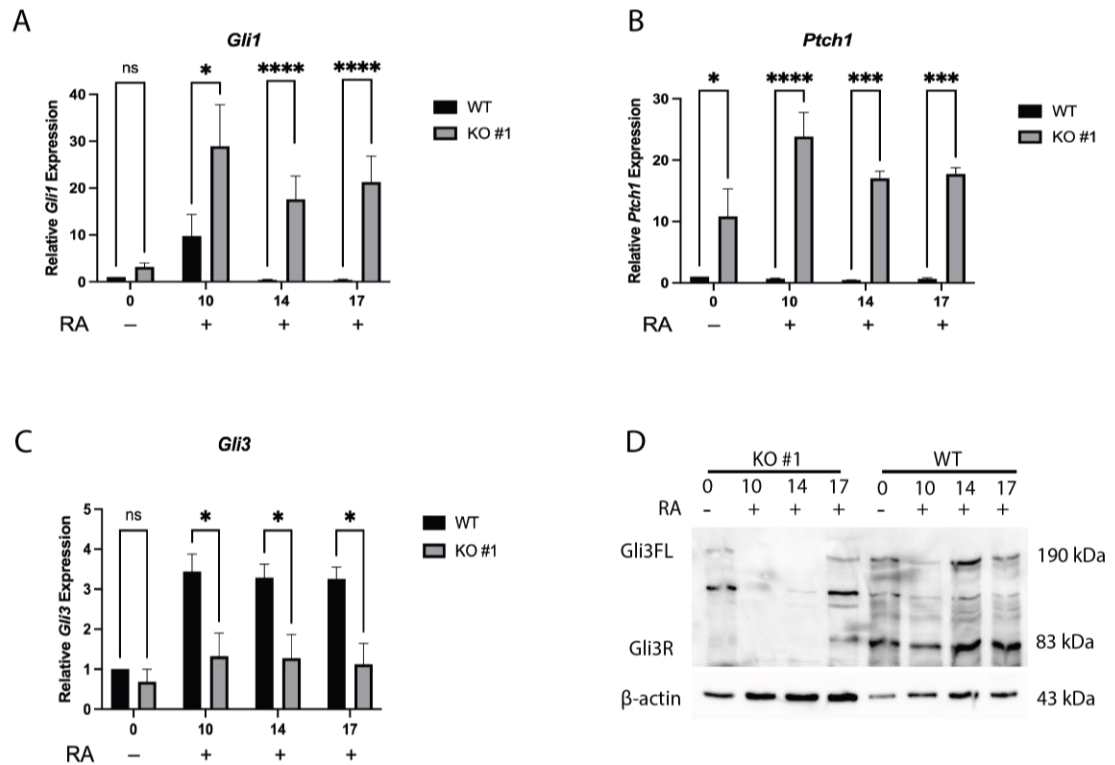


**Figure 2-11: *Sufu*<sup>-/-</sup> #1 maintains increased Hh signaling and causes the loss of Gli3**

Expression of (A) *Gli1* (B) *Ptch1* and (C) *Gli3* in wildtype (WT) and *Sufu*<sup>-/-</sup> KO #1 cells on days 0-17. (D) Immunoblot of Gli3 full-length (Gli3FL) and Gli3 repressor (Gli3R) in WT and *Sufu*<sup>-/-</sup> KO #1 cells on days 0-17. N=3. Bars represent mean values  $\pm$  s.e.m. P-values were determined by Two-way ANOVA with Sidak's post-hoc analysis. \* $P < 0.05$ , \*\*\* $P < 0.001$ , \*\*\*\* $P < 0.0001$ .

### 2.3.7 *Sufu* knockout delays and decreases the astrocyte cell fate

If the *Sufu* knockout induced Hh target genes what effect would this have on neural differentiation? To determine if KO cells could differentiate in the absence of RA, these cells were aggregated and replated in the absence or presence of RA. Both KO lines treated with RA showed  $\beta$ -III-tubulin signals at day 10 and GFAP signals on days 14 and 17; neither marker was detected in the absence of RA (Figure 2-12A). To determine if the timing or degree of differentiation was affected by the loss of SUFU, the expression of these markers was compared in each knockout line with that in WT cells at days 10, 14 and 17 in the presence of RA (Figure 2-12B). Densitometric analyses confirmed  $\beta$ -III-tubulin levels did not change between WT and KO cells (Figure 2-12C). Significantly, astrocyte differentiation was affected and GFAP signals on immunoblots were absent on day 10 and reduced on day 14 of RA treatment in *Sufu*<sup>-/-</sup> cells compared to WT (Figure 2-12B and D). The absence of GFAP on day 10 was interpreted cautiously, as in WT cells, we have seen inconsistencies in GFAP levels at this time point. Nevertheless, GFAP levels are consistently high in WT cells at day 14 (Figure 2-2C and Figure 2-15A) and it appeared removing SUFU delayed astrocyte differentiation when RA was present. To further confirm this result, RT-qPCR was used to measure expression of astrocyte markers *GFAP*, aldehyde dehydrogenase 1 family member L1 (*Aldh1l1*) and S100 calcium-binding protein B (*S100b*) (Figures 2-12, E-G, respectively). Consistent with immunoblotting results, *GFAP* expression was reduced on days 10 and 14, and unlike the immunoblotting was also reduced at day 17 of RA treatment (Fig. 2-12E). *Aldh1l1* expression, like GFAP, was also reduced in KO cells compared to WT at days 10, 14 and 17 of RA treatment (Fig. 2-12F). Interestingly, *S100b* expression was reduced at day 10 of RA treatment in KO compared to WT cells, however, it was not different from WT at day 14 and was increased compared to WT at day 17 (Fig. 2-12G).

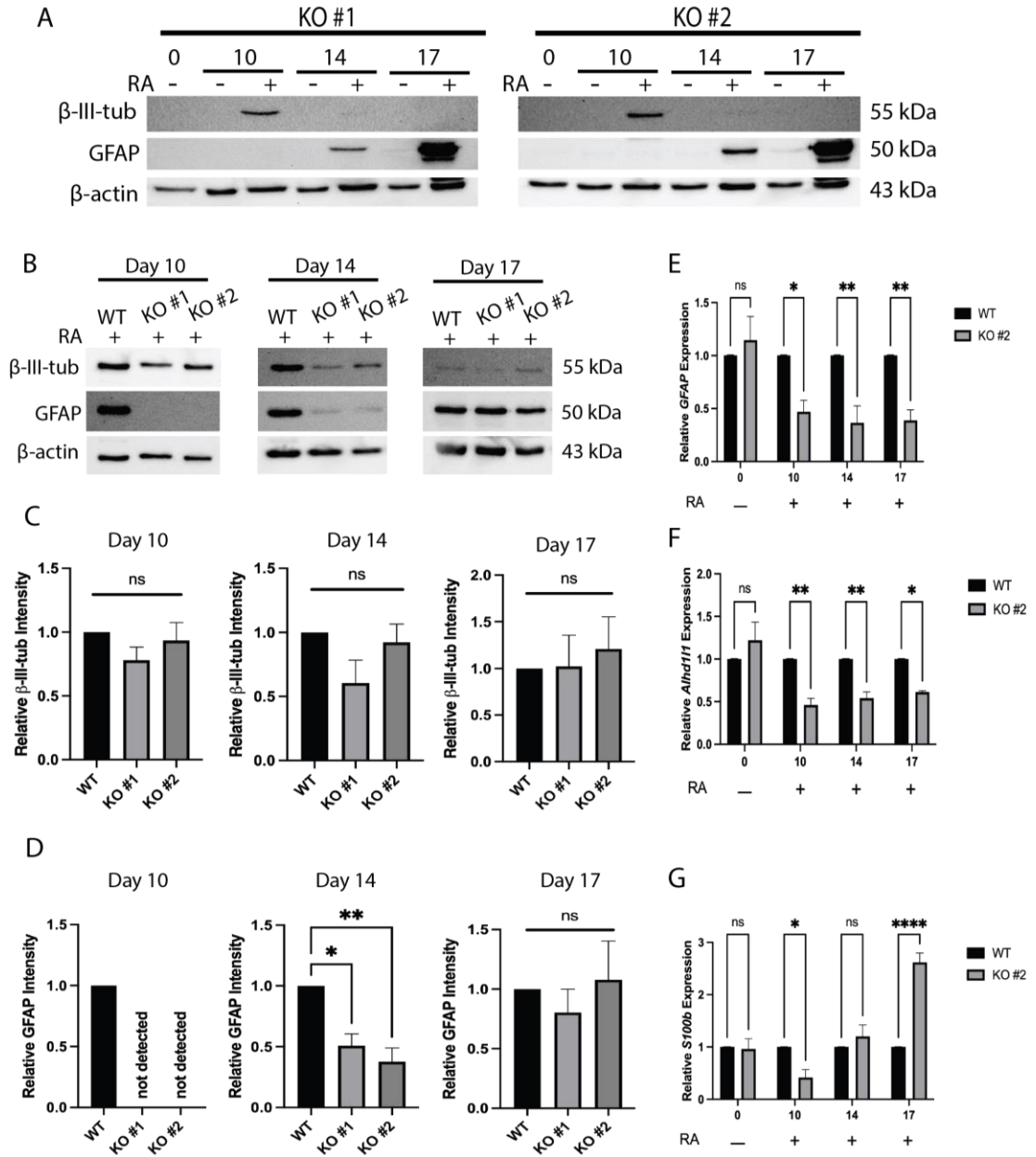


**Figure 2-12: *Sufu*<sup>-/-</sup> delays astrocyte formation without affecting neuron differentiation**

**(A)** Immunoblot of  $\beta$ -III-tubulin and GFAP on days 0-17 in *Sufu*<sup>-/-</sup> KO clones. **(B)** Immunoblots of  $\beta$ -III-tubulin and GFAP on day 10, day 14 and day 17 in wildtype (WT) and *Sufu*<sup>-/-</sup> clones, and densitometric analyses of immunoblots of **(B)** showing relative intensities of **(C)**  $\beta$ -III-tubulin and **(D)** GFAP. P-values were determined by One-way ANOVA with Tukey's post-hoc analysis. RT-qPCR of astrocyte markers **(E)** *GFAP*, **(F)** *Aldh1l1*, and **(G)** *S100b*. P-values were determined by Two-way ANOVA with Sidak's post-hoc analysis. N=3. Bars represent mean values  $\pm$  s.e.m. \* $P < 0.05$ , \*\* $P < 0.01$ .



To resolve the discrepancy between immunoblotting and RT-qPCR results of *GFAP*, immunofluorescence analysis with antibodies to  $\beta$ -III-tubulin and GFAP were used on WT and *Sufu*<sup>-/-</sup> cells. Given the immunoblotting results (Fig. 2-12B and D), we were expecting to see no differences in either marker between the two cell lines at day 17 of RA treatment. However, this analysis revealed a reduction in GFAP-positive staining in *Sufu*<sup>-/-</sup> cells (Figure 2-13A, quantified in B). This observed reduction also occurred despite the KO cells having increased cell viability (Fig. 2-13C) and increased total cells (Fig. 2-13D) as measured by trypan blue exclusion assay at both days 10 and 17 of RA treatment. However, since these cells are highly heterogenous and exist in areas of high-density, flow cytometry was used, and results confirmed this reduction showing *Sufu*<sup>-/-</sup> cells (~6-25%) had significantly less GFAP-positive staining compared to WT cells (~60-70%; Figure 2-13E and F). It should also be noted that although the immunoblot data at day 17 was inconsistent with the immunofluorescence and flow analysis, the flow cytometry had identified high GFAP levels (Figure 2-13E) in some *Sufu*<sup>-/-</sup> cells, even though overall there were fewer GFAP positive cells present in the KO line (Figure 2-13E). Nevertheless, these data support the idea that the loss of *Sufu* does not alter neuronal differentiation, but it does delay and decrease astrocyte differentiation.

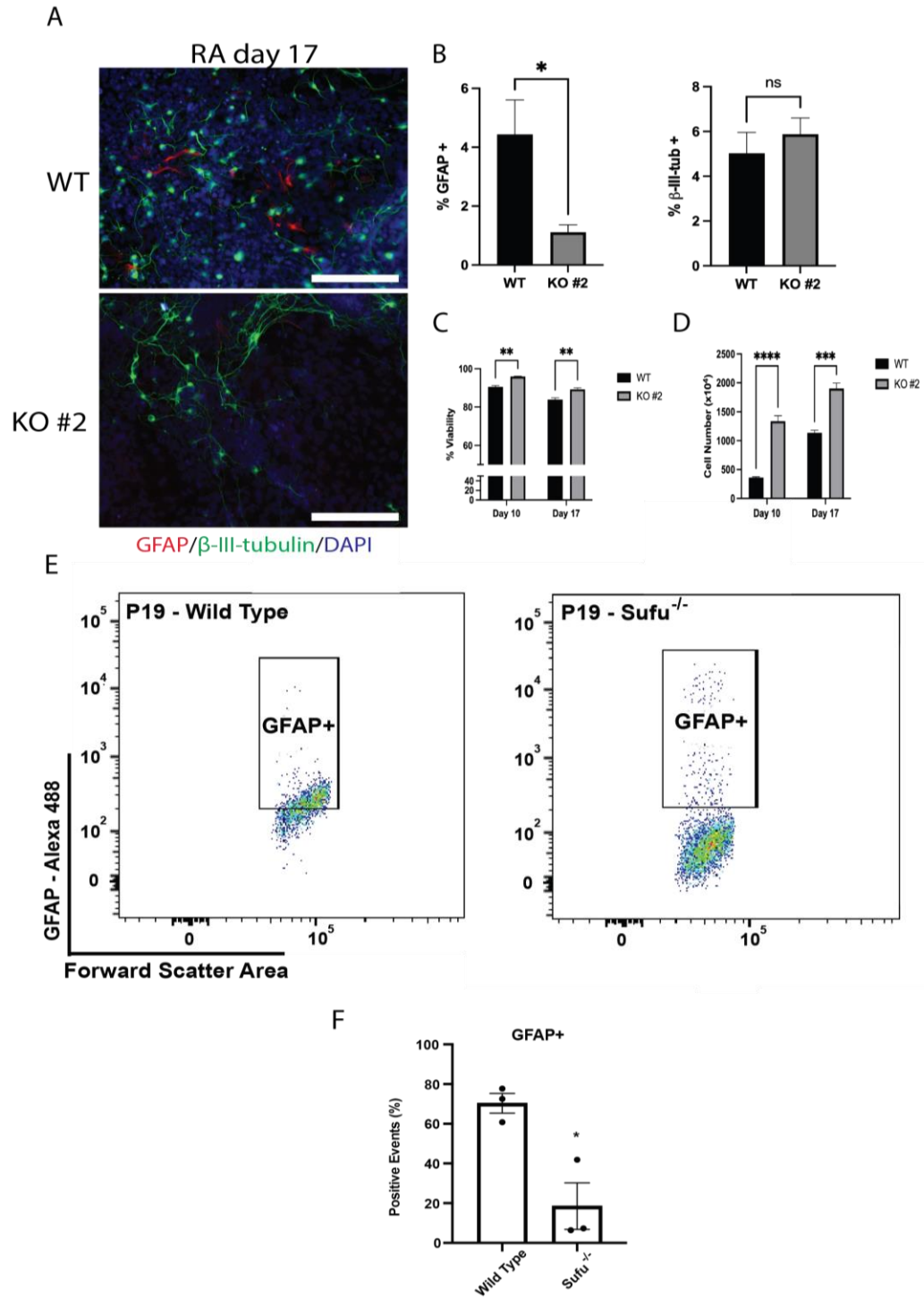


**Figure 2-13: *Sufu*<sup>-/-</sup> decreases astrocyte differentiation**

(A) GFAP (red) and  $\beta$ -III-tubulin (green) fluorescence and nuclear DAPI (blue) staining in wildtype (WT) and *Sufu*<sup>-/-</sup> KO clone #2 cells on day 17 of RA treatment. Scale bar = 200  $\mu$ m. (B) Quantification of positive cells from images in A. P-values were determined by Student's t-test. Trypan blue exclusion measuring (C) % cell viability and (D) total cell number at days 10 and 17 in WT and KO #2. P-values were determined by Two-way ANOVA with Sidak's post-hoc analysis. (E) Flow cytometry of GFAP-positive WT and *Sufu*<sup>-/-</sup> KO #2 cells on day 17 and quantified in F. P-values were determined by Student's t-test. N=3. Bars represent mean values  $\pm$  s.e.m. \* $P < 0.05$ , \*\* $P < 0.01$ , \*\*\* $P < 0.001$ , \*\*\*\* $P < 0.0001$ .

### 2.3.8 *Sufu* or *Gli3* overexpression partially rescues astrocyte phenotype

If the loss of *Sufu* resulted in delayed and decreased astrocyte differentiation (Figure 2-12 and Figure 2-13) and this was likely due to the loss of Gli3 (Figure 2-10D and Figure 2-11D), then overexpression of a CRISPR-insensitive chicken *Sufu* (pSUFU) or human *GLI3* (pGli3) in *Sufu* knockout cells should rescue the phenotype and astrocyte levels should increase in these mouse cells. Overexpression was confirmed by RT-qPCR of chicken *Sufu* and immunoblotting of human Gli3 (Figure 2-14). To determine the effect this overexpression had on astrocyte differentiation, GFAP levels were explored following pSUFU or pGli3 stable transfection in knockout cells. Results showed no GFAP detection on day 10, but there was an increase by day 14 of RA treatment, albeit not to the levels observed in the WT cells (Figure 2-15A and B). GFAP levels were maintained at day 17 in the human pGli3 stably transfected cells, but chicken pSUFU stably transfected cells showed significantly reduced levels compared to the WT or other transfected *Sufu*<sup>-/-</sup> cells (Figure 2-15A and B). Despite these minor differences, these results show that chicken *Sufu* and human *GLI3* overexpression partially rescue astrocyte differentiation and highlights not only the essential role of Gli3 in neural differentiation, but a major role for SUFU in regulating Gli3.

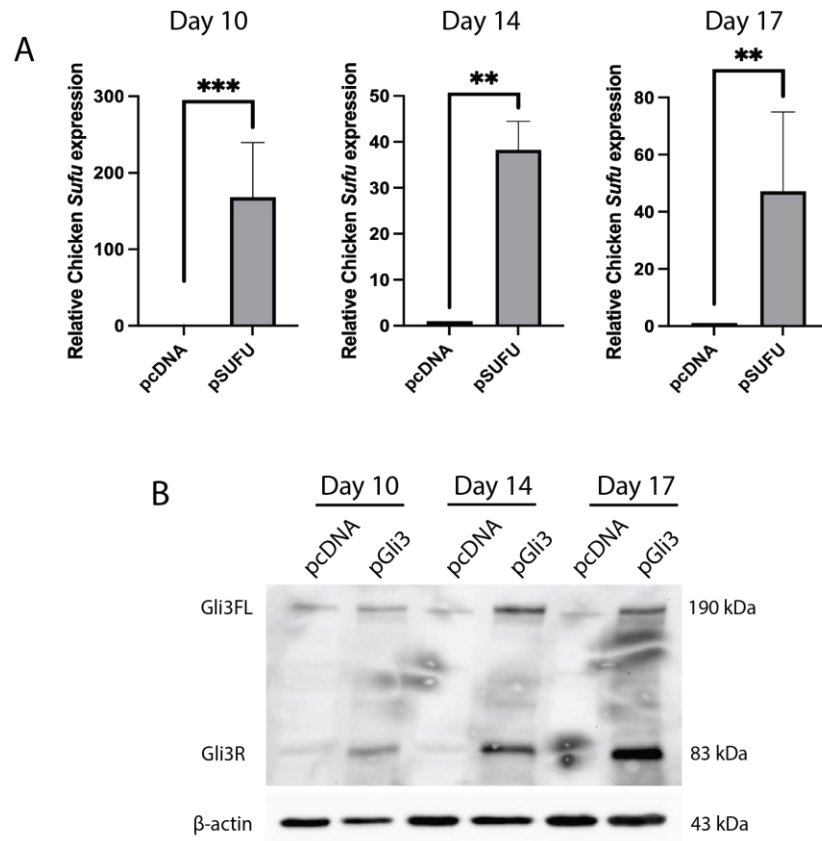


**Figure 2-14: pSUFU and pGli3 overexpression induces Chicken *Sufu* expression and rescued detection of Gli3**

(A) Chicken *Sufu* expression was detected using Chicken-specific RT-qPCR primers at days 10, 14 and 17 of RA treatment in pcDNA and pSUFU stably transfected *Sufu*<sup>-/-</sup> cells. (B) Gli3 full-length (Gli3FL) and repressor (Gli3R) was detected at days 10, 14 and 17 of RA in pGli3 stably transfected *Sufu*<sup>-/-</sup> cells. N=3. Bars represent mean values  $\pm$  s.e.m. P-values were determined by Student's t-test. \*\* $P < 0.01$ , \*\*\* $P < 0.001$ .

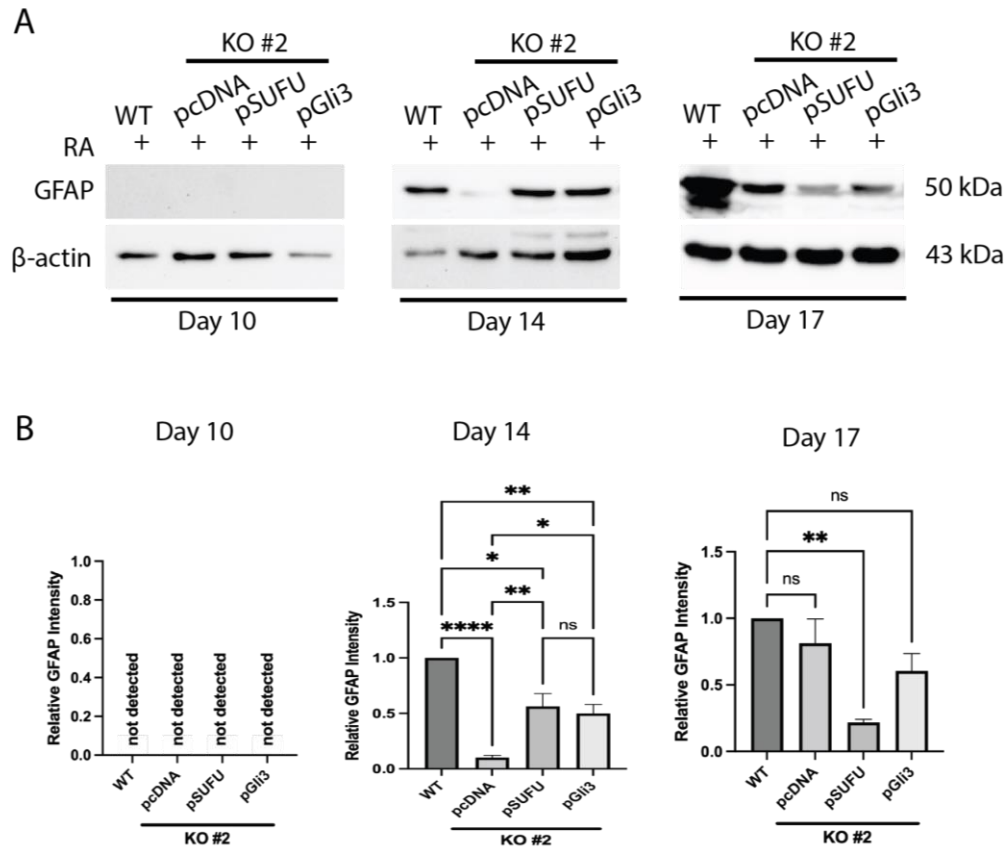


**Figure 2-15: *Sufu* or *Gli3* overexpression partially rescues the *Sufu*<sup>-/-</sup> phenotype**

(A) Immunoblot of GFAP on days 10, 14 and 17 in WT and *Sufu*<sup>-/-</sup> KO clone #2 cells stably transfected with pcDNA empty vector (pcDNA), pcDNA-chicken *Sufu* (pSUFU), or pcDNA-human *Gli3* (pGli3) vectors and treated with RA. (B) Densitometric analysis of GFAP from the immunoblot in A. N=3. Bars represent mean values  $\pm$  s.e.m. P-values were determined by One-way ANOVA with Tukey's post-hoc analysis. \* $P < 0.05$ , \*\* $P < 0.01$ , \*\*\*\* $P < 0.0001$ .

## 2.4 Discussion

Hh signaling is involved in neural tube closure and neural differentiation *in vivo* (Wilson and Maden 2005; Briscoe and Thérond 2013) where its activation results in transcription of target genes through Glis (Humke et al. 2010; Briscoe and Thérond 2013). Negative regulators of the pathway include Patched and SUFU (Briscoe and Thérond 2013), the loss of which results in medulloblastoma and Nevoid Basal Cell Carcinoma Syndrome (Hahn et al. 1996; Taylor et al. 2002; Urman et al. 2016; Smith et al. 2018). Using the mouse P19 cell model we report that Hh pathway activity is required for neural differentiation but increasing Hh pathway activity alone is not sufficient to induce neural cell fates. Furthermore, SUFU was found to be essential for *in vitro* neural differentiation as its loss caused the loss of Gli3, the induced transcription of Hh target genes and perturbed timing and proportion of astrocyte differentiation. Furthermore, human *Gli3* overexpression was sufficient to rescue GFAP, the astrocyte marker, in these SUFU deficient mouse cells, which indicates that Gli3 acts downstream or in parallel to the negative regulation imparted by SUFU.

RA-induced neural differentiation of P19 cells is well established (Jones-Villeneuve et al. 1982; McBurney et al. 1982, 1988; McBurney 1993), however few studies have explored Hh signaling in the model (Tan et al. 2010; Voronova et al. 2011; Lin et al. 2012). Voronova and colleagues (Voronova et al. 2011) also explored expression of Gli transcription factors during RA induced neurogenesis, and we have added to that work by reporting timeline expression of all components of the pathway. Specifically, we demonstrated that RA induced *Shh* expression (Figure 2-3A) where RA likely acts in these cells through the transcription factor FOXA1, which promotes the early expression of *Shh* (Tan et al. 2010); two other messages encoding Hh ligands (*Dhh* and *Ihh*) were also expressed (Figure 2-3A). IHH and DHH, like SHH, can activate the pathway as evident in long bone differentiation (St-Jacques et al. 1999; Bechtold et al. 2019) and gonad development (Bitgood et al. 1996; Clark et al. 2000; Bashamboo and McElreavey 2015). Similar results showing transcriptional activation of all Hh ligands was reported with human embryonic stem cells (hESCs) induced to form neural tissues (Wu et al. 2010). Thus, it is likely that SHH is responsible, but since transcripts encoding all ligands

are induced by RA it remains unclear which isoform triggers pathway activation in the P19 model. Although we, like others, have demonstrated the presence of Hh signaling in P19 differentiation, other signaling pathways including those linked to Wnt, Fgf and Yap are also involved (Tang et al. 2002; Chen et al. 2006; Jing et al. 2009; Lin et al. 2012). Considering our study, these other pathways require further investigation to determine if they too are temporally regulated to facilitate differentiation.

Utilization of RA to induce neural lineages *in vitro* goes beyond the P19 model, as RA is used for directed neural differentiation of human induced pluripotent stem cells and mouse embryonic stem cells (mESCs) (Fraichard et al. 1995; Mak et al. 2012). Many neural differentiation protocols also supplement RA with exogenous SHH or SAG in order to enhance the differentiation of neurons (Okada et al. 2004; Mak et al. 2012; Wu et al. 2012) and glial cell progenitors (Li et al. 2019). Like these previous results, co-treating P19 cells with RA and SAG at day zero in our protocol enhanced the differentiation of both neurons and astrocytes (Figure 2-4), although treating with SAG alone was not sufficient to induce differentiation. We also investigated the effect of inhibiting the Hh pathway using Cyc, where Cyc treatment inhibited neuron and astrocyte differentiation (Figure 2-4), a result consistent with previous work showing Cyc co-treatment with RA decreased expression of neural-related transcription factors in mESCs (Okada et al. 2004). *In vivo* studies also highlight the requirement of Hh signaling in neural differentiation and development, where mutations reducing Hh activity causes reduced neuron differentiation in the embryonic midbrain (Gazea et al. 2016), reduced neural progenitors in the developing cerebellum (Spassky et al. 2008), reduced neurogenesis of the developing telencephalon (Komada et al. 2008; Xu et al. 2010) or large-scale alterations to the size of interneuron differentiation regions in the neural tube (Ding et al. 1998; Rallu et al. 2002). Thus, the early activation of Hh signaling in the differentiation of neural lineages is a requirement, and we next sought to understand the importance of later-stage reduction of the Hh signal by SUFU.

SUFU regulation of Hh signaling involves the ubiquitin-proteasome pathway following Hh pathway activation (Yue et al. 2009). We showed Hh ligand expression is induced within 1 day of RA treatment (Figure 2-2) and given previous reports on SUFU



regulation, an early decrease in SUFU levels was expected. Our results, however, showed no significant change in SUFU levels during any stage of neurogenesis in P19 cells (Figure 2-6). Thus, it is likely that SUFU is being regulated through post-translational modifications to affect Hh signaling output, and although not explored here, it should be noted that differential phosphorylation and ubiquitination can both promote or inhibit SUFU stability and/or Gli interaction (Takenaka et al. 2007; Chen et al. 2011; Wang et al. 2016; Infante et al. 2018). CRISPR-Cas9, used to deplete SUFU from P19 cells, showed the loss of SUFU induces the ectopic transcription of Hh target genes (Figure 2-7, Figure 2-10, Figure 2-11) and while supported by studies using mice, mESCs and hESCs (Chen et al. 2009; Wu et al. 2010; Hoelzl et al. 2015; Urman et al. 2016; Hoelzl et al. 2017), this is in contrast with a study showing reduced Hh target expression in adult neural stem cells (Noguchi et al. 2019) and in another showing loss of *Sufu* reducing maximal Hh pathway activity in the developing mouse spinal cord (Zhang et al. 2017). Given previous work showing *Gli2* overexpression in P19 cells is sufficient to induce neuron differentiation in the absence of RA (Voronova et al. 2011), we were surprised to observe SUFU-deficient P19 cells did not differentiate towards the neuron lineage in the absence of RA (Figure 2-12A). That another study showed the knockdown of *Gli2* in YAP overexpressing P19 cells causes an increase in neuron differentiation (Lin et al. 2012), would indicate that other Gli's may be involved in the neural differentiation of P19 cells, specifically Gli3.

The connection between aberrant astrocyte differentiation and SUFU deficiency came from examining the transcriptional activation of Hh target genes (Figure 2-7, Figure 2-10, and Figure 2-11). *Gli1* and *Ptch1* expression was higher when *Sufu* was knocked out, but not *Gli3* (Figure 2-10). Previous reports in mouse embryonic fibroblasts and mouse embryos show that SUFU is required for proper Gli3 processing (Kise et al. 2009) and its absence leads to reduced or absent Gli3 protein (Chen et al. 2009; Makino et al. 2015), which also occurs with conditional *Sufu* knockouts in the embryonic and post-natal mouse brain (Kim et al. 2011, 2018; Yabut et al. 2015; Jiwani et al. 2020). We reported similar results with Gli3 in P19 cells and showed that it affects neural differentiation. In support, conditional knockouts of *Sufu* at various stages of mouse brain development results in decreased neuron differentiation and disorganized glial cell arrangements in the

cerebellum and forebrain (Yabut et al. 2015; Kim et al. 2018). Discrepancies, however, do exist even within Hh signaling in P19 cells (Voronova et al. 2011; Lin et al. 2012), and although these differences can be explained, our work has shown the knockout of *Sufu* was accompanied by the consistent upregulation of Hh target genes, like that seen in mouse retinal progenitor cells (Cwinn et al. 2011), mESCs (Hoelzl et al. 2015) and the developing mouse neocortex (Yabut et al. 2015) lacking SUFU. This upregulation did not result in neuron differentiation without RA treatment (Figure 2-12A) and this result is supported by work in SUFU-deficient mESCs (Hoelzl et al. 2015) and SHH treated hESCs (Wu et al. 2010) maintaining their pluripotent state without additional differentiation cues. Our results did show a delay and decrease in astrocyte differentiation with SUFU loss (Figure 2-12 and Figure 2-13), which may explain the disorganization of glial cells observed in conditional *Sufu* knockouts described in mouse embryos (Yabut et al. 2015; Kim et al. 2018). However, previous work has shown the same reduction in astrocyte differentiation in P19 cells overexpressing a dominant negative form of *Gli2*, thus causing a reduction in Hh pathway activity (Voronova et al. 2011). This, combined with our work, shows that Hh signaling is induced by RA and this induction is required for differentiation. The Hh pathway, however, must return to basal activity levels for proper astrocyte differentiation to occur. Given that glial cell populations are composed of astrocytes, oligodendrocytes and microglia, further research must be done to explore the effect of SUFU loss on these other lineages. In the developing mouse forebrain, an initial report suggests an essential role of SUFU in oligodendrocyte differentiation, however the molecular mechanisms involved remain to be resolved (Winkler et al. 2018). In addition to the delay in astrocyte formation (Figure 2-12 and Figure 2-13), there was a loss of *Gli3* in SUFU-deficient cells (Figure 2-10 and Figure 2-11) and we have provided evidence that ectopic expression of *Gli3* was sufficient to rescue the timing of glial cell differentiation (Figure 2-15). That *GLI3* was able to rescue the *Sufu* knockout phenotype is significant and supported by previous research showing *Gli3* repressor overexpression in the SUFU-deficient embryonic mouse cerebellum was sufficient to rescue morphology and increase GFAP levels (Kim et al. 2011). Together, our results show that SUFU imparts a negative regulation on the Hh pathway, likely by acting on *Gli3*, and is required during the specification of the astrocyte lineage.

## 2.5 References

- Bashamboo, A., and McElreavey, K. 2015. Human sex-determination and disorders of sex-development (DSD). *Semin. Cell Dev. Biol.* **45**: 77–83. Elsevier Ltd. doi:10.1016/j.semcdb.2015.10.030.
- Bechtold, T.E., Koyama, E., Kurio, N., Nah, H.D., Saunders, C., and Billings, P.C. 2019. The roles of Indian hedgehog signaling in TMJ formation. *Int. J. Mol. Sci.* **20**(24). doi:10.3390/ijms20246300.
- Bitgood, M.J., Shen, L., and McMahon, A.P. 1996. Sertoli cell signaling by Desert hedgehog regulates the male germline. *Curr. Biol.* **6**(3): 298–304. doi:10.1016/S0960-9822(02)00480-3.
- Brinkman, E.K., Chen, T., Amendola, M., and Van Steensel, B. 2014. Easy quantitative assessment of genome editing by sequence trace decomposition. *Nucleic Acids Res.* **42**(22): 1–8. doi:10.1093/nar/gku936.
- Briscoe, J., and Théron, P.P. 2013. The mechanisms of Hedgehog signalling and its roles in development and disease. *Nat. Rev. Mol. Cell Biol.* **14**(7): 418–431. doi:10.1038/nrm3598.
- Chen, M.H., Wilson, C.W., Li, Y.J., Law, K.K. Lo, Lu, C.S., Gacayan, R., Zhang, X., Hui, C.C., and Chuang, P.T. 2009. Cilium-independent regulation of Gli protein function by Sufu in Hedgehog signaling is evolutionarily conserved. *Genes Dev.* **23**(16): 1910–1928. doi:10.1101/gad.1794109.
- Chen, W., Caihong, X., Wei, B., Li, L., Lin, W., Chen, Y.-G., Ang, S.-L., and Jing, N. 2006. Cell aggregation-induced FGF8 elevation is essential for P19 cell neural differentiation. *Mol. Biol. Cell* **17**: 3075–3084. doi:10.1091/mbc.e05-11-1087.
- Chen, Y., Yue, S., Xie, L., Pu, X.H., Jin, T., and Cheng, S.Y. 2011. Dual phosphorylation of suppressor of fused (Sufu) by PKA and GSK3 $\beta$  regulates its stability and localization in the primary cilium. *J. Biol. Chem.* **286**(15): 13502–13511. doi:10.1074/jbc.M110.217604.
- Clark, A.M., Garland, K.K., and Russell, L.D. 2000. Desert hedgehog (Dhh) gene is required in the mouse testis for formation of adult-type Leydig cells and normal development of peritubular cells and seminiferous tubules. *Biol. Reprod.* **63**(6): 1825–1838. doi:10.1095/biolreprod63.6.1825.
- Cooper, A.F., Yu, K.P., Brueckner, M., Brailey, L.L., Johnson, L., McGrath, J.M., and Bale, A.E. 2005. Cardiac and CNS defects in a mouse with targeted disruption of suppressor of fused. *Development* **132**(19): 4407–4417. doi:10.1242/dev.02021.

- Cwinn, M.A., Mazerolle, C., McNeill, B., Ringuette, R., Thurig, S., Hui, C.C., and Wallace, V.A. 2011. Suppressor of fused is required to maintain the multipotency of neural progenitor cells in the retina. *J. Neurosci.* **31**(13): 5169–5180. doi:10.1523/JNEUROSCI.5495-10.2011.
- Dahmane, N., and Ruiz, A. 1999. Sonic hedgehog and cerebellum development. *Development* **3100**: 3089–3100.
- Ding, Q., Motoyama, J., Gasca, S., Mo, R., Sasaki, H., Rossant, J., and Hui, C. 1998. Diminished Sonic hedgehog signaling and lack of floor plate differentiation in Gli2 mutant mice. *Development* **125**: 2533–2543.
- Dunaeva, M., Michelson, P., Kogerman, P., and Toftgard, R. 2003. Characterization of the physical interaction of Gli proteins with SUFU proteins. *J. Biol. Chem.* **278**(7): 5116–5122. doi:10.1074/jbc.M209492200.
- Fraichard, A., Chassande, O., Bilbaut, G., Dehy, C., Savatier, P., and Samarut, J. 1995. In vitro differentiation of embryonic stem cells into glia and neurons. *J. Cell Sci.* **108**: 3181–3188. Available from <http://jcs.biologists.org/content/joces/108/10/3181.full.pdf>.
- Gazea, M., Tasouri, E., Tolve, M., Bosch, V., Kabanova, A., Gojak, C., Kurtulmus, B., Novikov, O., Spatz, J., Pereira, G., Hübner, W., Brodski, C., Tucker, K.L., and Blaess, S. 2016. Primary cilia are critical for Sonic hedgehog-mediated dopaminergic neurogenesis in the embryonic midbrain. *Dev. Biol.* **409**(1): 55–71. Elsevier. doi:10.1016/j.ydbio.2015.10.033.
- Hahn, H., Wicking, C., Zaphiropoulos, P.G., Gailani, M.R., Shanley, S., Chidambaram, A., Vorechovsky, I., Holmberg, E., Uden, A.B., Gillies, S., Negus, K., Smyth, I., Pressman, C., Leffell, D.J., Gerrard, B., Goldstein, A.M., Dean, M., Toftgard, R., Chenevix-Trench, G., Wainwright, B., and Bale, A.E. 1996. Mutations of the human homolog of drosophila patched in the nevoid basal cell carcinoma syndrome. *Cell* **85**(6): 841–851. doi:10.1016/S0092-8674(00)81268-4.
- Han, Y., Shi, Q., and Jiang, J. 2015. Multisite interaction with Sufu regulates Ci/Gli activity through distinct mechanisms in Hh signal transduction. *Proc. Natl. Acad. Sci.* **112**(20): 6383–6388. doi:10.1073/pnas.1421628112.
- Haycraft, C.J., Banizs, B., Aydin-Son, Y., Zhang, Q., Michaud, E.J., and Yoder, B.K. 2005. Gli2 and Gli3 localize to cilia and require the intraflagellar transport protein Polaris for processing and function. *PLoS Genet.* **1**(4): e53. doi:10.1371/journal.pgen.0010053.
- Hoelzl, M.A., Heby-Henricson, K., Bilousova, G., Rozell, B., Kuiper, R. V, Kasper, M., Toftgård, R., and Teglund, S. 2015. Suppressor of Fused plays an important role in regulating mesodermal differentiation of murine embryonic stem cells In vivo. *Stem Cells Dev.* **24**(21): 2547–2560. doi:10.1089/scd.2015.0050.

Hoelzl, M.A., Heby-Henricson, K., Gerling, M., Dias, J.M., Kuiper, R. V., Trünkle, C., Bergström, Å., Ericson, J., Toftgård, R., and Teglund, S. 2017. Differential requirement of SUFU in tissue development discovered in a hypomorphic mouse model. *Dev. Biol.* **429**(1): 132–146. Elsevier Inc. doi:10.1016/j.ydbio.2017.06.037.

Hui, C., and Angers, S. 2011. Gli proteins in development and disease. *Annu. Rev. Cell Dev. Biol.* **27**(1): 513–537. doi:10.1146/annurev-cellbio-092910-154048.

Humke, E.W., Dorn, K. V., Milenkovic, L., Scott, M.P., and Rohatgi, R. 2010. The output of Hedgehog signaling is controlled by the dynamic association between Suppressor of Fused and the Gli proteins. *Genes Dev.* **24**(7): 670–682. doi:10.1101/gad.1902910.

Infante, P., Faedda, R., Bernardi, F., Bufalieri, F., Severini, L.L., Alfonsi, R., Mazzà, D., Siler, M., Coni, S., Po, A., Petroni, M., Ferretti, E., Mori, M., De Smaele, E., Canettieri, G., Capalbo, C., Maroder, M., Screpanti, I., Kool, M., Pfister, S.M., Guardavaccaro, D., Gulino, A., and Di Marcotullio, L. 2018. Itch/ $\beta$ -Arrestin2-dependent non-proteolytic ubiquitylation of SuFu controls Hedgehog signalling and medulloblastoma tumorigenesis. *Nat. Commun.* **9**(1): 1–17. doi:10.1038/s41467-018-03339-0.

Jing, X.T., Wu, H.T., Wu, Y., Ma, X., Liu, S.H., Wu, Y.R., Ding, X.F., Peng, X.Z., Qiang, B.Q., Yuan, J.G., Fan, W.H., and Fan, M. 2009. DIXDC1 promotes retinoic acid-induced neuronal differentiation and inhibits gliogenesis in P19 cells. *Cell. Mol. Neurobiol.* **29**(1): 55–67. doi:10.1007/s10571-008-9295-9.

Jiwani, T., Kim, J.J., and Rosenblum, N.D. 2020. Suppressor of fused controls cerebellum granule cell proliferation by suppressing Fgf8 and spatially regulating Gli proteins. *Development* **147**(3): 1–17. doi:10.1242/dev.170274.

Jones-Villeneuve, E.M., McBurney, M.W., Rogers, K.A., and Kalnins, V.I. 1982. Retinoic acid induces embryonal carcinoma cells to differentiate into neurons and glial cells. *J. Cell Biol.* **94**(2): 253–262. doi:10.1083/jcb.94.2.253.

Kim, J.J., Gill, P.S., Rotin, L., van Eede, M., Henkelman, R.M., Hui, C.-C., and Rosenblum, N.D. 2011. Suppressor of Fused controls mid-hindbrain patterning and cerebellar morphogenesis via GLI3 repressor. *J. Neurosci.* **31**(5): 1825–1836. doi:10.1523/JNEUROSCI.2166-10.2011.

Kim, J.J., Jiwani, T., Erwood, S., Loree, J., and Rosenblum, N.D. 2018. Suppressor of fused controls cerebellar neuronal differentiation in a manner modulated by GLI3 repressor and Fgf15. *Dev. Dyn.* **247**(1): 156–169. doi:10.1002/dvdy.24526.

Kise, Y., Morinaka, A., Teglund, S., and Miki, H. 2009. SuFu recruits GSK3 $\beta$  for efficient processing of Gli3. *Biochem. Biophys. Res. Commun.* **387**(3): 569–574. Elsevier Inc. doi:10.1016/j.bbrc.2009.07.087.

- Komada, M., Saitsu, H., Kinboshi, M., Miura, T., Shiota, K., and Ishibashi, M. 2008. Hedgehog signaling is involved in development of the neocortex. *Development* **135**(16): 2717–2727. doi:10.1242/dev.015891.
- Li, S., Zheng, J., Chai, L., Lin, M., Zeng, R., Lu, J., and Bian, J. 2019. Rapid and Efficient Differentiation of Rodent Neural Stem Cells into Oligodendrocyte Progenitor Cells. *Dev. Neurosci.* **41**(1–2): 79–93. doi:10.1159/000499364.
- Lin, Y.T., Ding, J.Y., Li, M.Y., Yeh, T.S., Wang, T.W., and Yu, J.Y. 2012. YAP regulates neuronal differentiation through Sonic hedgehog signaling pathway. *Exp. Cell Res.* **318**(15): 1877–1888. doi:10.1016/j.yexcr.2012.05.005.
- Mak, S.K., Huang, Y.A., Iranmanesh, S., Vangipuram, M., Sundararajan, R., Nguyen, L., Langston, J.W., and Schüle, B. 2012. Small molecules greatly improve conversion of human-induced pluripotent stem cells to the neuronal lineage. *Stem Cells Int.* 2012. doi:10.1155/2012/140427.
- Makino, S., Zhulyan, O., Mo, R., Puvindran, V., Zhang, X., Murata, T., Fukumura, R., Ishitsuka, Y., Kotaki, H., Matsumaru, D., Ishii, S., Hui, C.C., and Gondo, Y. 2015. T396I mutation of mouse *Sufu* reduces the stability and activity of *Gli3* repressor. *PLoS One* **10**(3): 1–15. doi:10.1371/journal.pone.0119455.
- McBurney, M. 1993. P19 embryonal carcinoma cells. *Int. J. Dev. Biol.* **140**: 135–140.
- McBurney, M.W., Jones-Villeneuve, E.M.V., Edwards, M.K.S., and Anderson, P.J. 1982. Control of muscle and neuronal differentiation in a cultured embryonal carcinoma cell line. *Nature* **299**(5879): 165–167. doi:10.1038/299165a0.
- McBurney, M.W., Reuhl, K.R., Ally, a I., Nasipuri, S., Bell, J.C., and Craig, J. 1988. Differentiation and maturation of embryonal carcinoma-derived neurons in cell culture. *J. Neurosci.* **8**(3): 1063–73. Available from <http://www.ncbi.nlm.nih.gov/pubmed/2894413>.
- Noguchi, H., Castillo, J.G., Nakashima, K., and Pleasure, S.J. 2019. Suppressor of fused controls perinatal expansion and quiescence of future dentate adult neural stem cells. *Elife* **8**: 1–21. doi:10.7554/eLife.42918.
- Okada, Y., Shimazaki, T., Sobue, G., and Okano, H. 2004. Retinoic-acid-concentration-dependent acquisition of neural cell identity during in vitro differentiation of mouse embryonic stem cells. *Dev. Biol.* **275**: 124–142. doi:10.1016/j.ydbio.2004.07.038.
- Pearse, R. V., Collier, L.S., Scott, M.P., and Tabin, C.J. 1999. Vertebrate homologs of *Drosophila* Suppressor of fused interact with the *Gli* family of transcriptional regulators. *Dev. Biol.* **212**(2): 323–336. doi:10.1006/dbio.1999.9335.
- Rallu, M., Machold, R., Gaiano, N., Corbin, J.G., McMahon, A.P., and Fishell, G. 2002. Dorsoroventral patterning is established in the telencephalon of mutants lacking both *Gli3* and Hedgehog signaling. *Dev.* **129**: 4963–4974.

- Ran, F.A., Hsu, P.D., Wright, J., Agarwala, V., Scott, D.A., and Zhang, F. 2013. Genome engineering using CRISPR-Cas9 system. *Nat. Protoc.* **8**(11): 2281–2308. doi:10.1007/978-1-4939-1862-1\_10.
- Smith, M.J., Beetz, C., Williams, S.G., Bhaskar, S.S., Sullivan, J.O., Anderson, B., Daly, S.B., Urquhart, J.E., Bholah, Z., Oudit, D., Cheesman, E., Kelsey, A., McCabe, M.G., Newman, W.G., Evans, D.G.R., Smith, M.J., Williams, S.G., Urquhart, E., Bholah, Z., and William, G. 2018. Germline mutations in *SUFU* cause Gorlin Syndrome – Associated Childhood Medulloblastoma and redefine the risk associated with *PTCH1* mutations. *J. Clin. Oncol.* **32**(36): 4155–4161. doi:10.1200/JCO.2014.58.2569.
- Spassky, N., Han, Y.-G., Aguilar, A., Strehl, L., Besse, L., Laclef, C., Ros, M.R., Garcia-Verdugo, J.M., and Alvarez-Buylla, A. 2008. Primary cilia are required for cerebellar development and *Shh*-dependent expansion of progenitor pool. *Dev. Biol.* **317**: 246–259. doi:10.1016/j.ydbio.2008.02.026.
- St-Jacques, B., Hammerschmidt, M., and McMahon, A.P. 1999. Indian hedgehog signaling regulates proliferation and differentiation of chondrocytes and is essential for bone formation. *Genes Dev.* **13**(16): 2072–2086. doi:10.1101/gad.13.16.2072.
- Svärd, J., Henricson, K.H., Persson-Lek, M., Rozell, B., Lauth, M., Bergström, Å., Ericson, J., Toftgård, R., and Teglund, S. 2006. Genetic elimination of suppressor of fused reveals an essential repressor function in the mammalian hedgehog signaling pathway. *Dev. Cell* **10**(2): 187–197. doi:10.1016/j.devcel.2005.12.013.
- Takenaka, K., Kise, Y., and Miki, H. 2007. *GSK3 $\beta$*  positively regulates Hedgehog signaling through *Sufu* in mammalian cells. *Biochem. Biophys. Res. Commun.* **353**(2): 501–508. doi:10.1016/j.bbrc.2006.12.058.
- Tan, Y., Xie, Z., Ding, M., Wang, Z., Yu, Q., Meng, L., Zhu, H., Huang, X., Yu, L., Meng, X., and Chen, Y. 2010. Increased levels of *FoxA1* transcription factor in pluripotent P19 embryonal carcinoma cells stimulate neural differentiation. *Stem Cells Dev.* **19**(9): 1365–1374. doi:10.1089/scd.2009.0386.
- Tang, K., Yang, J., Gao, X., Wang, C., Liu, L., Kitani, H., Atsumi, T., and Jing, N. 2002. *Wnt-1* promotes neuronal differentiation and inhibits gliogenesis in P19 cells. *Biochem. Biophys. Res. Commun.* **293**(1): 167–173. doi:10.1016/S0006-291X(02)00215-2.
- Taylor, M.D., Liu, L., Raffel, C., Hui, C. chung, Mainprize, T.G., Zhang, X., Agatep, R., Chiappa, S., Gao, L., Lowrance, A., Hao, A., Goldstein, A.M., Stavrou, T., Scherer, S.W., Dura, W.T., Wainwright, B., Squire, J.A., Rutka, J.T., and Hogg, D. 2002. Mutations in *SUFU* predispose to medulloblastoma. *Nat. Genet.* **31**(3): 306–310. doi:10.1038/ng916.

- Tempe, D., Casas, M., Karaz, S., Blanchet-Tournier, M.-F., and Concordet, J.-P. 2006. Multisite Protein Kinase A and Glycogen Synthase Kinase 3 Phosphorylation Leads to Gli3 Ubiquitination by SCF TrCP. *Mol. Cell. Biol.* **26**(11): 4316–4326. doi:10.1128/MCB.02183-05.
- Urman, N.M., Mirza, A., Atwood, S.X., Whitson, R.J., Sarin, K.Y., Tang, J.Y., and Oro, A.E. 2016. Tumor-derived suppressor of fused mutations reveal hedgehog pathway interactions. *PLoS One* **11**(12): 1–10. doi:10.1371/journal.pone.0168031.
- Voronova, A., Fischer, A., Ryan, T., Al Madhoun, A., and Skerjanc, I.S. 2011. *Ascl1/Mash1* is a novel target of *Gli2* during *Gli2*-induced neurogenesis in P19 EC cells. *PLoS One* **6**(4). doi:10.1371/journal.pone.0019174.
- Wang, Y., Li, Y., Hu, G., Huang, X., Rao, H., Xiong, X., Luo, Z., Lu, Q., and Luo, S. 2016. *Nek2A* phosphorylates and stabilizes *SuFu*: A new strategy of *Gli2*/Hedgehog signaling regulatory mechanism. *Cell. Signal.* **28**(9): 1304–1313. Elsevier Inc. doi:10.1016/j.cellsig.2016.06.010.
- Wilson, L., and Maden, M. 2005. The mechanisms of dorsoventral patterning in the vertebrate neural tube. *Dev. Biol.* **282**: 1–13. doi:10.1016/j.ydbio.2005.02.027.
- Winkler, C.C., Yabut, O.R., Fregoso, S.P., Gomez, H.G., Dwyer, B.E., Pleasure, S.J., and Franco, S.J. 2018. The dorsal wave of neocortical oligodendrogenesis begins embryonically and requires multiple sources of sonic hedgehog. *J. Neurosci.* **38**(23): 5237–5250. doi:10.1523/JNEUROSCI.3392-17.2018.
- Wu, C.Y., Whye, D., Mason, R.W., and Wang, W. 2012. Efficient differentiation of mouse embryonic stem cells into motor neurons. *J. Vis. Exp.* **64**: 1–5. doi:10.3791/3813.
- Wu, S.M., Choo, A.B.H., Yap, M.G.S., and Chan, K.K.K. 2010. Role of Sonic hedgehog signaling and the expression of its components in human embryonic stem cells. *Stem Cell Res.* **4**(1): 38–49. doi:10.1016/j.scr.2009.09.002.
- Xu, Q., Guo, L., Moore, H., Waclaw, R.R., Campbell, K., and Anderson, S.A. 2010. Sonic Hedgehog Signaling Confers Ventral Telencephalic Progenitors with Distinct Cortical Interneuron Fates. *Neuron* **65**(3): 328–340. doi:10.1016/j.neuron.2010.01.004.
- Yabut, O.R., Fernandez, G., Yoon, K., Pleasure, S.J., Yabut, O.R., Fernandez, G., Huynh, T., Yoon, K., and Pleasure, S.J. 2015. Suppressor of Fused Is critical for maintenance of neuronal progenitor identity during corticogenesis. *Cell Rep.* **12**(12): 2021–2034. doi:10.1016/j.celrep.2015.08.031.
- Yue, S., Chen, Y., and Cheng, S.Y. 2009. Hedgehog signaling promotes the degradation of tumor suppressor *Sufu* through the ubiquitin-proteasome pathway. *Oncogene* **28**(4): 492–499. doi:10.1038/onc.2008.403.



Zhang, Z., Shen, L., Law, K., Zhang, Z., Liu, X., Hua, H., Li, S., Huang, H., Yue, S., Hui, C., and Cheng, S.Y. 2017. Suppressor of Fused Chaperones Gli Proteins To Generate Transcriptional Responses to Sonic Hedgehog Signaling. *Mol. Cell. Biol.* **37**(3): e00421-16. doi:10.1128/MCB.00421-16.

## Chapter 3

### 3 Never in Mitosis Kinase 2 regulation of metabolism is required for neural differentiation

Wnt and Hh are known signalling pathways involved in neural differentiation and recent work has shown the cell cycle regulator, Never in Mitosis Kinase 2 (Nek2) is able to regulate both pathways. Despite its known function in pathway regulation, few studies have explored Nek2 within embryonic development. The P19 embryonal carcinoma cell model was used to investigate Nek2 and neural differentiation through CRISPR knockout and overexpression studies. Loss of Nek2 reduced cell proliferation in the undifferentiated state and during directed differentiation, while overexpression increased cell proliferation. Despite these changes in proliferation rates, Nek2 deficient cells maintained pluripotency markers after neural induction while Nek2 overexpressing cells lost these markers in the undifferentiated state. Nek2 deficient cells lost the ability to differentiate into both neurons and astrocytes, although Nek2 overexpressing cells enhanced neuron differentiation at the expense of astrocytes. Hh and Wnt signaling were explored, however there was no clear connection between Nek2 and these pathways causing the observed changes to differentiation phenotypes. Mass spectrometry was also used during wildtype and Nek2 knockout cell differentiation and we identified reduced electron transport chain components in the knockout population. Immunoblotting confirmed the loss of these components and additional studies showed cells lacking Nek2 were exclusively glycolytic. Interestingly, hypoxia inducible factor 1 $\alpha$  was stabilized in these Nek2 knockout cells despite culturing them under normoxic conditions. Since neural differentiation requires a metabolic switch from glycolysis to oxidative phosphorylation, we propose a mechanism where Nek2 prevents HIF1 $\alpha$  stabilization, thereby allowing cells to use oxidative phosphorylation to facilitate neuron and astrocyte differentiation.

### 3.1 Introduction

Hedgehog (Hh) and Wnt signaling pathways are vital for neural development and are involved during *in vivo* and *in vitro* neural differentiation (Schuuring et al. 1989; Dahmane and Ruiz 1999; Tang et al. 2002; Min et al. 2011; Kim et al. 2018). During neurulation the notochord and floor plate secrete Hh, inducing ventral neural phenotypes, and the roof plate secretes Wnt, inducing dorsal neural phenotypes (Wilson and Maden 2005; Mulligan and Cheyette 2012; Briscoe and Théron 2013). These signals not only pattern the dorsal-ventral axis of the neural tube but are also vital for patterning its anterior-posterior axis (Mulligan and Cheyette 2012) and defining the midbrain-hindbrain boundary (Kim et al. 2011; Gibbs et al. 2017). Activation of the Hh pathway occurs when the Hh ligand binds to its receptor Patched (Ptch), which relieves the inhibition of Smoothed, allowing Smoothed to translocate to the plasma membrane (Rohatgi et al. 2007). Translocation causes the Suppressor of Fused (SUFU) and Gli complex to be recruited to the primary cilium where SUFU dissociates from the full-length form of Gli, which enters the nucleus to activate transcription (Humke et al. 2010; Tukachinsky et al. 2010). In the absence of ligand, SUFU-bound Gli is either sequestered in the cytoplasm or is targeted for partial proteosomal degradation converting Gli to a transcriptional repressor (Hui and Angers 2011; Briscoe and Théron 2013). In the case of the Wnt pathway, it is either canonical and involves  $\beta$ -catenin or non-canonical and linked to planar cell polarity or  $\text{Ca}^{2+}$  signaling. In either case, one of 19 vertebrate Wnt ligands binds the transmembrane receptor Frizzled (Fzd), which signals to Dishevelled (DVL) and in the canonical pathway causes the recruitment of the destruction complex (Cliffe et al. 2003; Wong et al. 2003; Stamos and Weis 2013) that includes Axin, adenomatous polyposis coli, glycogen synthase kinase 3 (GSK3), casein kinase 1, and  $\beta$ -TrCP, a ubiquitin ligase (Stamos and Weis 2013; Mukherjee et al. 2018). This recruitment and the destabilization of Axin attenuates the hyper-phosphorylation of  $\beta$ -catenin by GSK3 allowing  $\beta$ -catenin cytoplasmic accumulation and translocation to the nucleus where it interacts with TCF/LEF transcription factors inducing Wnt target gene transcription (Steinhart and Angers 2018).

Recently, Never in Mitosis Kinase 2 (Nek2) was reported as a novel regulator of both canonical Wnt and Hh pathways (Mbom et al. 2014; Cervenka et al. 2016; Wang et al. 2016; Zhou et al. 2017), but few studies have explored its role in embryonic development. What is known, however, is that Nek2 plays an essential role in left-right asymmetry of the *Xenopus* heart (Joseph Endicott et al. 2015a), its overexpression in the *Drosophila* eye ectopically induces wingless (Wnt1) signaling and reduces retinal neuron differentiation (Martins et al. 2017), and in mouse, *Nek2* expression is reported in the brain of the E10.5 embryo (Tanaka et al. 1997). The role of this protein in signaling, however, originated from reports of its involvement as a centrosomal linker protein during the cell cycle, showing Nek2 binding and phosphorylating DVL (Cervenka et al. 2016) and  $\beta$ -catenin (Mbom et al. 2014) at centrosomes. Nek2, serving as a Gli1/2 target gene (Zhou et al. 2017), also phosphorylates and stabilizes SUFU (Wang et al. 2016), placing it as negative regulator of the Hh pathway. Overexpression of *Nek2* has also been linked to multiple Wnt- and Hh-associated cancers, including those causing brain malignancies (Neal et al. 2014; Lin et al. 2016; Boulay et al. 2017; Liu et al. 2017; Yao et al. 2019; Xiang et al. 2022).

Given that Hh and Wnt signaling are essential in neural differentiation, and that Nek2 acts as a regulator of both pathways, we sought to explore the role of Nek2 in neural differentiation using P19 embryonal carcinoma cells. These cells can be differentiated towards neurons and astrocytes in the presence of retinoic acid (RA) (Jones-Villeneuve et al. 1982, 1983; McBurney et al. 1988; McBurney 1993; Spice et al. 2022), which affects Wnt (Schuurung et al. 1989; St-Arnaud et al. 1989; Papkoff 1994; Tang et al. 2002) and Hh (Voronova et al. 2011; Spice et al. 2022) signaling. Herein, we report the presence of Nek2 throughout RA-induced differentiation and through overexpression studies and CRISPR-Cas9 ablation, demonstrate an essential role of Nek2 in neuron and astrocyte differentiation. Furthermore, we show that *Nek2* overexpression is linked to increased Wnt signaling, however, proteomic analysis suggests an essential role of Nek2 outside of signaling and connects its involvement to metabolic regulation.

## 3.2 Materials and Methods

### 3.2.1 Cell Culture

Mouse P19 embryonal carcinoma cells were a generous gift from Dr. Lisa Hoffman, Lawson Health Research Institute, UWO. Cells were maintained in DMEM containing 5% fetal bovine serum (FBS, ThermoFisher) and 1% penicillin/streptomycin (ThermoFisher) on adherent tissue culture plates (Sarstedt). Wildtype and mutant cells were passaged every 4 days or when they reached a confluency of 70%, whichever occurred first. Following previously published protocols (McBurney et al. 1982; Spice et al. 2022), differentiation was induced in wildtype and mutant cells by plating  $1.05 \times 10^6$  cells on bacterial grade Petri dishes (Falcon) in the presence of 0.5  $\mu\text{M}$  retinoic acid (RA) for 4 days to form embryoid bodies (EB). These aggregates were collected and re-plated on adherent tissue culture dishes in the presence of 0.5  $\mu\text{M}$  RA, which in wildtype cells, develop into neurons after 10 days and form astrocytes by day 17. For BIO-treated experiments, cells were induced to differentiate in the presence of 0.5  $\mu\text{M}$  RA on days 0 and 4, 0.5  $\mu\text{M}$  RA treatments on days 0 and 4 plus 10 nM BIO (6-Bromoindirubin-3'-oxime, Sigma) treatment on day 0, or 10 nM BIO treatment on day zero plus 0.5  $\mu\text{M}$  RA on day 4. Cells were also treated with 10 nM BIO alone with no subsequent RA. For XAV treatments, cells were induced to differentiate in the presence of 0.5  $\mu\text{M}$  RA on days 0 and 4, plus 5  $\mu\text{M}$  XAV on day 0. For metabolic experiments cells were seeded and allowed to adhere for 16 hours, then treated with either media alone, DMSO, 2.5  $\mu\text{M}$  Oligomycin A (BioShop) or 50 mM 2-Deoxy-D-glucose (2-DG, Sigma) for 24 hours. Cell counts and viability were measured by trypan blue exclusion. Cells for all experiments were maintained at 37°C and 5% CO<sub>2</sub>.

### 3.2.2 Preparing CRISPR plasmids

Nek2 sgRNAs (Table 3-1) were cloned into the CRISPR-Cas9 plasmid pSpCas9(BB)-2A-Puro (PX459) V2.0 (Addgene plasmid 62988; <http://n2t/addgene:62988>) using the protocol by Ran et al. 2013 (Ran et al. 2013). Prior to cloning, sgRNAs were amplified and phosphorylated, then subsequently digested with the BbsI restriction enzyme along with the vector. Digested sgRNA and vector were incubated at room temperature for 1.5

hours in the presence of T7 ligase (New England Biolabs). Plasmids were transformed into transformation competent DH5alpha E. coli cells and positive colonies were collected using a Mini Prep kit (Qiagen) and sequenced using the U6 primer (Table 3-1) at the London Regional Genomics Centre (Robarts Research Institute, London, ON).

**Table 3-1: CRISPR-Cas9 gRNAs, primers for gRNA amplification and PCR around the cut site**

CRISPR-Cas9		
<i>Nek2</i> KO gRNA	CATCGTAATGGAATACTGTGAGG	
<i>Nek2</i> KD gRNA	CAAGCCATCAGAGTAGCGGTAGG	
	<b>Forward Primer (5' → 3')</b>	<b>Reverse Primer (5' → 3')</b>
<i>Nek2</i> KO gRNA	CACCCATCGTAATGGAATACTGTGAGG	AAACCCTCACAGTATTCCATTACGATG
<i>Nek2</i> KO PCR	TTTGTCTCACACCTTGGAAATG	TTATTAGATACGAACCGTGGGG
<i>Nek2</i> KD gRNA	CACCCAAGCCATCAGAGTAGCGGTAGG	AAACCCTACCGCTACTCTGATGGCTTG
<i>Nek2</i> KD PCR	CTGCAGAATGTCCAGAGCGT	CTGTAGCCAGGGAAACCGAT
<i>U6</i>	GGGCAGGAAGAGGGCCTAT	

### 3.2.3 Generating *Nek2* deficient cell lines

Two µg of sgRNA containing plasmid was incubated with 10 µL of Lipofectamine 2000 (Invitrogen) for 20 minutes and then added to high confluency P19 cells for 4 hours. Culture media was replaced, and cells were allowed to reach 70% confluency. Cells were then passaged to a 1 cell/50 µL concentration into a 96 well plate where they were incubated daily in 1 µg/mL puromycin (BioShop) selection medium for 4 days. After selection, cells were allowed to recover in compete medium until reaching 70% confluence. Mutant genotypes were identified by collecting genomic DNA (Qiagen DNeasy Blood & Tissue kit, 69504), which was amplified using PCR (DreamTaq Master Mix (2X), Thermo Scientific, K1081), a vapo.protect Thermocycler (Eppendorf) and site-specific primers (Table 3-1). Amplified DNA was sequenced at the London Regional Genomics Centre and pair-wise alignments were performed using Geneious 2021™.

Additional analysis of in/dels was performed using Synthego Performance Analysis, ICE Analysis. 2019. v3.0. Synthego; [Jan. 13, 2022].

### 3.2.4 Generating Nek2 Overexpression Cell Line

Two  $\mu\text{g}$  of plasmid was incubated in the presence of 10  $\mu\text{L}$  of Lipofectamine 2000 for 4 hours. Media was changed and cells were allowed to grow to 70% confluency before being passaged. Cells were incubated in selection media containing either 1 mg/mL hygromycin or 500  $\mu\text{g}/\text{mL}$  neomycin for 2 weeks, with selection media being changed every 48 hours, to generate stable lines. Plasmids used include: 1436 pcDNA3 Flag HA (Addgene plasmid #10792) and pCMV3-human NEK2-Myc (HG10054-CM, Sino Biological).

### 3.2.5 RT-qPCR

Real time reverse transcriptase PCR analysis was used to determine relative expression levels of various genes accompanying differentiation in wildtype and mutant cell lines. In wildtype cells, mRNA was collected at days 0, 1, 2, 3, 4, 6, 8 and 10 after RA treatment and in wildtype and mutant cells, mRNA was collected at days 0, 10, 14 and 17 after RA treatment using QIAshredder (Qiagen, 79654) and RNeasy (Qiagen, 74104) kits. RNA was reverse-transcribed into cDNA using a High-Capacity cDNA Reverse Transcription Kit (ThermoFisher Scientific, 4368814) and was amplified using the following primers: *L14*, *Nek2*, *Gli1*, *Ptch1*, *Ascl1*, *Dab2*, *Dkk1*, *c-Myc*, *Nanog* and *Oct4* (Table 3-2). PCR reactions containing 500 nM each of reverse and forward primers, 10  $\mu\text{L}$  of SensiFAST SYBR No-ROX Mix (FroggaBio, BIO-98050) and 1  $\mu\text{L}$  of cDNA, were run using a CFX Connect Real-Time PCR Detection System (Bio-Rad). Samples were analyzed using the comparative cycle threshold method ( $2^{-\Delta\Delta\text{Ct}}$ ) using *L14* as an expression control and comparing normalized expression values to undifferentiated wildtype cells to determine fold changes in expression.

**Table 3-2: Primers used for RT-qPCR**

qRT-PCR		
Gene	Forward Primer (5' → 3')	Reverse Primer (5' → 3')
<i>L14</i>	GGGTGGCCTACATTTCTTCG	GAGTACAGGGTCCATCCACTAAA
<i>Gli1</i>	GGAAGTCCTATTCACGCCTGA	CAACCTTCTTGCTCACACATGTAAG
<i>Ptch1</i>	AAAGAACTGCGGCAAGTTTTTG	CTTCTCCTATCTTCTGACGGGT
<i>Oct4</i>	CCCAATGCCGTGAAGTTGGA	GCTTTCATGTCCTGGGACTCCT
<i>Nanog</i>	TCTTCCTGGTCCCCACAGTTT	GCAAGAATAGTTCTCGGGATGAA
<i>Dkk1</i>	TGAAGATGAGGAGTGCGGCTC	GGCTGTGGTCAGAGGGCATG
<i>Dab2</i>	GGAGCATGTAGACCATGATG	AAAGGATTTCCGAAAGGGCT

### 3.2.6 Immunoblotting

Cells at various stages of differentiation in both wildtype and mutant lines were lysed using 100-500  $\mu$ L of 2% sodium dodecyl sulfate buffer with 10% glycerol, 5% 2-mercaptoethanol, 1:200 of 1X Halt Protease Inhibitor Cocktail (ThermoFisher Scientific, 1862209), at pH 6.8. Proteins were sonicated on ice for 30 seconds and quantified using a DC™ Protein Assay (Bio-Rad, 5000113) before loading 10  $\mu$ g of protein to 6-10% polyacrylamide gels. Proteins were separated for approximately 1.5 hours at 120V, and then transferred overnight at 20V to PVDF membranes (Bio-Rad, 1620177). Membranes were placed for 1 hour at room temperature in 5% skim milk in Tris-buffered saline containing 0.1% Tween-20 (TBS-T). After washing, blots were incubated overnight at 4°C in the following primary antibodies:  $\beta$ -III-Tubulin (TUJ1, 1:1000; Cell Signaling Technology, 5568), SUFU (1:1000; abcam, ab28083), GFAP (1:1000; Invitrogen, 14-9892-80), Nek2 (Santa Cruz Biotechnology, sc-55601), Dab2 (Cell Signaling Technology, 12906), ERBB (1:1000; Novus Biologicals, PP-H6705-00), Total OXPHOS (1:1000; abcam, ab110413), TOM20 (1:1000; Cell Signaling Technology, 42406), HIF1 $\alpha$  (ab179483) and  $\beta$ -actin (1:10,000; Santa Cruz Biotechnology, sc-47778). Blots were washed and then incubated for 2 hours at room temperature in host-specific HRP-conjugated secondary antibody (1:10,000, Sigma) in TBS-T containing 5% skim milk. After secondary antibody incubation and washing, blots were incubated in Immobilon® Classico Western HRP Substrate (Millipore, WBLUC0500) and imaged using a Chemi



Doc Touch System (Bio-Rad). Densitometry analysis was performed using ImageLab Software (Bio-Rad).

### 3.2.7 Immunofluorescence and Phase Contrast Imaging

Wildtype and Nek2 knockout cells were treated with 0.5  $\mu$ M RA as described (Spice et al. 2022) for 17 days on poly-L-lysine hydrobromide (Sigma, P5899) coated coverslips. Cells on coverslips were washed with PBS for 1 minute and then fixed with 4% paraformaldehyde in PBS for 10 minutes at room temperature. Ice-cold PBS was used to wash coverslips, then cells were permeabilized with 0.2% Triton-X-100 in PBS for 10 minutes at room temperature. Cells were again washed before being blocked for 30 mins at room temperature in PBS containing 1% bovine serum albumin, 22.52 mg/mL glycine and 0.1% Tween-20. Coverslips were then incubated overnight in a humidity chamber with the following primary antibodies:  $\beta$ -III-Tubulin (TUJ1, 1:400; Cell Signaling Technology, 5568) and GFAP (1:500; Invitrogen, 14-9892-80). After primary incubation, cells were washed and incubated with secondary antibodies in blocking solution for 1 hour at room temperature. The secondary antibodies were Alexa Fluor™ 660 Goat anti-Mouse IgG (Invitrogen, A21054) and Goat anti-Rabbit IgG Alexa Fluor Plus 488 (Invitrogen, A32731TR). Finally, coverslips were washed and mounted to slides using Slowfade™ Gold Antifade Mountant with DAPI (Invitrogen, S36942) and sealed with nail polish. Images were captured on a Zeiss AxioImager Compound Fluorescence Microscope (Integrated Microscopy Facility, Biotron, Western University, London, ON).

Wildtype and Nek2 mutant cells were treated with RA as described above, and after 4 days, EBs were imaged using a Leica DMIL LED microscope or a Zeiss inverted microscope and an OPTIKA Microscopes C-B5 camera with OPTIKA Lightview software. EB number per image area, EB area and aspect ratio were measured using ImageJ.

### 3.2.8 Cell Count and Viability Assays

Trypan blue exclusion assays were performed on wildtype and mutant cells in the undifferentiated state, after 4 days of RA treatment and after 2-DG or Oligomycin A treatment. In the undifferentiated state, 15,000 cells were plated on adherent tissue

culture dishes. Every 24 hours for 96 hours, cells were trypsinized and a 1:1 cell suspension to trypan blue ratio was added and total number of cells counted using a CellDrop BF Brightfield Cell Counter (DeNovix). For RA treatment, cells were processed as described previously (Spice et al. 2022) and EBs were collected after 4 days. EBs were vigorously resuspended in complete media, before being counted in a 1:1 cell suspension to trypan blue ratio. Total cell number was counted, and viability was compared to the number of dead cells.

### 3.2.9 Caspase 3 Activity Assay

Caspase 3 activity was measured using the Caspase-3 Colorimetric Activity Assay Kit (APT131, Millipore). Briefly, cells were treated with RA for 4 days to form EBs, and then collected and lysed according to manufacturer's instructions. Caspase-3 activity was determined through the detection of p-nitroaniline (pNA) in cytoplasmic lysates after incubation with a Caspase-3 specific substrate (Ac-DEVD-pNA). Readings were performed using a Modulus™ II Microplate Multimode Reader (Turner Biosystems) at 450nm, where background detection was subtracted and normalized to wildtype Caspase-3 activity.

### 3.2.10 Luciferase Assay

Wildtype and Nek2 mutant cells were transfected with 4 µg total of DNA using 10 µL of Lipofectamine 2000. Transfected plasmids included pRL-TK (Promega) alone, or pRL-TK and pGL3-BARL (β-catenin activated reporter luciferase, Promega) or pRL-TK and pGL3-8xGli (a gift from Philip Beachy, Stanford University). Following transfection, cells were incubated for 24 hours before passaging into a 96-well plate. Cells were allowed to adhere for 48 hours before the Dual-Gli® Luciferase Assay System (Promega, E2920) was used according to manufacturer's instructions. Briefly, Dual-Glo reagent was incubated in each well containing growth media for 15 minutes before measuring Firefly luminescence (from pGL3-BARL and pGL3-8xGli plasmids). Subsequently, Dual-Glo Stop & Glo reagent was added to each well and was incubated for 15 minutes before measuring Renilla luminescence (from pRL-TK plasmid). To calculate initial luminescence values, background luminescence was subtracted from each well, where

Firefly luminescence was divided by Renilla luminescence for each treatment. Relative luminescence was determined by dividing each well by the luminescence from WT cells transfected with pRL-TK only.

### 3.2.11 LC-Mass Spectrometry

Cells were differentiated as described, and cells were either centrifuged as EBs for collecting cells at days 1 and 4 of RA treatment or were trypsinized and centrifuged for adherent cells at days 0 and 10 of RA treatment. Three biological replicates of lysates of P19 cells were prepared through incubation in 8 M Urea, 50 mM ammonium bicarbonate (ABC), 10 mM DTT, 2% SDS at room temperature for 10 minutes and sonicated with a probe sonicator for 20 x 0.5s pulses to shear DNA. Lysates were quantified by using a Pierce™ 660 nm Protein Assay (ThermoFisher Scientific) and stored at  $-80^{\circ}\text{C}$  until future use. Lysates were reduced in 10 mM DTT for 30 min and alkylated in 100 mM iodoacetamide (IAA) for 30 min at room temperature in the dark. Next, lysate protein was precipitated in chloroform/methanol and prepared for in-solution digestion according to Kuljanin et al. (Kuljanin et al. 2017). On-pellet protein digestion was performed in 50 mM ABC (pH 8) by adding TrypLysC (Promega) at an enzyme: protein ratio at 1:25 and incubated overnight at  $37^{\circ}\text{C}$  in a ThermoMixer at 900rpm. Digestion buffer was acidified to 1% formic acid (FA) and vacuum centrifuged at  $45^{\circ}\text{C}$ . Digested peptides were desalted using in-house C18 stagetips prepared in a 200 $\mu\text{l}$  pipette tip. C18 stagetips were conditioned with 80% Acetonitrile (ACN)/0.1% trifluoroacetic acid (TFA) followed by 5% ACN/0.1% TFA before loading and washing peptides twice with 5% ACN/0.1% TFA. Desalted peptides were eluted with 80% ACN/0.1% TFA prior to vacuum centrifugation and resuspension in 0.1% FA. Final peptide concentrations were determined by BCA quantification prior to ultraperformance liquid chromatography tandem mass spectrometry (UPLC-MS/MS).

500ng of peptides per sample was analyzed by using an M-class nanoAquity UPLC system (Waters) connected to a Q Exactive mass spectrometer (Thermo Scientific). Buffer A consisted of Water/0.1% FA and Buffer B consisted of ACN/0.1% FA. Peptides were loaded onto an ACQUITY UPLC M-Class Symmetry C18 Trap Column (5 $\mu\text{m}$ , 180

m x 20 mm) and trapped for 5 min at a flow rate of 10 L/min at 99% A/1% B. Subsequently, peptides were separated on an ACQUITY UPLC M-Class Peptide BEH C18 Column (130 Å, 1.7 µm, 75µm × 250 mm) operating at a flow rate of 300 nL/min at 35°C using a non-linear gradient consisting of 1–7% B over 1 min, 7–23% B over 179 min, 23–35% B over 60 min, 35–98% B over 5 minutes, before increasing to 95% B and washing. Settings for data acquisition on the Q Exactive are outlined in Table 3-3. Raw UPLC-MS/MS files were processed in FragPipe 1.18.0 and data analysis was performed in Perseus software (v1.16.4). Statistical significance was determined using Student's t-test ( $p < 0.05$ ). Gene Set Enrichment Analysis (GSEA) using GSEA 4.2.3 was used to reference GO Biological Processes using Signal2Noise for ranking genes, all other settings were left at default.

**Table 3-3: Q Exactive Settings for Data Acquisition**

<b>QE Plus Setting</b>	<b>Value</b>
Scan Range	400-1500 m/z
MS1 AGC Target	3E6
MS1 Resolution	70K
MS2 Resolution	17.5K
MS2 AGC Target	2E5
Maximum IT	64ms
Loop Count	12
Top N	12
Isolation Window	1.2 m/z
Isolation Offset	0.5 m/z
NCE	25
Dynamix Exclusion	30
Charge Exclusion	1,7,8,>8
Fixed First Mass	100 m/z

### 3.2.12 Statistical Analysis

One-way ANOVA with Tukey's post-hoc analysis was used for wildtype timeline experiments and experiments containing only 3 groups. For experiments comparing expression or protein abundance over time across two cell lines a Two-way ANOVA was used with Sidak's multiple comparisons post-hoc analysis. All statistical analyses were performed using Prism Software (Prism version 9.3.1).

## 3.3 Results

### 3.3.1 Nek2 levels are unchanged during neural differentiation

Despite the reports showing that Nek2 regulates Hh and Wnt signaling (Mbom et al. 2014; Cervenka et al. 2016; Wang et al. 2016; Zhou et al. 2017) and both pathways are activated during P19 neural differentiation (Schuuring et al. 1989; Voronova et al. 2011; Spice et al. 2022), few publications have explored the role of Nek2 in embryonic development (Tanaka et al. 1997; Joseph Endicott et al. 2015b; Martins et al. 2017) and to our knowledge, few limited work exists on its involvement in neurogenesis. To first address this shortfall, *Nek2* gene expression (Figure 3-1) and protein levels (Fig. 3-2A and B) were explored throughout RA-induced differentiation, and results showed no significant change in either transcript or protein levels.

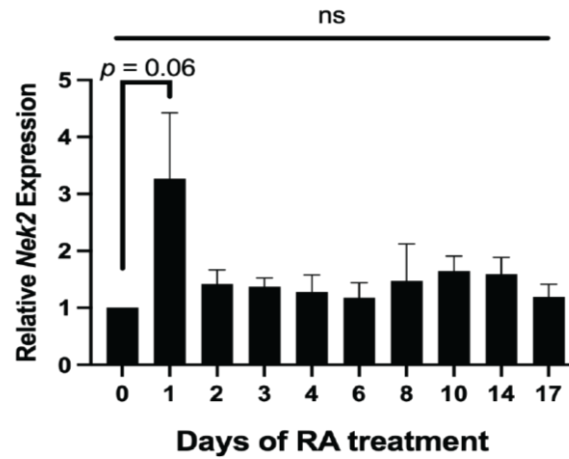


**Figure 3-1: *Nek2* gene expression does not change throughout RA-induced neural differentiation**

RT-qPCR of *Nek2* during days 0-17 of RA treatment. N=3. Bars represent mean values  $\pm$  s.e.m. Significance was determined by One-way ANOVA with Tukey's post-hoc analysis.

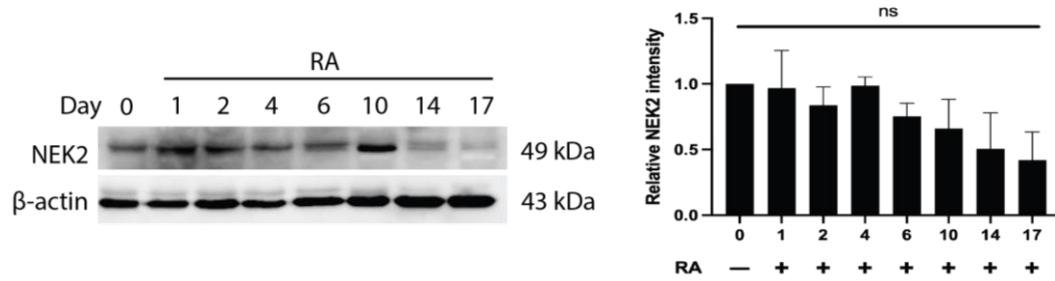


**Figure 3-2: Nek2 levels do not change during neural differentiation**

(A) Immunoblot of Nek2 at various timepoints between days 0-17 of RA treatment. (B) Densitometry of immunoblot in A. N=3. Bars represent mean values  $\pm$  s.e.m. P-values were determined by One-way ANOVA using Tukey's post-hoc analysis.

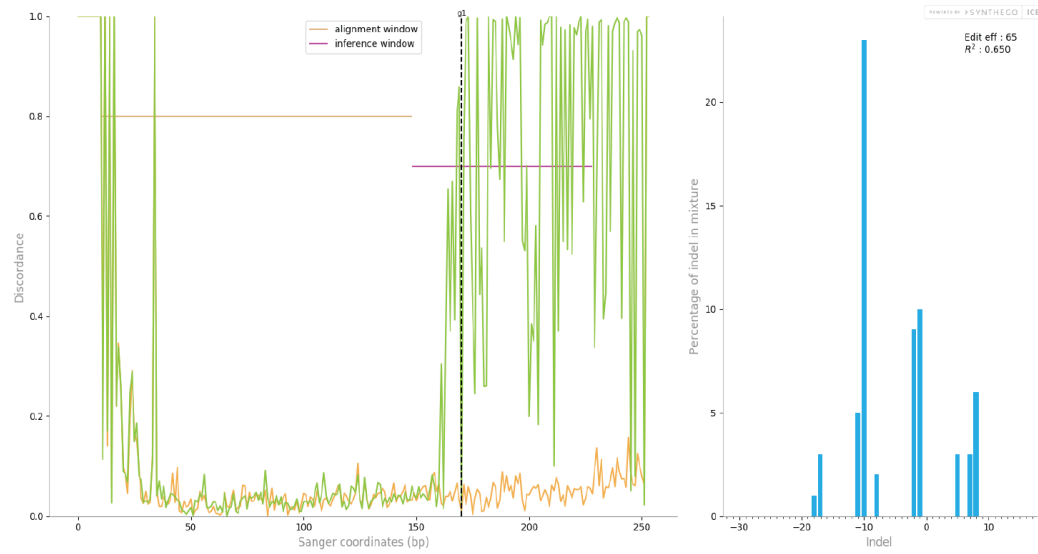
### 3.3.2 Nek2 regulates cell proliferation in undifferentiated cells

To determine the role of Nek2 in P19 cells, CRISPR-Cas9 was used to disrupt exon 2 of the coding region of the gene (gRNA sequence Table 3-1). This targeting resulted in a pool of alleles that consisted primarily of a 10 bp deletion, but also contained alleles of 1, 2, 8, 11, 17 and 18 bp deletions, as well as 5, 7 and 8 bp insertions (Figure 3-3A). This polyclonal pool was labelled knockout (KO) as all alleles resulted in a frameshift mutation and immunoblotting showed no detection of Nek2 protein in these cells (Fig. 3-4A and B). A second gRNA, targeting exon 3 (Table 3-1), resulted in a reduction in Nek2 levels (Fig. 3-4A and B) and identified alleles within these cells were either wildtype (WT) sequence or a 1 bp insertion (Figure 3-3B). These cells were labelled as knockdown (KD) cells and although the nature of the knockdown was not explored further, it may be the result of heterozygous alleles or in defects in pre-mRNA splicing (Tang et al. 2018). Cells were also transfected with either pcDNA or a plasmid containing human Nek2 (pNek2-Myc), the latter showing significantly increased levels of Nek2 protein over the pcDNA control (Fig. 3-4A and B).

As Nek2 is a known regulator of the cell cycle (Fry et al. 2012), cell counts were performed in undifferentiated cells, and results show that the Nek2 KO caused significantly fewer cells to be present after 72 and 96 hours (Fig. 3-4C); KD cells had significantly fewer cells only after 96 hours (Fig. 3-4C). *Nek2*-overexpressing cells showed the opposite results, with more cells present than the control at 96 hours (Fig. 3-4C). Thus, Nek2 loss resulted in decreased cell proliferation while its overexpression caused the opposite effect.



A



B

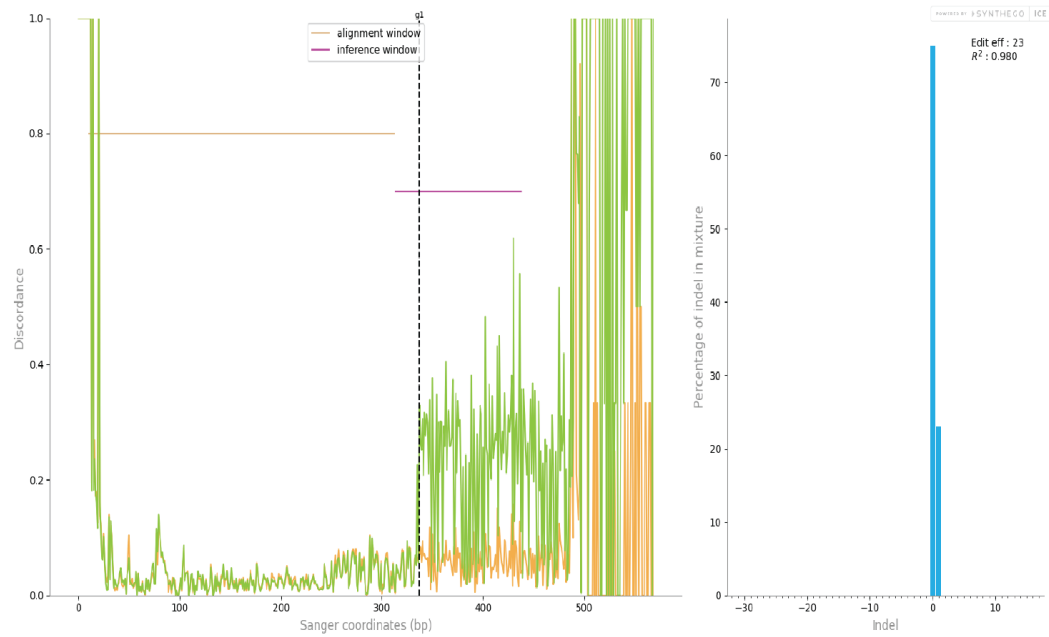


**Figure 3-3: Allele summary of NEK2 deficient cells**

Synthego ICE analysis showing alleles in the population of **(A)** Nek2 knockout (KO) and **(B)** Nek2 knockdown (KD) cells. Orange lines show WT sequence similarity to projected region, green lines show mutant sequence similarity. Dotted black line highlights the predicted cut site. Blue bars represent percentage of identified pool with the noted in/del.

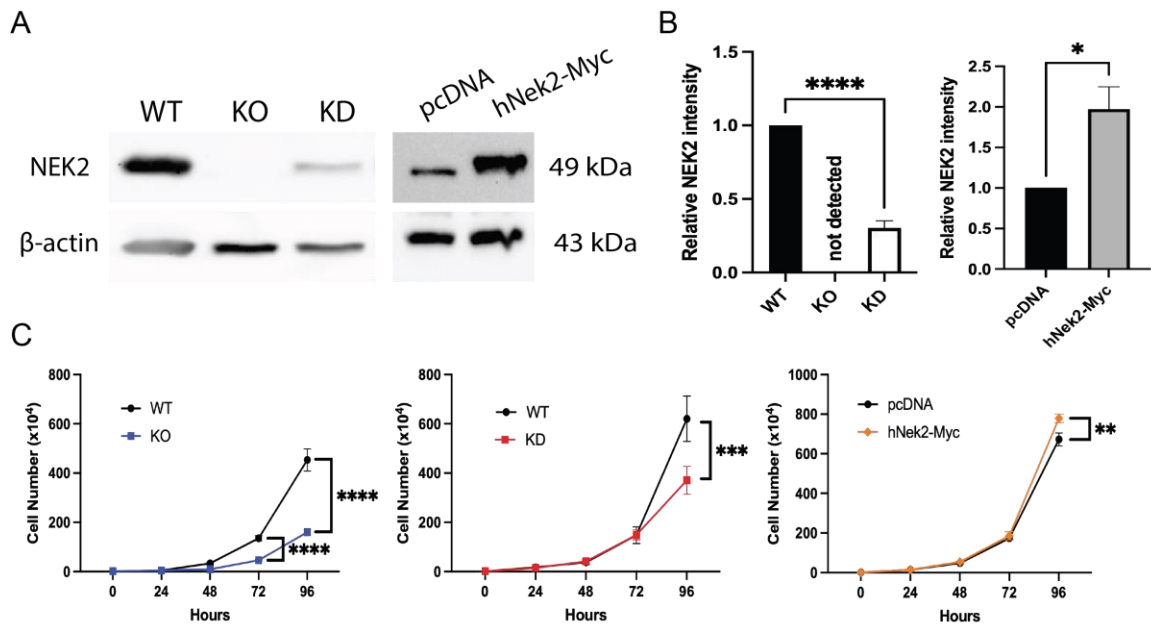


**Figure 3-4: Altering Nek2 levels changes proliferation rate of undifferentiated cells**

(A) Immunoblots of Nek2 in wildtype (WT), knockout (KO), knockdown (KD), pcDNA and hNek2-Myc transfected cells in the undifferentiated state. (B) Densitometry of immunoblots in A. Bars represent mean values  $\pm$  s.e.m. P-values were determined by One-way ANOVA using Tukey's post-hoc analysis. (C) Total cell counts of WT, KO, KD, pcDNA and hNek2-Myc transfected cells between 0-96 hours after plating in the undifferentiated state. Dots represent mean values  $\pm$  s.e.m. P-values were determined by Two-way ANOVA using Sidak's post-hoc analysis. \* $P < 0.05$ , \*\* $P < 0.01$ , \*\*\* $P < 0.001$ , \*\*\*\* $P < 0.0001$ .

The reduction in cell number in KO and KD cells was also observed after 4 days of RA treatment (Figure 3-5A) and resulted in dramatically reduced EB size (Fig. 3-6A and D) and organization (Fig. 3-6B), without altering the number of observed EBs (Fig. 3-6C and D). These changes in RA treated EBs appeared to be the result of a maintained reduction in proliferation (Figure 3-5A) without affecting caspase 3 activity (Figure 3-5B) or viability (Figure 3-5C). Significantly, *Nek2* overexpressing cells compared to the control also showed reduced EB size (Fig. 3-6A and D), while showing increased organization and an aspect ratio closer to 1 (Fig. 3-6B). Unlike the KO and KD cells, however, pNek2-Myc transfected cells had more EBs per image area compared to pcDNA transfected cells (Fig. 3-6C and D). Together, these data show that Nek2 is important for regulating the cell cycle in the undifferentiated state, and it appears to continue this regulation during the first days of neural induction.

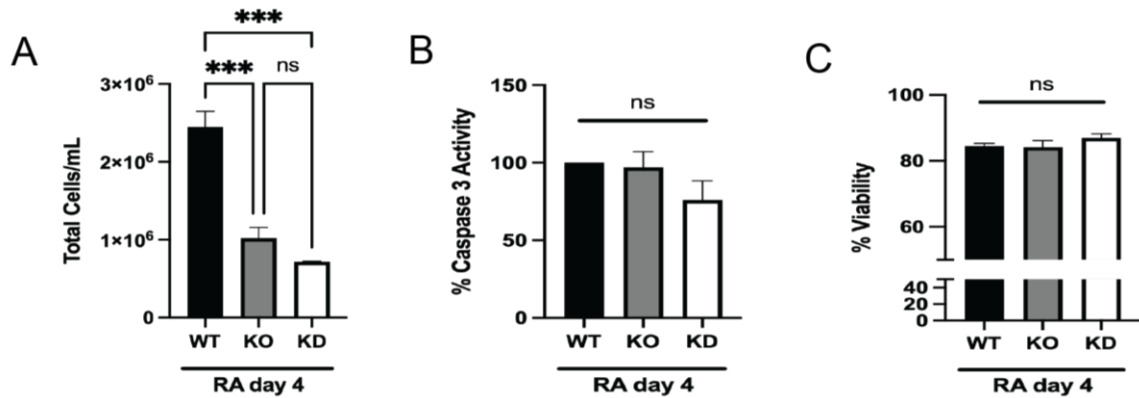
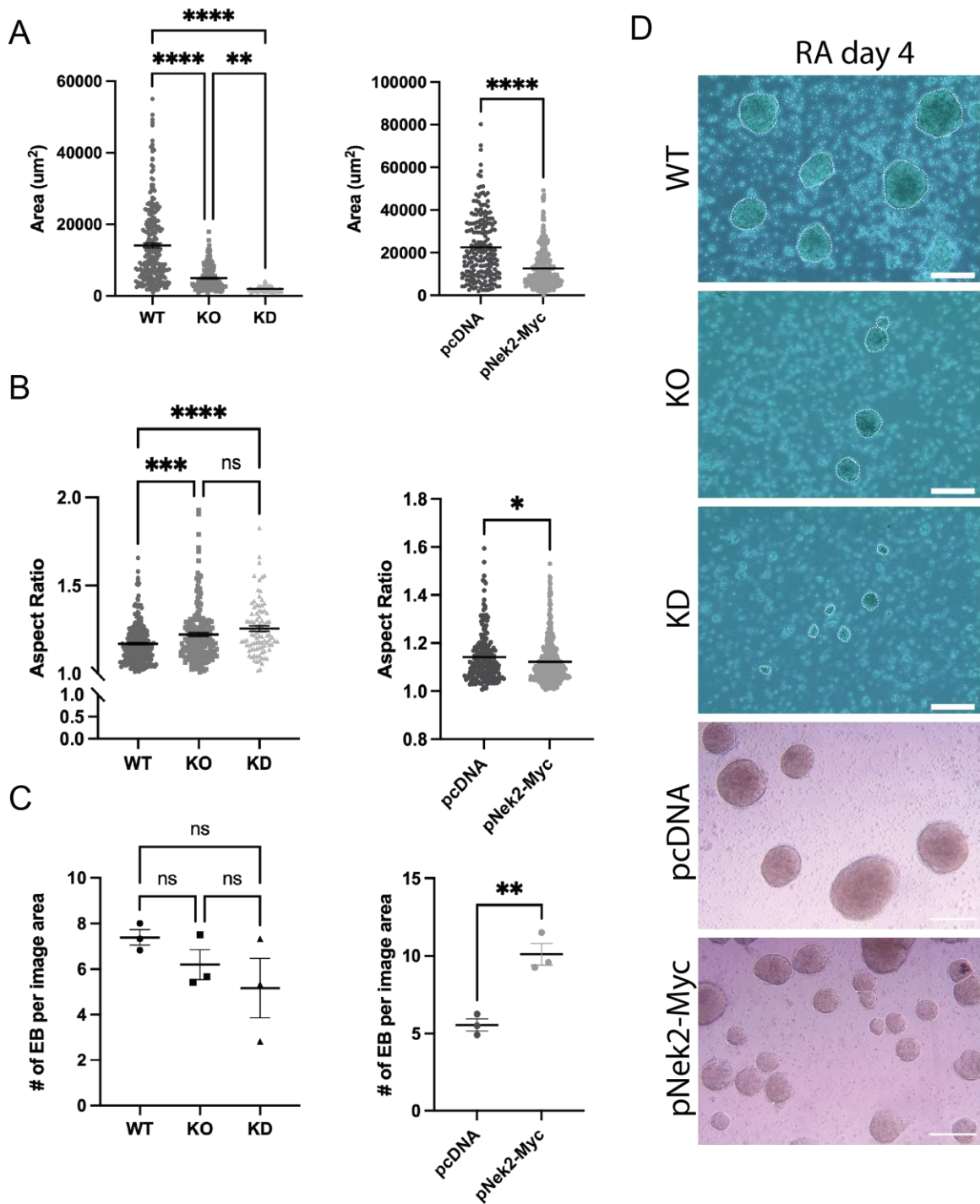


**Figure 3-5: Nek2 deficiency inhibits proliferation without affecting apoptosis**

(A) Total number of cells (B) Caspase 3 activity measured by cytoplasmic concentration of pNA after EBs being resuspended and (C) trypan blue exclusion test measuring cell viability in EB in wildtype (WT), Nek2 knockout (KO) and knockdown (KD) cells. N=3. Bars represent mean values  $\pm$  s.e.m. P-values were determined by One-way ANOVA with Tukey's post-hoc analysis. \*\*\* $P < 0.001$ , \*\*\*\* $P < 0.0001$ .

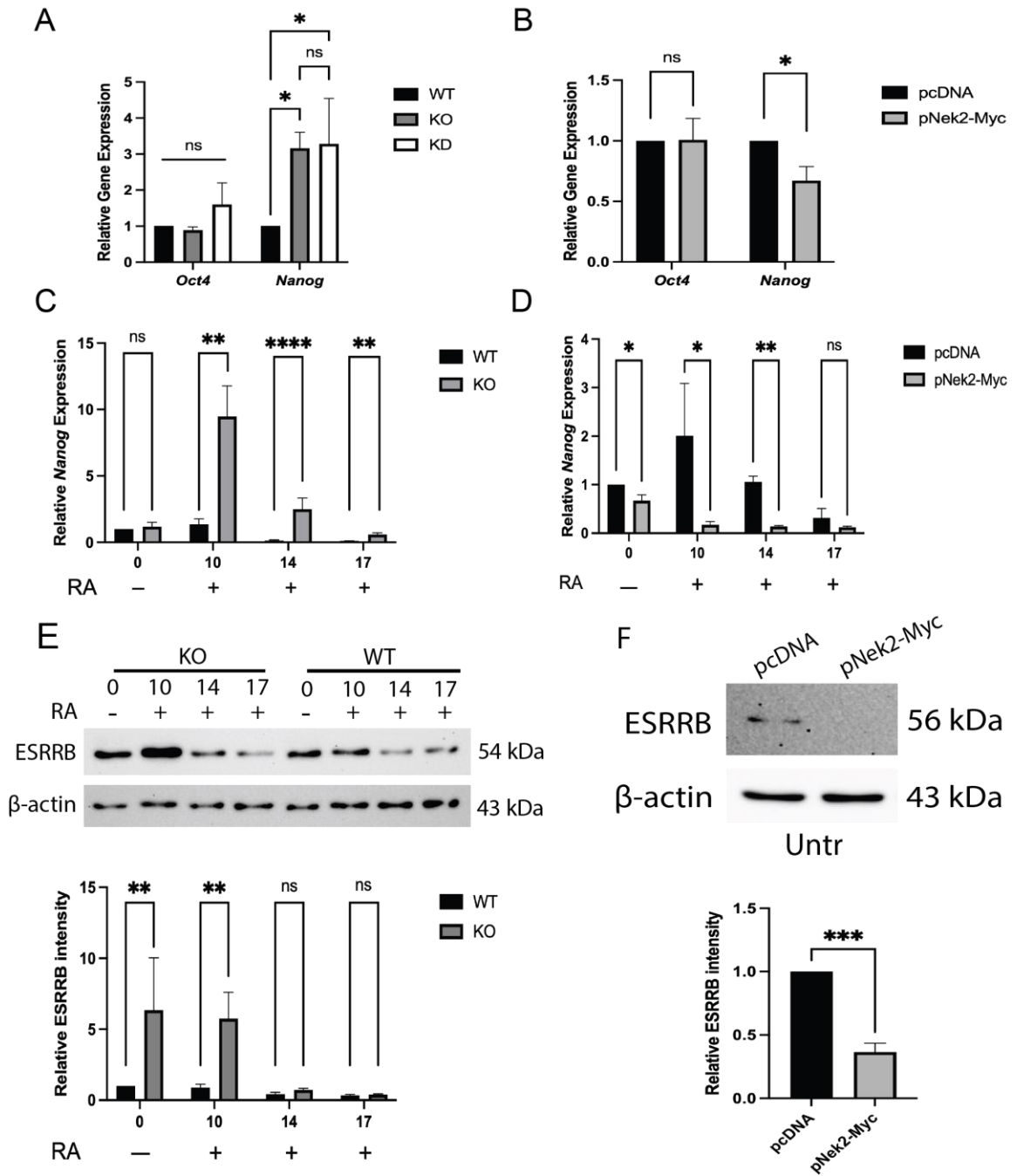


(A) Area, and (B) Aspect ratio (major axis/minor axis of EB from images in D formed after 4 days of RA treatment in wildtype (WT), Nek2 knockout (KO) and knockdown (KD) cells, and pcDNA and pNek2-Myc transfected cells. Points represent individual EB. (C) Number of EB per image area from images in D. Points represent mean number of EB across all images per replicate. Lines across points represent mean values  $\pm$  s.e.m. (D) Phase contrast images of EB. White dotted lines outline perimeter. Scale bar = 200  $\mu$ m. N=3. P-values were determined by One-way ANOVA with Tukey's post-hoc analysis. \* $P < 0.05$ , \*\* $P < 0.01$ , \*\*\* $P < 0.001$ , \*\*\*\* $P < 0.0001$ .

### 3.3.3 Nek2 promotes exit from pluripotency

Since Nek2 has been explored sparingly in the context of pluripotency (Van Hoof et al. 2009) but as shown can affect cell number, the expression and protein abundance of various factors was examined to determine if there was a relationship. RT-qPCR was used to measure the expression of known pluripotency transcription factors *Oct4* and *Nanog* (Gatie et al. 2022) in undifferentiated WT, KO, and KD cells and in those overexpressing *Nek2* compared to a pcDNA control. No significant change in *Oct4* levels were detected in any condition, but there was a significant increase in *Nanog* expression in KO and KD cells (Fig. 3-7A). Conversely, and relative to the control, *Nek2* overexpressing cells showed a decrease in *Nanog* levels (Fig. 3-7B) in the undifferentiated state. KO cells were further explored throughout RA-induced differentiation where expression of *Nanog* was elevated in RA-treated cells at days 10, 14 and 17 compared to WT controls (Fig. 3-7C). Again, *Nek2* overexpressing cells, relative to the control, had reduced *Nanog* expression at days 0, 10 and 14 of RA treatment (Fig. 3-7D). ESRRB, a marker of pluripotency (Gatie et al. 2022), was also explored in KO and WT cells throughout RA treatment and results showed that it was significantly higher than the WT controls on day 10 following RA treatment, and significantly higher in KO cells relative to WT at day 0 when RA was not present (Fig. 3-7E). In support, and relative to the pcDNA controls, *Nek2* overexpressing cells lost the ESRRB signal in untreated cells (Fig. 3-7F). Thus, markers of pluripotency decreased when *Nek2* was overexpressed and increased with *Nek2* loss, suggesting it is likely involved in influencing the state of cell pluripotency.





RT-qPCR of pluripotency markers *Oct4* and *Nanog* in untreated, undifferentiated (**A**) wildtype (WT), Nek2 knockout (KO) and knockdown (KD) cells, and (**B**) pcDNA and pNek2-Myc transfected cells. P-values were determined by One-way ANOVA with Tukey's post-hoc analysis. Expression of *Nanog* in (**C**) WT and KO cells and (**D**) pcDNA and pNek2-Myc transfected cells during 0-17 days of RA treatment. Immunoblotting of ESRRB in (**E**) WT and KO cells during days 0-17 of RA treatment and (**F**) untreated pcDNA and pNek2-Myc transfected cells. P-values were determined by Two-way ANOVA with Sidak's post-hoc analysis or by Student's t-test. N=3. Bars represent mean values  $\pm$  s.e.m. \* $P < 0.05$ , \*\* $P < 0.01$ , \*\*\* $P < 0.001$ , \*\*\*\* $P < 0.0001$ .

### 3.3.4 Nek2 is required for neural differentiation

To test the involvement of Nek2 in neural differentiation, antibodies to  $\beta$ -III-tubulin and GFAP were used to detect the presence of neurons and astrocytes, respectively, in WT and Nek2 deficient cells (KO and KD) and in cells overexpressing *Nek2* (pNek2-Myc) (Fig. 3-8). Compared to WT cells, both markers showed either reduced or absent  $\beta$ -III-tubulin (Fig. 3-8A and B, Fig. 3-9A and B) and GFAP levels (Fig. 3-8A and C, Fig. 3-9A and C) at days 10, 14 and 17 in KO and KD cells. Overexpression of *Nek2* caused the opposite to occur for  $\beta$ -III-tubulin, showing a significant increase at days 10 and 17 (Fig. 3-8A and B), while GFAP levels were absent in these cells at day 17 (Fig. 3-8A). Thus, the reduction or absence of Nek2 was sufficient to attenuate both neuronal and astrocyte cell fates. More importantly, overexpressing *Nek2* was sufficient to enhance the neuronal fate, but it also attenuated astrocyte formation. Immunofluorescence was used to corroborate the immunoblot findings at day 17 of RA treatment, and results confirmed no detection of either marker in KO cells (Fig. 3-8D). To test whether or not Nek2 KO cells remained stem-like in nature, RT-qPCR was used to detect *Nestin*, a neural stem cell marker (Lendahl et al. 1990; Morshead et al. 1994; Suzuki et al. 2010). Results, compared to undifferentiated controls, showed that *Nestin* expression increased in both wildtype and KO cell lines over time ( $P < 0.0001$ ), however, there was no significant difference between WT and KO cells at any of the timepoints tested (Fig. 3-8E). Thus, it appears Nek2 is required for the differentiation of neurons and astrocytes, and its overexpression promotes the formation of neuron but not astrocytes.

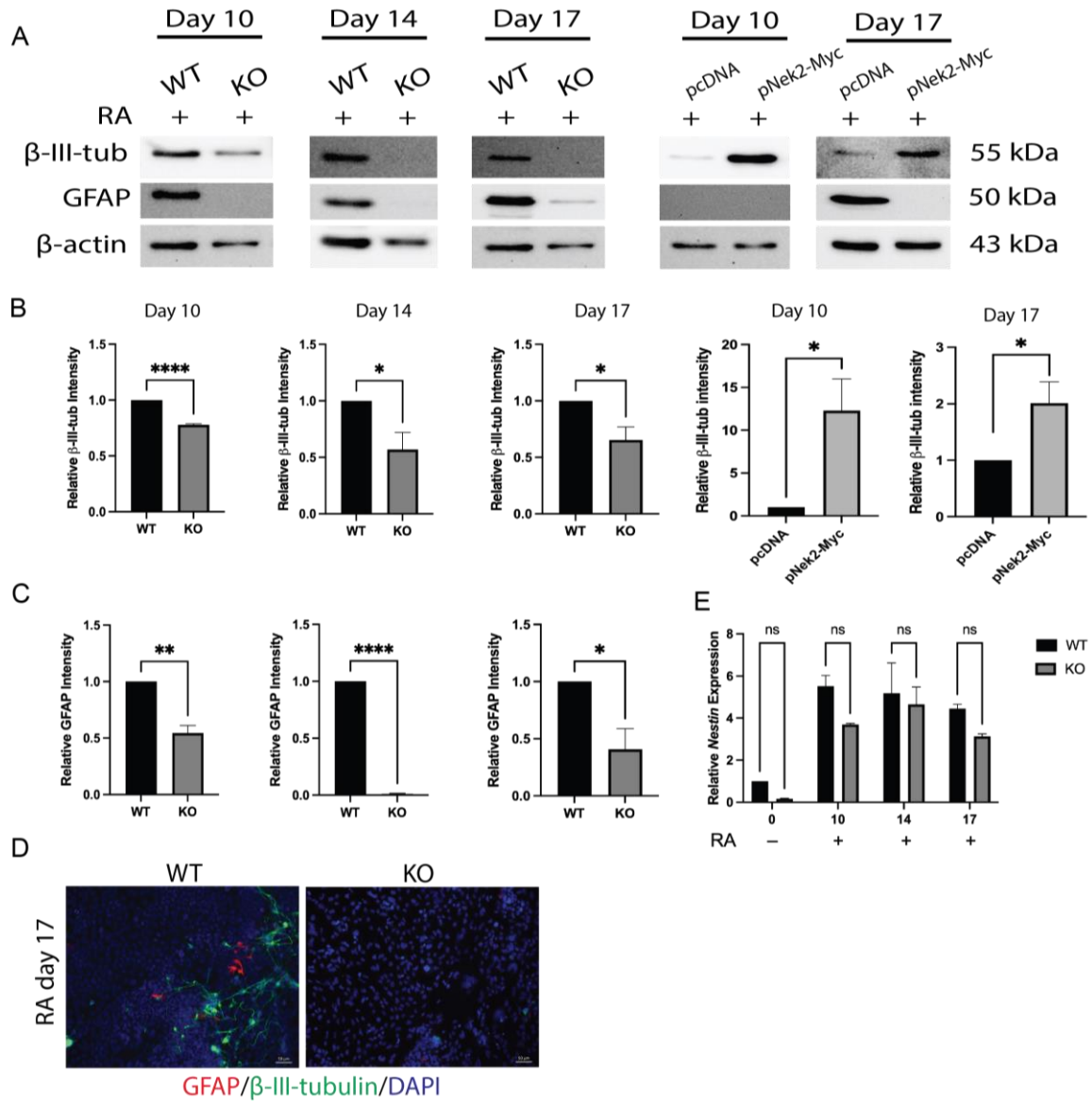


**Figure 3-8: Nek2 is required for neural differentiation**

(A) Immunoblot of neuron marker,  $\beta$ -III-tubulin, and astrocyte marker, GFAP, in wildtype (WT), Nek2 knockout (KO), pcDNA and pNek2-Myc transfected cells at various times during RA treatment. Densitometry of (B)  $\beta$ -III-tubulin and (C) GFAP from immunoblots in A). P-values were determined by Student's t-test. (D) Immunofluorescence of GFAP (red),  $\beta$ -III-tubulin (green), and DAPI (blue) staining in WT and KO cells at day 17 of RA treatment. (E) RT-qPCR of neural stem cell marker *Nestin* in WT and KO cells during days 0-17 of RA treatment. P-values were determined by Two-way ANOVA with Sidak's post-hoc analysis. N=3. Bars represent mean values  $\pm$  s.e.m. \* $P < 0.05$ , \*\* $P < 0.01$ , \*\*\*\* $P < 0.0001$ .

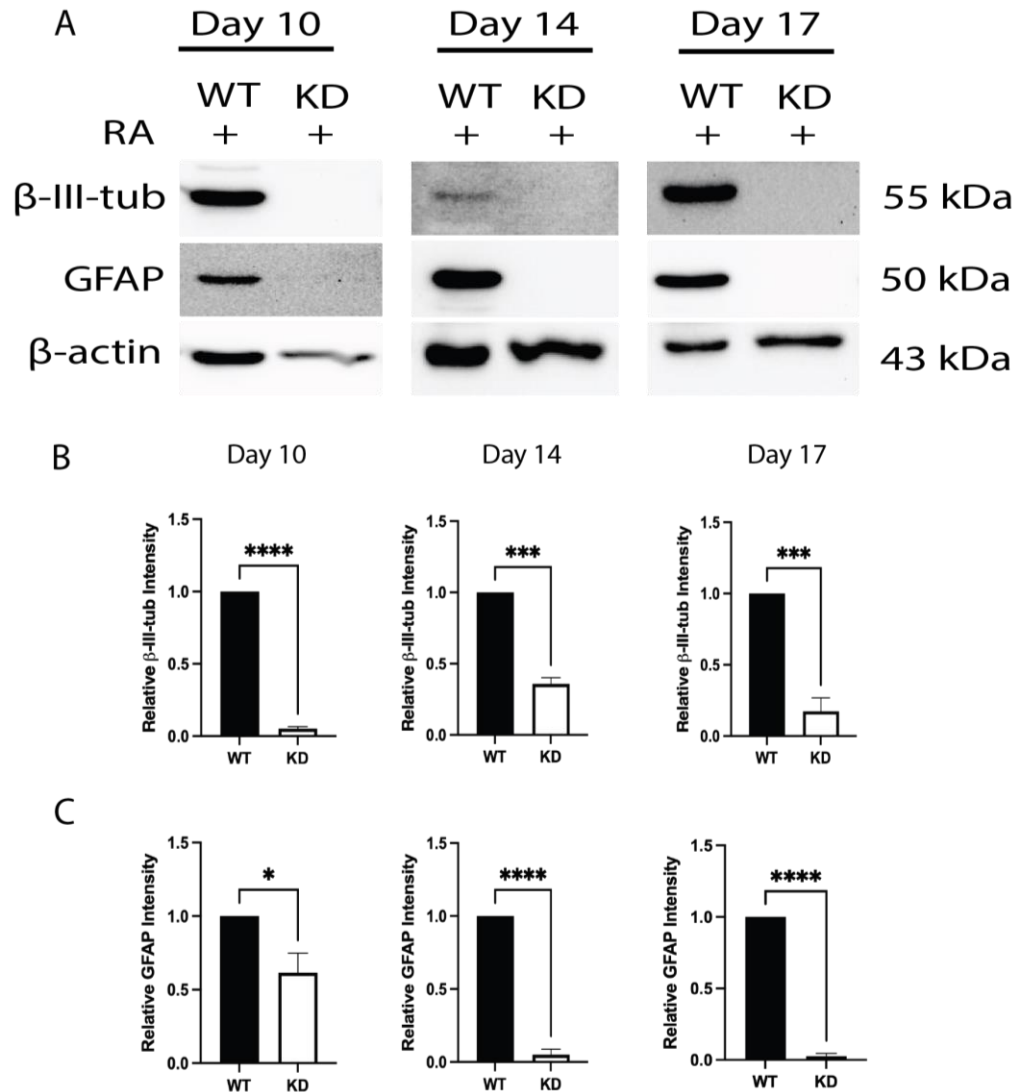


**Figure 3-9: NEK2 knockdown blocks differentiation of neurons and astrocytes**

(A) Immunoblot of neuron marker  $\beta$ -III-tubulin, astrocyte marker GFAP and  $\beta$ -actin in wildtype (WT) and Nek2 knockdown (KD) cells after differentiation in the presence of 0.5  $\mu$ M retinoic acid (RA) for 10, 14 and 17 days. Densitometry of immunoblot in A of (B)  $\beta$ -III-tubulin and (C) GFAP at the same time points. Bars represent mean values  $\pm$  s.e.m. N=3. P-values were determined by Student's t-test. \* $P < 0.05$ , \*\* $P < 0.01$ , \*\*\* $P < 0.001$ , \*\*\*\* $P > 0.0001$ .

### 3.3.5 Nek2 loss and overexpression alters Hh signalling

Canonical Hh and Wnt signalling both play an integral role in neural differentiation of P19 cells and have been linked to Nek2 (Mbom et al. 2014; Cervenka et al. 2016; Wang et al. 2016; Zhou et al. 2017). Wang et al. [19] and Zhou et al. [20] reported Nek2 serves as a negative regulator of Hh signalling and our previous report has shown that overactivation of Hh signalling through the loss of SUFU inhibited astrocyte differentiation in the P19 model (Spice et al. 2022). Therefore, Hh signalling was first explored as a potential mechanism for Nek2 in regulating neural differentiation. RT-qPCR was performed in untreated, undifferentiated KO and KD cells, where Hh target gene *Ptch1* was increased compared to WT cells (Fig. 3-10A). However, Hh targets *Gli1* and *Ascl1* were only elevated in KD and not KO cells (Fig. 3-10A). A Gli-responsive luciferase assay was also performed, which confirmed that untreated KO and KD cells had similar Gli-luciferase activity compared to WT cells treated with 10 nM SAG (Fig. 3-10B). Despite the Nek2 KO and Nek2 overexpression in cells showing opposite levels of pluripotency genes (Fig. 3-7), there was also an increase in *Ptch1* expression in pNek2-Myc transfected, undifferentiated cells (Fig. 3-10C). To get a better understanding how Hh signalling may be affected by altering Nek2 levels, RT-qPCR was also performed on Nek2-deficient and *Nek2* overexpressing cells throughout RA treatment (Fig. 3-11). Nek2 KO cells showed increased expression of *Gli1* at days 10 and 14 of RA treatment (Fig. 3-11A), whereas *Nek2* overexpressing cells showed decreased expression at day 10 (Fig. 3-11B). In Nek2 KO cells, *Ptch1* expression compared to WT controls occurred only at day 0 (Fig. 3-11C) and at later stages its amount was like that in controls. However, *Nek2* overexpressing cells had reduced expression compared to the controls at day 10 of RA treatment (Fig. 3-11D). Together, these data suggest that the presence of Nek2 acts to reduce Hh target gene expression at these later stages, however, the link between Nek2 and Hh remains unclear as the expression of target genes was not consistent when Nek2 levels were perturbed (Figure 3-11).

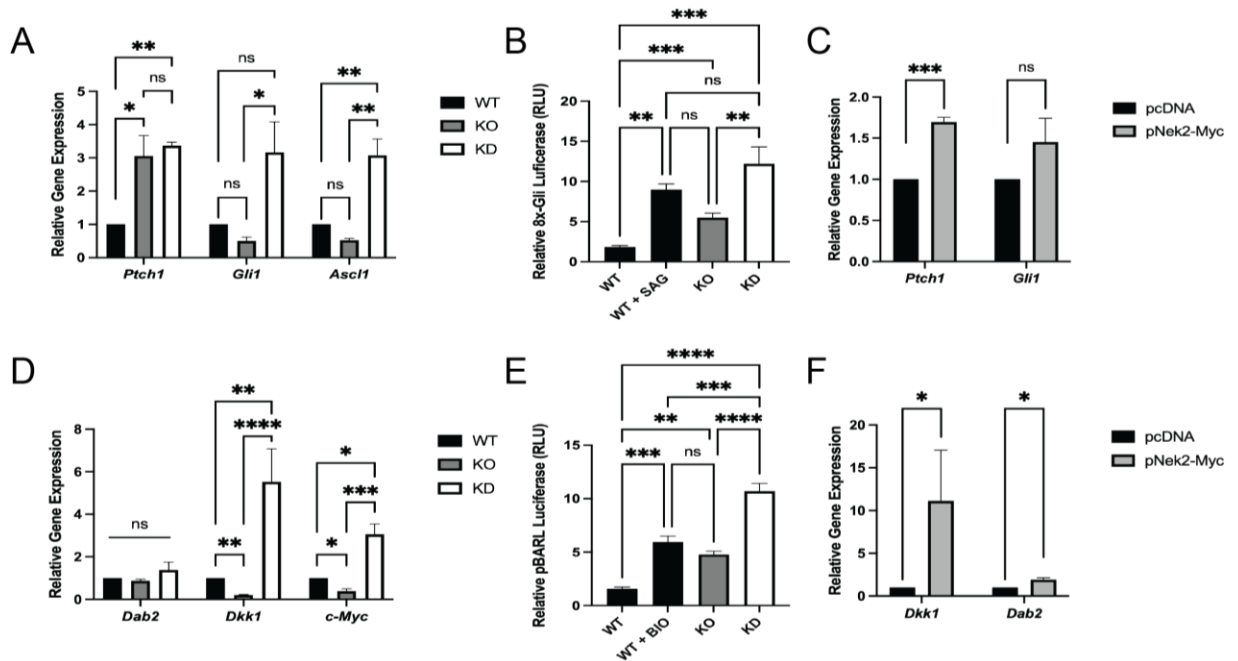


**Figure 3-10: Hh and Wnt signaling are perturbed in Nek2 deficient and overexpressing cells**

(A) RT-qPCR of Hh target genes *Ptch1*, *Gli1* and *Ascl1* in wildtype (WT), knockout (KO) and knockdown (KD) cells in undifferentiated cells. (B) Gli-responsive luciferase assay in untreated WT, KO and KD cells and WT cells with 10 nM SAG treatment after 24 hours. (C) RT-qPCR of Hh target gene *Ptch1* and *Gli1* in pcDNA and pNek2-Myc transfected cells. (D) RT-qPCR of Wnt target genes *Dab2*, *Dkk1* and *c-Myc* in WT, KO and KD undifferentiated cells. (E)  $\beta$ -catenin responsive luciferase assay in untreated WT, KO and KD cells and WT cells treated with 10 nM BIO after 24 hours. (F) RT-qPCR of Wnt target genes *Dkk1* and *Dab2* in pcDNA and pNek2-Myc transfected cells. P-values were determined by One-way ANOVA with Tukey's post-hoc analysis. N=3. Bars represent mean values  $\pm$  s.e.m. \* $P < 0.05$ , \*\* $P < 0.01$ , \*\*\* $P < 0.001$ , \*\*\*\* $P < 0.0001$ .



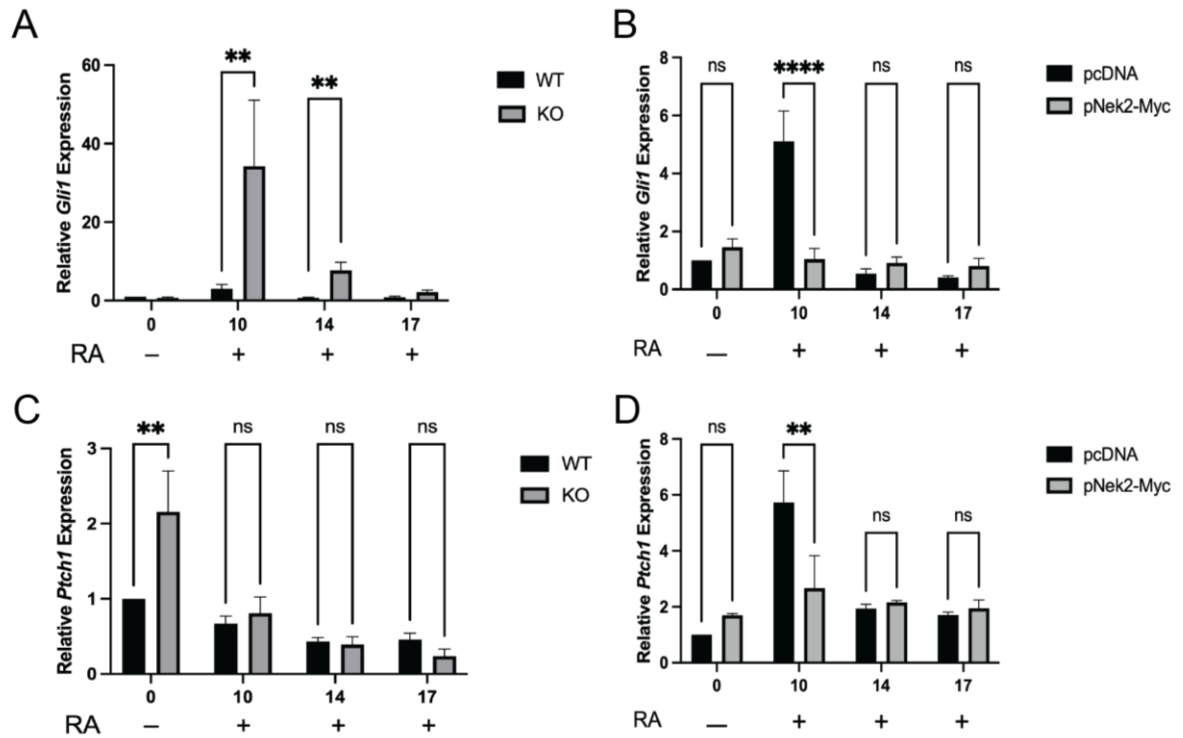


**Figure 3-11: Hh signaling is affected by perturbed Nek2 levels**

RT-qPCR of Hh target gene *Gli1* in (A) wildtype (WT) and Nek2 knockout (KO) cells, and (B) in pcDNA and pNek2-Myc transfected cells during days 0-17 of RA treatment. RT-qPCR of Hh target gene *Ptch1* in (C) WT and KO, and (D) pcDNA and pNek2-Myc transfected cells during days 0-17 of RA treatment. P-values were determined by Two-way ANOVA with Sidak's post-hoc analysis. N=3. Bars represent mean values  $\pm$  s.e.m. \*\* $P < 0.01$ , \*\*\*\* $P < 0.0001$ .

### 3.3.6 Nek2 loss and overexpression alters Wnt signalling

Since Nek2 is reported as a positive regulator of Wnt signalling through phosphorylation of DVL and  $\beta$ -catenin (Mbom et al. 2014; Cervenka et al. 2016), we also explored if the canonical Wnt pathway was linked to Nek2 and neural differentiation. RT-qPCR was performed in untreated, undifferentiated WT, KO and KD cells where the Wnt target gene *Dab2* showed no change in expression. However, other targets including *Dkk1* and *c-Myc* were reduced in KO cells and elevated in KD cells (Fig. 3-10D). To better understand these differences, experiments with a  $\beta$ -catenin-responsive luciferase assay was performed in untreated WT, KO and KD cells and in WT cells treated with 10 nM BIO after 24 hours. Results showed KO and KD cells had greater  $\beta$ -catenin-luciferase activity than WT cells, and comparable to when BIO was included as a treatment of WT cells (Figure 3-10E). Significantly, *Nek2* overexpressing cells also showed an increase in the expression of *Dkk1* and *Dab2* compared to that in controls (Figure 3-10F). Furthermore, we employed a similar strategy as that conducted for Hh signalling to investigate the potential link between Wnt and Nek2 at later stages involving RA-induced differentiation. RT-qPCR showed that target gene *Dkk1* was increased at day 10 in KO cells compared to WT controls (Fig. 3-12A), while *Nek2* overexpressing cells showed consistent increases in *Dkk1* expression at days 0, 14 and 17 of RA treatment; the apparent increase on day 10 was not significant (Fig. 3-12B). *Dab2* was also investigated, where KO cells showed significantly reduced expression only at day 17 compared to WT cells (Fig. 3-12C). In contrast, when *Nek2* was overexpressed in cells, *Dab2* was increased at days 14 and 17 of RA treatment (Fig. 3-12D). Thus, it appeared that the link between Wnt signalling and Nek2 in regulating neuronal development was clearer than Hh but still not definitive.

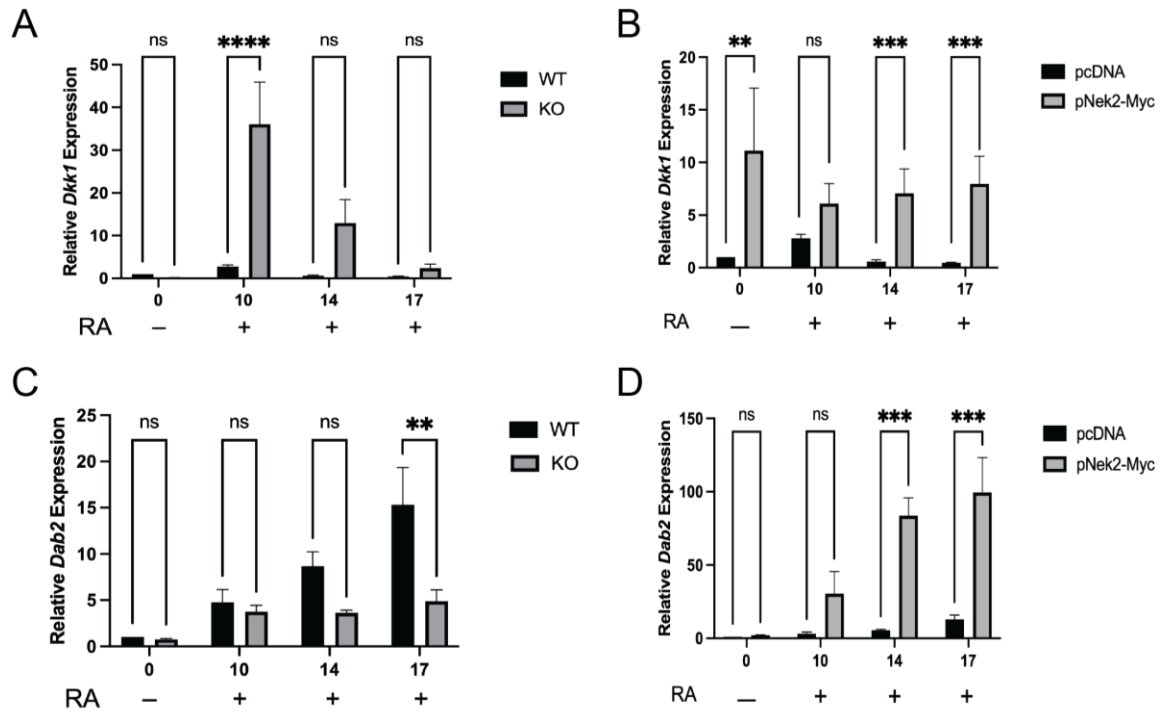


**Figure 3-12: Wnt signaling is affected by perturbed Nek2 levels**

RT-qPCR of Wnt target gene *Dkk1* in (A) wildtype (WT) and Nek2 knockout (KO) cells, and (B) in pcDNA and pNek2-Myc transfected cells during days 0-17 of RA treatment. RT-qPCR of Wnt target gene *Dab2* in (C) WT and KO, and (D) pcDNA and pNek2-Myc transfected cells during days 0-17 of RA treatment. P-values were determined by Two-way ANOVA with Sidak's post-hoc analysis. N=3. Bars represent mean values  $\pm$  s.e.m. \*\* $P < 0.01$ , \*\*\* $P < 0.001$ , \*\*\*\* $P < 0.0001$ .

Since *Wnt1* overexpression in P19 cells promotes neuron differentiation while inhibiting astrocyte differentiation (Tang et al. 2002) we employed a chemical strategy to further test this relationship between Nek2 and Wnt in neurogenesis. P19 cells were treated with BIO (Sklirou et al. 2017), an inhibitor of GSK3 that activates the Wnt pathway, and XAV (Huang et al. 2009), a tankyrase inhibitor which serves as a Wnt pathway antagonist. Co-treating cells with RA and BIO did not alter  $\beta$ -III-tubulin levels relative to RA alone (Fig. 3-13A and B), or when treated first with BIO before the addition of RA four days later. RA was the key inducer as BIO alone showed little to no  $\beta$ -III tubulin levels. The levels of GFAP, however, was greatly affected at later stages when the canonical Wnt pathway was activated by BIO in RA-treated cells (Figure 3-13A and C). XAV treatment, expected to produce opposite results, showed cells co-treated with it and RA inhibited both  $\beta$ -III-tubulin and GFAP detection (Fig. 3-13D-F). Together, these chemical and genetic results reveal a link between Nek2 and Wnt signalling, specifically on astrocyte differentiation, but the mechanism is still unclear on how the loss of Nek2 attenuates neuronal differentiation.

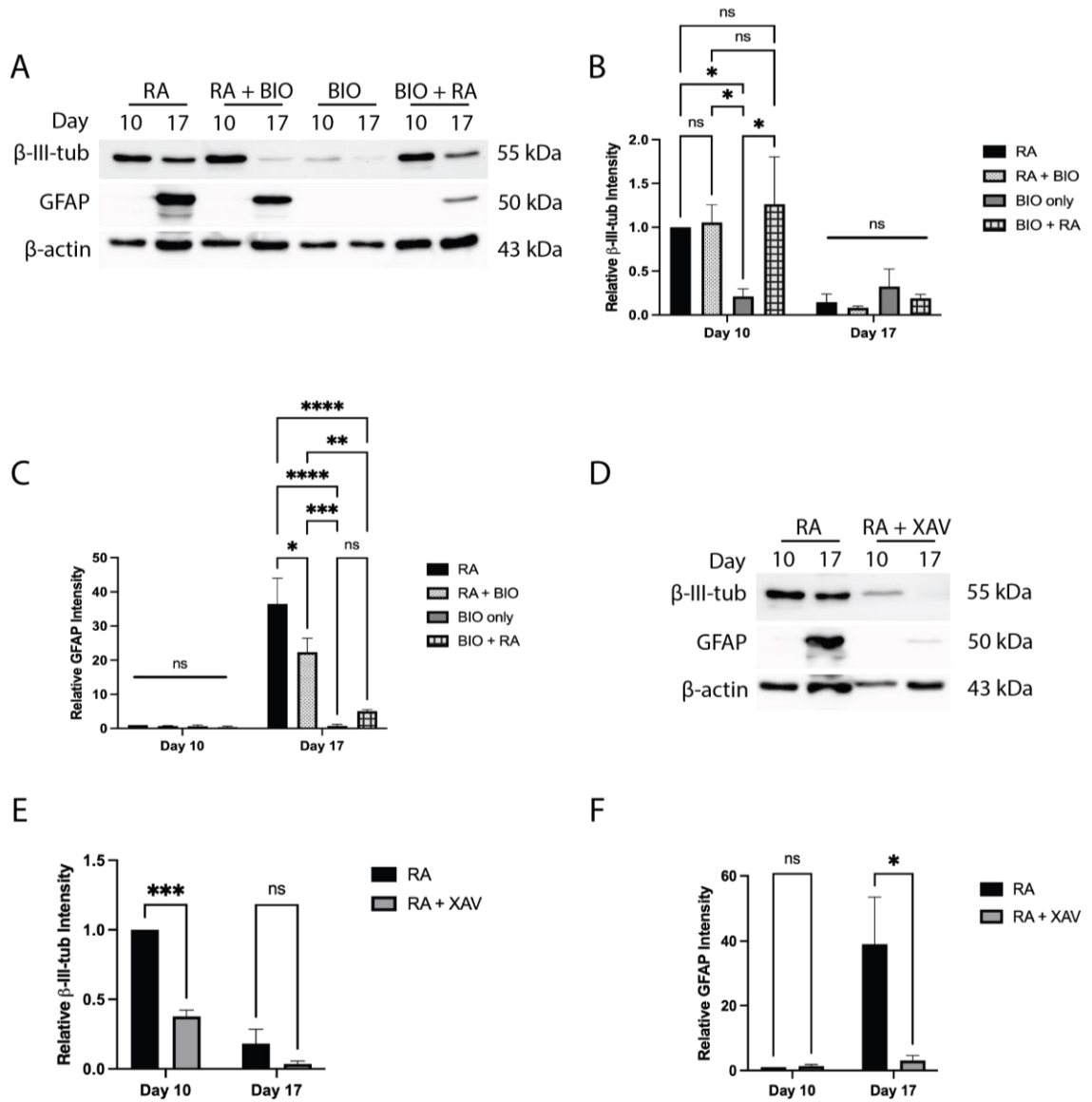


**Figure 3-13: Wnt is required for neural differentiation but is only sufficient to induce neurons**

(A) Immunoblot of  $\beta$ -III-tubulin and GFAP in wildtype cells at days 10 and 17 after treatment with 0.5  $\mu$ M on days 0 and 4 (RA), 0.5  $\mu$ M RA with 10 nM BIO on day 0 plus RA on day 4 (RA+BIO), 10 nM BIO treatment on day 0 (BIO) or 10 nM BIO treatment on day 0 plus RA on day 4 (BIO+RA). Densitometry analysis of the immunoblot in A for (B)  $\beta$ -III-tubulin and (C) GFAP. (D) Immunoblot of  $\beta$ -III-tubulin and GFAP in wildtype cells at days 10 and 17 after treatment with 0.5  $\mu$ M RA on days 0 and 4 (RA) or 0.5  $\mu$ M RA with 10  $\mu$ M XAV on day 0 plus RA on day 4. Densitometry analysis of the immunoblot in D of (E)  $\beta$ -III-tubulin and (F) GFAP. N=3. Bars represent mean values  $\pm$  s.e.m. P-values were determined by Two-way ANOVA with Sidak's post-hoc analysis. \* $P < 0.05$ , \*\* $P < 0.01$ , \*\*\* $P < 0.001$ , \*\*\*\* $P < 0.0001$ .

### 3.3.7 Proteomic analysis identifies several differentially abundant proteins in Nek2 deficient cells

Although canonical Hh and Wnt signalling is required in P19 cells for proper neural differentiation (Smolich and Papkoff 1994; Tang et al. 2002; Voronova et al. 2011; Spice et al. 2022), and there are relationships between these pathways and Nek2, our data strongly suggests that the loss of Nek2 influences neural cell lineages linked to pluripotency and cell proliferation. The data supports this early role, rather than being directly linked to regulating the Wnt and Hh signalling pathways. To investigate this further a proteomic approach comparing global protein abundance patterns was chosen to provide more information of the pathways involving Nek2 in P19 cells. Proteins were analyzed from cells collected at days 0, 1, 4 and 10 of RA induced differentiation of WT and KO cells (Fig. 3-14). Differential enrichment analysis identified 1780 differentially regulated proteins across all time points (Fig. 3-14C-F); however, only 3 proteins were upregulated in KO cells (Fig. 3-15A): Cth, Slc25a13 and Pla2g15. In exploring pathways enriched specifically at day 10 of RA treatment, KO cell pathway enrichment included proteins involved in fatty acid metabolism, the G2 DNA damage checkpoint and K63 linked deubiquitination (Fig. 3-15C). Sixteen proteins were found to be downregulated in KO cells (Fig. 3-15B), including Ndufb8, Ndufv1, Ndufa10, Ndufc2, Mtnd4, Ptgr1, Mtnd1, Ndufs1, Mtco2, Ndufa4, Ndufa12, Ndufa5, Ndufb1, Cox6b1, Mtnd5 and Gstp1, and pathway enrichment in WT cells included proteins involved in negative regulation of cell projection organization, negative regulation of neuron projection development and mitochondria localization (Fig. 3-15D). Other pathways enriched in the WT population include Myc targets, epithelial to mesenchymal transition proteins and those related to oxidative phosphorylation (Fig. 3-14G).

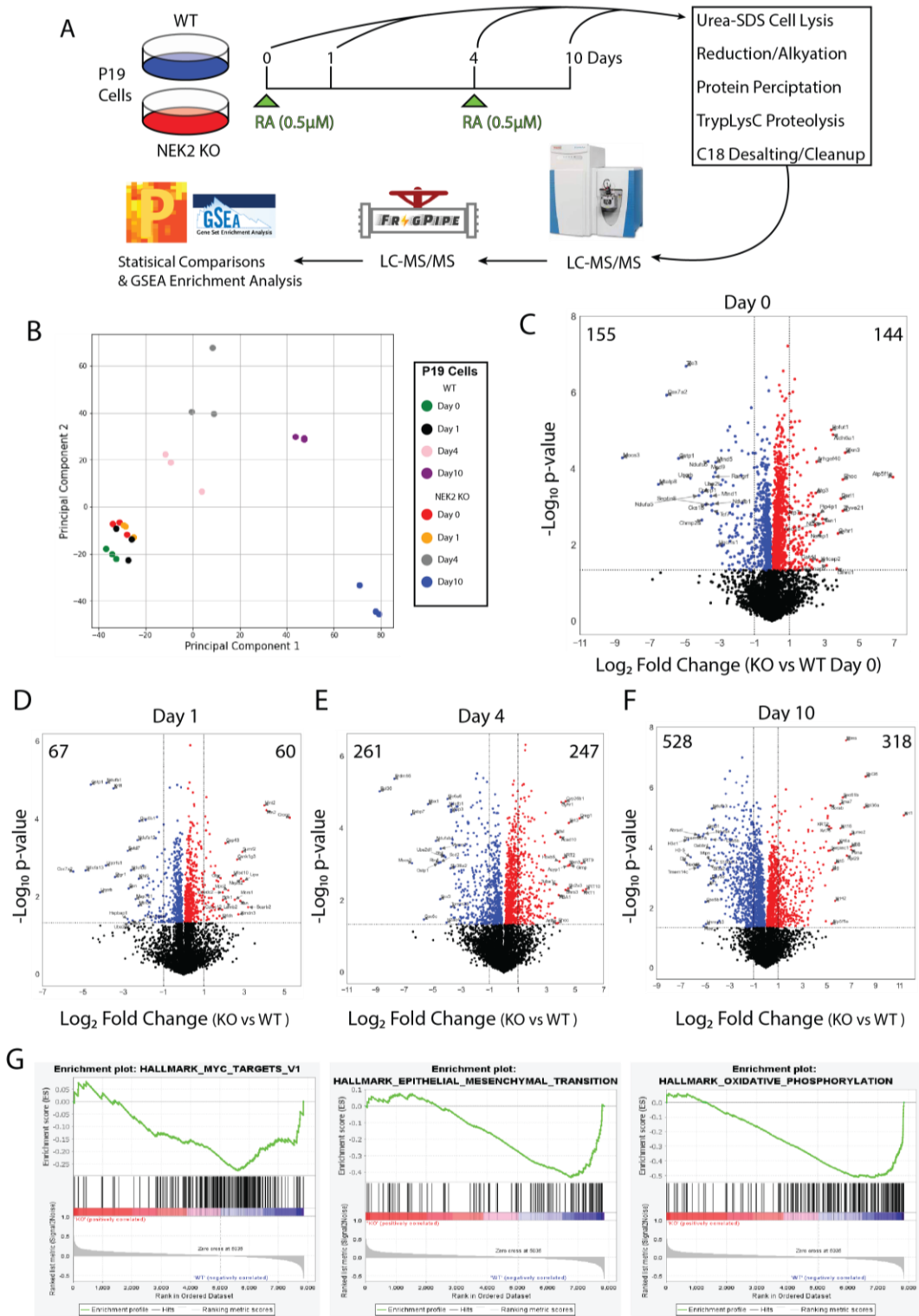


**Figure 3-14: LC-MS workflow and results of WT and KO cells**



**(A)** Workflow of LC-MS. **(B)** Principal component analysis of samples used for LC-MS showing clustering of biological replicates. Proteins identified as up or down regulated in KO cells compared to WT cells at days **(C)** 0, **(D)** 1, **(E)** 4 and **(F)** 10 of RA treatment. **(G)** GSEA Pathway Enrichment Analysis of proteins enriched in WT cells compared to KO cells.

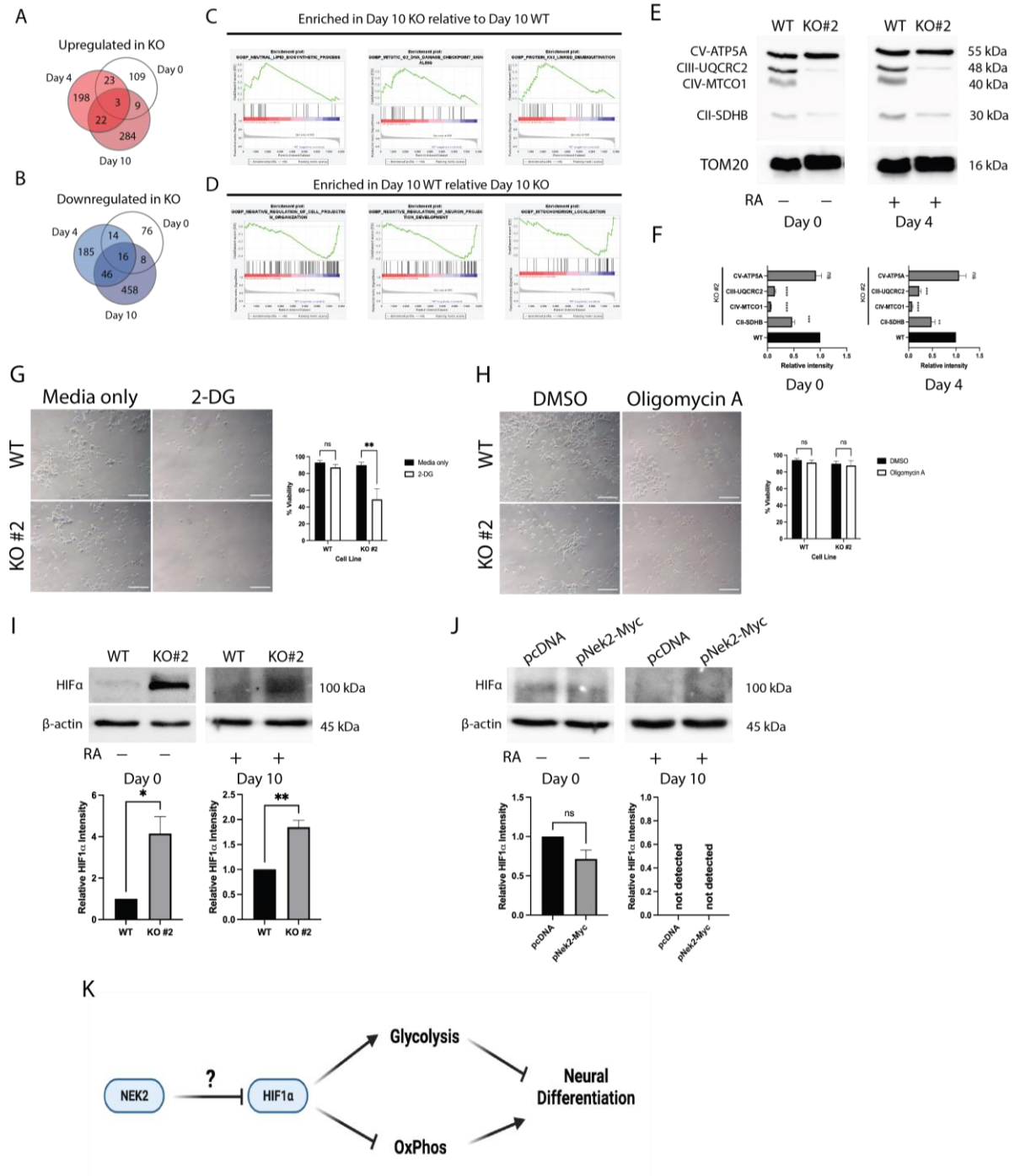


**Figure 3-15: Loss of Nek2 inhibits oxidative metabolism**

Proteins identified through LC-MS that are **(A)** upregulated and **(B)** downregulated in KO cells compared to WT cells at days 0, 4 and 10 of RA treatment. GSEA enrichment analysis of LC-MS results identifying pathways that are **(C)** enriched in KO cells compared to WT cells and **(D)** in WT cells compared to KO cells at day 10 of RA treatment. **(E)** Immunoblot of electron transport chain components, SDHB, MTCO1, UQCRC2 and ATP5A corresponding to subunits in complexes II-V, respectively, in WT and KO cells at days 0 and 4 of RA treatment. **(F)** Densitometry analysis of immunoblots in E. P-values were determined by One-way ANOVA with Tukey's post-hoc analysis. Phase contrast images and viability of cells determined through trypan blue exclusion in cells treated with **(G)** media only or 50 mM 2-DG, and **(H)** DMSO or 2.5  $\mu$ M oligomycin A for 24 hours. Scale bar = 200  $\mu$ m. P-values were determined by Two-way ANOVA with Sidak's post-hoc analysis. Immunoblot of HIF1 $\alpha$  in untreated and RA treated **(I)** WT and KO cells and **(J)** pcDNA and pNek2-Myc transfected cells. **(K)** Proposed mechanism of Nek2 action. Image created using BioRender. Bars represent mean values  $\pm$  s.e.m. **\*\*** $P < 0.01$ , **\*\*\*** $P < 0.001$ , **\*\*\*\*** $P < 0.0001$ .

### 3.3.8 Loss of Nek2 promotes glycolytic metabolism

Since most proteins negatively impacted in Nek2 KO cells involved complexes of the mitochondrial electron transport chain (ETC) and that WT cells compared to KO cells at day 10 had enriched proteins related to oxidative phosphorylation (OxPhos; Fig. 3-14), we wanted to test what metabolic pathway was being utilized in Nek2 KO cells.

Immunoblotting was used and like the LC-MS results, results showed KO cells at days 0 and 4 of RA treatment had reduced or absent ETC complexes II, III and IV (Fig. 3-15E and F). Furthermore, these cells were treated with either 50 mM 2-deoxy-D-glucose (2-DG) to inhibit glycolysis, or 2.5  $\mu$ M oligomycin A to inhibit OxPhos to determine if, compared to WT cells, they were reliant on one or the other metabolic pathways. Results showed WT cell viability was unaffected by either treatment (Fig. 3-15G and H, respectively) suggesting these cells likely have a bivalent metabolism in the undifferentiated state. However, 2-DG significantly reduced KO cell viability (Fig. 3-15H), implying these cells rely on glycolysis. As glycolytic genes are known to be upregulated in response to hypoxia-inducible factor 1 $\alpha$  (HIF1 $\alpha$ ) stabilization (Kierans and Taylor 2021), we explored HIF1 $\alpha$  levels in untreated, undifferentiated WT and KO cells (Fig. 3-15I) and in cells overexpressing *Nek2* (Fig. 3-15J). Under normoxic conditions, undifferentiated WT cells do not show HIF1 $\alpha$  stabilization at days 0 or 10 of RA treatment, whereas KO cells did show stabilization at these same timepoints (Fig. 3-15I). *Nek2* overexpressing cells showed very little HIF1 $\alpha$  stabilization at day 0 but was not different from pcDNA transfected controls at either timepoint (Fig. 3-15J). These results show that Nek2 is essential for maintaining ETC components and that the loss of Nek2 shifts P19 cells towards glycolysis and sustained HIF1 $\alpha$  stabilization (Fig. 3-15K).

### 3.4 Discussion

Nek2 has many roles within the cell and is involved in regulating centrosome dynamics, signaling pathways and metabolism, and although its importance is clear, few studies have explored this protein within normal development (Tanaka et al. 1997; Joseph Endicott et al. 2015a; Martins et al. 2017). We have shown that Nek2 is essential in the differentiation of both neurons and astrocytes in the P19 embryonal carcinoma model (Fig. 3-8 and 3-9) and previous reports have placed Nek2 as a regulator of the Hh and canonical Wnt pathways (Mbom et al. 2014; Cervenka et al. 2016; Lin et al. 2016; Wang et al. 2016; Zhou et al. 2017), which are required in this process (Schuurin et al. 1989; St-Arnaud et al. 1989; Papkoff 1994; Tang et al. 2002; Voronova et al. 2011; Spice et al. 2022) (Fig. 3-13). Towards that end, we sought to explore neural differentiation using the P19 model through the context of Wnt and Hh signaling, and although Nek2 appears to affect these pathways, the data did not indicate that their deregulation was the causative factor affecting neural differentiation. We did find that a reduced proliferative capacity of cells lacking Nek2 (Fig. 3-4 and 3-5) and a metabolic shift away from OxPhos towards exclusively glycolytic metabolism (Fig. 3-15) as the likely cause of this reduced differentiation potential when Nek2 is absent.

One of the main factors seeming to affect the differentiation of neurons and astrocytes was the reduced proliferative capacity of Nek2 KO cells. Without Nek2, undifferentiated cells had reduced numbers (Fig. 3-4) as did cells in EBs, where these EBs had reduced size and organization (Fig. 3-6) without altered cell viability or apoptosis (Fig. 3-5). Interestingly, the overexpression of *Nek2* resulted in the opposite phenotype, with increased proliferation in the undifferentiated state (Fig. 3-4) and reduced EB size, but increased EB number (Fig. 3-6). The loss of Nek2 was also reported to cause reduced proliferation in glioblastoma and medulloblastoma cell lines, however, this reduction was accompanied by increased apoptosis (Boulay et al. 2017; Xiang et al. 2022). Another report also observed the reduced ability of Nek2-depleted cells to form spheroids (similar to EBs) in a hepatocellular carcinoma cell line (Lin et al. 2016). This study by Lin et al. (Lin et al. 2016) also showed Wnt3a treatment resulted in an increase in spheroid number in *Nek2* expressing hepatocellular carcinoma cells, which parallels our results that

showed when *Nek2* was overexpressed it caused canonical Wnt signaling to be activated (Fig. 3-12) and an increased number of EB (Fig. 3-6). Despite the well-known phenomenon that pluripotent cells are highly proliferative (Liu et al. 2019), we were surprised that unlike hepatocellular carcinoma cells depleted of *Nek2* (Lin et al. 2016), our KO cells showed elevated pluripotency factors, *Nanog* and *ESRRB* (Fig. 3-7), and reduced proliferation rates (Fig. 3-4 and 3-5). These pluripotency factors were also reduced or absent when *Nek2* was overexpressed in P19 cells (Fig. 3-7), and this was accompanied by an increase in proliferation (Fig. 3-4). Despite the lack of information reported for *Nek2*, these differences in pluripotency and proliferation were noted but their significance remains unknown. A previous report in hESCs identified *Nek2* activity in the undifferentiated state and during early induction of differentiation (Van Hoof et al. 2009), which highlights that *Nek2* is likely playing a role, however the specifics of its role in pluripotency are unclear. Our results, with this previous report (Van Hoof et al. 2009), note *Nek2* is likely functioning earlier during the “decision-making” process involving pluripotency (Fig. 3-7) and/or cell fate determination that favors one lineage over the other (Fig. 3-8 and 3-9). Although we predicted the role of *Nek2* lay within regulation of Wnt or Hh, our results point to the regulation of pluripotency and the unlikelihood that *Nek2* in P19 cells is directly linked to Hh (Fig. 3-11) and/or canonical Wnt signaling (Fig. 3-12) in differentiation.

In addition to changes in pluripotency factors a proteomics approach revealed several proteins with differential enrichment in WT and KO cells and highlighted a reduction in mitochondrial ETC components in *Nek2* KO cells (Fig. 3-15). Further experiments, confirming these LC-MS results, showed that losing *Nek2* altered cellular metabolism, with KO cells becoming exclusively glycolytic (Fig 3-15). Experiments are underway using other cell lines to determine if *Nek2* KO influences cellular metabolism, especially in the light of the study by Zhou et al. (Zhou et al. 2021) who found in certain types of B-cell lymphomas that *Nek2* promotes proliferation but also glycolysis. We explored HIF1 $\alpha$  levels and results showed P19 cells lacking *Nek2* showed increased HIF1 $\alpha$  stabilization (Fig. 3-15I) and a concomitant reliance on glycolytic metabolism (Fig. 3-15G). The connection between metabolic changes and neural differentiation has been

reported in human induced pluripotent stem cell (hiPSC) derived neural precursors (NPCs) where there is a switch from aerobic glycolysis to OxPhos in neurons involving pyruvate kinase M1/2 (PKM) isoforms (Zheng et al. 2016). Given that Nek2 is also involved in PKM splicing (Gu et al. 2017; Zhou et al. 2021) and its loss causes P19 cells to become glycolytic (Fig. 3-15) and thus blocking neural differentiation (Fig. 3-8 and 3-9), it seems reasonable to propose its contribution in this process. HIF1 $\alpha$  has also been explored within neural differentiation where its overexpression in hiPSCs enhanced pluripotency and reduced neural differentiation (Cui et al. 2021), which was also observed in mESCs (Večeřa et al. 2017). Previous work with P19 cells has shown that there is a shift from glycolytic metabolism to OxPhos with RA induction and this promotes neuron differentiation (Vega-Naredo et al. 2014; Pashkovskaia et al. 2018). Interestingly, and in contrast to our proposed mechanism of cells grown under normoxic conditions (Fig. 3-15J), a previous report in P19 cells showed an increase in neuron differentiation under hypoxic conditions where HIF1 $\alpha$  was stabilized (Wu et al. 2008). Given our work, however, we have shown in P19 cells that altered metabolism and neural differentiation is the result of cells lacking Nek2, thus demonstrating an essential role for Nek2 in regulating this metabolic transition from glycolysis to OxPhos. Evidence would suggest the mechanism of Nek2 regulation likely involves HIF1 $\alpha$ , however the direct link between Nek2 and it remains to be established (Fig. 3-15J). These connections, in addition to the post-translational modifications Nek2 likely performs to promote or inhibit neural differentiation must be further examined and are currently under investigation.

### 3.5 References

- Boulay, G., Awad, M.E., Riggi, N., Archer, T.C., Iyer, S., Boonseng, W.E., Rossetti, N.E., Naigles, B., Rengarajan, S., Volorio, A., Kim, J.C., Mesirov, J.P., Tamayo, P., Pomeroy, S.L., Aryee, M.J., and Rivera, M.N. 2017. OTX2 activity at distal regulatory elements shapes the chromatin landscape of group 3 medulloblastoma. *Cancer Discov.* 7(3): 288–301. doi:10.1158/2159-8290.CD-16-0844.
- Briscoe, J., and Théron, P.P. 2013. The mechanisms of Hedgehog signalling and its roles in development and disease. *Nat. Rev. Mol. Cell Biol.* 14(7): 418–431. doi:10.1038/nrm3598.
- Cervenka, I., Valnohova, J., Bernatik, O., Harnos, J., Radsetoulal, M., Sedova, K., Hanakova, K., Potesil, D., Sedlackova, M., Salasova, A., Steinhart, Z., Angers, S., Schulte, G., Hampl, A., Zdrahal, Z., and Bryja, V. 2016. Dishevelled is a NEK2 kinase substrate controlling dynamics of centrosomal linker proteins. *Proc. Natl. Acad. Sci. U. S. A.* 113(33): 9304–9309. doi:10.1073/pnas.1608783113.
- Cliffe, A., Hamada, F., and Bienz, M. 2003. A role of Dishevelled in relocating Axin to the plasma membrane during Wingless signaling. *Curr. Biol.* 13: 960–966. doi:10.1016/S.
- Cui, P., Zhang, P., Yuan, L., Wang, L., Guo, X., Cui, G., Zhang, Y., Li, M., Zhang, X., Li, X., Yin, Y., and Yu, Z. 2021. HIF-1 $\alpha$  Affects the Neural Stem Cell Differentiation of Human Induced Pluripotent Stem Cells via MFN2-Mediated Wnt/ $\beta$ -Catenin Signaling. *Front. Cell Dev. Biol.* 9(June): 1–15. doi:10.3389/fcell.2021.671704.
- Dahmane, N., and Ruiz, A. 1999. Sonic hedgehog and cerebellum development. *Development* 3100: 3089–3100.
- Fry, A.M., O'Regan, L., Sabir, S.R., and Bayliss, R. 2012. Cell cycle regulation by the NEK family of protein kinases. *J. Cell Sci.* 125(19): 4423–4433. doi:10.1242/jcs.111195.
- Gatie, M.I., Cooper, T.T., Khazae, R., Lajoie, G.A., and Kelly, G.M. 2022. Lactate enhances mouse ES cell differentiation towards XEN cells in vitro. *Stem Cells: sxab022.* doi:10.1093/stmcls/sxab022.
- Gibbs, H.C., Chang-Gonzalez, A., Hwang, W., Yeh, A.T., and Lekven, A.C. 2017. Midbrain-Hindbrain Boundary Morphogenesis: At the Intersection of Wnt and Fgf Signaling. *Front. Neuroanat.* 11(August): 1–17. doi:10.3389/fnana.2017.00064.
- Gu, Z., Xia, J., Xu, H., Frech, I., Tricot, G., and Zhan, F. 2017. NEK2 promotes aerobic glycolysis in multiple myeloma through regulating splicing of pyruvate kinase. *J. Hematol. Oncol.* 10: 1–11. *Journal of Hematology & Oncology.* doi:10.1186/s13045-017-0392-4.
- Van Hoof, D., Muñoz, J., Braam, S.R., Pinkse, M.W.H., Linding, R., Heck, A.J.R., Mummery, C.L., and Krijgsveld, J. 2009. Phosphorylation Dynamics during Early



- Differentiation of Human Embryonic Stem Cells. *Cell Stem Cell* 5(2): 214–226. doi:10.1016/j.stem.2009.05.021.
- Huang, S.M.A., Mishina, Y.M., Liu, S., Cheung, A., Stegmeier, F., Michaud, G.A., Charlat, O., Wiellette, E., Zhang, Y., Wiessner, S., Hild, M., Shi, X., Wilson, C.J., Mickanin, C., Myer, V., Fazal, A., Tomlinson, R., Serluca, F., Shao, W., Cheng, H., Shultz, M., Rau, C., Schirle, M., Schlegl, J., Ghidelli, S., Fawell, S., Lu, C., Curtis, D., Kirschner, M.W., Lengauer, C., Finan, P.M., Tallarico, J.A., Bouwmeester, T., Porter, J.A., Bauer, A., and Cong, F. 2009. Tankyrase inhibition stabilizes axin and antagonizes Wnt signalling. *Nature* 461(7264): 614–620. Nature Publishing Group. doi:10.1038/nature08356.
- Hui, C., and Angers, S. 2011. Gli proteins in development and disease. *Annu. Rev. Cell Dev. Biol.* 27(1): 513–537. doi:10.1146/annurev-cellbio-092910-154048.
- Humke, E.W., Dorn, K. V., Milenkovic, L., Scott, M.P., and Rohatgi, R. 2010. The output of Hedgehog signaling is controlled by the dynamic association between Suppressor of Fused and the Gli proteins. *Genes Dev.* 24(7): 670–682. doi:10.1101/gad.1902910.
- Jones-Villeneuve, E.M., McBurney, M.W., Rogers, K.A., and Kalnins, V.I. 1982. Retinoic acid induces embryonal carcinoma cells to differentiate into neurons and glial cells. *J. Cell Biol.* 94(2): 253–262. doi:10.1083/jcb.94.2.253.
- Jones-Villeneuve, E.M., Rudnicki, M.A., Harris, J.F., and McBurney, M.W. 1983. Retinoic acid-induced neural differentiation of embryonal carcinoma cells. *Mol. Cell. Biol.* 3(12): 2271–2279. doi:10.1128/mcb.3.12.2271.
- Joseph Endicott, S., Basu, B., Khokha, M., and Brueckner, M. 2015a. The nima-like kinase nek2 is a key switch balancing cilia biogenesis and resorption in the development of left-right asymmetry. *Development* 142(23): 4068–4079. doi:10.1242/dev.126953.
- Joseph Endicott, S., Basu, B., Khokha, M., and Brueckner, M. 2015b. The nima-like kinase nek2 is a key switch balancing cilia biogenesis and resorption in the development of left-right asymmetry. *Dev.* 142(23): 4068–4079. doi:10.1242/dev.126953.
- Kierans, S.J., and Taylor, C.T. 2021. Regulation of glycolysis by the hypoxia-inducible factor (HIF): implications for cellular physiology. *J. Physiol.* 599(1): 23–37. doi:10.1113/JP280572.
- Kim, J.J., Gill, P.S., Rotin, L., van Eede, M., Henkelman, R.M., Hui, C.-C., and Rosenblum, N.D. 2011. Suppressor of Fused controls mid-hindbrain patterning and cerebellar morphogenesis via GLI3 repressor. *J. Neurosci.* 31(5): 1825–1836. doi:10.1523/JNEUROSCI.2166-10.2011.

- Kim, J.J., Jiwani, T., Erwood, S., Loree, J., and Rosenblum, N.D. 2018. Suppressor of fused controls cerebellar neuronal differentiation in a manner modulated by GLI3 repressor and Fgf15. *Dev. Dyn.* 247(1): 156–169. doi:10.1002/dvdy.24526.
- Kuljanin, M., Dieters-Castator, D.Z., Hess, D.A., Postovit, L.M., and Lajoie, G.A. 2017. Comparison of sample preparation techniques for large-scale proteomics. *Proteomics* 17(1–2): 1–2. doi:10.1002/pmic.201600337.
- Lendahl, U., Zimmerman, L.B., and McKay, R.D.G. 1990. CNS stem cells express a new class of intermediate filament protein. *Cell* 60(4): 585–595. doi:10.1016/0092-8674(90)90662-X.
- Lin, S., Zhou, S., Jiang, S., Liu, X., Wang, Y., Zheng, X., Zhou, H., Li, X., and Cai, X. 2016. NEK2 regulates stem-like properties and predicts poor prognosis in hepatocellular carcinoma. *Oncol. Rep.* 36(2): 853–862. doi:10.3892/or.2016.4896.
- Liu, H., Liu, B., Hou, X., Pang, B., Guo, P., Jiang, W., Ding, Q., Zhang, R., Xin, T., Guo, H., Xu, S., and Pang, Q. 2017. Overexpression of NIMA-related kinase 2 is associated with poor prognoses in malignant glioma. *J. Neurooncol.* 132(3): 409–417. Springer US. doi:10.1007/s11060-017-2401-4.
- Liu, L., Michowski, W., Kolodziejczyk, A., and Sicinski, P. 2019. The cell cycle in stem cell proliferation, pluripotency and differentiation. *Nat. Cell Biol.* 21(9): 1060–1067. Springer US. doi:10.1038/s41556-019-0384-4.
- Martins, T., Meghini, F., Florio, F., and Kimata, Y. 2017. The APC/C Coordinates Retinal Differentiation with G1 Arrest through the Nek2-Dependent Modulation of Wnt Signaling. *Dev. Cell* 40(1): 67–80. Elsevier Inc. doi:10.1016/j.devcel.2016.12.005.
- Mbom, B.C., Siemers, K.A., Ostrowski, M.A., Nelson, W.J., and Barth, A.I.M. 2014. Nek2 phosphorylates and stabilizes B-catenin at mitotic centrosomes downstream of Plk1. *Mol. Biol. Cell* 25(7): 977–991. doi:10.1091/mbc.E13-06-0349.
- McBurney, M. 1993. P19 embryonal carcinoma cells. *Int. J. Dev. Biol.* 140: 135–140.
- McBurney, M.W., Jones-Villeneuve, E.M.V., Edwards, M.K.S., and Anderson, P.J. 1982. Control of muscle and neuronal differentiation in a cultured embryonal carcinoma cell line. *Nature* 299(5879): 165–167. doi:10.1038/299165a0.
- McBurney, M.W., Reuhl, K.R., Ally, a I., Nasipuri, S., Bell, J.C., and Craig, J. 1988. Differentiation and maturation of embryonal carcinoma-derived neurons in cell culture. *J. Neurosci.* 8(3): 1063–73. Available from <http://www.ncbi.nlm.nih.gov/pubmed/2894413>.
- Min, T.H., Kriebel, M., Hou, S., and Pera, E.M. 2011. The dual regulator Sufu integrates Hedgehog and Wnt signals in the early *Xenopus* embryo. *Dev. Biol.* 358(1): 262–276. Elsevier Inc. doi:10.1016/j.ydbio.2011.07.035.

- Morshead, C.M., Reynolds, B.A., Craig, C.G., McBurney, M.W., Staines, W.A., Morassutti, D., Weiss, S., and van der Kooy, D. 1994. Neural stem cells in the adult mammalian forebrain: A relatively quiescent subpopulation of subependymal cells. *Neuron* 13(5): 1071–1082. doi:10.1016/0896-6273(94)90046-9.
- Mukherjee, A., Dhar, N., Stathos, M., Schaffer, D. V., and Kane, R.S. 2018. Understanding How Wnt Influences Destruction Complex Activity and  $\beta$ -Catenin Dynamics. *iScience* 6: 13–21. Elsevier Inc. doi:10.1016/j.isci.2018.07.007.
- Mulligan, K.A., and Cheyette, B.N.R. 2012. Wnt signaling in vertebrate neural development and function. *J. Neuroimmune Pharmacol.* 7(4): 774–787. doi:10.1007/s11481-012-9404-x.
- Neal, C.P., Fry, A.M., Moreman, C., McGregor, A., Garcea, G., Berry, D.P., and Manson, M.M. 2014. Overexpression of the Nek2 kinase in colorectal cancer correlates with beta-catenin relocalization and shortened cancer-specific survival. *J. Surg. Oncol.* 110(7): 828–838. doi:10.1002/jso.23717.
- Papkoff, J. 1994. Identification and biochemical characterization of secreted Wnt-1 protein from P19 embryonal carcinoma cells induced to differentiate along the neuroectodermal lineage. *Oncogene* 9(1): 313–317. England.
- Pashkovskaia, N., Gey, U., and Rödel, G. 2018. Mitochondrial ROS direct the differentiation of murine pluripotent P19 cells. *Stem Cell Res.* 30(June): 180–191. Elsevier. doi:10.1016/j.scr.2018.06.007.
- Ran, F.A., Hsu, P.D., Wright, J., Agarwala, V., Scott, D.A., and Zhang, F. 2013. Genome engineering using CRISPR-Cas9 system. *Nat. Protoc.* 8(11): 2281–2308. doi:10.1007/978-1-4939-1862-1\_10.
- Rohatgi, R., Milenkovic, L., and Scott, M.P. 2007. Patched1 regulates Hedgehog signaling at the primary cilium. *Science* (80-. ). 317(July): 372–377.
- Schuuring, E., van Deemter, L., Roelink, H., and Nusse, R. 1989. Transient expression of the proto-oncogene int-1 during differentiation of P19 embryonal carcinoma cells. *Mol. Cell. Biol.* 9(3): 1357–1361. doi:10.1128/mcb.9.3.1357-1361.1989.
- Sklirou, A.D., Gaboriaud-Kolar, N., Papassideri, I., Skaltsounis, A.L., and Trougakos, I.P. 2017. 6-bromo-indirubin-3'-oxime (6BIO), a Glycogen synthase kinase-3 $\beta$  inhibitor, activates cytoprotective cellular modules and suppresses cellular senescence-mediated biomolecular damage in human fibroblasts. *Sci. Rep.* 7(1): 1–13. Springer US. doi:10.1038/s41598-017-11662-7.
- Smolich, B.D., and Papkoff, J. 1994. Regulated Expression of Wnt Family Members during Neuroectodermal Differentiation of P19 Embryonal Carcinoma Cell:

Overexpression of Wnt-1 Perturbs Normal Differentiation-Specific Properties. *Dev. Biol.* 166: 300–310.

Spice, D.M., Dierolf, J., and Kelly, G.M. 2022. Suppressor of Fused regulation of Hedgehog Signaling is Required for Proper Astrocyte Differentiation. *bioRxiv*: 1–20. doi:10.1101/2021.08.24.457497.

St-Arnaud, R., Craig, J., McBurney, M.W., and Papkoff, J. 1989. The int-1 proto-oncogene is transcriptionally activated during neuroectodermal differentiation of P19 mouse embryonal carcinoma cells. *Oncogene* 4(9): 1077–1080. England.

Stamos, J.L., and Weis, W.I. 2013. The  $\beta$ -catenin destruction complex. *Cold Spring Harb. Perspect. Biol.* 5: a007898. doi:10.1101/cshperspect.a007898.

Steinhart, Z., and Angers, S. 2018. Wnt signaling in development and tissue homeostasis. *Development* 145(11): 1–8. doi:10.1242/dev.146589.

Suzuki, S., Namiki, J., Shibata, S., Mastuzaki, Y., and Okano, H. 2010. The neural stem/progenitor cell marker nestin is expressed in proliferative endothelial cells, but not in mature vasculature. *J. Histochem. Cytochem.* 58(8): 721–730. doi:10.1369/jhc.2010.955609.

Tanaka, K., Parvinen, M., and Nigg, E.A. 1997. The in vivo expression pattern of mouse Nek2, a NIMA-related kinase, indicates a role in both mitosis and meiosis. *Exp. Cell Res.* 237(2): 264–274. doi:10.1006/excr.1997.3788.

Tang, J.X., Chen, D., Deng, S.L., Li, J., Li, Y., Fu, Z., Wang, X.X., Zhang, Y., Chen, S.R., and Liu, Y.X. 2018. CRISPR/Cas9-mediated genome editing induces gene knockdown by altering the pre-mRNA splicing in mice. *BMC Biotechnol.* 18(1): 1–9. *BMC Biotechnology*. doi:10.1186/s12896-018-0472-8.

Tang, K., Yang, J., Gao, X., Wang, C., Liu, L., Kitani, H., Atsumi, T., and Jing, N. 2002. Wnt-1 promotes neuronal differentiation and inhibits gliogenesis in P19 cells. *Biochem. Biophys. Res. Commun.* 293(1): 167–173. doi:10.1016/S0006-291X(02)00215-2.

Tukachinsky, H., Lopez, L. V., and Salic, A. 2010. A mechanism for vertebrate Hedgehog signaling: Recruitment to cilia and dissociation of SuFu-Gli protein complexes. *J. Cell Biol.* 191(2): 415–428. doi:10.1083/jcb.201004108.

Večeřa, J., Kudová, J., Kučera, J., Kubala, L., and Pacherník, J. 2017. Neural differentiation is inhibited through HIF1  $\alpha$  /  $\beta$ -catenin signaling in embryoid bodies. *Stem Cells Int.* 2017. doi:10.1155/2017/8715798.

Vega-Naredo, I., Loureiro, R., Mesquita, K.A., Barbosa, I.A., Tavares, L.C., Branco, A.F., Erickson, J.R., Holy, J., Perkins, E.L., Carvalho, R.A., and Oliveira, P.J. 2014. Mitochondrial metabolism directs stemness and differentiation in P19 embryonal

carcinoma stem cells. *Cell Death Differ.* 21(10): 1560–1574. Nature Publishing Group. doi:10.1038/cdd.2014.66.

Voronova, A., Fischer, A., Ryan, T., Al Madhoun, A., and Skerjanc, I.S. 2011. *Ascl1/Mash1* is a novel target of *Gli2* during *Gli2*-induced neurogenesis in P19 EC cells. *PLoS One* 6(4). doi:10.1371/journal.pone.0019174.

Wang, Y., Li, Y., Hu, G., Huang, X., Rao, H., Xiong, X., Luo, Z., Lu, Q., and Luo, S. 2016. *Nek2A* phosphorylates and stabilizes *SuFu*: A new strategy of *Gli2*/Hedgehog signaling regulatory mechanism. *Cell. Signal.* 28(9): 1304–1313. Elsevier Inc. doi:10.1016/j.cellsig.2016.06.010.

Wilson, L., and Maden, M. 2005. The mechanisms of dorsoventral patterning in the vertebrate neural tube. *Dev. Biol.* 282: 1–13. doi:10.1016/j.ydbio.2005.02.027.

Wong, H.C., Bourdelas, A., Krauss, A., Lee, H.J., Shao, Y., Wu, D., Mlodzik, M., Shi, D.L., and Zheng, J. 2003. Direct binding of the PDZ domain of *Dishevelled* to a conserved internal sequence in the C-terminal region of *Frizzled*. *Mol. Cell* 12(5): 1251–1260. doi:10.1016/S1097-2765(03)00427-1.

Wu, L.Y., Wang, Y., Jin, B., Zhao, T., Wu, H.T., Wu, Y., Fan, M., Wang, X.M., and Zhu, L.L. 2008. The role of hypoxia in the differentiation of P19 embryonal carcinoma cells into dopaminergic neurons. *Neurochem. Res.* 33(10): 2118–2125. doi:10.1007/s11064-008-9728-3.

Xiang, J., Alafate, W., Wu, W., Wang, Y., Li, X., Xie, W., Bai, X., Li, R., Wang, M., and Wang, J. 2022. *NEK2* enhances malignancies of glioblastoma via *NIK/NF-κB* pathway. *Cell Death Dis.* 13(1): 1–13. Springer US. doi:10.1038/s41419-022-04512-6.

Yao, Y., Su, J., Zhao, L., Luo, N., Long, L., and Zhu, X. 2019. *NIMA*-related kinase 2 overexpression is associated with poor survival in cancer patients: A systematic review and meta-analysis. *Cancer Manag. Res.* 11: 455–465. doi:10.2147/CMAR.S188347.

Zheng, X., Boyer, L., Jin, M., Mertens, J., Kim, Y., Ma, L., Ma, L., Hamm, M., Gage, F.H., and Hunter, T. 2016. Metabolic reprogramming during neuronal differentiation from aerobic glycolysis to neuronal oxidative phosphorylation. *Elife* 5: e13374. doi:10.7554/eLife.13374.

Zhou, F., Huang, D., Li, Y., Hu, G., Rao, H., Lu, Q., Luo, S., and Wang, Y. 2017. *Nek2A/SuFu* feedback loop regulates *Gli*-mediated Hedgehog signaling pathway. *Int. J. Oncol.* 50(2): 373–380. doi:10.3892/ijo.2016.3819.

Zhou, L., Ding, L., Gong, Y., Zhao, J., Zhang, J., Mao, Z., Wang, Z., Zhang, W., and Zhou, R. 2021. *NEK2* Promotes Cell Proliferation and Glycolysis by Regulating *PKM2* Abundance via Phosphorylation in Diffuse Large B-Cell Lymphoma. *Front. Oncol.* 11(June): 1–15. doi:10.3389/fonc.2021.677763.

## Chapter 4

### 4 Discussion & Conclusions

#### 4.1 Summary of Key Findings

Neural development and differentiation require many signaling pathways and protein interactions to give rise to the distinct cell types of the central nervous system. Hh and Wnt signaling are two of the pathways that regulate this process, however, each pathway has many unique and overlapping players that act to regulate transcriptional output. Included in this group are SUFU and Nek2, which have distinct roles in neural differentiation, but their function(s) are not entirely understood or have never been explored. Within this work I hypothesized that if Hh and Wnt signaling are required in the RA-induced differentiation of P19 embryonal carcinoma cells, then loss of function of either SUFU or Nek2 would disrupt the regulation of these signaling pathways and block the differentiation of neural lineages.

In Chapter 2, I determined the timing of Hh signaling activity in P19 cells and sought to establish if Hh signaling is sufficient to induce differentiation and whether genetic ablation of SUFU would block differentiation. Through the investigation of *Gli1* target gene expression and the Gli3 full-length to repressor ratio, I determined that Hh signaling increases its activity one day after RA induction before returning to basal levels. Thus, Hh signaling is temporally regulated during P19 neural differentiation. To test if this activity is required for differentiation, I used a chemical activator and an inhibitor of the Smo transmembrane protein, that when active transduces the Hh signal. Co-treatment of P19 cells with RA and SAG, the activator, increased the differentiation of both neurons and astrocytes. However, SAG treatment alone was not sufficient to induce robust differentiation of either cell type. Conversely, co-treatment of cells with RA and the inhibitor, Cyc, reduced differentiation of neurons and blocked the formation of astrocytes. These results confirmed that Hh signaling is required to induce neural differentiation, however, Hh activity alone was not sufficient. The genetic loss of function in the *Sufu* gene using CRISPR provided evidence that the reduction of Hh signaling after neural induction was required. These experiments confirmed SUFU as a

negative regulator of the Hh pathway and SUFU loss increased Hh target gene expression throughout RA-induced differentiation. In fact, this increased target gene expression was linked to the loss of the Gli3 transcription factor, a negative transcriptional regulator (Altaba 1998; Bai et al. 2002; Buttitta et al. 2003; Motoyama et al. 2003). The loss of SUFU, and subsequent loss of Gli3 corresponding to the overactivity of Hh target gene expression, resulted in delayed and decreased astrocyte differentiation. However, this did not affect neuron differentiation. Given this data I concluded that Hh is required for neural differentiation, and at later stages the reduction of Hh signaling is also required for the proper timing and proportion of astrocyte differentiation.

Nek2 is another negative regulator of Hh signaling (Wang et al. 2016; Zhou et al. 2017). However, this protein has not been well studied in neural development. Nek2 regulates Hh signaling through SUFU (Wang et al. 2016) and given my discovery that SUFU is key in neural differentiation of P19 cells (Chapter 2), I predicted removing Nek2 using CRISPR would have similar effects (Chapter 3). Nek2, however, is also a positive regulator of canonical Wnt signaling (Mbom et al. 2014; Cervenka et al. 2016), a pathway required for neural differentiation of P19 cells. The presence and expression of Nek2 was confirmed in P19 cells, and in addition to the CRISPR studies, I used plasmid vectors to overexpress human *Nek2* in these cells. Changes in proliferation were identified as a major determinant from these studies, where loss of Nek2 reduced proliferation while overexpression had a profound increase that translated into changes in embryoid body formation. Given these changes, I explored if pluripotency genes were affected and surprisingly found that the loss of *Nek2* corresponded to an increase in the abundance of pluripotency markers; *Nek2* overexpressing cells showed reduced expression. Hh and Wnt target gene expression was also explored in *Nek2*<sup>-/-</sup> cells and although there were changes in Hh target gene expression, they were inconsistent and did not reveal a clear connection between Nek2 and Hh signaling. Wnt target genes showed similar inconsistencies in Nek2-deficient cells but were consistently upregulated in *Nek2* overexpressing cells. These same cells showed enhanced neuron differentiation at the expense of astrocytes, while P19 cells treated with XAV and expected to show little to no Wnt target gene expression, also showed reduced astrocyte differentiation. This data confirmed Nek2 as a positive regulator of Wnt signaling in neural differentiation. It is

interesting to note, cells lacking Nek2 did not differentiate into neurons or astrocytes, although they did express *Nestin*, a neural precursor marker. Since the results with Nek2 and Hh or Wnt signaling were confusing, I pursued a proteomics approach to examine the large-scale changes in protein abundance that exist between wildtype and *Nek2*<sup>-/-</sup> cells. These data suggested Nek2 in P19 cells is involved in the regulation of cellular metabolism and I determined that cells deficient of Nek2 caused the loss of mitochondrial electron transport chain components. Given these metabolic changes I also explored HIF1 $\alpha$ , where levels of this protein were found to increase in Nek2-deficient cells. Together, these data suggested a model of Nek2 regulation of differentiation, where through a currently unknown mechanism, Nek2 promotes the destabilization of HIF1 $\alpha$  and allows cells during later stages of differentiation to transition from a primarily glycolytic metabolism to oxidative phosphorylation. Although this process is required for neural differentiation, it may be more a general phenomenon in cells requiring this transition during lineage specification.

The presented work, shown as a model in Figure 4-1, confirms the requirement of both Hh and Wnt signaling in neural differentiation, and I have shown that SUFU, a negative regulator of Hh signaling, is essentially linked to the process. Furthermore, my data suggests Nek2 does not act as a regulator of the Hh signaling pathway. Instead, Nek2 acts much earlier, on metabolism and a model is presented that the protein is required for the transition of cells using glycolysis to ones using oxidative phosphorylation to generate ATP. Together, and despite cell specification and neural development having been extensively explored, this work provides evidence that the role of specific regulators of signaling, and metabolism are intricately linked in developing cells.



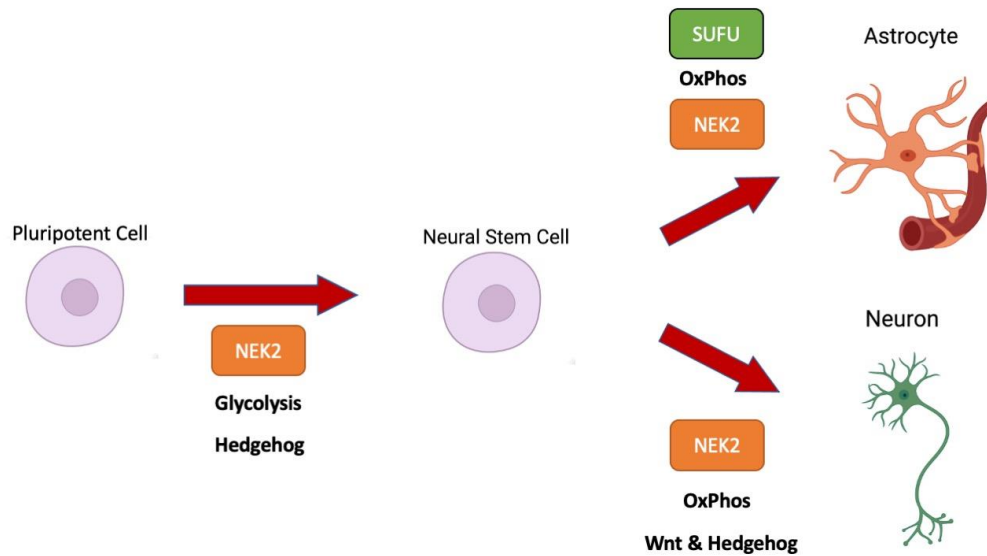


**Figure 4-1: Model for the role of SUFU and Nek2 in P19 neural differentiation**

In the process of a cell exiting pluripotency and becoming a neural stem cell, Hh signaling is activated early in this process (Chapter 2). Nek2 plays a role in this process by promoting the exit from pluripotency, while cells can become neural stem cells while being using exclusively glycolytic metabolism (Chapter 3). Neurons can differentiate in the presence of overactive Hh signaling (Chapter 2) and overactive Wnt signaling promotes neuron differentiation (Chapter 3). SUFU is required to return Hh signaling to basal levels to facilitate astrocyte differentiation (Chapter 2). Nek2 is required for the differentiation of both neurons and astrocytes to facilitate the switch from glycolysis to OxPhos (Chapter 3).

## 4.2 Discussion & Significance

### 4.2.1 Stem cell models of neural differentiation

The embryonal carcinoma cell line, mouse P19, was used in this work as an easy to manipulate model to study the molecular mechanisms of neural differentiation in vitro. Like P19 cells, embryonic stem cells (ESCs), cells derived from the inner cell mass of a blastocyst (Evans and Kaufman 1981), can also undergo neural differentiation. Initial and subsequent studies of ESC neural differentiation, like P19 cells, relied on cell aggregation in the presence of RA (Bain et al. 1995), however, some later protocols have been established to derive neural lineages in the absence of both aggregation and RA using specific serum-free media conditions (Ying et al. 2003; Abranches et al. 2009). Although these later protocols are in monolayer conditions, tight cell clustering is still required for neural induction of ESCs as the cells in these studies must form rosettes for differentiation to occur (Ying et al. 2003; Abranches et al. 2009). Interestingly, the neuroectodermal cell fate appears to be the default program in ESCs as simply the removal of Leukemia Inhibitory Factor (LIF), a chemical required to maintain ESCs in their pluripotent state (Silva et al. 2008; Wulansari et al. 2021), is sufficient to form rosettes and neural progenitors (Ying et al. 2003). Not only can ESCs be used to derive immature neurons and glial cells, but they can also be directed towards specific types of neurons from various brain regions. P19 cell differentiation allows for a heterogeneous mixture of undirected neuron differentiation in the presence of RA, whereas human ESCs (hESCs) and mouse ESCs (mESCs) can be induced to form midbrain dopaminergic neurons (Kawasaki et al. 2000; Perrier et al. 2004), motor neurons (Hu and Zhang 2010), cortical neurons (Gaspard et al. 2009), and GABAergic neurons (Gonzalez-Ramos et al. 2021) more homogeneously under specific culture conditions. Given the relative homogeneity of ESC neural differentiation conditions, ESCs have been used to study the role of histone regulation and epigenetics (Golebiewska et al. 2009; Yao et al. 2018), extracellular matrix components (Hashemi et al. 2013), and mitochondrial electron transport (Pereira et al. 2013) in neural differentiation. ESCs have also been used to explore how environmental toxins affect neural differentiation (He et al. 2012; Shan et al.

2021) and have provided a means to link basic biology with biotechnology (Kabiri et al. 2012). Similarities exist between the presented data using P19 cells and ESCs, as hESCs increase expression of Hh ligands with neural induction (Wu et al. 2010) and exogenous SHH similarly increases neural differentiation (Fraichard et al. 1995; Mak et al. 2012). Conversely, Hoelzl and colleagues derived mESCs carrying a Sufu knockout and showed no reported changes to the ectodermal lineage (Hoelzl et al. 2015), however specific markers for neural cell types were not explored. Additionally, ESC studies form the basis of understanding the metabolic switch from glycolysis to OxPhos during neuron differentiation (Zheng et al. 2016) and shows similar connections to HIF1 $\alpha$  overexpression and reduced neuron differentiation (Cui et al. 2021). Although ESC models are likely to continue to hold a prominent position in the future of studying neural differentiation, there will remain a place for embryonal carcinoma cells as they require fewer reagents and are less costly to maintain (Jones-Villeneuve et al. 1982; Witteveldt and Macias 2019). For example, P19 cells can be cultured in standard cell culture media and maintain their pluripotency, while mESCs require Wnt and MAPK inhibitors in addition to being cultured in LIF containing media (Witteveldt and Macias 2019). Using P19 cells as a launch point for early investigations into molecular mechanisms of neural differentiation, as they were used for my work, is essential for many labs before translating that work into more costly ESC or in vivo mouse models.

#### 4.2.2 SUFU is required to regulate Hh signaling during astrocyte differentiation

Hh signaling is known to play an important role in neuron and glial cell differentiation (Chiang et al. 1996; Ericson et al. 1996, 1997; Litingtung and Chiang 2000) and SUFU, acting as a negative regulator of signaling, is also required (Spice et al., 2022). SUFU acts to promote the phosphorylation of Gli3 (Kise et al. 2009), the primary transcriptional repressor of the Hh pathway (Altaba 1998; Bai et al. 2002; Buttitta et al. 2003; Motoyama et al. 2003). In my thesis I showed the essential role of SUFU in astrocyte differentiation, specifically its regulation of Gli3 (Chapter 2). In the absence of SUFU, I showed that the full-length and repressor forms of Gli3 were reduced or lost, and Hh

target gene expression was elevated (Chapter 2). This observation is supported by other *in vitro* models and in the developing mouse brain where *Sufu*<sup>-/-</sup> caused a reduction in Gli3 and overactivation of Hh signaling (Chen et al. 2009; Kim et al. 2011, 2018; Makino et al. 2015; Yabut et al. 2015; Jiwani et al. 2020).

Temporal regulation of Hh signaling is key to the proper timing and number of differentiated cell types (Agius et al. 2004; Ribes and Briscoe 2009). I demonstrated that Hh pathway activity is regulated temporally in the P19 model, where SUFU loss of function disrupted this regulation (Chapter 2). The constitutive overexpression of Hh target genes in SUFU-deficient cells did not affect the number of neurons (Chapter 2), which was unexpected as I and others have shown that exogenous SHH or SAG treatment increases neuron formation (Chapter 2) (Okada et al. 2004; Mak et al. 2012; Wu et al. 2012). It is interesting to note that the loss of *Sufu* in the adult or developing mouse brain results in decreased neuron differentiation (Yabut et al. 2015; Kim et al. 2018). Thus, SUFU likely plays multiple roles within the cell during neuron differentiation and more work is needed to completely understand its role. Similarly, additional studies are required to explore the intracellular localization and protein-interaction partners of SUFU in normal neuron differentiation. SUFU has many reported interacting proteins (Paces-Fessy et al. 2004) and posttranslational modifications can promote or inhibit Gli interactions (Takenaka et al. 2007; Chen et al. 2011; Wang et al. 2016; Infante et al. 2018).

The major finding of Chapter 2 was the reduced and delayed differentiation of astrocytes corresponding to overactive Hh signaling caused by SUFU loss. Astrocyte differentiation is regulated by Hh signaling by specifying astrocyte progenitors, but Hh activity needs to be reduced to facilitate terminal astrocyte differentiation. In chick spinal cord explants, exogenous SHH treatment reduces GFAP-positive astrocytes (Agius et al. 2004), while glial progenitors increase (Li et al. 2019). These results are supported by *Smo*<sup>-/-</sup> in the adult mouse forebrain, which causes increased GFAP levels (Garcia et al. 2010). In this same study the number of S100 $\beta$  expressing astrocytes was unaffected (Garcia et al. 2010), like the expression pattern of *S100 $\beta$ I* observed in SUFU-deficient cells (Chapter 2). The study by Garcia et al. 2010, like mine, suggest that SUFU is only required for the

detection and differentiation of GFAP-positive astrocytes. In contrast, SHH increased astrocyte differentiation of NG2 progenitor cells in the adult mouse brain after focal cerebral ischemia (Honsa et al. 2016). These differences, however, are likely due to the injury rather than normal development. If SUFU-deficient cells are not properly differentiating as astrocytes, and are still differentiating into neurons, what are the remaining cell types in the dish? Although not explored in the presented work, I can envision these cells are either blocked as astrocyte precursors or are being converted to oligodendrocyte precursor cells. Active Shh signaling is reported in astrocyte precursor cells (Yu et al. 2013) and exogenous SHH treatment of mature astrocytes during reprogramming to a precursor phenotype enhances this efficiency (Yang et al. 2019). Hh signaling also promotes oligodendrocyte differentiation in the telencephalon (Tekki-Kessarlis et al. 2001) and in primary oligodendrocyte progenitor cultures (Wang and Almazan 2016), where loss of *Sufu* promotes terminal oligodendrocyte differentiation through overactive Hh signaling (Winkler et al. 2018). More support for the prediction that SUFU-deficient P19 cells are committing to the oligodendrocyte lineage comes from Pozniak and colleagues, who show that Sox10 directly binds the promoter region of *Sufu* to block its expression and promote oligodendrocyte precursor specification (Pozniak et al. 2010). These reports underscore the idea that more work will be required in P19 cells to determine if astrocyte differentiation is impaired when SUFU is deficient and if this leads to an increase in the oligodendrocyte progenitor pool. Another possibility to explain the observed reduced astrocyte differentiation in SUFU-deficient cells could lie outside of the neural lineage. P19 cells are a heterogeneous mixture of neural cells and uncharacterized fibroblast-like cells following RA treatment (Jones-Villeneuve et al. 1983), where it remains a possibility that the SUFU-deficient cells could more readily become this uncharacterized cell type. Additionally, SUFU loss may be affecting neuroglial progenitor cell-cell communication. It is reported that differentiated neurons secrete factors that affect the timing of gliogenesis (Barnabé-Heider et al. 2005), thus it is also possible that although the loss of SUFU did not alter neuron differentiation it may have altered the proteins secreted by neurons which could alter astrocyte differentiation. This cell-cell communication would also be impacted by the types of neurons being differentiated with SUFU knockout, an avenue of investigation that was not explored in

the presented work. Given the heterogeneity of RA induced P19 neural differentiation, the model I describe to explain these presented data is but one possibility, and more work should be done to determine if the loss of SUFU is causing changes to the potential or identity of the glial progenitor pool, or if the neurons are driving the reported changes. Although the role of SUFU has been extensively studied in neural development, my work places SUFU as an essential regulator of oligodendrocyte and astrocyte differentiation.

### 4.2.3 Nek2 regulates metabolism during neural specification

Regulation of metabolism is intricately linked to pluripotency and cell differentiation. Pluripotent ESC and embryonal carcinoma cell lines use glycolysis or are bivalent, showing both glycolytic and oxygen-dependent metabolisms, to generate energy (Vega-Naredo et al. 2014; Gu et al. 2016; Shyh-Chang and Ng 2017; Pashkovskaia et al. 2018; Spice et al. 2022). It is generally accepted that the loss of pluripotency and the induction of a terminally differentiated fate coincides with a switch from either a glycolytic or bivalent metabolism to one using exclusively oxidative phosphorylation (OxPhos) (Gu et al. 2016; Shyh-Chang and Ng 2017). This holds true during neuron differentiation, where hiPSC derived neural precursors switch from aerobic glycolysis to OxPhos during terminal neuron differentiation (Zheng et al. 2016). This metabolic shift is also seen in P19 cells, where promoting OxPhos increases neuron differentiation, while inhibiting it reduces the number of neurons (Vega-Naredo et al. 2014; Pashkovskaia et al. 2018). Metabolism plays many roles in regulating differentiation by altering the presence of metabolites, such as lactate (Gatie et al. 2022), which can act as signaling molecules. Manipulating the levels of reactive oxygen species in the cell (Bigarella et al. 2014), and the availability of epigenetic modifying molecules generated through metabolic processes, can alter transcriptional output that influences cell fate and differentiation (Harvey et al. 2019). I showed that ablating *Nek2*, a known cell cycle regulator (Fry 2002; Rellos et al. 2007; Cervenka et al. 2016; Sahota et al. 2018), and Hh signaling modulator (Wang et al. 2016; Zhou et al. 2017), in P19 embryonal carcinoma cells caused them to rely on aerobic glycolysis and to lose the expression of mitochondrial electron transport chain components (Chapter 3). These cells also lost the ability to differentiate to neuron or astrocyte lineages, but were still expressing a neural precursor

marker, *Nestin* (Chapter 3). Previous reports with P19 cells exploring metabolism only reported on the effect of OxPhos inhibition on neuron differentiation (Vega-Naredo et al. 2014; Pashkovskaia et al. 2018), where I propose blocking OxPhos also inhibits astrocyte differentiation (Chapter 3). Given mature astrocytes are primarily glycolytic (Rose et al. 2020), it is possible these cells require a transient switch to OxPhos, but also may point to an essential neuron-astrocyte precursor communication link. The Nek2-mutant cell reliance on glycolysis is likely blocking neuron differentiation, while the loss of neurons may be causing the loss of astrocyte differentiation through the loss of currently unknown signaling molecule(s) secreted from terminally differentiated neurons. These questions were not further explored in this work, but I did explore a potential link between glycolysis and Nek2 through HIF1 $\alpha$ , a known activator of glycolytic gene expression (Sharp and Bernaudin 2004).

Under normoxic conditions HIF1 $\alpha$  is constitutively expressed but is rapidly degraded by the proteasome (Sharp and Bernaudin 2004; Cunningham et al. 2012). The destabilization of HIF1 $\alpha$  is usually performed by hydroxylases (Cunningham et al. 2012), however, it can also be performed by kinases (Mennerich et al. 2014), including GSK3 $\beta$ . The activity of GSK3 $\beta$  has been reported to reduce HIF1 $\alpha$  stabilization in COS7 cells, ovarian cancer cells and hepatocellular carcinoma cells (Sodhi et al. 2001; Flügel et al. 2007; Cassavaugh et al. 2011). Toward that end, I proposed a mechanism in P19 cells whereby Nek2 promotes destabilization of HIF1 $\alpha$ , causing OxPhos genes to increase their expression and promote the transition from neural precursors to neurons and astrocytes (Chapter 3). Although the direct link between Nek2 and HIF1 $\alpha$  has yet to be established, the GSK3 $\beta$  data suggests that Nek2 may directly or indirectly be involved with this process. GSK3 $\beta$  can also phosphorylate SUFU (Chen et al. 2011), like Nek2 (Wang et al. 2016). Thus, HIF1 $\alpha$  may be another shared target of these kinases and a decrease in Nek2 activity (or as evident by the loss of Nek2, this study), would promote HIF1 $\alpha$  stabilization. HIF1 $\alpha$  stabilization was found to accompany pluripotency in these cells and neural differentiation, occurring after neural precursor induction, is inhibited (Chapter 3). In support, embryonic and adult neural stem cells are reliant on glycolysis over OxPhos (Candelario et al. 2013), and there is stabilization of HIF1 $\alpha$  (Panchision

2009; Li et al. 2014; Zhao et al. 2014). In addition, HIF1 $\alpha$  loss of function in the mouse brain also causes reduced neural differentiation, which is directly linked to a reduced neuronal precursor pool (Tomita et al. 2003; Li et al. 2014). Although the link between Hh and Wnt signaling pathways and Nek2 showed no clear connection (Chapter 3), players in Notch signaling may be involved. Gustafsson et al. (2005) reported HIF1 $\alpha$  directly interacts with the intracellular domain of the cleaved Notch receptor to promote the expression of stem-related genes. Thus, I propose in P19 cells the loss of Nek2 function accompanied by HIF1 $\alpha$  stabilization, leads to the latter interacting with active Notch to promote the increase in pluripotency markers (Chapter 3) and inhibit neural differentiation (Panchision 2009). No evidence currently exists showing this interaction in P19 cells, but it is possible, and testing is required. Another connection between Nek2 and HIF1 $\alpha$  exists at the level of PKM2, pyruvate kinase M2. Nek2 is reported to regulate the PKM1 to PKM2 splicing switch (Gu et al. 2017; Zhou et al. 2021), while HIF1 $\alpha$  is reported to bind PKM2 to promote HIF1 $\alpha$  related transcription (Semenza 2011). The role of Nek2 within neural differentiation, pluripotency and regulation of metabolism is still unclear, however this work provides numerous platforms for future studies.

### 4.3 Limitations & Future Directions

The presented work confirms the role of Hh and Wnt signaling in neural differentiation and highlights new roles for SUFU in astrocyte differentiation, and Nek2 in neuron and astrocyte differentiation. The P19 cell model used to explore these questions, has its benefits and they have been previously discussed, but they are not stem cells per se and therefore not completely reminiscent of the embryo. Exploring neural differentiation and applying these same questions in human and/or mouse ESC will be necessary to fully appreciate the role of these protein regulators during development. Despite the extensive body of work that has already been reported for SUFU in P19 and ESCs (Wu 2010; Voronova et al. 2011; Hoelzl et al. 2015), much remains about the post-translational modifications and subcellular localization of SUFU during differentiation. Conversely, Nek2 has not been reported in mammalian neural differentiation, and this future work in ESC lines is required to corroborate my initial studies. Another limitation of the presented work, and a limitation with all cell lines, is the reduced complexity compared



to the embryo. Three-dimensional culture is partially replicated in this work as cells are required to be cultured as embryoid bodies for differentiation to occur (Jones-Villeneuve et al. 1982). Although organoids are a better *in vitro* system for studying neural differentiation within a 3D context, they too have limitations. Although not ideal, the packaging of P19 cells into embryoid bodies, and not in the embryo itself, likely recapitulates enough 3D complexity to create conditions required for transient stabilization of HIF1 $\alpha$  in neural progenitors (Panchision 2009; Li et al. 2014; Zhao et al. 2014).

The stabilization of HIF1 $\alpha$  in Nek2-deficient cells (Chapter 3) was an exciting discovery, as it linked the observed changes in metabolism to a known metabolic regulator. Nek2 was reported as a regulator of centrosome dynamics (Fry 2002; Rellos et al. 2007; Cervenka et al. 2016; Sahota et al. 2018); however, I have shown its involvement in regulating neural differentiation through metabolism (Chapter 3). Others have linked Nek2 to metabolism through PKM1/2 splicing (Gu et al. 2017; Zhou et al. 2021), but whether Nek2 directly interacts with HIF1 $\alpha$  remains to be determined. Loss of Nek2 also caused a reduction in electron transport chain components (Chapter 3) and although HIF1 $\alpha$  may be involved in these changes, the exact mechanism involving Nek2 remains unknown. Chromatin-immunoprecipitation studies of HIF1 $\alpha$  in Nek2-deficient cells must be undertaken to determine if this protein is regulating the expression of the electron transport chain subunits. Additionally, the proteomic data presented in Chapter 3 show multiple pathways are enriched in Nek2 deficient cells and these must be explored. Together, establishing a Nek2 interactome would be ideal to better understand the various roles of this protein. The strategy used in this thesis was based on the literature, and experiments were designed to explore Nek2 and its relation to Wnt and Hh signaling. Unfortunately, the results showed no connections between these pathways and the Nek2 protein, and I would suggest that co-immunoprecipitation studies, followed by mass spectrometry, must also be performed to provide an understanding of the proteins that interact with Nek2.

Neural differentiation has been studied now for decades, however, there is still much that is unknown about the signaling pathways and proteins that govern this process. Although

my work has limitations and proposes new questions that have yet to be answered, it nevertheless provides us with a better understanding of the complex processes required to specify neural cell types.

## 4.4 References

- Abranches, E., Silva, M., Pradier, L., Schulz, H., Hummel, O., Henrique, D., and Bekman, E. 2009. Neural differentiation of embryonic stem cells in vitro: A road map to neurogenesis in the embryo. *PLoS One* 4(7): e6286. doi:10.1371/journal.pone.0006286.
- Agius, E., Soukkaie, C., Danesin, C., Kan, P., Takebayashi, H., Soula, C., and Cochard, P. 2004. Converse control of oligodendrocyte and astrocyte lineage development by Sonic hedgehog in the chick spinal cord. *Dev Biol* 270(2): 308–321. doi:10.1016/j.ydbio.2004.02.015.
- Altaba, A.R.I. 1998. Combinatorial Gli gene function in floor plate and neuronal inductions by Sonic hedgehog. *Development* 125(12): 2203–2212.
- Bai, C.B., Auerbach, W., Lee, J.S., Stephen, D., and Joyner, A.L. 2002. Gli2, but not Gli1, is required for initial Shh signaling and ectopic activation of the Shh pathway. *Development* 129: 4753–4761.
- Bain, G., Kitchens, D., Yao, M., Huettner, J.E., and Gottlieb, D.I. 1995. Embryonic stem cells express neuronal properties in vitro. doi:10.1006/dbio.1995.1085.
- Barnabé-Heider, F., Wasylnka, J.A., Fernandes, K.J.L., Porsche, C., Sendtner, M., Kaplan, D.R., and Miller, F.D. 2005. Evidence that embryonic neurons regulate the onset of cortical gliogenesis via cardiotrophin-1. *Neuron* 48(2): 253–265. doi:10.1016/j.neuron.2005.08.037.
- Bigarella, C.L., Liang, R., and Ghaffari, S. 2014. Stem cells and the impact of ROS signaling. *Development* 141(22): 4206–4218. doi:10.1242/dev.107086.
- Buttitta, L., Mo, R., Hui, C.C., and Fan, C.M. 2003. Interplays of Gli2 and Gli3 and their requirement in mediating Shh-dependent sclerotome induction. *Development* 130(25): 6233–6243. doi:10.1242/dev.00851.
- Candelario, K.M., Shuttleworth, C.W., and Cunningham, L.A. 2013. Neural stem/progenitor cells display a low requirement for oxidative metabolism independent of hypoxia inducible factor-1 $\alpha$  expression. *J Neurochem* 125(3): 420–429. doi:10.1111/jnc.12204.
- Cassavaugh, J.M., Hale, S.A., Wellman, T.L., Howe, A.K., Wong, C., and Lounsbury, K.M. 2011. Negative regulation of HIF-1 $\alpha$  by an FBW7-mediated degradation pathway during hypoxia. *J Cell Biochem* 112(12): 3882–3890. doi:10.1002/jcb.23321.
- Cervenka, I., Valnohova, J., Bernatik, O., Harnos, J., Radsetoulal, M., Sedova, K., Hanakova, K., Potesil, D., Sedlackova, M., Salasova, A., Steinhart, Z., Angers, S., Schulte, G., Hampl, A., Zdrahal, Z., and Bryja, V. 2016. Dishevelled is a NEK2 kinase substrate controlling dynamics of centrosomal linker proteins. *Proc Natl Acad Sci U S A* 113(33): 9304–9309. doi:10.1073/pnas.1608783113.

- Chen, M.H., Wilson, C.W., Li, Y.J., Law, K.K. Lo, Lu, C.S., Gacayan, R., Zhang, X., Hui, C.C., and Chuang, P.T. 2009. Cilium-independent regulation of Gli protein function by Sufu in Hedgehog signaling is evolutionarily conserved. *Genes Dev* 23(16): 1910–1928. doi:10.1101/gad.1794109.
- Chen, Y., Yue, S., Xie, L., Pu, X.H., Jin, T., and Cheng, S.Y. 2011. Dual phosphorylation of suppressor of fused (Sufu) by PKA and GSK3 $\beta$  regulates its stability and localization in the primary cilium. *Journal of Biological Chemistry* 286(15): 13502–13511. doi:10.1074/jbc.M110.217604.
- Chiang, C., Litingtung, Y., Lee, E., Young, K.E., Corden, J.L., Westphal, H., and Beachy, P.A. 1996. Cyclopia and defective axial patterning in mice lacking Sonic hedgehog gene function. *Nature* 383: 407–413.
- Cui, P., Zhang, P., Yuan, L., Wang, L., Guo, X., Cui, G., Zhang, Y., Li, M., Zhang, X., Li, X., Yin, Y., and Yu, Z. 2021. HIF-1 $\alpha$  Affects the Neural Stem Cell Differentiation of Human Induced Pluripotent Stem Cells via MFN2-Mediated Wnt/ $\beta$ -Catenin Signaling. *Front Cell Dev Biol* 9(June): 1–15. doi:10.3389/fcell.2021.671704.
- Cunningham, L.A., Candelario, K., and Li, L. 2012. Roles for HIF-1 $\alpha$  in neural stem cell function and the regenerative response to stroke. *Behavioural Brain Research* 227(2): 410–417. doi:10.1016/j.bbr.2011.08.002.
- Ericson, J., Morton, S., Kawakami, A., Roelink, H., and Jessell, T.M. 1996. Two critical periods of Sonic Hedgehog signaling required for the specification of motor neuron identity. *Cell* 87(4): 661–673. doi:10.1016/S0092-8674(00)81386-0.
- Ericson, J., Rashbass, P., Schedl, A., Brenner-Morton, S., Kawakami, A., Van Heyningen, V., Jessell, T.M., and Briscoe, J. 1997. Pax6 controls progenitor cell identity and neuronal fate in response to graded Shh signaling. *Cell* 90(1): 169–180. doi:10.1016/S0092-8674(00)80323-2.
- Evans, M.J., and Kaufman, M.H. 1981. Establishment in culture of pluripotential cells from mouse embryos. *Nature* 292: 154–156.
- Flügel, D., Görlach, A., Michiels, C., and Kietzmann, T. 2007. Glycogen Synthase Kinase 3 Phosphorylates Hypoxia-Inducible Factor 1 $\alpha$  and Mediates Its Destabilization in a VHL-Independent Manner. *Mol Cell Biol* 27(9): 3253–3265. doi:10.1128/mcb.00015-07.
- Fraichard, A., Chassande, O., Bilbaut, G., Dehy, C., Savatier, P., and Samarut, J. 1995. In vitro differentiation of embryonic stem cells into glia and neurons. *J Cell Sci* 108: 3181–3188.

- Fry, A.M. 2002. The Nek2 protein kinase: A novel regulator of centrosome structure. *Oncogene* 21(40 REV. ISS. 4): 6184–6194. doi:10.1038/sj.onc.1205711.
- Garcia, A.D.R., Petrova, R., Eng, L., and Joyner, A.L. 2010. Sonic Hedgehog regulates discrete populations of astrocytes in the adult mouse forebrain. *Journal of Neuroscience* 30(41): 13597–13608. doi:10.1523/JNEUROSCI.0830-10.2010.
- Gaspard, N., Bouchet, T., Herpoel, A., Naeije, G., van den Aemele, J., and Vanderhaeghen, P. 2009. Generation of cortical neurons from mouse embryonic stem cells. *Nat Protoc* 4(10): 1456–1463. doi:10.1038/nprot.2009.157.
- Gatie, M.I., Cooper, T.T., Khazae, R., Lajoie, G.A., and Kelly, G.M. 2022. Lactate Enhances Mouse ES Cell Differentiation Toward XEN Cells In Vitro. *Stem Cells* 40(3): 239–259. doi:10.1093/stmcls/sxab022.
- Golebiewska, A., Atkinson, S.P., Lako, M., and Armstrong, L. 2009. Epigenetic landscaping during hESC differentiation to neural cells. *Stem Cells* 27(6): 1298–1308. doi:10.1002/stem.59.
- Gonzalez-Ramos, A., Waloschková, E., Mikroulis, A., Kokaia, Z., Bengzon, J., Ledri, M., Andersson, M., and Kokaia, M. 2021. Human stem cell-derived GABAergic neurons functionally integrate into human neuronal networks. *Sci Rep* 11(1): 22050. Nature Publishing Group UK. doi:10.1038/s41598-021-01270-x.
- Gu, W., Gaeta, X., Sahakyan, A., Chan, A.B., Hong, C.S., Kim, R., Braas, D., Plath, K., Lowry, W.E., and Christofk, H.R. 2016. Glycolytic Metabolism Plays a Functional Role in Regulating Human Pluripotent Stem Cell State. *Cell Stem Cell* 19(4): 476–490. Elsevier Inc. doi:10.1016/j.stem.2016.08.008.
- Gu, Z., Xia, J., Xu, H., Frech, I., Tricot, G., and Zhan, F. 2017. NEK2 promotes aerobic glycolysis in multiple myeloma through regulating splicing of pyruvate kinase. *J Hematol Oncol* 10: 1–11. *Journal of Hematology & Oncology*. doi:10.1186/s13045-017-0392-4.
- Gustafsson, M. V., Zheng, X., Pereira, T., Gradin, K., Jin, S., Lundkvist, J., Ruas, J.L., Poellinger, L., Lendahl, U., and Bondesson, M. 2005. Hypoxia requires Notch signaling to maintain the undifferentiated cell state. *Dev Cell* 9(5): 617–628. doi:10.1016/j.devcel.2005.09.010.
- Harvey, A., Caretti, G., Moresi, V., Renzini, A., and Adamo, S. 2019. Interplay between Metabolites and the Epigenome in Regulating Embryonic and Adult Stem Cell Potency and Maintenance. *Stem Cell Reports* 13(4): 573–589. doi:10.1016/j.stemcr.2019.09.003.
- Hashemi, M.S., Ghaedi, K., Salamian, A., Karbalaie, K., Emadi-Baygi, M., Tanhaei, S., Nasr-Esfahani, M.H., and Baharvand, H. 2013. Fndc5 knockdown significantly decreased neural differentiation rate of mouse embryonic stem cells. *Neuroscience* 231: 296–304. IBRO. doi:10.1016/j.neuroscience.2012.11.041.

- He, X., Imanishi, S., Sone, H., Nagano, R., Qin, X.Y., Yoshinaga, J., Akanuma, H., Yamane, J., Fujibuchi, W., and Ohsako, S. 2012. Effects of methylmercury exposure on neuronal differentiation of mouse and human embryonic stem cells. *Toxicol Lett* 212(1): 1–10. Elsevier Ireland Ltd. doi:10.1016/j.toxlet.2012.04.011.
- Hoelzl, M.A., Heby-Henricson, K., Bilousova, G., Rozell, B., Kuiper, R. v, Kasper, M., Toftgård, R., and Teglund, S. 2015. Suppressor of Fused Plays an Important Role in Regulating Mesodermal Differentiation of Murine Embryonic Stem Cells In Vivo. *Stem Cells Dev* 24(21): 2547–2560. doi:10.1089/scd.2015.0050.
- Honsa, P., Valny, M., Kriska, J., Matuskova, H., Harantova, L., Kirdajova, D., Valihrach, L., Androvic, P., Kubista, M., and Anderova, M. 2016. Generation of reactive astrocytes from NG2 cells is regulated by sonic hedgehog. *Glia* 64(9): 1518–1531. doi:10.1002/glia.23019.
- Hu, B.-Y., and Zhang, S.-C. 2010. Directed differentiation of neural-stem cells and subtype-specific neurons from hESCs. *Methods in Molecular Biology* 636: 123–137. doi:10.1007/978-1-60761-691-7.
- Infante, P., Faedda, R., Bernardi, F., Bufalieri, F., Severini, L.L., Alfonsi, R., Mazzà, D., Siler, M., Coni, S., Po, A., Petroni, M., Ferretti, E., Mori, M., De Smaele, E., Canettieri, G., Capalbo, C., Maroder, M., Screpanti, I., Kool, M., Pfister, S.M., Guardavaccaro, D., Gulino, A., and Di Marcotullio, L. 2018. Itch/ $\beta$ -Arrestin2-dependent non-proteolytic ubiquitylation of SuFu controls Hedgehog signalling and medulloblastoma tumorigenesis. *Nat Commun* 9: 976. doi:10.1038/s41467-018-03339-0.
- Jiwani, T., Kim, J.J., and Rosenblum, N.D. 2020. Suppressor of fused controls cerebellum granule cell proliferation by suppressing Fgf8 and spatially regulating Gli proteins. *Development* 147(3): 1–17. doi:10.1242/dev.170274.
- Jones-Villeneuve, E.M., McBurney, M.W., Rogers, K.A., and Kalnins, V.I. 1982. Retinoic acid induces embryonal carcinoma cells to differentiate into neurons and glial cells. *J Cell Biol* 94(2): 253–262. doi:10.1083/jcb.94.2.253.
- Jones-Villeneuve, E.M., Rudnicki, M.A., Harris, J.F., and McBurney, M.W. 1983. Retinoic acid-induced neural differentiation of embryonal carcinoma cells. *Mol Cell Biol* 3(12): 2271–2279. doi:10.1128/mcb.3.12.2271.
- Kabiri, M., Soleimani, M., Shabani, I., Futrega, K., Ghaemi, N., Ahvaz, H.H., Elahi, E., and Doran, M.R. 2012. Neural differentiation of mouse embryonic stem cells on conductive nanofiber scaffolds. *Biotechnol Lett* 34(7): 1357–1365. doi:10.1007/s10529-012-0889-4.
- Kawasaki, H., Mizuseki, K., Nishikawa, S., Kaneko, S., Kuwana, Y., Nakanishi, S., Nishikawa, S.I., and Sasai, Y. 2000. Induction of midbrain dopaminergic neurons from

ES cells by stromal cell-derived inducing activity. *Neuron* 28(1): 31–40.  
doi:10.1016/S0896-6273(00)00083-0.

Kim, J.J., Gill, P.S., Rotin, L., van Eede, M., Henkelman, R.M., Hui, C.-C., and Rosenblum, N.D. 2011. Suppressor of Fused controls mid-hindbrain patterning and cerebellar morphogenesis via GLI3 repressor. *Journal of Neuroscience* 31(5): 1825–1836.  
doi:10.1523/JNEUROSCI.2166-10.2011.

Kim, J.J., Jiwani, T., Erwood, S., Loree, J., and Rosenblum, N.D. 2018. Suppressor of fused controls cerebellar neuronal differentiation in a manner modulated by GLI3 repressor and Fgf15. *Developmental Dynamics* 247(1): 156–169.  
doi:10.1002/dvdy.24526.

Kise, Y., Morinaka, A., Teglund, S., and Miki, H. 2009. Sufu recruits GSK3 $\beta$  for efficient processing of Gli3. *Biochem Biophys Res Commun* 387(3): 569–574. Elsevier Inc. doi:10.1016/j.bbrc.2009.07.087.

Li, L., Candelario, K.M., Thomas, K., Wang, R., Wright, K., Messier, A., and Cunningham, L.A. 2014. Hypoxia inducible factor-1 $\alpha$  (HIF-1 $\alpha$ ) is required for neural stem cell maintenance and vascular stability in the adult mouse SVZ. *Journal of Neuroscience* 34(50): 16713–16719. doi:10.1523/JNEUROSCI.4590-13.2014.

Li, S., Zheng, J., Chai, L., Lin, M., Zeng, R., Lu, J., and Bian, J. 2019. Rapid and Efficient Differentiation of Rodent Neural Stem Cells into Oligodendrocyte Progenitor Cells. *Dev Neurosci* 41(1–2): 79–93. doi:10.1159/000499364.

Litingtung, Y., and Chiang, C. 2000. Control of Shh Activity and Signaling in the Neural Tube. *Developmental Dynamics* 219: 143–154.

Mak, S.K., Huang, Y.A., Iranmanesh, S., Vangipuram, M., Sundararajan, R., Nguyen, L., Langston, J.W., and Schüle, B. 2012. Small molecules greatly improve conversion of human-induced pluripotent stem cells to the neuronal lineage. *Stem Cells Int* 2012: 140427. doi:10.1155/2012/140427.

Makino, S., Zhulyan, O., Mo, R., Puvindran, V., Zhang, X., Murata, T., Fukumura, R., Ishitsuka, Y., Kotaki, H., Matsumaru, D., Ishii, S., Hui, C.C., and Gondo, Y. 2015. T396I mutation of mouse Sufu reduces the stability and activity of Gli3 repressor. *PLoS One* 10(3): 1–15. doi:10.1371/journal.pone.0119455.

Mbom, B.C., Siemers, K.A., Ostrowski, M.A., Nelson, W.J., and Barth, A.I.M. 2014. Nek2 phosphorylates and stabilizes B-catenin at mitotic centrosomes downstream of Plk1. *Mol Biol Cell* 25(7): 977–991. doi:10.1091/mbc.E13-06-0349.

Mennerich, D., Dimova, E., and Kietzmann, T. 2014. Direct phosphorylation events involved in HIF-1 $\alpha$  regulation: the role of GSK-3 $\beta$ ; *Hypoxia* 2: 35–45.  
doi:10.2147/hp.s60703.

Motoyama, J., Milenkovic, L., Iwama, M., Shikata, Y., Scott, M.P., and Hui, C.C. 2003. Differential requirement for Gli2 and Gli3 in ventral neural cell fate specification. *Dev Biol* 259(1): 150–161. doi:10.1016/S0012-1606(03)00159-3.

Okada, Y., Shimazaki, T., Sobue, G., and Okano, H. 2004. Retinoic-acid-concentration-dependent acquisition of neural cell identity during in vitro differentiation of mouse embryonic stem cells. *Dev Biol* 275: 124–142. doi:10.1016/j.ydbio.2004.07.038.

Paces-Fessy, M., Boucher, D., Petit, E., Paute-Briand, S., and Blanchet-Tournier, M.-F. 2004. The negative regulator of Gli, Suppressor of fused (Sufu), interacts with SAP18, Galectin3 and other nuclear proteins. *Biochemical Journal* 378(2): 353–362. doi:10.1042/bj20030786.

Panchision, D.M. 2009. The role of oxygen in regulating neural stem cells in development and disease. *J Cell Physiol* 220(3): 562–568. doi:10.1002/jcp.21812.

Pashkovskaia, N., Gey, U., and Rödel, G. 2018. Mitochondrial ROS direct the differentiation of murine pluripotent P19 cells. *Stem Cell Res* 30(June): 180–191. Elsevier. doi:10.1016/j.scr.2018.06.007.

Pereira, S.L., Grãos, M., Rodrigues, A.S., Anjo, S.I., Carvalho, R.A., Oliveira, P.J., Arenas, E., and Ramalho-Santos, J. 2013. Inhibition of mitochondrial complex III blocks neuronal differentiation and maintains embryonic stem cell pluripotency. *PLoS One* 8(12): 1–16. doi:10.1371/journal.pone.0082095.

Perrier, A.L., Tabar, V., Barberi, T., Rubio, M.E., Bruses, J., Topf, N., Harrison, N.L., and Studer, L. 2004. Derivation of midbrain dopamine neurons from human embryonic stem cells. *Proc Natl Acad Sci U S A* 101(34): 12543–12548. doi:10.1073/pnas.0404700101.

Pozniak, C.D., Langseth, A.J., Dijkgraaf, G.J.P., Choe, Y., Werb, Z., and Pleasure, S.J. 2010. Sox10 directs neural stem cells toward the oligodendrocyte lineage by decreasing Suppressor of Fused expression. *Proc Natl Acad Sci U S A* 107(50): 21795–21800. doi:10.1073/pnas.1016485107.

Rellos, P., Ivins, F.J., Baxter, J.E., Pike, A., Nott, T.J., Parkinson, D.M., Das, S., Howell, S., Fedorov, O., Qi, Y.S., Fry, A.M., Knapp, S., and Smerdon, S.J. 2007. Structure and regulation of the human Nek2 centrosomal kinase. *Journal of Biological Chemistry* 282(9): 6833–6842. Currently published by Elsevier Inc; originally published by American Society for Biochemistry and Molecular Biology. doi:10.1074/jbc.M609721200.

Ribes, V., and Briscoe, J. 2009. Establishing and interpreting graded Sonic Hedgehog signaling during vertebrate neural tube patterning: the role of negative feedback. *Cold Spring Harb Perspect Biol* 1(2): 1–16. doi:10.1101/cshperspect.a002014.



- Rose, J., Brian, C., Pappa, A., Panayiotidis, M.I., and Franco, R. 2020, November 5. Mitochondrial Metabolism in Astrocytes Regulates Brain Bioenergetics, Neurotransmission and Redox Balance. *Frontiers Media S.A.* doi:10.3389/fnins.2020.536682.
- Sahota, N., Sabir, S., O'Regan, L., Blot, J., Zalli, D., Baxter, J., Barone, G., and Fry, A. 2018. NEKs, NIMA-Related Kinases. In *Encyclopedia of Signaling Molecules*. Edited by S. Choi. Springer International Publishing, Cham. pp. 3407–3419. doi:10.1007/978-3-319-67199-4\_17.
- Semenza, G.L. 2011. Regulation of metabolism by hypoxia-inducible factor 1. *Cold Spring Harb Symp Quant Biol* 76: 347–353. doi:10.1101/sqb.2011.76.010678.
- Shan, W., Hu, W., Wen, Y., Ding, X., Ma, X., Yan, W., and Xia, Y. 2021. Evaluation of atrazine neurodevelopment toxicity in vitro-application of hESC-based neural differentiation model. *Reproductive Toxicology* 103(101): 149–158. Elsevier Inc. doi:10.1016/j.reprotox.2021.06.009.
- Sharp, F.R., and Bernaudin, M. 2004. HIF1 and oxygen sensing in the brain. *Nat Rev Neurosci* 5(6): 437–448. doi:10.1038/nrn1408.
- Shyh-Chang, N., and Ng, H.H. 2017. The metabolic programming of stem cells. *Genes Dev* 31(4): 336–346. doi:10.1101/gad.293167.116.
- Silva, J., Barrandon, O., Nichols, J., Kawaguchi, J., Theunissen, T.W., and Smith, A. 2008. Promotion of reprogramming to ground state pluripotency by signal inhibition. *PLoS Biol* 6(10): 2237–2247. doi:10.1371/journal.pbio.0060253.
- Sodhi, A., Montaner, S., Miyazaki, H., and Gutkind, J.S. 2001. MAPK and akt Act cooperatively but independently on hypoxia inducible factor-1 $\alpha$  in rasV12 upregulation of VEGF. *Biochem Biophys Res Commun* 287(1): 292–300. Academic Press. doi:10.1006/bbrc.2001.5532.
- Spice, D.M., Cooper, T.T., Lajoie, G.A., and Kelly, G.M. 2022. Never in Mitosis Kinase 2 regulation of metabolism is required for neural differentiation. *Cell Signal* 100: 110484. doi: 10.1016/j.cellsig.2022.110484.
- Takenaka, K., Kise, Y., and Miki, H. 2007. GSK3 $\beta$  positively regulates Hedgehog signaling through Sufu in mammalian cells. *Biochem Biophys Res Commun* 353(2): 501–508. doi:10.1016/j.bbrc.2006.12.058.
- Tekki-Kessarlis, N., Woodruff, R., Hall, A.C., Gaffield, W., Kimura, S., Stiles, C.D., Rowitch, D.H., and Richardson, W.D. 2001. Hedgehog-dependent oligodendrocyte lineage specification in the telencephalon. *Development* 128(13): 2545–2554. doi:10.1242/dev.128.13.2545.

- Tomita, S., Ueno, M., Sakamoto, M., Kitahama, Y., Ueki, M., Maekawa, N., Sakamoto, H., Gassmann, M., Kageyama, R., Ueda, N., Gonzalez, F.J., and Takahama, Y. 2003. Defective Brain Development in Mice Lacking the Hif-1  $\alpha$  Gene in Neural Cells. *Mol Cell Biol* 23(19): 6739–6749. doi:10.1128/mcb.23.19.6739-6749.2003.
- Vega-Naredo, I., Loureiro, R., Mesquita, K.A., Barbosa, I.A., Tavares, L.C., Branco, A.F., Erickson, J.R., Holy, J., Perkins, E.L., Carvalho, R.A., and Oliveira, P.J. 2014. Mitochondrial metabolism directs stemness and differentiation in P19 embryonal carcinoma stem cells. *Cell Death Differ* 21(10): 1560–1574. Nature Publishing Group. doi:10.1038/cdd.2014.66.
- Wang, L.C., and Almazan, G. 2016. Role of Sonic Hedgehog Signaling in Oligodendrocyte Differentiation. *Neurochem Res* 41(12): 3289–3299. Springer US. doi:10.1007/s11064-016-2061-3.
- Wang, Y., Li, Y., Hu, G., Huang, X., Rao, H., Xiong, X., Luo, Z., Lu, Q., and Luo, S. 2016. Nek2A phosphorylates and stabilizes SuFu: A new strategy of Gli2/Hedgehog signaling regulatory mechanism. *Cell Signal* 28(9): 1304–1313. Elsevier Inc. doi:10.1016/j.cellsig.2016.06.010.
- Winkler, C.C., Yabut, O.R., Fregoso, S.P., Gomez, H.G., Dwyer, B.E., Pleasure, S.J., and Franco, S.J. 2018. The dorsal wave of neocortical oligodendrogenesis begins embryonically and requires multiple sources of sonic hedgehog. *Journal of Neuroscience* 38(23): 5237–5250. doi:10.1523/JNEUROSCI.3392-17.2018.
- Witteveldt, J., and Macias, S. 2019. Differentiation of Mouse Embryonic Stem Cells to Neuronal Cells Using Hanging Droplets and Retinoic Acid. *Bio Protoc* 9(21): 1–8. doi:10.21769/bioprotoc.3417.
- Wu, C.Y., Whye, D., Mason, R.W., and Wang, W. 2012. Efficient differentiation of mouse embryonic stem cells into motor neurons. *Journal of Visualized Experiments* (64): 1–5. doi:10.3791/3813.
- Wu, S.M., Choo, A.B.H., Yap, M.G.S., and Chan, K.K.K. 2010. Role of Sonic hedgehog signaling and the expression of its components in human embryonic stem cells. *Stem Cell Res* 4(1): 38–49. Elsevier B.V. doi:10.1016/j.scr.2009.09.002.
- Wulansari, N., Sulistio, Y.A., Darsono, W.H.W., Kim, C.H., and Lee, S.H. 2021. LIF maintains mouse embryonic stem cells pluripotency by modulating TET1 and JMJD2 activity in a JAK2-dependent manner. *Stem Cells* 39(6): 750–760. doi:10.1002/stem.3345.
- Yabut, O.R., Fernandez, G., Yoon, K., Pleasure, S.J., Yabut, O.R., Fernandez, G., Huynh, T., Yoon, K., and Pleasure, S.J. 2015. Suppressor of Fused Is critical for maintenance of

- neuronal progenitor identity during corticogenesis. *Cell Rep* 12(12): 2021–2034. The Authors. doi:10.1016/j.celrep.2015.08.031.
- Yang, H., Liu, C., Fan, H., Chen, B., Huang, D., Zhang, L., Zhang, Q., An, J., Zhao, J., Wang, Y., and Hao, D. 2019. Sonic Hedgehog Effectively Improves Oct4-Mediated Reprogramming of Astrocytes into Neural Stem Cells. *Molecular Therapy* 27(8): 1467–1482. Elsevier Ltd. doi:10.1016/j.ymthe.2019.05.006.
- Yao, M., Zhou, X., Zhou, J., Gong, S., Hu, G., Li, J., Huang, K., Lai, P., Shi, G., Hutchins, A.P., Sun, H., Wang, H., and Yao, H. 2018. PCGF5 is required for neural differentiation of embryonic stem cells. *Nat Commun* 9: 1436. Springer US. doi:10.1038/s41467-018-03781-0.
- Ying, Q.L., Stavridis, M., Griffiths, D., Li, M., and Smith, A. 2003. Conversion of embryonic stem cells into neuroectodermal precursors in adherent monoculture. *Nat Biotechnol* 21(2): 183–186. doi:10.1038/nbt780.
- Yu, K., McGlynn, S., and Matise, M.P. 2013. Floor plate-derived sonic hedgehog regulates glial and ependymal cell fates in the developing spinal cord. *Development* 140(7): 1594–1604. doi:10.1242/dev.090845.
- Zhang, Z., Shen, L., Law, K., Zhang, Z., Liu, X., Hua, H., Li, S., Huang, H., Yue, S., Hui, C., and Cheng, S.Y. 2017. Suppressor of Fused Chaperones Gli Proteins To Generate Transcriptional Responses to Sonic Hedgehog Signaling. *Mol Cell Biol* 37(3): 1–18. doi:10.1128/mcb.00421-16.
- Zhao, Y., Matsuo-Takasaki, M., Tsuboi, I., Kimura, K., Salazar, G.T. a., Yamashita, T., and Ohneda, O. 2014. Dual functions of hypoxia-inducible factor 1 alpha for the commitment of mouse embryonic stem cells toward a neural lineage. *Stem Cells Dev* 23(18): 2143–2155. doi:10.1089/scd.2013.0278.
- Zheng, X., Boyer, L., Jin, M., Mertens, J., Kim, Y., Ma, L., Ma, L., Hamm, M., Gage, F.H., and Hunter, T. 2016. Metabolic reprogramming during neuronal differentiation from aerobic glycolysis to neuronal oxidative phosphorylation. *Elife* 5: e13374. doi:10.7554/eLife.13374.
- Zhou, F., Huang, D., Li, Y., Hu, G., Rao, H., Lu, Q., Luo, S., and Wang, Y. 2017. Nek2A/SuFu feedback loop regulates Gli-mediated Hedgehog signaling pathway. *Int J Oncol* 50(2): 373–380. doi:10.3892/ijo.2016.3819.
- Zhou, L., Ding, L., Gong, Y., Zhao, J., Zhang, J., Mao, Z., Wang, Z., Zhang, W., and Zhou, R. 2021. NEK2 Promotes Cell Proliferation and Glycolysis by Regulating PKM2 Abundance via Phosphorylation in Diffuse Large B-Cell Lymphoma. *Front Oncol* 11(June): 1–15. doi:10.3389/fonc.2021.677763.

## Curriculum Vitae

<b>Name:</b>	Danielle Spice
<b>Post-secondary Education and Degrees:</b>	<p>The University of Western Ontario London, Ontario, Canada 2012-2016 B.Sc.</p> <p>The University of Western Ontario London, Ontario, Canada 2016-2022 Ph.D.</p>
<b>Honours and Awards:</b>	<p><b>Natural Sciences and Engineering Research Council of Canada Postgraduate Scholarship – Doctoral</b>, 2018-2021, \$21,000/yr for 3 years</p> <p><b>Queen Elizabeth II Graduate Scholarship in Science &amp; Engineering</b>, 2017-2019, \$15,000</p> <p><b>Mitacs Accelerate Internship</b>, 2012-2013, \$13,334</p> <p><b>Ian Clarke Graduate Scholarship in Biology</b>, 2018-2019, \$1000</p> <p><b>Cells I See Grand Prize – Till &amp; McCulloch Stem Cell Meetings</b>, 2020, \$750</p> <p><b>Laudenbach Memorial Award</b>, 2019-2020, \$600</p> <p><b>Best Basic Science Poster – Till &amp; McCulloch Stem Cell Meetings</b>, 2020, \$500</p>
<b>Related Work Experience</b>	<p><b>Teaching Assistant</b> Department of Biology The University of Western Ontario 2016-2022</p> <p><b>Teaching Assistant Training Program Instructor</b> Centre for Teaching and Learning The University of Western Ontario 2020-2022</p> <p><b>COVID Relief Teaching Fellow</b> Department of Biology The University of Western Ontario</p>

2020

**Educational Content Developer**

Wize® Prep

2017-2022

**Publications:**

**Spice, D.M.**, Cooper, T., Lajoie, G.A., and G.M. Kelly. “Never in Mitosis Kinase 2 regulation of metabolism is required for neural differentiation.” 2022. *Cellular Signaling*. 100, 110484. doi: 10.1016/j.cellsig.2022.110484

**Spice, D.M.**, Dierolf, J., and G.M. Kelly. “Suppressor of Fused Regulation of Hedgehog Signaling is Required for Proper Astrocyte Differentiation.” 2022. *Stem Cells and Development*. Online ahead of print. doi: 10.1089/scd.2022.0131

Gatie, M.I., **Spice, D.M.\***, Garha, A., McTague, A., Ahmer, A., Timoshenko, A.V., and G.M. Kelly. “*O*-GlcNACylation and Regulation of Galectin-3 in Extraembryonic Endoderm Differentiation.” 2022. \*Co-first author. *Biomolecules*. 12, 623. doi: 10.3390/biom12050623

Abbasi, S., Adoungotchodo, A., Ansari, U., ... **Spice, D.**, et al. “Evaluation of Tavakol et al.: Harnessing organs-on-a-chip to model tissue regeneration.” 2021. *Cell Stem Cell* 28 (6): 979-982. doi: 10.1016/j.stem.2021.05.011

Deol, G.S.J., Cuthbert, T.C., Gatie, M.I., **Spice, D.M.**, Hilton, L.R., and G.M. Kelly. “Wnt and Hedgehog Signaling Regulate the Differentiation of F9 Cells into Extraembryonic Endoderm”. 2017. *Front. Cell Dev. Biol.* 5: 93. doi: 10.3389/fcell.2017.00093

Dickson, B.J., Gatie, M.I.\*, **Spice, D.M.**, and G.M. Kelly. “Nox1 and Nox4 are Required for the Differentiation of Mouse F9 Cells into Extraembryonic Endoderm”. 2017. \*Co-first author, *PLOS ONE* 12 (2): e0170812. doi: 10.1371/journal.pone.0170812